RECLAMATION
Managing Water in the West

Design Standards No. 13

Embankment Dams

Chapter 13: Seismic Analysis and Design
Phase 4: Final

Mission Statements

The U.S. Department of the Interior protects America's natural resources and heritage, honors our cultures and tribal communities, and supplies the energy to power our future.

The mission of the Bureau of Reclamation is to manage, develop, and protect water and related resources in an environmentally and economically sound manner in the interest of the American public.

Design Standards Signature Sheet

Design Standards No. 13

Embankment Dams

DS-13(13)-8: Phase 4: Final
May 2015

Chapter 13: Seismic Analysis and Design

U.S. Department of the Interior
Bureau of Reclamation

Foreword

Purpose

The Bureau of Reclamation (Reclamation) design standards present technical requirements and processes to enable design professionals to prepare design documents and reports necessary to manage, develop, and protect water and related resources in an environmentally and economically sound manner in the interest of the American public. Compliance with these design standards assists in the development and improvement of Reclamation facilities in a way that protects the public's health, safety, and welfare; recognizes needs of all stakeholders; and achieves lasting value and functionality necessary for Reclamation facilities. Responsible designers accomplish this goal through compliance with these design standards and all other applicable technical codes, as well as incorporation of the stakeholders' vision and values, that are then reflected in the constructed facilities.

Application of Design Standards

Reclamation design activities, whether performed by Reclamation or by a non-Reclamation entity, must be performed in accordance with established Reclamation design criteria and standards, and approved national design standards, if applicable. Exceptions to this requirement shall be in accordance with provisions of *Reclamation Manual Policy*, Performing Design and Construction Activities, FAC P03.

In addition to these design standards, designers shall integrate sound engineering judgment, applicable national codes and design standards, site-specific technical considerations, and project-specific considerations to ensure suitable designs are produced that protect the public's investment and safety. Designers shall use the most current edition of national codes and design standards consistent with Reclamation design standards. Reclamation design standards may include exceptions to requirements of national codes and design standards.

Proposed Revisions

Reclamation designers should inform the Technical Service Center (TSC), via Reclamation's Design Standards Website notification procedure, of any recommended updates or changes to Reclamation design standards to meet current and/or improved design practices.

Chapter Signature Sheet
Bureau of Reclamation
Technical Service Center

Design Standards No. 13

Embankment Dams

Chapter 13: Seismic Analysis and Design

DS-13(13)-8:[1] Phase 4: Final
May 2015

Chapter 13 – Seismic Analysis and Design is an existing chapter within Design Standards No. 13 and has been revised to include:

- A risk-informed approach to dam safety, consistent with policies of the Bureau of Reclamation Dam Safety Office

- Updated practices for:
  - assessment of liquefaction potential
  - strengths of foundation and embankment materials for assessing stability and deformation
  - analysis of deformation

- Additional information on seismic loadings and their use for dam-safety analysis

- Design features for new dams and modifications of existing dams

---

[1] DS-13(13)-8 refers to Design Standards No. 13, chapter 13, revision 8.

Prepared by:
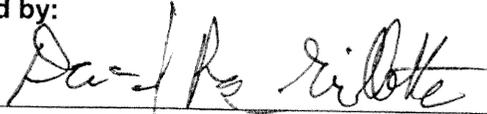
David Rees Gillette, P.E.   PE   5/1/2015

David Rees Gillette, P.E.   Date

Civil Engineer, Geotechnical Engineering Group 4, 86-68314

Peer Review

Robert L. Dewey, P.E.   5/1/2015

Robert L. Dewey, P.E.   Date

Civil Engineer, Geotechnical Engineering Group 4, 86-68313

Security Review:

Ashok Chugh   5/2/2015
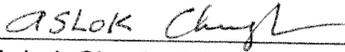
Ashok Chugh, P.E.   Date

Civil Engineer, Geotechnical Engineering Group 1, 86-68311

Recommended for Technical Approval:
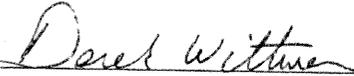
Derek T. Wittwer   5/1/15

Derek T. Wittwer, P.E.   Date

Manager, Geotechnical Engineering Group 4, 86-68314

Submitted:

Daniel W. Osmun   5/1/15
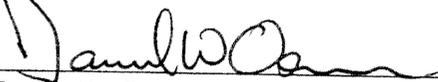
Daniel W. Osmun, P.E.   Date

Chief, Geotechnical Services Division, 86-68300

Approved:

Thomas A. Luebke   12/17/15

Thomas A. Luebke, P.E.   Date

Director, Technical Service Center

Abbreviations and Acronyms

1D	one-dimensional
2D	two-dimensional
A_{max}	peak horizontal acceleration at the ground surface
ASTM	American Society for Testing Materials
atm	atmospheric pressure
BPT	Hammer penetration tests
CR	Comprehensive Review
CPT	Cone Penetrometer Test
CPTu	CPT with measurement of pore-water pressure (u)
CRR	Cyclic Resistance Ratio
$CRR_{M=7.5,\sigma'=1}$	CRR normalized to standard magnitude and overburden
CSR	Cyclic Stress Ratio
$CSR_{M=7.5,\sigma'=1}$	CSR normalized to standard magnitude and overburden
DCPT	Dynamic Cone Penetration Test
DSS	Direct Simple Shear (Test)
ECPT	Electronic Cone Penetrometer Test
FDM	Finite Difference Method
FEM	Finite Element Method
FS	factor of safety
g	acceleration due to earth's gravity
ICOLD	International Commission on Large Dams
LL	liquid limit
M	earthquake magnitude
MCE	Maximum Credible Earthquake
MSF	Magnitude Scaling Factor (also known as DWF for duration weighting factor, or simply K_M)
M_W	earthquake moment magnitude

NCEER	National Center for Earthquake Engineering Research
OSHA	Occupational Safety and Health Administration
PFM	Potential Failure Mode
PHA	peak horizontal ground acceleration
PI	Plasticity Index
PSHA	Probabilistic Seismic Hazard Analysis
Reclamation	Bureau of Reclamation
TSC	Technical Service Center
u	pore-water pressure
UHS	uniform-hazard response spectra
USCS	Unified Soil Classification System
USGS	United States Geological Survey
V_S	shear wave velocity
VST	Field Vane Shear Test

Contents

Contents (continued)

Contents (continued)

Figures

Figures (continued)

Appendices

A   Earthquake Loadings for Analysis of Embankment Dams

B   Assessment of Liquefaction Potential Using the Cone Penetration Test

C   Assessment of Liquefaction Potential Using the Standard Penetration Test

D   Becker-Hammer Penetration Test for Gravelly Soils

E   Assessment of Liquefaction Potential by Shear-Wave Velocity

F   Soil Strengths for Seismic Analysis

G   Improving the Seismic Resistance of Existing Dams

Chapter 13

Seismic Analysis and Design

13.1   Introduction

13.1.1 Applicability

The procedures contained in this chapter are applicable to the seismic analysis and design of embankment dams constructed or evaluated by the Bureau of Reclamation (Reclamation).

This design standard is not a textbook or an exhaustive manual of earthquake engineering, nor can it be considered applicable to all dams and all site conditions. New developments are relatively frequent, particularly in the area of liquefaction assessment. The user of this design standard should maintain currency with the state of practice as it evolves.

Thorough, independent, expert review is essential at all stages of an investigation or design.

13.1.2 Deviations From Standard

Deviations from this standard should be noted in documentation of the design or analysis. Rationale for deviations from this standard should be approved and documented.

The user must be aware that the state of practice in earthquake geotechnical analysis is constantly evolving, and portions of this design standard may be superseded.

13.1.3 References

References are listed in full in Section 13.1, "References," at the end of this chapter. Most references are available in journals or conference proceedings. Many references are also available in Reclamation's Library and/or the Technical Service Center (TSC) Geotechnical Services Division library, both located in Denver.

13.1.4   Organization of This Chapter

Because of the rapidly changing state of knowledge on seismic analysis of embankment dams, Chapter 13, "Seismic Analysis and Design," of *Design Standards No. 13 – Embankment Dams*, was written to provide general information in the chapter itself, with details of specific testing and analysis methods in appendices. This "modular" approach is intended to allow information on specific topics to be updated, as required by advances in knowledge, without the need to rewrite the entire chapter.

Sections 13.2 through 13.11, and appendices A through F, discuss methods and guidelines for assessing the earthquake resistance of existing or proposed embankment dams. Section 13.12 provides general recommendations on earthquake-resistant design of new embankment dams. Section 13.13 and appendix G describe methods for improving the earthquake resistance of existing dams.

13.1.5   Definitions of Terms

This section provides only basic definitions of technical terms; detail is provided in subsequent sections and appendices.

Claylike soils: Claylike and sandlike or granular soils have different behavior under cyclic loading, so they require different analytical techniques and concepts. A soil is considered claylike if it has sufficient plastic fines to have the general characteristics of a clay, including a unique curve of void ratio *versus* effective confining stress in normal consolidation, and undrained shear strength and cyclic resistance that are functions of the stress history. Fine-grained soils (more than 50 percent fines) can be either claylike or sandlike in their behavior, depending on the amount of clay particles they contain. Soils that are classified as coarse grained under the Unified Soil Classification System (USCS) may actually be claylike in behavior if the fines are plastic and are more than about 25 to 35 percent, by weight (depending their plasticity), which is enough to cause the sand and gravel to "float" within a matrix of finer particles.

Cyclic failure: The term "cyclic failure" is used to describe yield and large permanent strain in claylike soils. (In laboratory testing, cyclic failure is often defined as 2 or 3 percent cyclic strain.) The occurrence of cyclic failure does not necessarily result in serious damage to the embankment or appurtenant structures; that is specific to each dam and its foundation soils. Following cyclic failure, the soil could either deform plastically, with little loss of shearing resistance with further strain, or show a large decrease, depending on the clay's sensitivity and the amount of strain the earthquake causes.

Cyclic mobility: Refer to the definition of **Liquefaction**, below. Cyclic mobility is a category of soil liquefaction in which strains tend to be limited by increases in shearing resistance following an initial nearly complete loss of effective stress and shearing resistance. This occurs in medium-density granular soils, and it may help to explain why liquefaction has occurred without instability or very large deformations.

Cyclic Stress Ratio and Cyclic Resistance Ratio (CSR and CRR): These are, respectively, measures of the loading imposed on the soil by an earthquake and of its resistance to liquefaction or cyclic failure. They are expressed as ratios of cyclic shear stress to effective overburden stress, with adjustments for earthquake magnitude (as a proxy for duration), static stresses, and other factors. In the CSR, the cyclic stress is the peak cyclic stress imposed by the earthquake on a horizontal surface. The CRR is a property of the soil and is *an index of* the cyclic stresses that it could withstand without liquefaction or cyclic failure. **As the terms are usually used, CRR greater than CSR does not necessarily preclude liquefaction or cyclic failure; instead, they are defined so that, if the CSR is equal to the CRR, the probability of liquefaction or cyclic failure is about 15 percent.**

Earthquake magnitude: The earthquake magnitude is a measure of the amount of energy released by an earthquake. Historically, the magnitude was quantified using the well-known Richter scale; however, the Richter scale has no direct connection with the mechanics of an earthquake, instead being defined by the response of one particular model of seismograph at a specified difference from the source. In the United States, the Richter scale has largely been replaced by the moment magnitude, M_W, which varies with the logarithm of the energy released. Numerical values of the two scales are very similar for moderate to large earthquakes, but in very large earthquakes, the two diverge because the Richter scale becomes insensitive to changes in energy released.

Granular soils: Granular soils are those with little or no plasticity or content of clay minerals, whose behavior in compression or shear is sandlike, as distinguished from claylike behavior. Granular soils are less compressible and more pervious than claylike soils. They do not have a unique curve of void ratio versus effective stress in normal consolidation. Their density is therefore less influenced by stress history, particularly in clean sands and gravels. Some nonplastic or slightly plastic, fine-grained soils are sandlike in behavior, although they are more strongly affected by stress history.

Liquefaction: A loose soil tends to contract when sheared; however, if it is saturated with water, which is practically incompressible, no volume change can occur unless the water is able to drain from the pore space. Without volume change, particle contacts disrupted by shearing are not reestablished as they would be in drained shearing or in a dilative soil. The effective confining stress and, therefore, the soil's shearing resistance, are reduced nearly to zero as a result.

This phenomenon is referred to as "liquefaction." It has caused slope failures, bearing capacity failures, and large deformations of gently sloping ground. It can result from either cyclic loading from an earthquake, or monotonic loading, as occurred during construction of the hydraulic fill for Fort Peck Dam.

Many definitions have been proposed for the term *liquefaction*. One definition, from Professor H.B. Seed, is:

> "…a condition where a soil will undergo **continued** deformation at a constant low residual stress or with low residual resistance due to the buildup and maintenance of high pore-water pressures, which reduce the effective confining pressure to a very low value..." (Seed, 1979) (emphasis added).

This is often called *flow liquefaction* to distinguish it from cyclic mobility. In *cyclic mobility*, the soil may initially contract, generating very high pore pressure and little shearing resistance at smaller strains, but dilate at larger strains, causing a reduction in pore pressure and some recovery of shearing resistance. There are other definitions as well, including "pore pressure nearly equal to 100 percent of the initial effective confining stress" and "double-amplitude axial strain greater than 5 percent in cyclic triaxial tests." The latter of these definitions is, of course, specific to laboratory testing, not field performance. The former can apply to measured pore-water pressure in the laboratory, or for identifying soils that liquefied in flat ground during earthquakes, where sand boils or upwelling water may be the only evidence that liquefaction has occurred, because there has been no significant ground deformation.

In this design standard, the term "liquefaction" will be used to include both flow liquefaction and cyclic mobility.

Potential failure mode: A specific mechanism by which a dam could fail, including the initiating event or loading; e.g., an earthquake or filling of the reservoir, and each condition or subsequent event that must occur for the dam to breach. A single initiating event can be associated with more than one potential failure mode.

Pseudostatic analysis: Analysis of the dynamic stability of a slope using typical slope-stability methods (method of slices or sliding blocks), but with a horizontal force applied to the slide mass to model the effect of horizontal acceleration.

Residual undrained shear strength, S_{ur}: The shearing resistance that can be mobilized at large strains in liquefied soils in the field and be maintained until excess pore-water pressures have dissipated. It is a gross-scale property, and it can be much lower than the steady-state shearing resistance measured on a laboratory specimen ($S_{u\text{-}ss}$). S_{ur} is most commonly estimated by correlation between some index of density (such as the Cone Penetration Test [CPT] or the

Standard Penetration Test [SPT]), and back-analyzed shear strength from actual flow slides. Refer to appendix E for details of estimating S_{ur}.

Spectral acceleration and response spectrum: Spectral acceleration is equal to the peak acceleration calculated when an earthquake ground-motion record excites a damped lumped-mass oscillator with a particular period of oscillation. For embankment dams, its primary use is selecting appropriate ground motions for analysis. Spectral acceleration is plotted against oscillator period for a range of periods, to form the response spectrum of the record. For dynamic analysis, ground motions are selected on the basis of whether their response spectrum is realistic for a specific earthquake source (a fault or a zone of seismicity). For more information, refer to appendix A.

Steady-state undrained shear strength, $S_{u\text{-}ss}$: $S_{u\text{-}ss}$ is the shearing resistance that can be mobilized in liquefied soil at a constant void ratio. It is not equivalent to the residual undrained shear strength, S_{ur}, which is the strength that actually governs the stability or deformation of a slope. Because of potential for changes in void ratio in the field, S_{ur} can be much lower than $S_{u\text{-}ss}$; S_{ur} ordinarily cannot be greater than $S_{u\text{-}ss}$. Refer to appendix F for details.

Yield acceleration: The minimum horizontal acceleration that must be applied to a slide mass in pseudostatic analysis to reduce the factor of safety (FS) against sliding to below 1.0, implying that yield and deformation would occur. Most slope-stability computer programs allow a pseudo-static acceleration to be applied; the acceleration is simply varied until the calculated value of FS is just below 1.0.

13.2   Reclamation's Approach to Seismic Analysis of Embankment Dams

13.2.1   Effects of Earthquakes on Embankment Dams

Historically, embankment dams have usually performed well in earthquakes (Seed et al., 1978; Resendiz et al., 1982; Ambraseys, 1988; Harder, 1991). However, earthquakes can adversely affect embankment dams in a number of ways. The most obvious way is causing instability or large deformations of the embankment or abutments, whether due simply to strong shaking, or aggravated by increases in pore pressure and resulting decreases in strength caused by cyclic loading. Sheffield Dam in Santa Barbara, California, failed in 1925, when loose, saturated foundation soils became liquefied. It suffered near-total loss of strength because of the shaking, and the entire embankment slid downstream on the weakened layer (Seed, Lee, and Idriss, 1969). In the 2001 Bhuj earthquake in India, the foundations of several small dams liquefied, and their upstream slopes became unstable, but the earthquake occurred in the dry season and the reservoirs were nearly empty, so no actual breaches occurred (Singh, Roy, and Jain, 2005).

(The outcome could have been very different if the reservoirs held more water at the time.) The most studied case of liquefaction and instability of a dam is Lower San Fernando Dam, where a hydraulic-fill portion of the embankment was liquefied by the 1971 San Fernando earthquake and slid away from the remainder, leaving only about 3 feet of freeboard remaining to contain the reservoir (Seed, Seed, Harder, and Jong, 1989; Castro, Seed, Keller, and Seed, 1992). Other famous examples of earthquake-induced liquefaction are the overturning of the Kawagishi Cho Apartment Building in Niigata, Japan (Seed, 1987), and the failure of the El Cobre tailings dam in Chile (Dobry and Alvarez, 1967).

Dams have also apparently failed due to erosion through cracks caused by an earthquake (e.g., Rogers Dam in the 1954 Fallon, Nevada, earthquake) (Ambraseys, 1988), and at least one dam has failed due to fault rupture in its foundation (Lower Howell Dam in the 1906 San Francisco earthquake) (Bray, 1990). Interestingly, Upper Howell Dam, which also crosses the San Andreas Fault, did not fail; the difference may have been the presence of an outlet pipe through the Lower Howell embankment. Causes of failure cannot always be determined because the evidence is often washed away.

13.2.2   Reclamation's Risk-Informed Dam-Safety Decision Process

Since the 1990s, decision making for Reclamation's dam-safety program has focused primarily, though not exclusively, on quantifying the level of risk a structure poses to human life (the probability and consequences of dam failure). This is a significant departure from customary deterministic standards, such as minimum factors of safety against liquefaction or slope instability, or a requirement for the dam to withstand the Maximum Credible Earthquake (MCE) for the site. Therefore, this chapter is intended primarily to support probabilistic risk analysis, and it does not provide deterministic guidelines or standards. Deterministic analysis is discussed only to provide Reclamation personnel with historic context.

Reclamation's interim dam-safety public protection guidelines (Reclamation, 2011) address both the probability of failure of a dam in any year, and the loss of life that would be expected if the dam were to fail. In brief, the probability of seismic failure is quantified by decomposing all identified Potential Failure Modes (PFMs) into the component events and conditions that all must occur for each PFM to occur. Then, the probability of each PFM is calculated, beginning with assigning probabilities to each component; the probabilities often vary with the severity of the earthquake loading and the reservoir level at the time of the postulated earthquake. The annual probability of each PFM is calculated from the component probabilities and the annual probability for a particular level of seismic loading, and the results are summed for all levels of loading. Depending on the situation of each dam, the calculations may be very simple, requiring only

hand calculations, or very complex, requiring detailed calculations that may include computer-aided Monte Carlo analysis (in addition to the engineering analyses needed to develop the component probabilities). Risk analysis procedures are described in other Reclamation and Corps of Engineers publications, primarily manuals of best practices.

Consequences of a breach are generally estimated based on case histories of dam failures and other floods. However, very few of those cases resulted from seismic dam failure; therefore, risk analysts need to consider how earthquake shaking and infrastructure damage would influence the effectiveness of warning and evacuation.

13.2.3 Liquefaction, Cyclic Mobility, Cyclic Failure, and Cyclic Strain Potential

A large portion of this chapter is devoted to assessing liquefaction potential of granular soils, analyzing the stability and deformation of dams with liquefiable foundations or embankments, and designing modifications for those that are not adequately stable. Granular soils are defined for this purpose as soils lacking appreciable plasticity, so that they show sandlike behavior, rather than claylike behavior under seismic loading. Boulanger and Idriss (2004) suggest that the Plasticity Index (PI) can be used to distinguish between the two soil types, with the boundary occurring at a PI of 4 to 7. Note that this is a distinction between sandlike and claylike behavior for selecting the appropriate set of engineering procedures for evaluating stress-strain behavior; it does NOT distinguish liquefiable from nonliquefiable soils. Some soils that are classified as ML or MH may actually need to be treated as granular soils for liquefaction assessment.

Cyclic mobility is most likely to occur in medium-density granular materials, roughly speaking those with adjusted Standard Penetration Test (SPT) blow counts, $(N_1)_{60cs}$, of 15 to 30. (Refer to appendix C for a detailed discussion of SPT and its use in liquefaction assessment.) Cyclic mobility is thought to have governed the behavior of many historic cases of lateral spreading in gently sloping ground. There, cyclic mobility can allow ground deformations of several inches to several feet, in contrast with flow liquefaction, involving slope instability and much greater deformation. With a steeper slope, the occurrence of initial liquefaction and cyclic mobility would not necessarily cause instability or deformations large enough to cause failure of a dam. However, the stability of steep slopes after initial liquefaction and cyclic mobility is not well understood, and there are few or no applicable case histories to provide guidance. Refer to appendix F for more detailed discussion of the shear strength of soils for seismic analysis.

The great majority of the case-history data used to establish correlations for liquefaction potential came from sites where there were no large deformations, so

the occurrence of liquefaction was identified from indirect evidence such as settlement or "sand volcanoes" caused by relief of high excess pore pressures. The lack of significant deformations resulted, at least in part, from the terrain being fairly flat. However, at some sites, initial liquefaction occurred, but the soil probably recovered part of its shearing resistance at larger strains (after the phase transformation); therefore, large deformations did not occur on gentle slopes. Given the historic absence of large deformations with medium-density soils, it may be tempting to conclude that very large deformations do not occur with medium-density soils. However, with a relatively gentle slope, the factor of safety against sliding may be only slightly below 1.0, so very little recovery of shearing resistance would be needed to halt sliding. It is, therefore, not reliable to predict the stability of steep slopes from the behavior of gentle slopes.

For dam-safety analyses, one should always try to have corroborating tests of multiple types (SPT, CPT, etc.), rather than rely solely on a single type of testing to assess liquefaction resistance. There may not always be consistency among the results of different tests; if not, the user must consider the reliability and applicability of the tests to the materials being tested.

Cyclic failure of sensitive, fine-grained soils can resemble liquefaction of granular soils. Clayey soils begin to show small permanent strains (several percent) at cyclic shear stresses of 80 to 90 percent of their monotonic peak strength. With stresses nearing or exceeding the peak strength, strains and deformations could be very large. If the soils are sensitive (i.e., their remolded undrained strength is only a small fraction of the peak), the resulting reduction in shear resistance can lead to post-earthquake instability similar to what occurs with liquefied granular soils. The cyclic behavior of fine-grained soils is described separately from granular soils because some different concepts and different empirical correlations apply. (See section 13.7.)

This chapter provides only guidance for designers and analysts, not a complete description of theory and practice for liquefaction assessment. For additional information on liquefaction in general, see Seed (1987), National Center for Earthquake Engineering Research (NCEER) (1997), Seed et al. (2003), and Idriss and Boulanger (2008). New developments in the field occur frequently, so the user is advised to maintain familiarity with new publications as they become available.

13.2.4   General Sequence of Analysis

The assessment of the behavior of an embankment dam under seismic loading typically includes the following eight basic steps:

1. Identifying and characterizing potential sources of earthquake loading, whether known faults or historic seismicity not associated with known faults.

2. Determining the appropriate loadings to apply in the analysis, which may include:

    - Location of and maximum earthquake magnitude from identified faults or zones of seismicity.

    - Peak ground accelerations (vertical and horizontal) or other parameters indicating the intensity of loading, such as spectral acceleration for periods of oscillation that would strongly affect the dam (appendix A).

    - Hazard curves, which show the annual frequency of exceedance for peak acceleration or other index of loading. (The reciprocal of the exceedance frequency is called the "return period," but that does not mean that the exceedance is periodic.)

    - Uniform hazard spectra, indicating the peak spectral acceleration for the full range of relevant periods of oscillation, for an exceedance frequency. For embankment dams, the relevant range is generally 0 to about 3 seconds.

    - Ground motion acceleration records (time histories) for use in analyzing dynamic response and deformation.

3. Collecting and portraying site geology to show embankment and abutment geometry, stratigraphy, piezometric levels, etc., to help identify any weak layers or zones. This will help identify which point data should be grouped for inferring soil-mass characteristics. Correlations for liquefaction triggering and post-liquefaction undrained strength are generally based on mean data for the strata that have liquefied (or not) in earthquakes. Therefore, it is important to separate data from individual strata so that the correct ones are included in estimating the "representative value" for the weakest materials, which may govern the overall behavior of the dam.

4. Determining the properties of the embankment and foundation soils, including as needed:

    - Basic index properties including soil type under the Unified Soil Classification System (USCS), Atterberg limits, grain-size distribution, moisture content, and degree of saturation)

    - Dynamic properties, primarily stiffness and damping

    - Density, and indirect indices of density, such as in situ penetration resistance

- Liquefaction potential of granular soils

- Sensitivity of claylike soils

- Preconsolidation pressure

- Shearing resistance of soils, in monotonic loading or cyclic loading

5. Analyzing the post-earthquake stability of the embankment if there would be a drastic loss of shear strength due to liquefaction, large strains in sensitive clay, or other cause.

6. Predicting the extent of deformations resulting from earthquake shaking and/or reduction in material strengths.

7. Determining the potential for dam failure by overtopping of the deformed embankment, erosion through cracks in the embankment, or other PFMs.

8. Evaluating other structures, such as spillway walls adjacent to the embankment, whose failure could cause failure of the embankment dam by allowing overtopping or by creating unfiltered exit points for internal erosion. (Structural analysis of appurtenant features is outside of the scope of this publication.)

This list of basic steps is not exhaustive. Other failure modes are possible, including internal erosion caused by fault rupture in the foundation, and overtopping by seiche waves. They would require different analyses that are not detailed in this chapter.

If the embankment would become unstable or otherwise create excessive risk of dam failure, some form of corrective action may be required, which could be modifying the dam, restricting the reservoir level, or protecting the public by other means. In Reclamation's dam-safety program, a decision to take corrective action for an existing dam is generally made considering the probability and consequences of dam failure. Hence, it is generally necessary to analyze the dam with consideration of the full reasonable range of material properties and embankment behavior, for a range of earthquake loadings, rather than simply performing deterministic analyses with the MCE for the site (which was once typical practice at Reclamation). Other dam owners and regulatory agencies have different requirements.

The appropriate level of detail for the various analyses must be judged for each dam, based on the costs and potential benefits of more detailed investigation. For example, it may be adequate to show that deformations would be very small relative to the available freeboard, rather than undertake a major study to predict the actual magnitude of deformations.

13.2.5 Site Geology in Embankment Analysis

Site geology is of great importance in liquefaction and stability analysis. The stratigraphy and groundwater govern the extent and continuity of potentially liquefiable materials in the foundation and, therefore, govern which samples and in situ tests should be used in characterizing a particular unit. There needs to be consistency between the forward analysis of the dam being assessed and the back analysis of historic field performance from which some procedures were developed. The degree of continuity is important because it can have a major effect on stability and deformation. Without a large test trench, it is not possible to observe the continuity of material types and densities from one drill hole or in situ test location to another, so it must be inferred. This requires an understanding of the depositional environment. All geologic information and test data should be portrayed on cross sections of the foundation and embankment, preferably oriented both upstream-downstream and cross-valley. Stratigraphy drawn between locations needs to be informed by the depositional history.

13.2.6 Uncertainty in Analyses

The practice of earthquake geotechnical engineering is in a state of development and change, and there is no consensus within the profession on many of the individual procedures for assessing liquefaction potential, shear strength, and embankment deformation. In addition to uncertainty in methodology, interpreting gross-scale soil properties and pore-pressure response from field and lab data has its own set of uncertainties. All predictions of ground motion, liquefaction potential, material strengths, embankment deformation, etc., must be considered in that light.

For example, most published methods for assessing liquefaction potential are based on the behavior of shallow soils (having low effective overburden pressure) in flat ground where there is little or no shear stress on horizontal surfaces. In contrast, the foundations of large dams have high overburden pressure and large static shear stresses. To extrapolate from the case histories to the foundation of a dam, the empirical liquefaction procedures require adjustments derived largely from theory and laboratory testing (K_σ and K_α, which are defined and discussed in detail in subsequent sections). The values of the adjustments are sensitive to a number of different factors that are not easily measured, which introduces additional uncertainty into estimating the likelihood of liquefaction.

Sometimes, one test or analytical procedure may indicate that a dam would behave acceptably, while another test or procedure shows it would not. The engineer needs to understand the analyses and their pitfalls, so that the uncertainties can be recognized and accounted for in risk analysis and decision making. **For assessing liquefaction resistance for high-hazard dams,**

corroborating tests of different types should always be performed, rather than relying solely on one test; e.g., supplementing Becker Hammer Penetration Tests (BPT) in gravelly soils with measurement of shear-wave velocities. (These tests are described in subsequent sections and in appendices D and E, respectively, in greater detail.)

Material properties are both **uncertain** and **variable** from point to point within a deposit, or even within an embankment zone. Uncertainty results, in large part, from the fact that mechanical properties are generally measured in the laboratory or field under conditions that do not precisely mimic the stress path, strain rate, etc., that would occur during an earthquake, or from inferring the properties indirectly by correlation. Laboratory tests and most in situ tests measure the behavior of small, relatively uniform samples with dimensions of a few inches, with controlled stress and strain conditions. These tests are not able to capture the gross-scale behavior of large, nonhomogeneous deposits. Dam embankments and foundations have dimensions of hundreds or thousands of feet, with significantly varying material properties in even the most homogeneous of foundations. Stress and strain conditions under earthquake loading are not entirely understood or easily replicated in the lab. Furthermore, maximum strains and strain rates are limited in laboratory tests, whereas the seismic behavior of an embankment dam may depend on material behavior at very large strains and high strain rates.

13.2.7 The Roles of Precedent and Analysis

For seismic analysis of dams, neither theory nor precedent is adequate on its own. Numerical procedures may be based on sophisticated theory and constitutive models based on laboratory testing, but the constitutive models are merely idealizations of nonhomogeneous deposits of mineral particles, generally treating them as continua. Analytical results are necessarily based on a number of simplifications and assumptions that cannot be verified. Therefore, back analysis of historic performance of dams in earthquakes is needed to validate the models. The number of instructive case histories is limited, and embankments and foundations are all different, so it is very unlikely that there would be directly relevant case histories that could provide a clear, purely empirical indication of the behavior of a particular dam in a particular earthquake. Theory and *back analysis* are needed to understand the case histories so that the lessons can be extended to the dam under study through *forward analysis*. This requires knowledge of both the underlying theory, to understand historic performance, and the historic performance to validate and calibrate theory and analytical methods.

13.3 Seismic Loadings for Analysis and Design

13.3.1 Current Reclamation Practice

Site-specific seismotectonic studies are usually performed for existing Reclamation dams and proposed dam sites by either the TSC's Seismotectonics and Geophysics Group or by a consultant. The scope of investigations depends on the analyses that are expected for the dam, the consequences of dam failure, the quality and quantity of available information, and the sensitivity of the overall results to variation in the plausible loadings. For example, a well-built dam on a rock foundation in an area of moderate seismicity would not receive the same level of effort as a dam on an alluvial foundation in a highly active seismic zone.

This chapter does not provide guidance on how to select earthquake loadings for use in analysis. However, appendix A provides a general description of seismotectonic studies and determining what products are required for various types of analysis.

Prior to and during seismotectonic studies, there must be communication between the seismologists and the analysts that will use the results. To provide the most useful results, the seismologists must be aware of the site geology and topography, the general nature and size of the dam, and the type of analysis that is planned. Communication is very important to efficient and correct selection of ground motions.

13.3.2 Products of Seismotectonic Studies

Depending on the level of analysis, seismotectonic studies for a given dam could include any or all of the following:

- Identification of seismogenic sources. These can be either identified faults (which do not necessarily have surface expression but may have been inferred from geophysical exploration or previous seismic activity) or zones of seismicity without identified causative faults. Evaluation of fault sources generally includes general geologic information, fault geometry (length, strike, dip, and down-dip extent), style of slip (i.e., strike-slip fault versus thrust fault versus normal fault), fault segmentation, and rate of slip. In the past, this would also have included the MCE from each source, but that is no longer part of Reclamation's practice.

- Hazard curves that give the annual exceedance frequency for values of peak horizontal ground acceleration (PHA) or other parameters, such as the spectral acceleration for a particular response period. In probabilistic risk analysis, exceedance probabilities are generally assumed to equal the

exceedance frequencies. The spectral acceleration indicates how strongly a particular earthquake record with its unique frequency content would excite a given structure. PHA is equal to the spectral acceleration for a response period of 0.0 second. For some structures, the spectral acceleration corresponding to the fundamental period of the structure can be applied as pseudo-static loading; however, for embankment dams, the primary use of spectral-acceleration hazard for periods other than 0.0 second is in selecting ground motions for detailed response or deformation analysis. Refer to appendix A for further explanation.

- Uniform-hazard response spectra (UHS), showing the spectral accelerations associated with a given exceedance frequency, plotted as a function of oscillator period. For embankment dams, their primary use is in selecting ground-motion time histories for dynamic response and deformation analysis.

- Earthquake ground-motion time histories. Appropriate records for a given structure and type of analysis are selected by comparison of the acceleration response spectrum with the UHS for the oscillation periods of greatest importance, the duration, and time histories of velocity and displacement, all of which are interrelated.

There is no simple rule for deciding which seismotectonic studies are needed, *a priori*, that is, without having already performed some basic evaluation of the dam and its foundation. It depends on the nature of the dam, its foundation, and appurtenant structures, the level of seismicity at the site, and the potential consequences of damage or failure of the dam. At minimum, one should examine the site geology, previous analyses, and the most recent Comprehensive Review (CR).

13.4   Investigations of Embankment and Foundation Materials

13.4.1 Phased Exploration Philosophy

An investigation program is required to determine the mechanical properties of the dam and its foundation. At the beginning of the investigation, very general questions are considered, such as "Could the embankment or the foundation soil be liquefied by plausible earthquakes?" Then, as the investigation proceeds, the questions become more specific, such as "At a depth of 27 feet, what does the cone penetrometer test indicate about the density of the foundation alluvium?" It is generally most cost-effective to conduct a phased investigation, beginning with information already available (construction and instrumentation records, reports of previous investigations), then proceeding to gather general information (surface geology, topography), and, finally, to collecting more specific data (penetration

resistance, laboratory testing, etc.). The more general information helps one determine the specific questions that need to be answered in order to answer the general question of the dam's safety against earthquake loading. Drilling, in situ testing, and laboratory work are costly, so they should be used after the data needs have been well defined from information that is already available or less expensive to obtain.

Much like developing the scope for a seismotectonic study, there are no simple rules for designing a field exploration program. If, for example, it has already been shown that modification is necessary, and the cost of the modification is not very sensitive to reasonable variation of the post-liquefaction strength of the foundation materials, there would be little justification for large expenditures in an effort to refine the strength estimate. In contrast, a decision to modify or not modify a structure usually involves enough difference in cost that larger investigation expenditures are warranted if there is a reasonable chance of a successful outcome, i.e., showing that a costly modification is not necessary, or that a less costly one would suffice.

13.4.2 General Sequence and Methods of Investigation

This section provides an overview of the investigation of a dam and its foundation for seismic analysis, and selection of relevant methods for a particular dam. Investigation techniques are detailed in Reclamation's *Engineering Geology Field Manual* (Reclamation, 1998, 2001).

All field and laboratory testing should comply with the most recent version of applicable standards from the American Society for Testing and Materials (ASTM). A number of these standards are cited by number and title in this chapter. The last two digits of each standard number indicate the year of the most recent version of the standard (e.g., D 7382 08 to indicate 2008). The standards are frequently updated, so there may be a newer version than what is cited here; hence, they are not referenced in the text by year of publication.

13.4.2.1 Search of Existing Information

13.4.2.1.1 File Data (Bureau of Reclamation)

This may include previous geologic or geotechnical investigations, instrumentation readings, operational records, and records from construction, including photos and geologic mapping of foundation excavations, design changes, borrow areas, and embankment compaction. In evaluating an existing dam, mapping or photographs of the prepared embankment foundation could be of great value. For Reclamation dams, likely sources would include the Dam Safety Office file station; files of the regional office, area office, and water district; and the National Archives. In particular, geologic and construction

records often reside in regional or area offices, rather than at the TSC or Dam Safety Office.

13.4.2.1.2 File Data (External)

Reclamation has some dams that were designed or constructed by others. Files of the previous owners or operators, or of design consultants, may contain valuable information on construction and operational history. Local residents and construction personnel may have valuable memories of the way things were constructed.

13.4.2.1.3 Published Data

Agency and industry publications, and technical journals and conference papers may contain information on the site, construction, operation or maintenance of the structure. State agencies or the United States Geologic Survey (USGS) may have general geologic information for the vicinity of the site.

13.4.2.2   Surface Investigations

13.4.2.2.1 Ground Reconnaissance

The investigation or design team should spend enough time at the site to become familiar with the visible features of not only the immediate site, but of the surrounding area that may be relevant (such as possible borrow areas, access for drilling, appurtenant structures, etc.) It is always helpful for the team to visit the site, because that can create a better understanding of the site than can be obtained from viewing drawings and photographs.

13.4.2.2.2 Surface Topographic and Geologic/Geotechnical Mapping

The required scales and coverage can generally be determined from available file information and the initial reconnaissance.

13.4.2.2.3 Surface Geophysics

Surface geophysics are generally limited to measurements of shear-wave velocity (V_S) by seismic refraction, Spectral Analysis of Surface Waves (SASW) (Stokoe et al., 1988), or Multi-channel Analysis of Surface Waves (MASW) (Park et al., 1999; Stokoe et al., 2004). Of these, MASW is preferred because it can better detect low-velocity layers within stiffer material. While VS can be used to predict liquefaction potential or liquefaction probability (appendix E), surface methods should not be used on their own to determine liquefaction resistance for a high-hazard dam, whether existing or proposed. They can, however, be used to supplement other types of testing, and they can be of value for interpolating VS data between locations of down-hole and cross-hole measurements, for determining gross-scale stratigraphy, and for estimating the dynamic properties of the embankment and foundation for site-response analysis.

Occasionally, use is made of surface electromagnetic tests, such as resistivity for general stratigraphy, and self-potential for identifying areas of higher water levels or higher seepage flow.

13.4.2.3   Subsurface Investigations

Subsurface investigations are described in greater detail in Chapter 12, "Foundation and Earth Materials Investigation," *of Design Standard No. 13 - Embankment Dams*, as well as Reclamation's *Engineering Geology Field Manual*, Volumes I and II (Reclamation, 1998, 2001). Only brief descriptions of the various tools available are provided here. A detailed review and assessment of various methods for liquefaction potential can be found in research report DSO 07 09 (Reclamation, 2007). **One important finding of that report is that no single tool should be relied on for assessing liquefaction potential for an important structure.**

Investigations of foundation materials beneath an embankment can be expensive and difficult because they may require large drilling equipment, different drilling methods, or road construction; however, the material beneath the embankment is the most important. Drilling and testing at the toe are not, in general, sufficient to characterize materials under the slopes. In addition to potential differences in geology, some weak materials may have been removed during foundation preparation and replaced with embankment fill; other material may have consolidated or densified under the weight of the embankment. The required extent of investigation under the embankment slopes needs to be judged on the basis of how the material would affect stability or deformation, which may require some preliminary stability analysis.

13.4.2.3.1 Test Pits/Test Trenches

Test pits or trenches are generally excavated by bulldozer or backhoe or, occasionally, by hand. They allow quick, low-cost sampling and visual examination of the soil in place, in the form of relatively undisturbed block samples or highly disturbed "grab samples" of excavated material. They can be particularly useful for exposing heterogeneous soils, like alluvium, for visual study of layering and lensing, including the arrangement of any gravel and cobbles that could affect in situ test results and their interpretation. It is often possible to make in situ measurements of density and other properties. The cost of test pits or trenches increases rapidly with depth, however, and they are generally impractical for investigations more than about 20 feet below the surface. Potentially liquefiable materials occur only below the water table, and it is generally not feasible to examine them directly without dewatering. Properties of the material above the water table have been used to infer the properties of similar material below it, but the deeper material could be significantly different due to different deposition or different stress history, so caution is required.

To the extent practical, the geologists and engineers who will actually perform the analyses should be present to see the soils in place, rather than rely solely on logs and photographs by field personnel.

Tests pits create safety issues for both personnel and the dam. If personnel are to enter pits for testing or sampling, the pits must be designed in accordance with

applicable safety regulations, generally the most recent version of *Reclamation Safety and Health Standards* (Bureau of Reclamation, 2014) and the Occupational Safety and Health Administration. This may require shoring or flattened slopes. In some jurisdictions, permits are required. At the toe of a dam, test pits or other excavations have the potential to reduce the stability of a slope, or to shorten seepage paths, thus increasing the seepage gradient, or to create new seepage paths. Test pits should only be used after careful evaluation of the potential impacts on seepage and stability.

13.4.2.3.2 Electronic Cone Penetrometer Test

The Electronic Cone Penetrometer Test (CPT or ECPT) is used in seismic investigations to assess the shear strength and liquefaction resistance of foundation soils, and to help determine the stratigraphy, using empirical correlations with the tip and sleeve resistance, and with pore-water pressure response. For general information on CPT analysis and test procedures, refer to Lunne, Robertson, and Powell (1994); for its use in assessing liquefaction potential, see appendix B of this chapter. When soil conditions are suitable, CPT has several distinct advantages over most other in situ methods; these include a nearly continuous profile of measurements, almost complete standardization of equipment, and the fact that all measurements occur at the penetrometer itself, which means there is no concern about energy transfer from hammer to the rods to the tip, friction on the rods, drilling disturbance, etc., all of which complicate the interpretation of hammer-driven penetration tests (SPT, BPT, dynamic cone penetration test). Many cone penetrometers are equipped with transducers to measure pore-water pressure (u), and are referred to as the CPTu or "piezocone." This device can be used to measure in situ static pore pressure, and to estimate permeability, in addition to the tip and sleeve. Abrupt changes in pore pressure during advancement of the cone can signal changes in material type.

Although no samples are retrieved with the CPT, it is rapid and relatively inexpensive, making it attractive for inferring stratigraphy and material properties between widely spaced drill holes that include soil sampling. The CPT cannot, however, be used as a stand-alone tool for assessing foundation properties without sampling. CPT measurements in gravelly material may be invalid because of the size of the particles relative to the size of the cone, but the CPT can sometimes be pushed through gravelly material and record valid measurements below it. Therefore, the presence of gravel layers does not necessarily mean that CPT cannot be used at a site. One can also predrill holes through denser material and backfill them with loose, coarse, sand or pea gravel to provide lateral support for the CPT rods to prevent buckling in hard pushing.

Reclamation's CPT rig is equipped with a small-diameter push sampler, which, in the right conditions, can retrieve samples large enough for testing basic index properties, but too small and too disturbed for laboratory strength or consolidation testing.

The Seismic Cone Penetrometer Test (SCPT or SCPTu) is the same thing as CPT or CPTu, except that it includes accelerometers within the penetrometer, allowing downhole shear-wave velocity measurements between pushes.

13.4.2.3.3 SPT

Currently, in 2015, the SPT is the "workhorse" of liquefaction assessment in Reclamation practice, as it has been for decades. The SPT is now generally considered to be inferior to the CPT in measuring soil properties at sites where the geology is suitable for the CPT. The SPT has been in use for many years, and the profession has more experience with it than with other methods. The SPT has two major advantages over the CPT: (1) it provides a sample of the material being tested, and (2) because it is performed in a drill hole, it can be used in many locations where overly coarse or very strong material prevent the cone penetrometer from being pushed to the necessary depth. (The latter is a problem for many Reclamation dams with coarse alluvium in their foundations.) On the other hand, the SPT is less repeatable, and it is sensitive to seemingly minor changes in equipment and procedures. Because SPT results are sensitive to variations in procedure, SPTs for liquefaction assessment must be performed strictly in accordance with the standards of Reclamation and of the American Society for Testing and Materials. Procedures for analyzing liquefaction potential with the SPT are described in appendix C.

13.4.2.3.4 BPT

The BPT uses a truck-mounted, diesel pile hammer to drive 6.7-inch-diameter casing into the ground to test the density of materials that are too coarse to be tested meaningfully by the SPT or CPT. BPT requires a specialty drilling contractor, but it is relatively fast and inexpensive once the rig is on site. At present, the main use of the BPT in earthquake engineering is to estimate the equivalent SPT blow count that would have been measured if not for the effect of gravel. The result is used in determining liquefaction potential, or for other purposes, the same way that an actual SPT blow count is used. The procedures are described in appendix D. It should be noted that in very coarse materials (containing cobbles or large amounts of gravel greater than about 2 inches in diameter), the BPT may experience the same problems the SPT does with fine to medium gravels. In such cases, interpretation of equivalent SPT blow counts from BPT data may not be valid. Interpretation is made more complicated by friction on the drill string, which is simply hammered into the ground, rather than being in a drill hole of larger diameter like the SPT drill string is. There is also variation in the performance of the diesel hammer with driving resistance, altitude, throttle opening, etc. As a result, BPT-SPT correlations require some measure of the energy transferred to the drill string. (Refer to appendix D.) The BPT does not produce samples for examination or testing because the casing is driven with a plugged bit. However, the same rig can be used to drill a second hole with the bit not plugged, using compressed air to lift the cuttings into a "cyclone" for sampling. The samples are highly disturbed; small-scale stratigraphy and structure are completely lost, and sample water contents are meaningless. Even grain-size distributions can be affected. Note also that

Reclamation generally prohibits drilling with compressed air in embankment cores or transition zones because of the potential for damage.

13.4.2.3.5 Borehole Geophysics

For seismic analysis, the most important geophysical measurement is the shear-wave velocity, V_S, which provides both elastic material properties for use in dynamic response analysis and an index of liquefaction potential. V_S can be measured several different ways, including the surface measurements mentioned above; down-hole testing, with the source on the ground surface and the receiver in a drill hole; cross-hole testing, with the source in one drill hole and the receiver in another; and with the suspension logger, which contains both source and receiver on one instrument lowered into a drill hole. Appendix E describes the use of V_S in liquefaction assessment. Less commonly, other geophysical tests (e.g., electrical resistivity, natural gamma-ray intensity) are used to help correlate the stratigraphy.

13.4.2.3.6 Borehole Instrumentation

Most commonly, this is piezometers installed to measure pore-water pressure for use in liquefaction analysis. It may also include inclinometers to monitor slope movements, or settlement reference points.

13.4.2.3.7 Field Vane Shear Test

The Field Vane Shear Test (VST) is used primarily in soft to medium, saturated cohesive soils, where it can be helpful in determining peak, post-peak, and remolded strengths. These values are commonly required for estimating yield acceleration and estimating the amount of deformation an earthquake would cause. The VST is particularly good for identifying sensitive materials that could contribute to post-earthquake instability. It has also been proposed for measuring the post-liquefaction, residual undrained shear strength of nonplastic silts and silty sands, if they are sufficiently low in permeability (Charlie et al., 1995; Holzer et al., 1999). Note, however, that like laboratory strength testing, VST strength measurements cannot account for the effects of void redistribution following an earthquake or other "gross-scale" effects. Appendix F discusses soil strengths for seismic analysis, including the use of VST.

13.4.2.4 Undisturbed Samples and Laboratory Shear Testing

Some procedures for liquefaction assessment and strength measurement require undisturbed samples for laboratory testing. While no drilling method can yield samples that are truly undisturbed, plastic silty and clayey materials can often be sampled with little enough disturbance that valid laboratory tests can be performed, provided that sampling disturbance is accounted for with a procedure such as Stress History and Normalized Soil Engineering Properties (SHANSEP) (Ladd, 1991; Ladd and DeGroot, 2004). Seismic behavior of cohesive materials is discussed below, in Section 13.7, and in Appendix F, "Soil Strengths for Seismic Analysis."

In contrast, clean or silty nonplastic materials are quite difficult to sample without disturbance, and the results of undrained strength tests are quite sensitive to minor disturbance and changes in void ratio (Castro et al., 1992; Yoshimi et al., 1984). Some success has been achieved by freezing the ground prior to sampling (Sego et al., 1994). It is, however, quite expensive and can only be used in materials that are coarse and clean enough to drain freely, so that volume changes in the water, due to freezing and thawing, do not disturb the structure of the soil or affect the void ratio. Because of the care needed in drilling, the large diameter of the samples and drill holes typically required, and the complexity of testing, any program of undisturbed sampling and laboratory testing of nonplastic material is likely to be quite costly.

In addition to the disturbance issue cited above, there are other limitations on lab testing. The strain in triaxial testing is limited to about 10 percent, and the validity of the measurements tends to decline even before 10 percent is reached because of sample distortion, in contrast with much larger strains and remolding that occur in earthquake-induced deformation. Triaxial cyclic testing is more readily available than Direct Simple Shear (DSS) testing. However, the stresses and strains in DSS testing more nearly resemble those in an embankment foundation subjected to horizontal shaking, because the major principal stress is approximately vertical at the beginning of the test, and the cyclic shear strains are predominantly horizontal. In both monotonic and cyclic testing, DSS tends to give lower shear resistance than in triaxial compression (Finn et al. 1971; Seed and Peacock, 1971). Most importantly, perhaps, there is great difficulty in interpreting what the results of laboratory testing mean for field behavior. As discussed in appendix F, the behavior of liquefiable granular soils is heavily influenced by phenomena that occur on large scales and cannot be evaluated with test specimens that are only a few inches in dimension.

Laboratory vane shear testing on undisturbed samples is fast and inexpensive. It does, however, require undisturbed samples, and it is limited to cohesive materials without significant gravel or coarse sand. The measured peak strength may require empirical corrections like those used for VSTs, but this has not been checked against field performance. Regardless of sample quality, the laboratory vane should be considered an "index" of the shear strength, rather than a direct measurement, similarly to the pocket penetrometer. That is, it can be useful for comparisons among samples and to provide a general description, but it does not provide a strength value that can be relied on for analysis.

13.5   Dynamic Site Response

13.5.1 Introduction

Analysis of the dynamic response of a site may be required for several different purposes. The most common use related to embankment dams is determination of

the cyclic stresses for finding CSR for use in the Seed-Lee-Idriss empirical approach to liquefaction assessment using the SPT (Seed, 1979, 1987), updates of it, and similar methods using CPT and V_S as indices of in situ density. (These procedures are described briefly in section 13.6, and in detail in appendices B through E.) The cyclic stresses for liquefaction analysis are usually calculated by equivalent-linear response analysis, which consists of iterative linear-elastic response analyses. For each iteration, the material properties are adjusted until the results converge to a single set of output values (described below). Other uses of dynamic response analysis can include estimating dynamic loads for structures on the ground surface and predicting stress time histories for use in selecting and interpreting laboratory cyclic shear tests. Equivalent-linear response analysis does not by itself predict permanent deformation, but the output acceleration time history can be used in simplified deformation analysis by the Newmark method, and for developing acceleration time histories for deformation analysis. This section is primarily directed at determination of CSRs for liquefaction assessment, but the analytical techniques can be applied to other problems as well.

Permanent deformations can also be analyzed using nonlinear Finite-Element-Method (FEM) or Finite-Difference Method (FDM) programs such as PLAXIS and FLAC (Plaxis bv, 2014; Itasca, 2014); at present (2015), Reclamation generally uses FLAC. This can include modelling the progressive build-up of excess pore-water pressure and the resulting softening, during the course of an earthquake, although nonlinear deformation analysis can also be done with simpler models that do not actually calculate changes in pore pressure. This chapter does not cover the specifics of constitutive models or nonlinear analysis.

13.5.2   Dynamic Material Properties

In equivalent-linear response analysis, the shear modulus, G, and the damping coefficient, β, for each material are adjusted at each iteration to reflect the decrease in G that generally occurs with increasing strain. After the initial iteration, G and β for subsequent iterations are estimated as functions of the strains in the previous iteration; eventually, the strains converge. Strain softening in these analyses is typically modeled using empirical curves of G/G_{max}, where G_{max} is the shear modulus at small strains. Curves for G/G_{max} and strain-dependent damping coefficients for different materials are included with various equivalent-linear response programs commonly used by Reclamation, including the two-dimensional (2D) programs QUAD4M (Hudson et al., 1994) and QUAKE/W (Geo-Slope International, Ltd., 2014), and several versions of the one-dimensional (1D) program SHAKE (Idriss and Sun, 1992; Ordoñez, 2011). Different modulus and damping curves are needed for different material types.

Material properties for response analysis are best determined by in situ measurements of shear-wave velocity, and sampling to determine the unit weight. The small-strain shear modulus G_{max} can be calculated by:

$$G_{max} = \rho \, V_S^2 \qquad\qquad\qquad \text{Equation 1}$$

where V_s is the shear-wave velocity and ρ is the mass density in consistent units (slugs per cubic foot if V_S is in feet per second to give G in lb/ft^3; or tonne per cubic meter if V_S is in meters per second to give G in kPa). The dynamic properties can also be measured using laboratory resonant column tests (which is how most G/G_{max} relationships have been determined). G_{max} can also be measured in the laboratory with resonant column or cyclic triaxial tests, but these are not considered as reliable as field V_S used with equation 1, due in large part to sampling disturbance (Stokoe, 2004). Empirical correlations have also been proposed to predict G_{max} from SPT (Seed et al., 1986) or from CPT (Robertson and Campanella, 1983), but use of a correlation like that introduces significant uncertainty.

Shear-wave velocities for use in response or deformation analysis are NOT normalized for overburden stress the way they are when used as an index of density for liquefaction triggering analysis.

13.5.3 Seismic Loading

Dam-safety practice at the Bureau of Reclamation has changed from the conventional standards-based approach, in which dams are required to withstand the most severe loadings possible at the site without failure, to the use of probabilistic risk analysis to inform dam-safety decisions (Reclamation, 2011). It is therefore necessary to evaluate a dam's performance and its likelihood of failure under both extreme earthquakes and smaller ones. It is not unusual for the greatest contributions to the risk to result from smaller earthquakes because of their much higher probability of occurrence, even if the probability of failure is much smaller in the smaller earthquakes.

For higher level analyses, the Reclamation Seismotectonics and Geophysics Group usually provides the analysts with a Probabilistic Seismic Hazard Analysis (PSHA), and earthquake ground motions for selected return periods. The PSHA yields curves indicating the annual probability of exceedance for PHA and spectral acceleration for selected oscillation periods. For simpler seismic geotechnical analyses, this may be all the information that is required, but for more detailed analyses, the hazard curves are used to select ground motions that can be associated with a particular return period. This allows a risk estimating team to estimate the likelihood of dam failure resulting from loadings with various annual probabilities, so that an annual probability of dam failure can be calculated.

For a given earthquake scenario; i.e., a given combination of fault geometry, area of fault rupture, the values of PHA and spectral acceleration, and the ground motions vary with location relative to the dam and foundation; refer to figure 13.5.3-1. Estimates of peak ground acceleration and/or ground motions are

most often provided for a level rock outcropping or the surface of stiff soil, shown at point A in figure 13.5.3-1. However, the widely used Seed-Lee-Idriss simplified method for assessing liquefaction potential (described in later sections) requires as input the peak acceleration of the *soil* surface, at Point B, which can be slightly lower than to much higher than at Point A. The acceleration of the embankment crest, Point C, can be even higher because the shape of the embankment cross section affects the response. The simplified method was developed from 1D response analyses for level sites, so it is not strictly correct to apply it under a dam embankment. As needed, the Seismotectonics and Geophysics Group can provide hazard curves and earthquake records to represent motion at a soft soil surface (Point B), at the contact between soil and bedrock, or at a greater depth in the foundation, (Point D). One-dimensional response analysis using SHAKE or a similar program can use a record representing Point A, B, or D. FEM or FDM codes like FLAC usually require the ground motion to be put in at the base of the model, Point D. To obtain a record for Point D, usually, a rock-outcrop record (for Point A) is numerically "deconvolved" to account for the response of the material between the base elevation and the surface. Because of these differences, it is important for the engineer to clearly specify to the seismologist the desired location of the earthquake loadings, and for the seismologists to clearly identify the location to the analysts. The intended use of the loadings in analysis, and the nature of the structure being analyzed, should be communicated to the seismologists as early in the process as possible, so that the seismotectonic study can be tailored to the specific needs of the analysis.
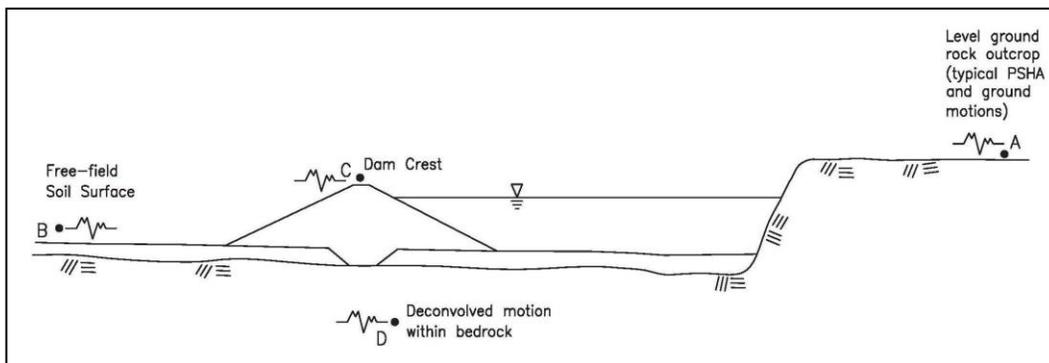
Figure 13.5.3-1. Locations requiring specific ground-motion records.

13.6   Evaluating Liquefaction Potential

13.6.1   General

The dam embankment and foundation materials must be investigated to determine their susceptibility to liquefaction under earthquake loading that could occur at the site. Soils are susceptible to liquefaction if they are saturated (or nearly so) and loose enough to be contractive under cyclic shearing. Because

water is nearly incompressible, the soil cannot contract until water is expelled from the void space. Unless the soil is highly pervious relative to the duration of the earthquake, this causes the pore-water pressure to become nearly equal to the total confining stress; that causes the effective stress and shearing resistance to both approach zero. This condition may persist after shaking ends, or it may be momentary in medium-density soils that dilate at larger strains and recover some of their shearing resistance. If the shearing resistance remains very low at large strains, there can be instability and flow, or sliding on weak layers. Low-density, nonplastic soils are the most vulnerable because fairly small, undrained strains can disrupt the intergranular contacts. The investigation should include review of available geologic, design, and construction records for the site, and laboratory and in situ testing as appropriate. Ruling out liquefaction potential requires proof that the soil is unsaturated, or sufficiently dense or sufficiently clayey that liquefaction would not occur with the earthquake being considered.

The potential for liquefaction to occur in granular soils under a given earthquake loading may be assessed by a variety of means, both indirect empirical correlations and laboratory tests that simulate the cyclic loading on the soil. In current practice, liquefaction potential is usually identified by correlations between the severity of cyclic loading and in situ tests that provide an index of density. The overall approach was pioneered by Professor Bolton Seed and coworkers at the University of California at Berkeley, beginning in the 1970s, and subsequently updated by others, most notably NCEER (1997), Cetin et al. (2004), and Idriss and Boulanger (2008, 2010). In the original work, the SPT and relative density (D_r) were used as the indices, but shear-wave velocity, V_S, and the CPT have been added.

There are other valid approaches to liquefaction assessment including, for example, liquefaction assessment based on cyclic shear strain or strain energy, rather than cyclic shear stress (Yokel et al., 1980; Liang et al., 1995; Dobry and Abdoun, 2011), laboratory cyclic testing, and sophisticated computer codes that couple the dynamic response with increases in pore pressure and deformation. Though not presently used by Reclamation, they may, with future development, prove valuable in practice, as well as provide insight into the mechanisms of liquefaction.

For liquefaction analysis, noncohesive sandlike soils are distinguished from claylike, fine-grained soils primarily by behavior, rather than by classification under the USCS. Claylike soils tend to be less vulnerable to liquefaction because, unlike clean sand, the soil skeleton can rebound elastically somewhat when disturbed, maintaining higher effective stress. In comparison with liquefying nonplastic material, plastic soils that are vulnerable to loss of strength tend to require more cyclic strain before that occurs. The behavior of the soil is governed primarily by the nature of the fines if the fines content is large enough that any sand particles are mostly "floating" in a matrix of finer material. This typically requires from about 20 percent fines with a PI greater than 12, to 35 percent

for less plastic material (Cetin et al., 2004). For soils that are classified as fine-grained (silt or clay) or that have enough fines to govern the behavior, Idriss and Boulanger (2004) made the distinction between claylike and granular behavior at a PI of 4 to 7, on the basis of consolidation and stress-strain behavior. **This is not a distinction between liquefiable material and material that would not lose very much strength from cyclic loading; it is a distinction between materials with different types of behavior, which therefore require different testing and analysis approaches.** Coarser, nonplastic silt would generally behave more like a granular soil than a cohesive, fine-grained soil. Note also that the PI is measured on the fraction of the sample passing the No. 40 U.S. standard sieve. The distinction between granular and claylike material at a PI of 4 to 7 may not hold if there is a large amount of plus-No. 40 material in the sample, and there is a "gray area" for granular soils with plastic fines. Fine-grained and plastic soils are discussed in greater detail in section 13.7, below.

When site conditions deviate from those under which an empirical procedure was developed, it may not be applicable, and other types of testing and analysis may be necessary. The available methods for assessing liquefaction potential all entail substantial uncertainty, and any of them may not work well at every site. For a high-hazard dam, it should be standard practice to use more than one method at the site to permit greater confidence in the conclusions or to help identify situations where additional investigation is needed.

13.6.2   Computing the CSR for Liquefaction Triggering Analysis

13.6.2.1   Basic Form and Equations

In most empirical methods for liquefaction assessment based on in situ tests as indices of density, the CSR is used as the measure of loading. Adjustments are made to the CSR for conditions that differ from the reference condition, which is level ground, 1 atm of effective overburden stress, and earthquake magnitude M_W, equal to 7.5. The CSR is defined as the "average" peak cyclic shear stress resulting from the earthquake on a horizontal plane, τ_{avg}, divided by the (pre-earthquake) vertical effective stress, σ_v'. For liquefaction triggering analysis, τ_{avg} is defined by an equivalent-linear analysis, assuming no generation of excess pore-water pressure, for consistency with how the correlations were developed (NCEER, 1997; Youd et al., 2001).

The CSR takes the form of:

$$\text{CSR} = \tau_{avg}/\sigma_v' = 0.65\ \tau_{max}/\sigma_v' \qquad\qquad \text{Equation 3}$$

where the peak cyclic shear stress, τ_{max}, is determined by a level of analysis appropriate to the structure and earthquake loadings, as discussed below. Because most of the cycles of shear stress caused by an earthquake have peaks smaller

than the overall maximum, the average cyclic shear stress is generally assumed to be 0.65 times the peak shear stress induced by the earthquake (Seed and Idriss, 1971). The adjustment was originally applied for comparing field performance with laboratory cyclic shear testing, so that the earthquake-induced τ_{avg} would be approximately equivalent in severity to uniform laboratory cyclic loading of τ_{max}. This remains as part of standard practice.

The preferred approach for estimating the value of τ_{max} in each stratum is equivalent-linear site-response analysis with a 1D computer program (such as SHAKE2000) or a 2D FEM program (like QUAD4M or QUAKE/W), with ground motions and soil properties selected specifically for the site. Although it is less desirable, the peak cyclic stress can also be estimated using a simplified equation that was developed from the results of numerous 1D response analyses:

$$\tau_{max} = (A_{max})(\sigma_v)r_d \qquad\qquad \text{Equation 4}$$

where A_{max} is the PHA **at the ground surface**, expressed as a fraction of earth's gravity, σ_v is the total overburden stress (which can also be thought of as the weight of the overlying soil), and r_d is an empirical "stress reduction coefficient" or "mass participation factor." Several different relationships for r_d have been proposed since the 1970s. All are equal to 1.0 at the ground surface, decreasing with depth.

It is incorrect and potentially very unconservative to use a bedrock or rock-outcrop PHA for A_{max} in the simplified equation. Therefore, if one has only rock-outcrop motions (Point A in figure 13.5.3-1) to work with, it is generally necessary to perform a dynamic response analysis to determine A_{max} at the soil surface (Point B). On level terrain, A_{max} is commonly anywhere from 80 to more than 200 percent of the rock outcrop PHA (Stewart et al., 2003; Boore, 2004). The actual ratio would depend on the frequency content of the earthquake, the shear-wave velocity profile, and the strain levels, which govern the amount of damping and shear-modulus degradation that occur in the soil. **Usually,** the surface acceleration is substantially higher than the rock-outcrop value for the same earthquake. There are also effects from the shape of the embankment, and the acceleration at the dam crest can be significantly greater than if it were a level ground surface. Unfortunately, there is no simple, precise way of estimating amplification factors, although some general trends are shown in Stewart et al. (2003). Any estimate of amplification without site-response analysis would entail rather large uncertainty.

Figure 13.6.2.1-1 (redrawn from Idriss, 1999) shows the variation of r_d with depth and earthquake magnitude for typical soil sites. It was developed by back-calculating r_d from shear stresses calculated in a large number of SHAKE91 runs with varied soil profiles and ground motions. Note that uncertainty is not portrayed; for a given soil profile and earthquake, the actual values of r_d could differ significantly from those shown in figure 13.6.2.1-1, depending on the site's

response characteristics (primarily the profile of shear-wave velocity), the frequency content of the earthquake (which is somewhat dependent on magnitude; hence, the separate curves for different magnitudes), and the amount of strain softening that occurs in each layer. (Some earlier r_d relationships included only one curve or range of curves for all magnitudes, rather than being a function of magnitude as well as depth.) Site-specific response analysis is needed if plausible variation in r_d could influence the overall outcome of the analysis, possibly including 2D analysis.
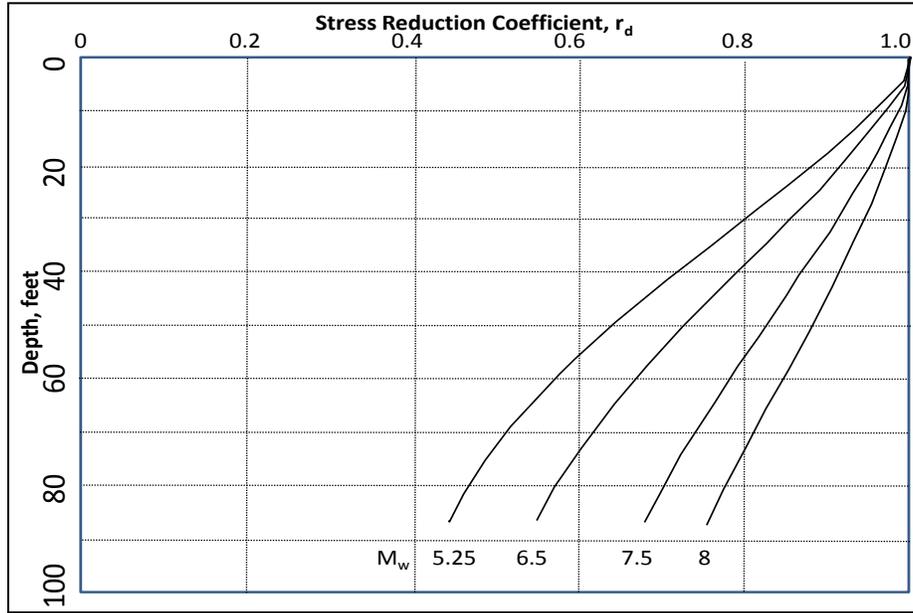
Figure 13.6.2.1-1. Stress reduction coefficient (mass participation factor), r_d, as a function of depth (based on Idriss, 1999).

For use in a spreadsheet or other computer program, the r_d curves in figure 13.6.2.1-1 can be calculated by:

$$r_d = e^{(\alpha(z) + \beta(z)M_w)}$$ Equation 5

where the depth z is in feet, M_W is the moment magnitude, and:

$$\alpha = -1.012 - 1.126 \sin(z/38.49 + 5.133)$$
$$\beta = 0.106 + 0.118 \sin(z/37.00 + 5.142)$$

The arguments of the sines are in radians.

Figure 13.6.2.1-1 does not show any variability in r_d for a given depth and magnitude, but it has been presented in other publications (Cetin et al., 2004; Kishida, 2008). Using a large set of ground motions and soil profiles (different from those used for figure 13.6.2.1-1), Cetin et al. calculated upper and lower

bounds on r_d separated by a factor of 2 or more at a depth of 100 feet. Kishida found comparable variability in a study of sites in the Sacramento-San Joaquin Delta, even with a fairly narrow range of V_s profiles. Typically, higher shear-wave velocities result in higher values of r_d at greater depths. However, the differences among Cetin et al., Kishida, and Idriss were very small in the back analyses of historic liquefaction cases because the depths were mostly less than 25 feet. Since r_d is, by definition, 1.0 at the ground surface, it is impossible for the models to differ by more than a few percent at those depths, and the effect is minor compared to the uncertainty in other parameters. In contrast, for *forward* analysis of a typical dam, the materials of greatest concern are those below 25 to 250 feet of stiff compacted fill. Both Cetin et al. and Kishida found that the range of possible values becomes very wide at greater depths, so the "actual" r_d profile for a given site and ground-motion record could differ substantially from the average values shown in figure 13.5.3-1. Uncertainty in the value of r_d becomes more important with increasing depth, and site-specific response analysis is needed for the cyclic shear stresses if the precise value could affect the overall outcome of the analysis.

Equivalent-linear analysis is called that because it is simply a linear response analysis, but with iteration and adjustment of the material properties for each layer (shear modulus and damping ratio), as functions of the peak strain in the previous iteration. This allows for strain softening, until the predicted material properties match the input properties. A single value of each parameter is used in each iteration, and the analysis does not account for progressive softening due to excess pore-water pressure or liquefaction during the course of the earthquake. Therefore, a CSR from equivalent linear analysis is less a prediction of the actual stresses than it is an easily calculated, fairly consistent "index" of loading with which liquefaction potential can be correlated.

Even though softening due to generation of excess pore pressure in liquefying layers could have a substantial effect on the actual site response, site-response analysis to find CSR for triggering correlations should generally not include it. Instead, all materials are treated as though no excess pore pressure would develop (Youd, 1997; Youd et al., 2001). The CSR is an *index* of loading severity, rather than an actual prediction of cyclic stresses. This is necessary for consistency with the way that the triggering correlations were developed, using equivalent-linear analysis, with material properties kept constant all the way through each iteration. There is an exception, however. For an embankment, 2D response analysis (using an FEM program such as QUAD4M or QUAKE/W) is generally more realistic than 1D analysis (using some version of SHAKE) and is preferred. One caution for 2D analysis is that liquefaction of one zone of the foundation or embankment could cause the cyclic shear loads to be "shed" onto other zones. This would increase the cyclic stresses on the other zones in a way that equivalent-linear analysis does not account for. If liquefaction is indicated in limited zones, and the resulting load shedding could significantly affect the CSR in other zones, it may be appropriate to rerun the analysis, with

greatly reduced stiffness for the liquefied material (keeping other materials the same). This behavior is modeled directly in nonlinear analysis (which is outside the scope of this chapter.

Equivalent-linear response analysis can be misleading if only the cyclic shear *stresses* are considered. If the calculated *strains* are high, exceeding about 0.1 percent in a soft layer (one having low shear modulus and shear-wave velocity), SHAKE (or other program) would have predicted a very large amount of strain softening. This can cause very small cyclic shear stress and CSR to be predicted under severe loading, in both the soft layer and layers above it because the soft layer cannot transmit the forces to the overlying material in the analysis. Liquefaction-triggering curves based on CSR would indicate little potential for liquefaction; however, high predicted cyclic *strains* would indicate that liquefaction is possible, or even likely, in a susceptible soil, regardless of how low the CSR is (Dobry and Abdoun, 2011). Also, if there has been that much strain softening, the assumptions of the equivalent-linear analysis have most likely been violated.

If predicted cyclic shear strains exceed 0.1 percent, liquefaction cannot be ruled out on the basis of a low CSR; liquefaction may even be likely. If the value of G_{max} or V_S is erroneously low, or if the modulus-degradation curve drops off too rapidly with increasing strain, the result would be overprediction of cyclic strains and underprediction of cyclic stresses. Softer materials may show less decrease in modulus *for a given strain* than would stiffer materials and would therefore require different modulus-degradation curves. In checking the reasonableness of results, it can be helpful to examine a stress-strain curve for the soil, to determine whether the predicted shear strain is possible with the peak shear stress predicted by the equivalent-linear analysis. Higher-level analyses may be needed.

In a 2D, equivalent-linear program like QUAD4M, strain softening could cause loads to be shed onto stiffer elements adjacent to the softest ones, compounding the effect.

The CSR should be calculated using the effective stress that would exist immediately before the earthquake, which may not be the same as its value during the in situ testing. The effective stress for CSR calculation is most commonly calculated assuming steady-state seepage with the reservoir filled to the top of active storage. For some dams, it may be reasonable to assume lower levels if steady-state seepage is not expected to ever develop. (This scenario might occur with a thick clayey core and a reservoir that is not kept full for most of the year.) In contrast, normalizing the SPT blow count, the CPT tip resistance, or the shear-wave velocity for assessing liquefaction resistance requires the piezometric conditions that existed at the time of testing.

13.6.2.2   Adjustments for "Reference" Conditions

Liquefaction triggering correlations are usually presented for standard "reference" conditions that rarely exist in dam foundations (level ground, effective overburden stress of 1.0 atm, M_W equal to 7.5). Adjustments are required for other conditions because smaller earthquakes generally produce fewer cycles of shaking than larger earthquakes do, and because a soil's susceptibility to liquefaction depends on its static stress state, along with its density and the intensity of cyclic loading. There are differences in the adjustment factors among the original Seed-Lee-Idriss procedure and the various updates, and it is preferable that each method be used as consistently as is practical with its development. Ideally, one would not, for example, use the liquefaction triggering model by Cetin et al. with the overburden adjustment from Idriss and Boulanger. However, in the back analyses of most of the historic liquefaction events, using different adjustment curves would have caused only minor differences in the back-calculated values of $CSR_{M=7.5,\sigma'=1}$ and in the outcome that would be predicted with any particular combination of $CSR_{M=7.5,\sigma'=1}$ and soil properties. In forward analysis of an embankment dam, static stress conditions are often quite different from the historic cases. Any uncertainty caused by mixing of procedures is likely overshadowed by uncertainty in the adjustment factors when large corrections are made.

For use in most empirical liquefaction procedures, adjustments must be made either to the CSR (from response analysis or equation 1), or to the cyclic *resistance* ratio, CRR, to account for loading conditions that differ from the reference conditions, which are level ground, 1 atm ≈ 1 ton/ft^2 of effective overburden stress, and an earthquake magnitude of 7.5. CRR is a property of the soil, equal to the value of CSR to which it can be subjected without the probability of liquefaction exceeding 15 percent. It is not a deterministic measurement of resistance. Adjusting the CSR gives the normalized value $CSR_{M=7.5,\sigma'=1}$, which is directly comparable with the normalized $CRR_{M=7.5,\sigma'=1}$, predicted as a function of penetration resistance or SWV, adjusted to reference conditions. This process can also be done in reverse, comparing the unadjusted CSR with the CRR that would be predicted for the actual stress conditions and M_W (rather than the reference conditions), by applying the inverses of the adjustments to the $CRR_{M=7.5,\sigma'=1}$ predicted from soil properties.

Some publications use the notation CSR* in place of $CSR_{M=7.5,\sigma'=1}$ (Cetin et al., 2004; Kayen et al., 2007). This simplification is acceptable in Reclamation reports, provided that CSR* is defined in the text. Similarly, CRR* may be used for $CRR_{M=7.5,\sigma'=1}$.

There are three main adjustment factors:

1.   Magnitude Scaling Factor (MSF) (also known as DWF, for duration-weighting factor, or simply as K_M)

2. K_α, which accounts for the effect of nonlevel ground, and

3. K_σ, which accounts for the effect of high overburden stress

More commonly, the three adjustments are considered part of the loading on the soil, as in equation 6a. In the reversed procedure, they are considered properties of the soil in situ, as in equation 6b. **For comparing loading and resistance, CSR is adjusted by equation 6a to yield $CSR_{M=7.5,\sigma'=1}$ for comparison with $CRR_{M=7.5,\sigma'=1}$ estimated from in situ testing, OR, $CRR_{M=7.5,\sigma'=1}$ is adjusted by equation 6b to obtain CRR, which is directly comparable with the unadjusted CSR. Only 6a or 6b is applied, not both.**

$$CSR_{M=7.5,\sigma'=1} = CSR / (MSF \cdot K_\alpha \cdot K_\sigma) \qquad \text{Equation 6a}$$

$$CRR = CRR_{M=7.5,\sigma'=1} \times (MSF \cdot K_\alpha \cdot K_\sigma) \qquad \text{Equation 6b}$$

At this point, the analysis of potential for liquefaction or cyclic failure of claylike soils diverges from that for granular soils. Claylike soils are covered in detail in section 13.7 below.

13.6.2.3 Adjustment of CSR for Earthquake Duration (Magnitude Scaling Factor)

Earthquakes of larger magnitudes (M) typically produce more cycles of strong motion. Typically, this ranges from about three-fourths of a cycle with a magnitude of 5.25 or less, to about 25 cycles with a magnitude of 8.5. (One full cycle would be loading to the maximum shear stress occurring once in each direction; three-fourths of a cycle corresponds to loading to the peak acceleration in one direction, and somewhat less in the other direction.) Therefore, for a given value of CSR, an earthquake of greater magnitude constitutes more severe loading, analogous to fatigue in metals. The empirical curves for liquefaction potential in appendices B, C, and E are standardized for earthquakes of magnitude 7.5; MSF is 1.0 by definition for M = 7.5, smaller for larger earthquakes, and larger for smaller earthquakes. Therefore, MSF is applied to a CSR from an earthquake of any other magnitude to obtain the equivalent $CSR_{M=7.5}$ to be used in the empirical correlations in the appendices.

The MSF is applicable primarily to liquefaction triggering analysis using equivalent-linear response analysis. In a coupled nonlinear analysis, the development of excess pore-water pressure is modeled progressively with time, so the effect of greater numbers of cycles is accounted for in the constitutive model, rather than by this separate factor. (MSF can, however, be used as an approximate check on the results of a nonlinear model.)

The effect of the number of cycles is known to be more severe in looser soils (Boulanger and Idriss, 2014). However, typical practice at present (2015) is to

assume that MSF is a function of earthquake magnitude only, which does not introduce a large amount of error.

For granular soils, the MSF is given by:

$$MSF = 6.9 \ e^{(-M/4)} -.058 \hspace{4cm} \text{Equation 7}$$

up to a maximum MSF of 1.8 for M=5.25 or smaller (Idriss, 1999). MSF decreases with increasing earthquake magnitude because soils are more prone to liquefaction with more cycles of loading. MSF is capped at 1.8 because there is no further reduction in the effective number of cycles with magnitudes below about 5.25.

Generally similar results were obtained by Cetin et al. (2004) using regression analysis of a very large number of case histories of liquefaction. The Idriss and Cetin curves are within about 10 percent of each other for magnitudes greater than 6.0. However, they diverge more at smaller magnitudes, with Cetin et al. being higher (less conservative). The difference may have resulted from the small number of case histories in the data base with smaller magnitudes (less than 6.0), which may not have been sufficient to constrain the regression results for lower magnitudes.

In addition to earthquake magnitude, the number of cycles of loading is also affected somewhat by distance from the earthquake source, tending to increase with increasing distance (while the peak acceleration decreases with distance). There are also sites, such as Mexico City and Jackson Lake Dam in Wyoming, that tend to continue to vibrate or "ring" for a long time after the shock wave from the fault has passed because of the effect of a basin full of softer material surrounded by stiffer bedrock. These effects are not explicitly accounted for in current procedures. There are, however, a very small number of sites where ringing or a very long subduction earthquake could produce an atypically large number of cycles, requiring a lower value of MSF (indicating a higher value of $CSR_{M=7.5,\sigma'=1}$), rather than simply using equation 7. This would require counting of cycles in site-specific ground motions, similar to what was done by Seed and Idriss (1982), and by Idriss (1999), in developing equation 7 and its predecessors. (For a description, refer to Idriss and Boulanger, 2008.)

13.6.2.4 Adjustment of CSR for Effective Overburden Stress (K_σ)

Soils under higher confining stresses are, for a given relative density (D_r), more prone to exhibit the contractive behavior that causes liquefaction than the same material at lower confining stresses. **The detrimental effect of high effective overburden stress on liquefaction resistance must therefore be accounted for by the factor K_σ.** Most empirical liquefaction procedures were developed primarily from case histories with pre-earthquake vertical effective stresses less than, or only a little more than, 1 atm ($\approx$1 ton per square foot). Large embankment dams may exert 10 times that amount. K_σ was not actually included

in the original studies of liquefaction potential. It was developed subsequently, based primarily on laboratory testing, to extend the correlations to greater depths (Seed et al., 1983; Hynes and Olsen, 1999; Youd et al., 2001). Originally, it was, by definition, exactly 1.0 for any effective overburden stress up to 1 ton per square foot. Now, it is considered to be exactly 1.0 with an effective overburden stress of 1 atm, and greater than 1.0 with overburden less than 1 atm, providing a small beneficial effect by reducing the value of $CSR_{M=7.5, \sigma'=1}$ at shallow depths (Cetin et al., 2004; Idriss and Boulanger, 2008, 2010). The use of K_σ is, therefore, required for both low and high effective overburden, in both forward analysis and back analysis. However, values of K_σ greater than 1.0 are seldom of consequence for an embankment dam, because the effective overburden is generally much higher than 1 atm. The Boulanger (2003b) K_σ relationship was based on a combination of theory and laboratory cyclic shear testing at a wide range of confining stresses. In contrast, Cetin et al. (2004) included effective overburden as one of the independent variables in a regression analysis; therefore, K_σ effects are built into the Cetin correlation, instead of being applied to CRR or CSR as a separate adjustment. The two K_σ relationships diverge rapidly from each other with increasing overburden stress, with Cetin's being about 20 percent lower (more conservative) at 2 atm (beyond which Cetin et al. do not recommend using it, because of the lack of supporting field data).

Figure 13.6.2.4-1 provides values of Kσ as a function of both effective overburden and the density of the soil, as indicated by SPT or CPT.
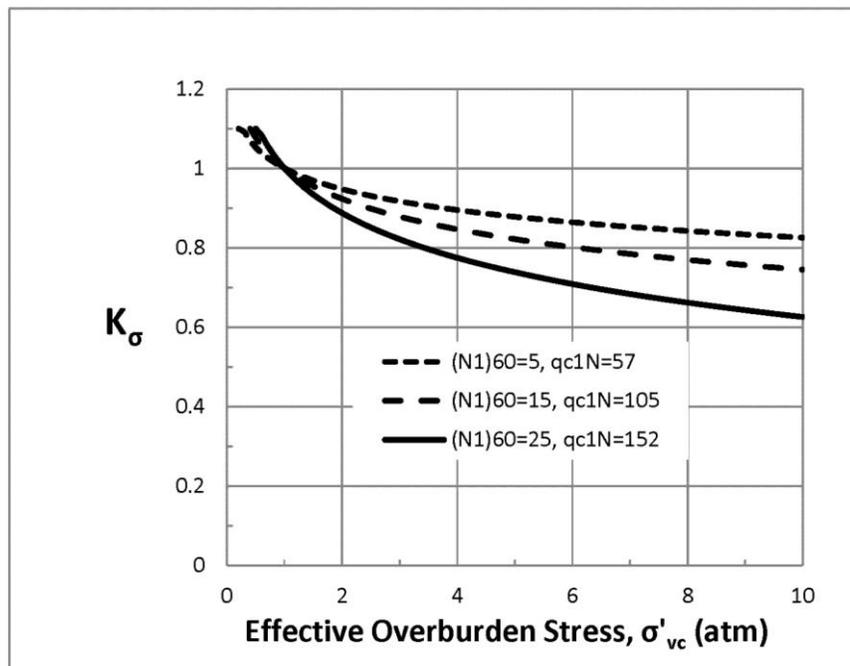

Figure 13.6.2.4-1. K$_\sigma$ relationship to account for effect of vertical effective stress on liquefaction triggering, based on Boulanger and Idriss (2004).

For use in a spreadsheet or other computer program, the value of K_σ can be calculated with equation 8a and 8b, 8c, or 8d:

$$K_\sigma = 1 - C_\sigma \ln\left(\frac{\sigma'_{vc}}{P_a}\right) \le 1.1 \hspace{3cm} \text{Equation 8a}$$

where

$$C_\sigma = \frac{1}{18.9 - 17.3 D_R} \le 0.3 \hspace{3cm} \text{Equation 8b}$$

$$C_\sigma = \frac{1}{18.9 - 2.55\sqrt{(N_1)_{60}}} \le 0.3 \hspace{3cm} \text{Equation 8c}$$

$$C_\sigma = \frac{1}{37.3 - 8.27(q_{c1N})^{0.264}} \le 0.3 \hspace{3cm} \text{Equation 8d}$$

in which P_A is atmospheric pressure, $(N_1)_{60}$ is the normalized SPT blow count, and q_{c1N} is the normalized CPT tip resistance. Refer to appendices C and B for determination of $(N_1)_{60}$ and q_{c1N}, respectively.

With low overburden pressure, K_σ is not allowed to exceed 1.1 in the liquefaction triggering methods of Idriss and Boulanger (2008, 2010), or 1.3 using Cetin et al. (2004) or Moss et al. (2006). Again, the difference here is fairly minor in the back analysis of historic liquefaction cases, and the upper bound on K_σ is unlikely to appear in forward analysis of an embankment dam or its foundation, because the effective overburden pressure is generally much higher than 1 atm.

In critical cases; i.e., those where a major decision depends on the precise value of K_α and/or K_σ, laboratory testing to determine site-specific values may be appropriate, instead of the chart and empirical equations.

For most projects, values of K_σ from figure 13.6.2.4-1 or equation 8a (which are equivalent) are sufficient. However, to some extent, the value is material-specific, in addition to being governed by σ' and density. Montgomery et al. (2013) reevaluated the available lab data, including removing data from clayey soils and dense sands, because they are not very relevant to sand liquefaction. They found that the relationship shown in figure 13.6.2.4-1 is reasonable to use for clean sands. The picture is less clear for silty sands. Figure 13.6.2.4-1 and equation 8a may be slightly unconservative, although that could be offset by the effect of fines in the procedure for adjusting penetration resistance (SPT and CPT) for overburden. The error in using them for silty sand is, therefore, likely to be minor. Montgomery et al. found that the widely used NCEER relationship (NCEER, 1997; Youd et al., 2001) is somewhat conservative when applied to sand. For unusual materials, it may be more appropriate to use laboratory cyclic shear testing (triaxial or simple shear) to develop material-specific K_σ, if a major decision rests on the precise value, so that the potential cost savings from higher (less conservative) values for K_σ might

offset the additional cost. Because soil fabric is likely to affect the value of K_σ, undisturbed samples are preferred for lab testing.

The value of σ_v' and, therefore, the value of K_σ depend on the piezometric conditions. The vertical effective stress for determining K_σ should be determined from the piezometric conditions that will be *assumed for the time of the earthquake,* typically steady-state seepage with the reservoir at the top of active storage, not the piezometric level at the time of exploration, which may be different.

Similar to the magnitude scaling factor, the effect of K_σ is computed directly in a coupled nonlinear analysis, but K_σ can be of value as an approximate check on the nonlinear model.

13.6.2.5 Adjustment of CSR for Horizontal Shear Stress in Nonlevel Ground (K_α)

The empirical relationships for liquefaction resistance were based entirely on data from sites that are nearly level, where the shear stress on horizontal planes was, therefore, nearly zero. Laboratory cyclic shear tests show that liquefaction resistance varies with the amount of static shear or deviator stress on the material before the cyclic loading is applied. For denser materials, particularly under low overburden stress, the testing shows substantial benefit from the static shear stress, whereas the liquefaction resistance of loose materials is generally reduced. In medium-dense to dense soils, the "prestress" helps by preventing or reducing reversals in the direction of the shear stress. In loose soils, the prestress is harmful to the cyclic resistance because it causes the in situ stresses to be closer to the undrained yield strength. The effect of nonlevel ground on liquefaction potential should be accounted for by the factor K_α, but cautiously.

The coefficient α is the ratio of the static shear stress on the horizontal plane, τ_s, to the pre-earthquake effective overburden stress, σ_{vc}'. The determination of τ_s would generally require static FEM modeling. K_α is a function of α, but also of the effective overburden stress and the soil's density (as indicated by the normalized SPT blow count $(N_1)_{60}$ or the normalized CPT tip resistance, q_{c1N}). Figure 13.6.2.5-1, from Idriss and Boulanger (2008), provides estimates of K_α for granular soils.

Figure 13.6.2.5-1 has two separate plots, one for pre-earthquake effective overburden stress of 1 atmosphere (approximately 1 ton per square foot), and one for 4 atm. The two are only slightly different for blow counts $(N_1)_{60CS}$ less than 12, but the difference is significant for higher blow counts. Increasing overburden stress causes the curves to be rotated downward, giving lower K_α values. The right-hand plot shows that, with 4 atm of effective overburden stress, the division between benefit and harm from K_α occurs at a normalized SPT blow count of about 14, or normalized CPT tip resistance of about 100. Under a large

embankment dam, the effective overburden stress could be much higher than 4 atm, which would cause further downward rotation of the curves.
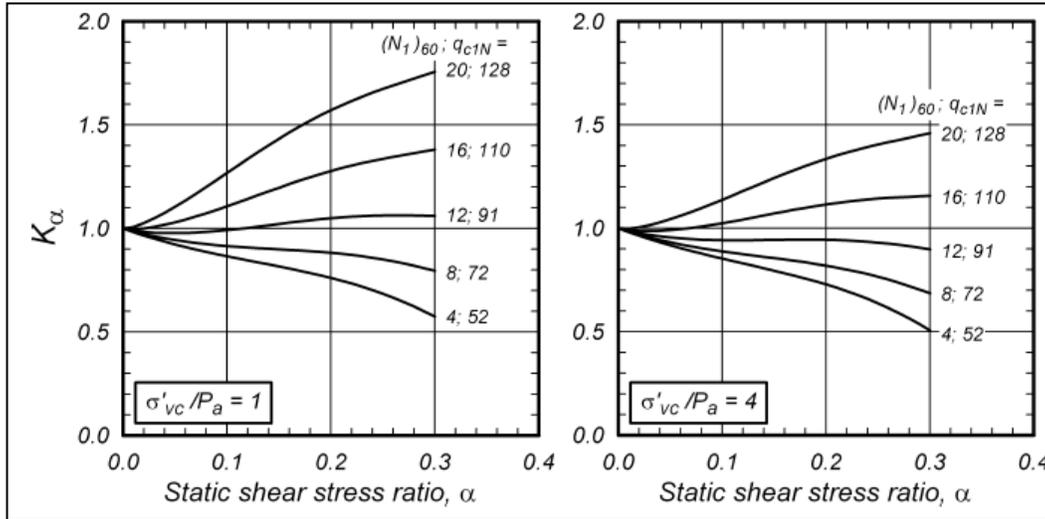
 Figure 13.6.2.5-1. K$_\alpha$ as a function of penetration resistance and in situ stress conditions. Note that curves for 4 atm are rotated downward from curves for 1 atm. Effective overburden stress greater than 4 atm would cause further rotation (Idriss and Boulanger, 2003, 2008).

Idriss and Boulanger (2003a, 2008) also present empirical equations for K$_\alpha$ that can be programmed in a spreadsheet or dedicated program; these are shown below as equation 9a through 9j. Because of the complexity of the equations, it may be easier to pick values from figure 13.6.2.1-1, unless a very large number of data are to be analyzed.

$$K_\alpha = a + b \cdot exp\left(\frac{-\xi_R}{c}\right) \qquad\qquad \text{Equation 9a}$$

where

$$a = 1267 + 636\alpha^2 - 634exp(\alpha) - 632 \cdot exp(-\alpha) \qquad \text{Equation 9b}$$

$$b = exp(-1.11 + 12.3\alpha^2 + 1.31 \cdot \ln(\alpha + 0.0001)) \qquad \text{Equation 9c}$$

$$c = 0.138 + 0.126\alpha + 2.52\alpha^3 \qquad \text{Equation 9d}$$

$$\alpha = \frac{\tau_s}{\sigma'_{vc}} \qquad\qquad \text{Equation 9e}$$

$$\xi_R = \frac{1}{Q - \ln\left(\frac{100(1+2K_0)\sigma'_{vc}}{3P_a}\right)} - \sqrt{\frac{(N_1)_{60}}{46}} \qquad \text{Equation 9f}$$

$$\xi_R = \frac{1}{Q - \ln\left(\frac{100(1 + 2K_0)\sigma'_{vc}}{3P_a}\right)} - (0.478(q_{c1N})^{0.264} - 1.063) \qquad \text{Equation 9g}$$

The authors state that this equation empirical equation is limited specific values of q_{c1N}, α, and ξ_R:

$$q_{c1N} \geq 21 \qquad \qquad \text{Equation 9h}$$

$$\alpha \leq 0.35 \qquad \qquad \text{Equation 9i}$$

$$-0.6 \leq \xi_R \geq 0.1 \qquad \qquad \text{Equation 9j}$$

The curves and equations for predicting K_α were developed from cyclic triaxial and direct-simple-shear testing with varying levels of static shear prestress applied before the cyclic shear stress. These were generally CK_0U tests with cyclic loading centered about the K_0 condition, and cyclic direct simple-shear tests with an initial horizontal shear stress. In both of these, the cyclic stress and the initial prestress were in the same direction, so the tests could not capture the effects of shaking that is not parallel with the static shear stress. The static shear stress in the foundation of a dam is ordinarily perpendicular to the axis of the dam, but the earthquake motions can occur in any direction. Boulanger and Seed (1995) showed that beneficial effect from K_α in medium-dense to dense soil is mostly lost if the cyclic stress is not parallel with the static shear stress. (For combinations of density and static prestress, where figure 13.6.2.5-1 predicts K_α to be less than 1.0, there is little effect.) Similar results were obtained by Kammerer et al. (2004) in a subsequent study that included cyclic loading occurring in multiple directions within one test, more like in an actual earthquake. This suggests that, unless the dam was constructed in a narrow canyon that would prevent strain in the cross-valley direction, K_α could be significantly lower than what is shown in figure 13.6.2.5-1. **Until this issue is better resolved, skepticism is warranted regarding the beneficial effects from K_α in high-density soils, whereas detrimental effects in loose materials appear to be very likely.** In risk analysis, it may be appropriate to consider some *probability* (not *certainty*) of benefit from K_α; i.e., $K_\alpha > 1$, in estimating liquefaction probability.

For determining K_α, α should be calculated for the seepage and reservoir loading conditions that would exist immediately prior to the earthquake, usually steady-state seepage with the reservoir at the top of active storage. The seepage forces in an embankment influence the horizontal shear stress and the effective vertical confining pressure.

In the special case of a normalized blow count of 13 to 16, or normalized CPT tip resistance of 95 to 110, K_α is approximately 1.0 for all values of α, which is sometimes convenient. For higher blow counts, a component of shaking perpendicular to the static shear stress may reduce the value of K_α to

approximately 1.0. In such cases, K_α can be assumed equal to 1.0, with little loss of accuracy, thereby saving the effort of FEM analyses to find the static shear stresses. This cannot be done with lower blow counts, or with much higher overburden stresses, which would cause the curves on the right-hand portion of figure 13.6.2.5-1to be rotated downward.

Similar to MSF and K_σ, K_α is directly applicable only in simplified liquefaction analysis based on equivalent-linear response analysis. A coupled nonlinear analysis would account for K_α effects directly, but published relationships for K_α can provide an approximate check on the nonlinear model. As in the case of K_σ, site-specific laboratory cyclic triaxial or simple shear testing may occasionally be helpful for determining K_α., although neither can account for the effect of nonparallel shaking, for which specialized equipment is required.

13.6.3   Appropriate Level of Analysis for τ_{max} and CSR

Cyclic stress ratios can be estimated by several different means, as described above. The appropriate level of effort for estimation of the CSRs must be judged for each application, considering the validity of the assumptions of each approach, the cost of analysis, and the likelihood and consequences of making a biased determination from simpler analyses.

The actual PHA or spectral acceleration at the ground surface can be anywhere from 0.7 to 3 times the acceleration at a rock outcrop (Stewart et al., 2003).

It is relatively easy to implement 1D site response with some version of the program SHAKE, which models the soil profile as a stack of shear beams of varying stiffness. ("SHAKE" is used here to refer to all versions, including: SHAKE91, [Idriss and Sun, 1992]; SHAKE96, which is identical, except for having larger arrays to allow longer earthquake records; or the newer SHAKE2000 [Ordoñez, 2011].) The earthquake record can be put into the soil column at any location, so it can be used with a soil-surface record, a bedrock record (at depth), or a rock-outcrop record. Strictly speaking, SHAKE is only applicable to level ground, and it tends to underestimate the acceleration and shear stresses near the crest and upper surfaces of dam embankments. Hence, it would not generally be appropriate for assessing the liquefaction potential of hydraulic fill embankments. However, in dam foundations, the results are in reasonable agreement with those from 2D analysis, and SHAKE can be used for preliminary assessments of liquefaction potential (although K_α effects need to be accounted for). If the calculated CSR from the earthquake is obviously much higher or lower than the CRR, it may not be necessary to pursue further analysis because there will be a clear answer. SHAKE is also a quick, inexpensive tool for studying the sensitivity of the cyclic stresses to changes in earthquake record or soil properties. As with 2D FEM analysis, the peak cyclic shear stress from SHAKE is used in equation 3 for each layer.

As discussed above, SHAKE and the simplified equation with r_d (equation 4) would not be appropriate for assessing the liquefaction potential of a dam embankment (except, perhaps, for preliminary studies) because they are 1D analyses and do not correctly model the response of the upper part of the embankment. Even for level ground, equation 4 may not be appropriate for unusual sites with ground motions or soil profiles that differ substantially from the typical sites on which the r_d curves are based. There, SHAKE would be preferable because it can explicitly account for the soil profile and the characteristics of the ground motion.

More correct but more labor-intensive, is the use of a 2D, FEM code such as QUAD4M (Hudson et al., 1994) or QUAKE/W (Geo-Slope International, 2014) with earthquake records that are specifically selected for the site. The peak shear stress from this analysis, τ_{max}, would be used in equation 3.

With either 1D or 2D equivalent-linear analysis, misleading results can occur because of extreme strain softening being predicted in soft layers. The predicted cyclic strains must be examined to determine whether they are high enough to cause liquefaction, even if the cyclic shear stress from equivalent-linear analysis is predicted to be low because of major strain softening. **A low CSR from equivalent-linear analysis does not actually indicate that there is no potential for liquefaction if it is accompanied by large strains.** This is a limitation of the equivalent-linear methodology. Liquefaction can occur in loose soils with cyclic shear strains less than 0.1 percent, regardless of what cyclic stresses are predicted by SHAKE (Dobry and Abdoun, 2011).

As discussed above, the simplified equation for CSR requires the *soil-surface* PHA and r_d from either figure 13.6.2.1-1 or equation 5. If the soil-surface PHA has not been provided but ground-motion records are available for a bedrock outcrop, it can be found using SHAKE. However, in equation 3, it is preferable to use the peak shear stresses from SHAKE, using actual soil properties and earthquake records selected specifically for the site, rather than introduce the uncertainty inherent in r_d. (The relationships for r_d were developed from a large number of SHAKE analyses using a wide range of soil profiles and earthquake ground motions that may not be appropriate for the site being analyzed. Unfortunately, A_{max} amplification ratios are not easily determined without a response analysis.

Originally, the factors MSF, K_α, and K_σ were considered to be adjustments to the CRR of the soil as indicated by testing, rather than adjustments to the CSR that would be imposed by the earthquake loading (Seed and Idriss, 1982). (Again, CRR is simply the maximum CSR to which the soil could be subjected to without the probability of liquefaction exceeding 15 percent. It is also referred to as CSR_L in some publications.) Thus, rather than dividing the CSR by those factors, as described above, the CRR is multiplied by them. The net effect in the analysis is the same. For this document, MSF was associated with the CSR because the

magnitude, like the PHA, is a component of the earthquake loading, not a soil property. (K_α and K_σ are kept with MSF, both for convenience and because they represent the effects of loads on the soil, rather than properties of the soil.) This way, different earthquakes can be evaluated with changes made only in $CSR_{7.5}$ and the determination of the minimum soil properties required to resist liquefaction, rather than redetermining CRR for each SPT interval for each earthquake. MSF is, in fact, a function of both M_W and soil properties, but the error introduced by making it solely a function of M_W is relatively minor.

How should the CSR be determined? In general, dynamic response analysis is preferred over the simplified equation using r_d, because response analysis is specific to the shear-wave-velocity profile at the site and ground motions specifically selected to portray the nearby seismogenic sources. In contrast, the r_d curves are averages from a larger number of 1D response analyses using SHAKE, and there is considerable variation from different ground motions and velocity profiles. It is recognized, however, that the simplified equation must be used sometimes because it requires less labor and does not require site-specific ground motions; however, if the overall result is not clear because of uncertainty in CSR, a higher level of analysis is required.

Many earlier liquefaction triggering charts were developed using a single r_d curve, but figure C4 (in appendix C) was developed using the magnitude-specific r_d by Idriss (1999), shown above as figure 13.6.2.1-1. Because the frequency content of earthquake ground motions and the amount of strain softening tend to vary with changes in earthquake magnitude, r_d also varies with magnitude and not just with depth.

The factor K_α applied to $CSR_{7.5}$ accounts for the effect of static horizontal shear stress on cyclic resistance, but it does not account for how the shape of the embankment affects the dynamic response. For that, 2D response analysis is superior and should be performed.

There are two important cautions about using equivalent-linear response analysis (such as SHAKE or QUAKE/W). First, the cyclic shear *strains* need to be checked, not just the stresses. In some cases, soft layers (having low shear-wave velocity) within stiffer material are predicted to undergo very large strain, resulting in extensive strain softening, and a predicted cyclic-stress ratio that is low enough not to indicate liquefaction with figure C4. However, if calculated cyclic strains actually exceed 0.1 percent in loose or medium-density sand, it would likely be liquefied (Dobry and Abdoun, 2011). Such large computed strains could also result from unrealistic inputs for the shear modulus at small strains and the modulus degradation at larger strains. The equivalent-linear approach uses a constant value of shear modulus for each iteration; it does not allow for progressive strain softening during the course of the earthquake. A layer could actually experience large cyclic shear stress early in the earthquake, even if extensive strain softening could occur later in the earthquake, and this

would not be apparent in the output. It may be instructive to compare the predicted stress and strain against a monotonic or cyclic laboratory stress-strain curve to see whether it is possible for that level of strain to develop without the soil having been stressed above the value predicted by SHAKE.

Second, if large strain and drastic strain softening are predicted, the response analysis may indicate a "base-isolation" effect, so that overlying layers do not appear to "feel" the strong shaking. In reality, the strain softening would not occur instantaneously (as equivalent-linear analysis assumes, in effect), so the overlying layers could actually be subject to strong motion early in the earthquake, even if the analysis doesn't show that. Again, this is a limitation of the equivalent-linear method, and it is not always possible to get realistic results from equivalent-linear analysis.

13.6.4   In-Place Density as an Indication of Liquefaction Potential

Generally, liquefiable materials are loose, noncohesive materials from fluvial and lacustrine deposition and are composed of silts, sands, and gravels. Aeolian (wind-deposited) soils like loess are also commonly quite loose and liquefiable. Fill in modern embankments is usually compacted thoroughly during placement and, therefore, would not be liquefiable; however, hydraulic fill embankments and some embankments constructed prior to the mid-1900s may not be sufficiently dense to preclude liquefaction. Some older embankments were compacted by small horse-drawn equipment, or not at all. One should consider the possibility of liquefaction of hydraulic fills, even under fairly mild earthquake loading, and of lightly compacted embankment fills under moderate to severe loading.

Usually, the density of soils is not actually determined for liquefaction assessment because of the difficulty of sampling and testing saturated noncohesive material. Instead, empirical correlations with indirect indices of density are almost always used, primarily the SPT, CPT, and V_S.

When D_r values are available, a chart by Seed and Peacock (1971), shown in figure 13.6.4-1, can provide some general guidance, although it is based on few data and relative density is not necessarily the best index of liquefaction potential. (If SPT or CPT data are available, those should take precedent over D_r.) Seed and Peacock's chart suggests that a relative density greater than about 75 percent would generally preclude liquefaction, unless the loading is unusually severe, in which case 80 to 85 percent might be required to completely preclude high excess pore-water pressure. Materials with relative densities below 50 percent are quite susceptible to liquefaction; those above 65percent would typically display cyclic mobility and limited strains, rather than flow liquefaction, unless settlement and

void redistribution after the earthquake could create a weak layer at the top of the liquefied layer. (Appendix F discusses this important phenomenon in greater detail.)
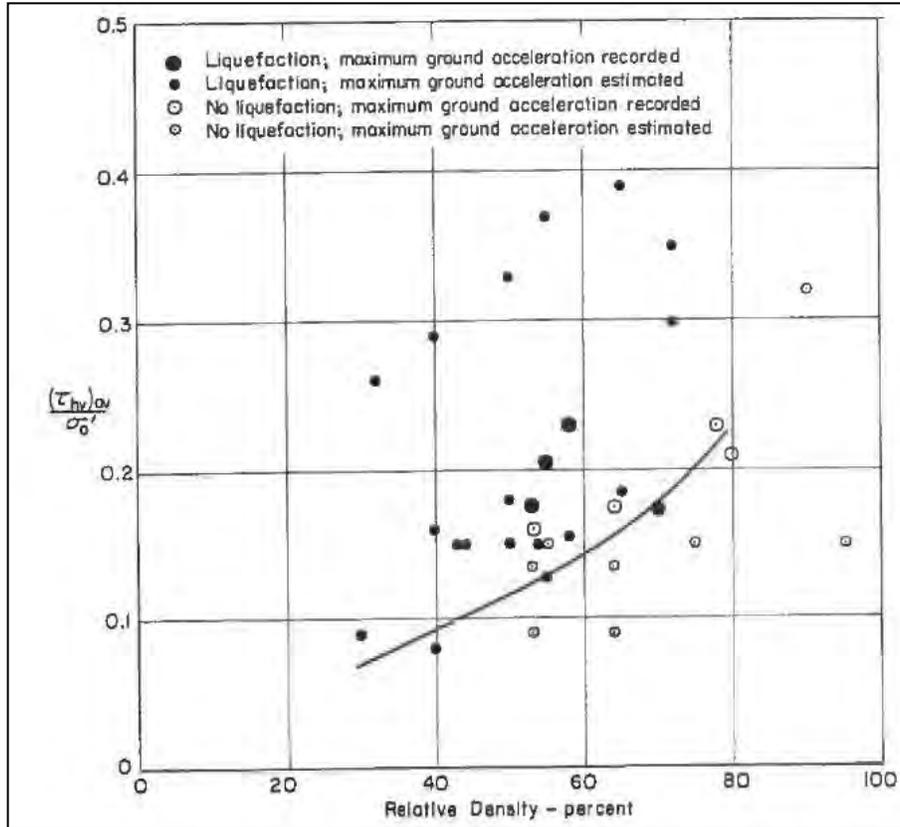
Figure 13.6.4-1. CSR and relative density of soils subjected to earthquake loading, with and without liquefaction (Seed and Peacock, 1971). Note: $(\tau_{hv})_{av} / \sigma'_o$ is equivalent to $0.65\, \tau_{max} / \sigma'_v$.

Relative-density determinations depend on three different measurements (laboratory minimum, laboratory maximum, and in situ density), each of which is subject to error and variability. Determining the in situ density can be difficult, especially below the water table where it may not even be feasible, and measuring the laboratory minimum density is quite sensitive to technique. The relative density test was developed in the 1940s but was not standardized until the 1960s. Hence, some of the data used to develop figure 13.6.4-1 (published in 1971) may not have been determined by the methods that are now standard. The minimum density requires careful loose placement of soil into a mold of known volume by hand (ASTM D 4254 00). The maximum density can be determined by either a mold on a vibrating table (ASTM D 4253 00) or with a vibratory hammer to compact the soil in a mold (ASTM D 7382 08). The vibrating table must be properly calibrated; problems have occurred when it was not done. Although the calibration of Reclamation's tables is checked regularly, that does not always occur in private labs and other government labs. Reclamation usually obtains

maximum densities with the vibratory hammer test, with designation
ASTM D 7382 08. It sometimes yields maximum densities that are higher than
those from the vibratory table, so the relative density calculated from an in situ
density would be slightly lower than if the conventional vibratory table is used for
the maximum.

The determination of in situ density at depth can be rather difficult. It is well
established that piston samplers tend to cause volume changes in clean sands
during insertion. Loose sands tend to densify, while dense sands tend to loosen.
The only reliable method for sampling clean sands with less than 10 percent fines
is to freeze the deposit and cut cores of the frozen material. An application of this
method is described by Sego et al. (1994). Silty sands and silts (SM and ML) are
usually easier to sample and less subject to disturbance from thin-wall tube or
piston sampling, especially if they are slightly plastic and cohesive. This is
because these soils are approximately undrained during the sampling process, due
to their lower permeability. If the fines content is 20 percent or greater, one can
usually assume undrained behavior during sampling. Tube sample density
measurements are possible, with large-diameter tubes being preferred. Often,
silty sand can be sampled with simple thin-wall tube samplers because there is
sufficient cohesion to hold the soil in the tube. However, it is recommended that
a piston sampler (such as the Osterberg type) be used. Tube samples can be
X-rayed to evaluate layering before they are extruded from the tubes. The
samples should be shipped vertically, with vibrations kept to a minimum,
although changes in density can occur even with the most careful handling.
Allowing drainage of nonplastic tube samples before they are shipped would
change the moisture content, but it can impart a small negative pore-water
pressure (capillarity) that helps keep the sample intact. Hand-carved cylindrical
undisturbed samples have been obtained in open excavation and can yield
excellent undisturbed specimens for cyclic triaxial testing, provided that the
materials that are sufficiently fine-grained and near enough to the ground surface
for access in open excavation.

The in situ density of near-surface material can often be measured using
sand-cone density tests, following ASTM D 1556 07, or in small test pits whose
volume is measured by replacement with sand of known density or with water,
following ASTM standard D 4914 08 or D 5030/5030M 13a. In some cases, the
foundation alluvium may be accessible downstream of the dam, where test pits
can be excavated easily above the water table. The test standards provide criteria
for sand-cone and test-pit size as a function of the size of the particles. The
criteria are based on obtaining a representative sample of sufficient size for index
testing, and making the pit large enough that . In studies of density of natural
deposits, such as alluvium, it is important to obtain a good number of tests for
statistical evaluation because of potential errors in testing and the inherent natural
variability of the deposits. In many cases, it is difficult to gain access to deposits;
expensive, steel-cased, caisson-type shafts would be required. These
measurements have been performed at Jackson Lake Dam (Miedema and

Farrar, 1988) and Mormon Island Auxiliary Dam (Hynes-Griffin, 1987). If measurements are to be performed in test pits or shafts, size requirements and Occupational Safety and Health Administration (OSHA) confined-space safety requirements, such as ventilation, must be planned in advance.

Layering is a major problem with in situ density measurement. Most alluvial soils and hydraulic fills are deposited in layers of fairly uniform particle diameters with varying thicknesses. If the maximum density test mixes layers, the calculated relative density will be erroneously low. This is because combining multiple uniform layers into one laboratory sample results in a more widely graded mixture with higher minimum and maximum densities. Occasionally, this leads to calculated relative densities of zero or less.. To avoid these problems, extra care should be taken in the field investigation to confine density measurements to individual layers. In addition, because these errors cannot always be avoided, there should be a good number of tests from which to evaluate in situ densities. It is difficult to create materials with relative densities of 20 percent or less (except small laboratory-scale placements), and measured values that low can generally be assumed to be invalid due to mixing of layers.

Similar difficulties can arise when trying to characterize the density of material containing large particles. While the actual in situ density of such materials can be measured by large-diameter ring-density tests instead of the usual sand cone tests, these tests are more likely to be affected by layers of differing density, and there is no simple way to compare the measured density with a reference density, such as the laboratory maximum. When the oversized material is a small fraction of the total, it is common practice to simply subtract off the weight and volume of oversized particles and calculate the density of the remaining "matrix" material; the result is then compared with minimum and maximum densities measured on the matrix with the oversized particles removed. This procedure can produce approximately valid results when the oversized fraction is small, but not if it is large. Under a given compactive effort, the matrix does not become as dense adjacent to the surfaces of the oversized particles as it does when no oversized material is present. With large amounts of oversized material, it may be necessary to run a series of laboratory density tests with varying amounts of smaller oversized particles to establish a trend that can be projected for the whole material gradation.

In wet or saturated soils containing fines, measures must be taken to avoid squeezing of the test hole during sand cone or test pit tests. These measures may include the use of wood cribbing to support the weight of the technician and/or the backhoe, and ensuring that the sides of the pit are stable. Severe squeezing of the hole is indicated by abnormally high values of relative density or computed degree of saturation, but a small amount of squeezing could be difficult to detect from the appearance of the excavation. Very little squeezing would be needed to increase the measured relative density by 10 or 20 percentage points above its true value.

For soils containing fines in excess of about 10 to 15 percent, the relative density test cannot be performed, and Proctor-type impact compaction tests are required instead (ASTM D 698 12). No liquefaction criteria have been published based on the relative compaction (RC), equal to the in situ density divided by the laboratory maximum density, expressed as a percentage. However, for a preliminary assessment of liquefaction potential of sandy soils, an estimate of the equivalent relative density can be obtained from equation 10, from Lee and Singh (1971). Equation 10 is a correlation between relative compaction and relative density in soils where both D_r and RC are valid.

$$RC = 80 + 0.2 \, D_r \hspace{4cm} \text{Equation 10}$$

Combining equation 10 and figure 13.6.4-1, soils with relative compaction less than 90 percent would be quite vulnerable to liquefaction, and liquefaction would be unlikely for soils much over 95 percent of their laboratory maximum density. Neither equation 10 nor figure 13.6.4-1 is a particularly tight correlation, so this range should only be considered a general indication, not a criterion. When greater certainty is needed, additional tests should be performed to further evaluate liquefaction resistance.

13.6.5 SPT for Assessing Liquefaction Potential and Liquefaction Probability

The standard penetration test (SPT) is currently the most used means of assessing liquefaction potential in Reclamation's practice. The test consists of using a 140-pound drop hammer to drive a split-barrel sampler in a drillhole and recording N, the number of 30-inch drops of the hammer to drive the sampler 1 foot. Once the blow counts have been recorded, they are adjusted to standard test conditions, so that they can be compared with an empirical correlation for liquefaction potential (or liquefaction probability). **Reclamation and ASTM standard procedures must be followed, most importantly ASTM D 6066 11 for test procedures, and Reclamation's policy and dam-safety requirements for drilling in embankments.** These includes requirements for:

- Sufficient depth of drilling fluid or water in the drill holes to minimize heave or loosening of the bottom of the hole

- Controlled rate of removal of samplers and bits to avoid creating suction that would cause heave

- Measurements of the energy imparted to the rods by each drop hammer

- Avoiding hydraulic fracturing by excessively high fluid pressure

Appendix C describes the procedures for adjusting the test data and assessing liquefaction potential using the SPT. They were developed primarily by the late

Professor Bolton Seed and coworkers at the University of California at Berkeley (Seed et al., 1985), with refinements added by later investigators. The SPT liquefaction procedures are primarily applicable to cohesionless, clean sands and silty sands. They may be unnecessarily conservative if applied to materials with PIs exceeding 5 to 10, it is not clear to what extent (NCEER, 1997). Thus, as currently formulated, the SPT interpretation can be used to show that there is low likelihood of liquefaction in more plastic soils, but it would not conclusively indicate high likelihood.

Interpretation of SPT data can be quite complex, especially when the test conditions differ from standard conditions used to develop the correlations. The results of the test are strongly influenced by the presence of gravel, the design of the hammer, the depth of testing, and many other factors. Empirical adjustments or corrections have been developed to account for many of these factors, but there remains a substantial amount of uncertainty in the results. The energy from the hammer blow is transmitted to the sampler by a wave of compression traveling down the rods, and energy can be lost to friction, loose rod connections, etc. At very small or very large depths, the energy actually imparted to the sampler can be much smaller than what occurs at the intermediate depths from which the liquefaction correlation was primarily developed. For gravelly conditions or depths less than 10 feet, other investigative tools may be more appropriate than the SPT.

The procedure for assessing liquefaction potential with SPT data may be summarized as follows:

1. Obtain SPT data (N, drill logs) and soil samples in accordance with current Reclamation and ASTM standards.

2. Adjust each measured SPT N value to standard conditions (as described in appendix C), including hammer energy, effective overburden stress, nonstandard equipment or procedures (best avoided so no adjustment is needed), fines content, and possible interference from cobbles or gravel too coarse for meaningful testing.

3. Calculate the CSRs induced in each layer by each earthquake under consideration, then adjust them for magnitude and in situ static stress conditions as described above.

4. Use empirical curves or equations in appendix C to estimate the probability that each interval would be liquefied by the earthquake.

5. Present and evaluate results. The complete set of data and results should be presented in tabular form. For ease of interpretation, the data should also be presented on geologic cross sections to aid in inferring soil-mass characteristics from point data of index properties and density.

In soil that could contain gravel or cobbles, SPT blow counts are commonly recorded for each 0.1 foot of penetration, or as the cumulative penetration after each blow. This can help one to detect and adjust for gravel interfering with penetration, which would increase the blow count above what "should" be measured if there were no gravel interference. On a plot of cumulative blow count *versus* depth, an abrupt increase in slope may indicate that the sampler has reached gravelly material, in which case the blow count may not be meaningful. However, the absence of an abrupt change does not necessarily mean that there is no gravel interference because the whole test interval could have been affected. Blow counts need to be evaluated with close attention to recovery percentages and material descriptions from the field and laboratory. Even if there is no concern about gravel at a particular site, it is a good idea to look for changes in slope because that can aid in understanding the layering within a test interval. If gravel adjustments might be necessary, the geologists or engineers who will log the samples need to be made aware of what details will be needed.

Spreadsheets are a convenient way to analyze, tabulate, and plot SPT and other in situ data, and the results of analysis for each interval of each drill hole. They make it easy to redo calculations with different assumptions about earthquake loading.

13.6.6   Cone Penetration Test for Assessing Liquefaction Potential and Liquefaction Probability

The cone penetration test, or CPT, (also referred to as the electric cone penetration test, or ECPT, to distinguish it from the earlier mechanical cone penetrometer or Dutch cone) has gained favor in recent years as an indication of liquefaction potential and probability (Robertson and Wride, 1997; Stark and Olson 1995; Moss et al., 2006; Idriss and Boulanger, 2008; Boulanger and Idriss, 2014). Its use in liquefaction analysis is conceptually very similar to the SPT. The tip of the penetrometer is a 60-degree circular cone, generally having a diameter of 3.57 cm (1.40 in) and a projected end area of 10 cm^2 (1.55 in^2). It is pushed into the ground at a rate of 1 to 2 cm/s (0.4 to 0.8 in/s), while the resistance to penetration is measured at intervals of 2 to 5 cm by an electronic load cell. Another load cell measures the frictional resistance on a cylindrical sleeve immediately above the conical tip. The tip measurement is an index of soil density and correlates with resistance to liquefaction. The tip and sleeve measurements are used together to produce a rough estimate of soil classifications. Many cone penetrometers also have pressure transducers to measure changes in pore water pressure due to penetration; these are referred to as piezocones or CPTU, where the "U" indicates pore pressure). Pore-water pressure measurements can help in identifying changes in material type, measuring static pore-water pressures, and estimating consolidation parameters.

Appendix B discusses procedures for assessing liquefaction potential using CPT data. Standard CPT procedures are presented in ASTM D 5778 12.

The use of CPT data in assessing liquefaction potential or probability is analogous to the use of SPT as described above in section 13.6.5, except that adjustments specific to CPT data are made in Step 2. The measure of earthquake loading is the cyclic stress ratio, CSR, calculated in the same manner as for the SPT empirical procedures.

Although the CPT does not retrieve a soil sample like the SPT does, it has definite advantages over the SPT. The CPT produces a nearly continuous record of penetration resistance, unlike the SPT, which provides a single value of penetration resistance at intervals of 2.5 feet or more. Because the cone penetrometer is advanced by a steady push, not by hammering, and forces are measured at the tip of the rods, there is no concern about hammer energy, wave transmission, or energy losses along the rods. Those can be problematic for the SPT, particularly for very shallow or very deep tests. Also, the CPT is generally much faster and less costly to use where large amounts of data are required, and CPT data are generally more repeatable than SPT data. As described in appendix B, different methods of assessing liquefaction potential use different approaches for adjusting the tip resistance to account for the effects of fines. It can be a function of the actual fines contents from nearby drilling samples, or of the sleeve resistance. In the latter approach, the adjustment is, in effect, a function of the *behavior* of the fines, not the *percentage* of fines. Some researchers have favored this approach because different types of fines (clays or silts with varying plasticity) would have different effects on penetration resistance and liquefaction potential for a given percentage of fines. Several different methods for this adjustment have been proposed and are in use. Currently (2015), there is no consensus within the profession on which method to use. Refer to appendix C.

Because the CPT does not produce soil samples for classification or laboratory testing like the SPT does, soil classifications are based on the CPT sleeve and tip measurements; these are, however, are only rough estimates (especially in thinly stratified materials). It is, therefore, necessary to include adequate drilling and sampling in the exploration program to verify interpretations of soil properties from cone penetration data. While the CPT is often a good choice for determining stratigraphy over a large site, some drilling is still required to obtain soil samples, preferably with SPTs to corroborate the indications of the CPT. Reclamation's CPT rig is equipped for direct-push sampling, although the samples are of very small diameter, and not all materials can be sampled successfully, particularly if gravel is present.

Sometimes the material to be tested is found under compacted embankment fill or other material that is too stiff or dense to push the CPT through. In these cases, a hole can be predrilled through the overlying material. Before the CPT is pushed,

the hole is usually backfilled with uncompacted coarse sand or pea gravel to provide lateral support to keep the rods from buckling during hard pushing.

13.6.7   Becker Hammer Penetration Test and Other Methods for Gravelly Soils

The Becker hammer penetration test (BPT) uses a truck-mounted, diesel pile hammer to drive 6.7-inch outside-diameter, double-wall pipe, while the number of blows required to drive it each foot is recorded. Because of its large diameter, it can be used in soils that are too gravelly to produce meaningful SPT or CPT data. Empirical correlations have been developed to estimate the equivalent SPT blow count, N_{60}, that would be measured if there were no effect of gravel interference (Harder, and Seed, 1986; Sy and Campanella, 1994; Ghafghazi et al., 2014). (N_{60} is the SPT blow count adjusted for driving energy, but not yet normalized for overburden stress or adjusted for fines content.) The Becker-equivalent N_{60} is used in the same way as an actual SPT blow count, but rather significant uncertainty is introduced by the correlation. Appendix D presents details of BPT test procedures and procedures for estimating Becker-equivalent SPT blow counts.

The BPT has several advantages over the SPT. First, the large penetrometer tip diameter allows penetration testing of gravelly material that is too coarse to be meaningfully tested by the SPT. The SPT sampler has an inside diameter of 1.375 inches; if sufficiently numerous, particles with diameters as small as 0.5 inch can cause interference that elevates the blow count above what "should" be measured. Second, the BPT produces a more continuous profile of penetration resistance. Blow counts are typically recorded for each foot of penetration, in contrast with a minimum of 2.5 feet between SPT tests. Finally, production is typically much faster with the BPT than the SPT because the testing is continuous. Unlike the BPT, the SPT requires alternate drilling and testing, which requires tripping the rods out of the hole and back in with each change from drill bit to sampler and back. Although mobilizing a BPT rig can be expensive, testing is rapid and relatively inexpensive once the rig is on site. Sometimes, however, it is necessary to predrill through dense material overlying the soil to be tested, as sometimes occurs when testing under an embankment. Predrilling and any necessary road construction can increase the cost considerably. (The Becker drill rig is larger and heavier than typical SPT rigs, so larger roads and more gradual turns may be required.)

The BPT, as standardized for evaluation of liquefaction resistance, uses a plugged bit at the tip of the driven pipe. Therefore, the BPT, like the cone penetrometer, provides a measure of the resistance to driving, but it does not provide a sample for classification or lab testing. It is important that the investigation program includes drilling and sampling adequate to provide material index properties for interpreting the BPT data. Having SPT holes next to some of the BPT soundings

at a site allows comparison of Becker-equivalent N_{60} values against actual N_{60} values in layers where the SPT is valid, and site-specific "fine tuning" of the correlations. Because of the greater uncertainties in interpretation, there is little justification for using the BPT at sites where all of the necessary information can be obtained by SPT and/or CPT. Some sampling by SPT or other methods is required to obtain the soil gradation; otherwise, the BPT data must be assumed to represent clean sand, which would have less liquefaction resistance than silty sand or silt with the same blow count. Test pits or shafts can be very helpful for viewing the composition and structure of coarser materials in place.

Interpretation of BPT data is greatly complicated by the friction on the sides of the drill string. The method of Harder and Seed (1986) assumes that the friction is fairly similar from site to site, which makes the method simple to implement. The method proposed by Sy and Campanella (1994) explicitly accounts for the effects of side friction, but it requires the additional time and expense of a pile driving analyzer for every BPT sounding, and wave-equation analyses for selected blows. One newer development is the instrumented BPT (iBPT), which is related to the Sy and Campanella method but uses instruments for energy measurement at both the *tip* of the drill string and the *top*, essentially eliminating the issue of energy losses due to friction (Ghafghazi et al., 2014). Although Reclamation has no experience with it to date (2015), iBPT is now considered to be the state-of-the-art procedure. Differences between the methods of interpreting BPT data and their use in practice are described in appendix D. Further developments may occur and should not be neglected simply because they are not included in this chapter.

A possible alternative to the BPT for gravelly soils is the Dynamic Cone Penetration Test (DCPT), which was developed in China and is currently being studied for use in the United States (Cao et al., 2013). It is not discussed further in this design standard, but the DCPT is inexpensive and rapid, so it should not be ignored if it is shown to be of value.

13.6.8   Shear-Wave Velocity for Assessing Liquefaction Potential and Liquefaction Probability

The shear-wave velocity, V_S, of a granular soil generally increases with increasing density, as does the soil's resistance to liquefaction. Empirical correlations have been developed between V_S measured in situ and liquefaction resistance (Andrus and Stokoe , 2000; Andrus et al., 2004; Kayen et al., 2013). These can be valuable in soils that are too coarse for meaningful penetration testing, and for verification of soil properties from other methods. Empirical procedures for assessing liquefaction potential using shear-wave velocities are described in detail in appendix E. The measure of earthquake loading is the cyclic stress ratio, CSR, calculated in the same manner as for the SPT and CPT empirical procedures.

The shear-wave velocity is generally measured either between drill holes (cross-hole measurements), or from the surface to a downhole receiver, which may be incorporated into a cone penetrometer (Robertson et al., 1992). Cross-hole measurements are preferred for their greater accuracy but they are more expensive and time-consuming because of the need for multiple cased holes at each location. There have been advances in surface methods that have increased acceptance of surface geophysics for detecting liquefiable materials, notably Multichannel Analysis of Surface Waves or MASW (Park et al., 1999), but cross-hole measurement is still the primary method for Reclamation dams.

Measurements of shear-wave velocity involve very small strains, whereas liquefaction is a large-strain phenomenon. Also, V_S is relatively insensitive to changes in relative density, but predicted liquefaction resistance is very sensitive to variation or small measurement errors in V_S. Therefore, one would not expect a correlation between V_S and liquefaction resistance to be particularly "tight." It is possible that weakly cemented soils may give high shear-wave velocities without having high resistance to liquefaction; in other words, they may be stiff at very small strains without being dense or highly resistant to liquefaction.

Low shear-wave velocities do not necessarily indicate liquefiable material if they were measured in soils with plasticity. Hence, it is necessary to obtain soil samples for classification and/or laboratory testing, in addition to the shear-wave velocity measurements.

For dam-safety analyses, corroborating tests of a different type (SPT, CPT, etc.) should always be performed, rather than relying solely on V_S (or any single method) to assess liquefaction resistance.

13.6.9 Laboratory Cyclic Shear Tests for Assessing Liquefaction Potential

Liquefaction potential has been evaluated by laboratory cyclic triaxial or simple-shear tests (Ishihara, 1993; Seed and Peacock, 1971; Pillai and Stewart, 1994; and Yoshimi et al., 1984). Such tests were used to develop many of the principles used in empirical liquefaction assessments, including MSF, K_α, and K_σ, described in section 13.5.7 above. Currently, laboratory shear tests for liquefaction potential are used primarily in research because high-quality, undisturbed samples are expensive and difficult to obtain and test. It is quite difficult to sample noncohesive, clean sand and gravel without disturbance that affects the void ratio (or to account for the effects of disturbance), except with extraordinary measures like ground freezing. More importantly, the behavior of a large soil mass, such as a dam's foundation, is not directly analogous to behavior of laboratory shear specimens, because of heterogeneity and other large-scale effects that cannot be captured in small specimens. For these reasons, and because of the expense, Reclamation has not used laboratory cyclic shear tests for

liquefaction potential since the 1990s; however, an engineer may find records of such testing and should understand the implications.

There may, however, be sites for which laboratory shear tests are the only effective means, if empirical methods do not provide sufficient confidence. In particular, fine-grained or plastic materials may not be clearly liquefiable or nonliquefiable from in situ testing, but they are easier to sample and test than clean sands. Laboratory tests can provide a general indication of their behavior, such as how much excess pore pressure is generated from cyclic loading, whether shear resistance increases with consolidation, etc. (For such materials, the field vane shear test (VST) can be quite helpful in determining peak and remolded strengths, although it does not permit strain measurements or indicate resistance to cyclic loading.) Some nonlinear FEM and FDM codes require stress-strain parameters that can only be measured in laboratory tests (although nonlinear analysis is outside the scope of this chapter). More extensive use of laboratory tests has been made for evaluating post-liquefaction strength, most notably in the steady-state procedure described by Poulos et al. (1985), which attempts to compensate for sampling disturbance and changes in void ratio by careful and time-consuming field measurements, with theoretical adjustments for the changes.

In loose, liquefiable soils, cyclic strains (sometimes even monotonic strains) can rearrange the particles enough that particle contacts are disrupted so they can no longer carry the effective stress. The total confining stress is thereby transferred to the pore water, partially or completely, and the effective stress is reduced. The resistance to continuing large deformation can be much lower than the initial loading that caused the strain (strain softening). Cyclic laboratory tests may be used to simulate the buildup in pore-water pressure occurring during earthquake loading and the corresponding decrease in strength during the course of the earthquake. As cycling continues through the test, the pore pressure can increase until it reaches the total stress acting on the sand, either permanently (as in flow liquefaction of loose sand) or during only part of each subsequent cycle (cyclic mobility of medium-density sand). The difference between the two behaviors is very important. The number of cycles required to reach liquefaction is a function of the density of the sand and of the magnitude of the applied cyclic stress.

Liquefaction in a cyclic laboratory test is generally defined either as the occurrence of pore pressure equal to 100 percent of the initial effective confining stress, or as the occurrence of 3 to 5 percent double-amplitude (peak-to-peak) strain in a cyclic triaxial or simple-shear test. In denser sands, the strain criterion may be reached well before the pore pressure reaches the level of the effective confining stress (or the initial vertical effective stress in cyclic simple-shear tests). If it is not accompanied by very high excess pore-water pressure, the strain criterion for liquefaction can be misleading (overly conservative) for such materials. A few percent shear strain in the embankment or foundation would not cause large deformations and major loss of freeboard, although it could affect appurtenant structures within the embankment or cause cracking that might lead

to internal erosion. The user of cyclic test data must, therefore, be aware of how "liquefaction" was defined for each test program.

The practicality of laboratory shear testing for a site-specific liquefaction analysis of noncohesive materials, whether for triggering or for residual undrained shear strength, can be limited by the difficulty of obtaining sufficiently undisturbed samples and by the expense (especially if gravel is present). Conventional sampling may be feasible in low-plasticity silts or silty sands; however, in noncohesive material without much capillarity to hold a sample together, ground freezing may be the only method that produces samples that can really be considered undisturbed (Yoshimi et al., 1994). The decision to pursue a laboratory liquefaction testing program (inevitably expensive) should be made only after careful examination of the alternatives and the likely benefit of such a program. The considerations would include whether samples would cohere enough for undisturbed sampling with available methods.

13.7   Fine-Grained and Claylike Soils

13.7.1   General

Under strong earthquake loading, plastic, claylike soils may undergo a drastic loss of shearing resistance due to liquefaction or sensitivity, or they may simply yield and deform in a ductile manner. (Sensitivity is defined as the ratio of the peak strength in monotonic loading to the remolded strength.) The mere occurrence of yield and deformation is not necessarily a threat to the safety of the dam, although the deformation could encroach on the freeboard; crack the embankment, which could allow internal erosion; or damage appurtenant structures. If they are saturated and not highly overconsolidated, the shear strength of clays under seismic loading is generally governed by undrained shearing, which generally makes them weaker than nonliquefied granular material, so they can be the "weak link" for instability or deformation that is not governed by liquefied soil.

Liquefaction is primarily a phenomenon of noncohesive (granular) soils (clean sands or sand-gravel mixtures, silty sands with nonplastic fines, nonplastic silts, etc.). Clayey soils tend to be more resistant to liquefaction. For example, from laboratory cyclic shear tests on mine tailings, Ishihara (1993) determined that, for PIs greater than 10, the resistance to liquefaction increases with increasing PI. This finding is consistent with the observed performance of the Mochi-Koshi gold tailings dam in a major earthquake; nonplastic material liquefied, but a clayey silt layer with a PI of 10 did not (Ishihara, 1993). Where liquefaction has occurred in clays, it has been near the ground surface, where the effective preconsolidation stress is low and the soil has not been consolidated to a low void ratio and low water content. Under an embankment dam of even moderate size, clayey soils are generally consolidated to water contents well below their liquid limit, unlike the Mochi-Koshi tailings. Claylike soils generally require higher strains to reach a

state of liquefaction when they do, it is most likely in the form of cyclic mobility, rather than flow liquefaction (Bray and Sancio, 2006).

Clay and claylike soils differ from granular soils in several important ways. Unlike granular soils, their void ratio is determined primarily by the effective preconsolidation pressure. The greater compressibility of their soil skeleton and their ability to rebound somewhat with decreases in effective stress makes clays less susceptible to rearrangement and loss of particle contacts when disturbed by small shear strains, compared to clean sand. (This also makes them easier to sample and test.) In monotonic tests, claylike soils can often be sheared through several tens of percent strain without drastic loss of shearing resistance; *usually,* they do not show "brittle" behavior in the form of a sudden drop in shearing resistance after yield. There are exceptions to this; clays with high sensitivity can behave somewhat like liquefied sands, with drastic loss of shearing resistance occurring with full or partial remolding

The state of the art on the cyclic resistance of fine-grained soils was summarized by Boulanger and Idriss (2004). They present procedures for predicting cyclic failure of clayey soils in much the same framework as the Seed-Lee-Idriss assessment of liquefaction potential for sands. There are, however, different methods for determining the Cyclic Resistance Ratio (CRR) and different values of empirical adjustments such as MSF and K_α. (The term *cyclic failure,* as used here, would include liquefaction of clays, but would also include the more common situation of yielding without such drastic loss of strength.) The procedure is not detailed here, although there are some important points for embankment dams. They recommend that the distinction between granular soils and claylike soils be made at a PI of 4 to 7, with higher PI indicating more claylike behavior; the difference in behavior is not a sharp transition. Note that this is a distinction between sandlike and claylike behavior for the purpose of choosing an appropriate set of engineering procedures for evaluating stress-strain behavior, NOT a criterion for ruling out liquefaction potential. (For the latter, refer to section 13.7.2 below.) Atterberg limits are measured on the fraction passing the U.S. No. 40 sieve (0.425 mm), and coarser particles in significant quantities can affect whether this criterion is appropriate for a given soil. For soils with a PI just above or just below 7, or soils that contain large amounts of material coarser than the No. 40 sieve, case-by-case judgments are required. **These judgments should be made with direct examination and handling of the samples by the engineers that will do or direct the analysis.**

Embankment dams generally induce high static horizontal shear stresses in their foundations under the slopes. (In the Boulanger and Idriss clay procedure, this results in much lower K_α than in sands, for a given value of α.) If the foundation consists of normally consolidated to lightly overconsolidated clayey soil, the yield acceleration (the threshold acceleration for intermittent slope instability) is typically small. Therefore, it is frequently the post-yield behavior of the clayey soils that is most important in determining whether embankment deformation

would be excessive. (Appendix F provides recommendations for selecting strength parameters for use in analysis.) There are, however, exceptions, for example, when very small deformations could cause damage to appurtenant structures within the embankment or greatly increase the risk of dam failure by erosion through cracks.

This does not, however, mean that nonliquefied clay foundations would not undergo large strains or suffer major reductions in strength due to earthquake loading. Clays typically begin to show small permanent strains (tenths of a percent to a few percent) with cyclic loads as low as 80 percent of the peak undrained shear strength if there are numerous cycles of loading (Boulanger and Idriss, 2004). Once the peak strength has been reached, very large strains can occur with repeated or sustained loading. After large strains (several percent to tens of percent), the shearing resistance may drop considerably to a post-peak or "softened" value, then continue to decrease as the clay is sheared to the point of being remolded. The ultimate reduction can be as little as 30 percent in material that is only slightly sensitive, to 90 percent or more in very sensitive soil. (In this context, sensitive soils are those that undergo a major loss of shearing resistance when remolded or subjected to large strains, such as might occur if an earthquake caused a slide plane to move several feet. There have been cases of drastic earthquake-induced losses of strength in sensitive clays (Boulanger et al., 1998; Stark and Contreras, 1998). Once remolded, very sensitive clays can behave much like liquefied soils. However, sensitivity of claylike soils differs from liquefaction in that much higher strains are generally needed to cause the major loss of strength in clays, and the excess pore-water pressure ratio remains well below 100 percent, except in the most sensitive soils. Also, it requires a different set of test procedures and analyses.

High sensitivity is most likely to occur in clays with high water content or high liquidity index, with low to medium PI, and low overconsolidation ratio. Aged clays, and marine clays that have had their original saline pore fluid leached out and replaced by fresh water can be extremely sensitive, although such soils are rarely found at Reclamation dam sites. Sensitivity tends to increase with increasing water content and decreasing PI. High overburden stresses, such as those found under medium or high embankment dams, tend to reduce sensitivity and increase the amount of strain required to cause yield. Sensitivity decreases with decreasing water content and liquidity index; typically, but not always, these are low in soil consolidated under the weight of a large dam embankment.

Whether sensitive or not, fine-grained soils in the embankment or foundation often govern the yield acceleration of the embankment slopes because the undrained strength is the "weak link" for stability. With normally consolidated or lightly overconsolidated clay in the foundation, the yield acceleration can be much smaller than it would be for a dam on a foundation of bedrock or dense soil. In other words, contractive material would yield in undrained shear with each dynamic load cycle that exceeds the yield acceleration. Sensitive clay could lose

enough strength to allow instability or very large dynamic deformation. Insight can often be gained from a simple calculation of the pseudostatic yield acceleration, assuming peak and post-peak undrained shear strengths, and comparing the result with the expected peak ground acceleration. If there is no liquefaction potential and A_{max} is less than or only slightly greater than the yield acceleration, there is not likely to be a problem with the embankment itself. (Appurtenant structures could be damaged.)

The field vane shear test (VST) can be very useful for assessing the peak shear strength and residual (remolded) shear strength of fine-grained soils. (Refer to ASTM D 2573 for test procedures.) A drastic reduction in the shearing resistance after the peak would indicate high sensitivity and the potential for instability or large deformations. The VST does not, however, indicate the amount of strain required to cause full or partial remolding during an earthquake, except qualitatively. The stresses and strains around the vane device are complex and different from the simple cylinder ordinarily assumed in calculating the shear strength from the measured torque on the rod. Empirical correction factors are used to correct for that (e.g., Bjerrum, 1973), but the factors were back-calculated from cases of static slope instability; they include effects of strain rate, drainage, anisotropy, and stress path that may not be fully relevant to rapid shearing by earthquake ground motions. Because the VST does not provide any quantitative indication of the strain required to mobilize the peak shearing resistance, or the strain associated with decreases after the peak, a combination of test methods is likely to be necessary. This would likely include triaxial and/or direct simple-shear tests, with the highest strains and strain rates the test equipment allows, along with VST to determine sensitivity and remolded strength. The cone penetrometer test (CPT) can also measure peak and remolded strength throughout a deposit quickly and at low cost. High sensitivity is detected thereby, but the measurement of remolded strength by CPT is not precise, and like VST, the CPT cannot indicate how much strain is required for full or partial remolding to occur.

Appendix F provides greater detail on peak, post-peak, and remolded strengths of clays for seismic stability and deformation analysis. Characterization of clay strengths may require a detailed investigation that includes consolidation testing, and laboratory and field strength testing. The undrained behavior of clays is quite dependent on the stress history, so oedometer consolidation tests should be included in any program of testing for undrained strength of claylike materials.

13.7.2   Assessing Liquefaction Potential of Fine-Grained and Clayey Soils

A number of investigators have proposed the use of index properties to rule out liquefaction potential in fine-grained soils. This concept originated with the so-called "Chinese criteria," published in 1979 by Wang (1979), and tentatively

adopted by Seed et al. (1983), but later superseded. A newer set of criteria by Bray and Sancio (2006) is shown below and; it is considered to have superseded the earlier criteria. From a large set of case histories and laboratory testing, Bray and Sancio concluded:

- If the PI is greater than 18, the soil may be considered nonliquefiable.

- If the PI is greater than 12, the soil may be considered nonliquefiable, provided that the water content is less than 85 percent of the Liquid Limit (LL).

- If a soil does have some plasticity, even if the PI is less than 12, it may be considered nonliquefiable, provided that the water content is less than 80 percent of the LL.

A soil that does not satisfy at least one of these criteria should be considered liquefiable, unless it can be shown otherwise by laboratory shear testing, in situ penetration resistance, or other evidence. If the PI is between 12 and 18, or if the water content is between 80 and 85 percent of the LL, Bray and Sancio considered the soil to be moderately susceptible or potentially susceptible to liquefaction, and further evaluation is required. Laboratory shear testing is generally feasible for materials with even a small amount of plasticity.

Satisfying the criteria does not rule out severe strength loss from cyclic loading or large permanent shear strains. Sensitivity and potential for undrained yield must be evaluated and accounted for in deformation and post-earthquake stability analyses.

Also, water contents are quite susceptible to change during sampling, handling, and shipping. **The use of criteria based on water content to rule out liquefaction potential is contingent upon a valid water content, which requires that samples are sealed immediately and protected from heat and direct sunlight, and that the water content is measured as soon as possible after sampling.**

It is preferable for liquid and plastic limits to be measured on samples that have not been completely air dried because drying may cause changes in mineralogy, especially in residual soils and those derived from decomposed volcanic materials.

It is important to remember that Atterberg limits are measured on the fraction passing the No. 40 U.S. Standard sieve, whereas the water content is measured on the whole sample. Modest amounts of coarser material surrounded by a matrix of minus-No. 40 material would affect the water content of the whole sample without affecting the behavior significantly. If the amount of material retained on the No. 40 sieve is not large , the water content can be adjusted as follows:

$$w_{adj} = \frac{w - 0.03 * \text{(percentage retained on \#40 sieve)}}{\text{(percentage passing \#40 sieve)}} \qquad \text{Equation 11}$$

with water contents w and w_{adj} expressed as percentages. In effect, all of the water in the sample is assumed to be associated with the fraction of the material finer than the No. 40 sieve, except for an amount equal to 3 percent of the weight of the coarser material. The fraction of the material passing the No. 40 sieve (the minus No. 40 fraction) is not generally measured in Reclamation practice, except when a full gradation curve is required. **The minus No. 40 fraction should be determined whenever these criteria are to be used.** (Interpolating between the percentages passing the No. 30 and No. 50 should be adequate, if those are available.)

This set of criteria supersedes an earlier set that Reclamation used, informally known as the "Chinese criteria." They indicated that liquefaction could be ruled out on the basis of either a high liquid limit or a high content of particles smaller than 0.005 millimeter, but both of these criteria have proven ineffective, and Reclamation no longer uses them. Refer to section 13.11.2, below, for further discussion of earlier practices. The Chinese criteria did include a comparison of the water content and the liquid limit, similar to Bray and Sancio (2006), but it was slightly less conservative, predicting that no liquefaction would occur with water contents as high as 90 percent of LL.

The VST and CPT can indicate the peak undrained strength and show whether a plastic fine-grained soil or a silty or clayey sand would undergo a drastic loss of strength following cyclic failure. However, these tests provide little indication of the level of shaking required to cause liquefaction of marginal soils, and there is no way to obtain a stress-strain curve from them. However, permanent shear strains in plastic materials begin to accumulate with cyclic stresses as low as 80 or 90 percent of the peak strength (Boulanger and Idriss, 2004), which does provide a rough indication of the minimum cyclic stress for very high excess pore-water pressure to occur.

13.7.3 Granular Soils with Plastic Fines

If a soil classified as SC or GC (clayey sand or clayey gravel) consists primarily of material that passes the No. 40 sieve and has a PI greater than 7, it would be reasonably to treat it as a clay-like. It is generally accepted that the strength of a soil is governed by the finest 20 to 35 percent of its grain-size distribution because the coarser material is essentially suspended in the finer fraction. (The percentage would depend on the properties of the finer fraction.) Atterberg limits are measured on the fraction that passes the U.S. Standard No. 40 sieve (0.42 mm), rather than on the "fines," as defined by the No. 200 sieve (0.075 mm). Therefore, if the finest 35 percent would pass the U.S. Standard No. 40 sieve, the Atterberg limits of the soil should, at least in theory, indicate the behavior as a

whole. While this may be true on a small scale, no soil is completely uniform, with the plastic fines and plus No. 40 fraction being evenly distributed. There may be layers within a sample that have less than 35 percent minus No. 40 particles and/or a PI less than 7, even if the whole sample has higher values. Grain-size data reported on drill logs or laboratory reports may actually be averages for nonuniform material within the sample. To allow for nonuniformity, it is suggested that SC and GC should only be treated as fine-grained soils if more than 50 to 60 percent passes the No. 40 sieve. This guidance is tentative because there is no general consensus regarding the amount of fines for the transition from fines-controlled to coarse-controlled behavior, or about how to account for the amount of sand between the No. 40 and No. 200 sieves. (See, for example, Armstrong and Malvick, 2014).

Liquefaction triggering analyses based on penetration resistance or shear-wave velocity generally include an adjustment for the presence of fines. For plastic soils, it would be conservative, perhaps overly so, to apply a fines adjustment developed from nonplastic soils. Ishihara (1993) suggested that if the PI is greater than 10, there is an increase in liquefaction resistance.

13.8   Post-Earthquake Stability Analysis

13.8.1   General

If liquefaction or major loss of shear strength from other effects is likely to result from an earthquake, the post-earthquake static stability of the embankment must be analyzed assuming appropriate reduced strengths for the liquefied or sensitive material. Granular materials that would not be liquefied but would undergo pore-pressure increase may also require reduced strengths.

Liquefaction of soil does not necessarily mean complete loss of strength, particularly for materials of medium density (roughly speaking, having normalized, fines-adjusted SPT blow counts, $(N_1)_{60cs}$, of 15 to 30). A variety of direct and empirical means have been proposed for evaluating the post-liquefaction strength of soils, as described in appendix F.

Stability analyses should be made in accordance with Reclamation's *Design Standard No. 13 – Embankment Dams,* Chapter 4, "Static Stability Analysis."

13.8.2   Continuity or Connectivity of Liquefiable Deposits

Even if SPT, CPT, or other data indicate that portions of a deposit are potentially liquefiable under a particular earthquake, these zones may be sufficiently isolated

and discontinuous that they would not cause a large reduction in the strength of the soil mass as a whole. There is some minimum areal extent of liquefied material required for a slide to occur. Judging the continuity or connectivity of liquefiable materials requires both relatively close spacing of test data and an understanding of the mode of deposition of the soil. The definition of "close spacing," as used here, is a function of the mode of deposition (alluvial, lacustrine, etc.), the size of a potential failure mass, and the variability in soil properties from point to point within the deposit. All available information, including material types, blow counts, and geophysical data, should be presented on cross sections, profiles, and plan views. Interpolation and extrapolation of soil properties need to be informed by the geologic processes that created the deposits. Correlations used to estimate material properties need to be used as consistently as practical with the way that they were developed. For example, correlations between SPT blow count and residual undrained shear strength were generally developed using the mean blow count for the layers that were involved. It is necessary to understanding the deposition to be able to determine which data should be included in the mean for the site being studied.

13.8.3 Seepage Conditions

Stability and liquefaction stability analysis should be made with the piezometric surface that would exist just prior to the earthquake. Usually, this can be assumed to be steady-state seepage with the reservoir at the top of active conservation. Other seepage conditions may also need to be considered, depending on typical operation of the reservoir and how flood-storage space is used.

13.8.4 Material Strength

Appendix F provides guidance on the selection of material strengths for stability and deformation analysis.

To the extent practical, the foundation and embankment should be subdivided into zones of material with similar properties. Where the foundation is very heterogeneous or apparently chaotic, it may not be practicable to divide it into zones for each material. In such cases, the overall behavior of a zone could be considered to be the average strength over the weakest plausible failure surface through the zone. This surface need not be completely planar, but it may be appropriate to exclude some low values if they occur very far above or below a surface formed by the others. Geologically informed cross sections are needed for making these judgments. If there is not a distinct weak layer, a reasonable approximation is to assume the 33rd percentile of all the strength measurements in the zone. However, the minimum area that constitutes a plausible failure surface

is not always obvious, making it more difficult to decide which data to include in the average. Some insight may be gained from 3D stability or deformation using either a limit-equilibrium program like CLARA (O. Hungr Geotechnical Research Inc., 2010), or an FEM or FDM program like FLAC3D.

Layering and strength anisotropy can be important. In a dam's foundation, the dominant direction of shearing is usually approximately horizontal, and a single continuous weak layer could govern the strength as a whole. In contrast, a steeply inclined sliding surface may have to cut through a number of layers with different strengths. In that case, the strength would be similar to the average of the layers. The strength of the zone, as a whole, is effectively anisotropic, regardless of anisotropy within the individual layers. Some slope stability programs allow anisotropic strength functions, which, in this situation, would allow a single strength function to cover all orientations.

For nonliquefied zones of dilatant material, regardless of type, drained strength parameters should generally be used. The undrained strength could actually be higher than the drained strength, but that should not be relied upon, because it depends on negative excess pore-water pressure, which could be lost due to cavitation, preexisting bubbles, or water flowing in from the reservoir or adjacent zones with higher pore-water pressure.

For nonliquefied zones of contractive material (materials that would generate excess pore pressure but not be liquefied), undrained strengths are usually appropriate for both granular and fine-grained materials.

For liquefied zones, undrained residual strength S_{ur} should be used, as described in appendix G, which provides procedures for estimating S_{ur} based on field and laboratory measurements. Estimates of residual undrained strength are highly uncertain, and a parametric study may be useful to understand the sensitivity of the factor of safety to varied strength assumptions.

13.8.5 Failure (Sliding) Surface

Two general types of failure surface geometries should be analyzed and reported:

1. The failure surface that has the lowest factor of safety overall.

2. Failure surfaces (upstream- and downstream-facing) that would result directly in release of the reservoir.

The failure surface with the lowest factor of safety overall may or may not be one that would release the reservoir. In some cases, the surface with the overall lowest factor of safety may be of little consequence for dam safety because it

would only affect a small portion of the embankment, leaving the crest
and important zoning intact.

The stability of an embankment on a liquefied foundation is very sensitive to the
physical extent of liquefaction. If there is liquefaction only under the downstream
toe and a small portion of the downstream slope, the embankment may be entirely
stable, or any instability that might occur would not affect the dam's ability to
safely contain the reservoir. With liquefied material extending farther upstream
under the embankment, the factor of safety would decrease for failure surfaces
that have potential to breach the embankment. It may be useful to do slope
stability analysis prior to an extensive exploration program to improve
understanding of what information is needed and to focus the drilling effort
accordingly.

13.8.6 Factors of Safety and Likelihood of Dam Breach

In the risk-informed dam-safety paradigm Reclamation has used since the 1990s,
there are no specific minimum post-earthquake static FS that must be met.
Instead, FS for new or modified dams must simply be high enough that the risk of
dam failure is sufficiently low to meet risk guidelines. In a decision about
acceptability of an existing dam or a design, consideration may be given to
uncertainty in the supporting analyses and to potential for future changes in the
state of practice. The level of risk depends on the annual probability of various
levels of earthquake loading, the likelihood of a breach with each loading, and the
consequences of a breach (typically considering only the potential for loss of
human life under the public protection guidelines). The likelihood of instability
is, of course, lower with higher FS, and the likelihood of a breach of the
embankment, given occurrence of instability, depends on the position and shape
of the sliding surface. (Risk-analysis procedures are not presented here, except as
necessary for context. Refer to the most recent versions of Reclamation and the
Corps of Engineers' best-practice manuals for dam-safety risk analysis, and to
Bureau of Reclamation (2011) for decision guidelines.

Estimating the likelihood of instability, given occurrence of liquefaction,
generally requires three steps: (1) analysis of stability with ranges of plausible
values for the more critical parameters, to determine how variation affects the FS;
(2) judgment regarding the relative likelihood of different values of the
parameters within their respective ranges; and (3) judgment of the likelihood of
instability given different values of FS. In many cases involving foundation
liquefaction, the most critical parameter is not the strength of the liquefied
material, but its extent. Consideration must be given not only to the numerical
values of FS from the stability analyses, but also to any conservatism or
unconservatism in the assumptions, e.g., whether benefit from 3D effects is being
neglected, or whether continuity of weak material is being assumed for all the
stability runs, even though continuity is far from certain.

Obviously, if the stability analysis predicts FS less than 1.0 for a sliding surface that leaves no remnant of embankment above the reservoir, the probability of a breach would be very high. Otherwise, the likelihood of a breach after instability must be judged from the condition of the expected remnant. Considerations would include the potential for internal erosion through the remnant (which may have damaged core and filters), for retrogressive sliding that would cause the remnant to fall below the reservoir, or for failure of appurtenant features such as the outlet works. Damage to appurtenant features could lead to embankment failure (by internal erosion, for example); it could also prevent the reservoir from being drawn down following the earthquake. In judging the likelihood of dam failure following instability, consideration must be given not only to the overall most critical sliding surface, but also to the potential for other surfaces to move, even if they have slightly higher FS.

For new dams, it should be standard practice to treat or remove all weak, potentially liquefiable, or sensitive material from the foundation, with a generous margin for possible future changes in the state of practice. Provided the treatment is done, gravity-driven post-earthquake instability should not be an issue for a new dam, although dynamic deformation could be an issue.

13.9   Analysis of Embankment Deformation

13.9.1   General Approach

Even if an embankment and its foundation soil would not liquefy sufficiently to allow gravity-driven instability, permanent deformations may still occur. Settlement can result from densification of foundation or embankment material, but the dominant cause is likely to be shear strains, with or without formation of a distinct sliding surface. If deformation is large enough to allow overtopping of the embankment, a rapid breach of the dam would generally be expected. Deformation without overtopping could also cause failure by creating cracks that would lead to internal erosion, or by damaging appurtenant structures. Note that deformation may result from cross-valley shaking, as well as upstream-downstream movement.

Methods of evaluating seismic deformation range from comparing case histories of dams subjected to similar loading, through simple sliding block analysis, to nonlinear FEM or FDM analysis. In general, analysis should proceed from the simplest analysis, to more rigorous methods, until an acceptable and justifiable result is obtained. Typical Reclamation practice is described below.

If deformations could affect retaining walls, conduits, or other structures within the embankment, evaluation of the impact should be made in cooperation with the relevant Reclamation design group.

13.9.2 Conditions Indicating Deformation Analysis is Not Required

Numerous dams have been subjected to moderate seismic loading with little or no deformation or damage. Experience has shown that a well-built embankment on a good foundation is not likely to be damaged in a moderate earthquake (Seed, Makdisi, and De Alba, 1978; USSD, 1992, 2000, 2014). Figure 13.9.2-1, replotted from Swaisgood (1993) with additional data added, shows historic crest settlements of embankment dams that have been subjected to major earthquakes as a function of the reported peak horizontal acceleration (PHA). (Physical locations of PHA values relative to the embankment and foundation the dam may not be consistent from site to site.) At some of the sites. liquefaction occurred, but slope instability did not (only deformation). The settlements have been normalized by the combined height of embankment and alluvium. There is a clear trend of increasing settlement with increasing A_{max}, and a weaker trend of increasing settlement with increasing earthquake magnitude. It is important to note that very few of the settlement data are above 1 percent, and those that were all occurred at dams having some identifiable adverse condition, such as hydraulic fill or a landslide in the foundation.

Figure 13.9.2-1. Earthquake-induced settlements of embankment dams. Replotted from Swaisgood (1993), with additional data from Lekkas (2009).

Deformation analysis is generally not required if all the following conditions are satisfied:

1. The dam and foundation materials are not subject to liquefaction and do not include sensitive clays.

2. The dam is well built and compacted to at least 95 percent of the laboratory maximum dry density, or to a relative density greater than 75 percent.

3. The slopes of the dam are 2.5:1 (horizontal:vertical) or flatter, and/or the phreatic line is well below the downstream face of the embankment.

4. The PHA at the base of the embankment is no more than 0.35 g.

5. The static FS for all potential failure surfaces involving loss of crest elevation (i.e., slides other than shallow surficial slides) are greater than 1.5, with pore-water pressures that could reasonably be expected immediately prior to the earthquake (typically steady-state seepage with the reservoir at the top of active or joint-use storage).

6. The minimum freeboard with active or joint-use storage is at least 3 to 5 percent of the embankment height, and never less than 3 feet. (Required freeboard to accommodate reservoir seiche waves or coseismic movement of faults at the dam or in the reservoir is a separate issue.)

7. There are no appurtenant features that would be harmed by small movements of the embankment, or that could create potential for internal erosion or other potential failure mode.

If all of these criteria except No. 4 are met, potential deformations can be assessed by simplified methods, with no need for site-specific numerical analysis with a sliding-block or nonlinear deformation code. If PHA is only slightly smaller than the yield acceleration, deformation can still occur from permanent shear and volumetric strains, but it would generally be minor. Even if yield is expected, the deformation can still be small. The amount of deformation would depend on the peak acceleration and the number of loading cycles that reach or exceed the yield acceleration. Calculation of yield acceleration should incorporate undrained shear strengths for clayey materials and any other materials that are not free-draining and could be contractive. For materials that are dilatant, very free-draining, or dry, the drained strength would be used.

Higher-level analysis may be needed if there are criteria that are not met (other than No. 4), if simplified deformation analysis shows that settlement could significantly encroach on the embankment freeboard, or if differential settlement could be large. For example, simplified methods would not be appropriate for

assessing potential for deformation resulting from subduction zone earthquakes of unusually long duration. Even a well-built dam on a good foundation would require further evaluation, most likely using time-dependent, Newmark sliding-block approach (Newmark, 1965) or a nonlinear FEM or FDM code. (Refer to section 13.9.4 below.)

The list of conditions above does not address the potential for embankment cracking (transverse or longitudinal) or damage to appurtenant features (such as outlet-works tunnels), which must be considered as separate issues.

13.9.3 Newmark Sliding-Block Approach

In his 1965 Rankine Lecture, Professor Nathan M. Newmark proposed a simple technique for predicting a dam's deformation under earthquake shaking, applicable only when there are no liquefiable materials or sensitive clays (Newmark, 1965). The sliding mass is treated as a rigid block sliding on an inclined plane, with the base subjected to a ground motion acceleration record. Whenever the horizontal acceleration of the foundation opposite to the direction of sliding exceeds the "yield acceleration," the slope accelerates out from under the slide mass, which moves down the slope. However, if the slope is statically stable, the motion ceases when the acceleration of the ground reverses, so the slide mass moves in intermittent pulses of "stick and slip" corresponding to the stronger cycles of shaking. The yield acceleration is determined by calculating the inertial force required to lower the FS against sliding to 1.0, usually with a limit-equilibrium, slope-stability program such as UTEXAS2 (Edris and Wright, 1992) or SLOPE/W (Geo-Slope International, Ltd., 2014).

Based on bench-scale models and numerical analysis of a large number of slopes with typical earthquake motions, Newmark provided a simple chart solution that can be used for very preliminary estimates of the order of magnitude of movements. However, the method as originally formulated did not take into account the elastic response of the embankment, which affects the acceleration of the slide mass. Makdisi and Seed (1977) modified Newmark's method to include the dynamic response and produced a new chart solution, which Reclamation later incorporated into the computer program SEIDA, described below. Although it is not the preferred sliding-block method for Reclamation dams, it is included here for screening-level studies when peak ground acceleration and earthquake magnitude are the only available loading parameters, i.e., response spectra (spectral accelerations for different oscillation periods) are unavailable.

The preferred method for using Newmark's sliding-block approach is a site-specific, numerical analysis that incorporates dynamic site response and earthquake ground motions that are appropriate for the specific site and earthquake source. Reclamation has used its own computer program DYNDSP (Reclamation, 1983) in combination with dynamic response analysis, and QUAKE/W combined with SLOPE/W (Geo-Slope International, Ltd., 2014).

Although these methods (including the site-specific analysis) have been able to calculate movements that are fairly consistent with field observations, the calculations must be regarded as general indications, not precise predictions, of the amount of deformation. If liquefaction or generation of high excess pore pressure is expected to occur, the Newmark approach with reduced strengths may be useful for estimating upper and lower bounds on the expected movement, but no more than that. If instability is predicted by a post-earthquake static FS less than 1 or only slightly above it, the Newmark approach cannot be used in any form.

Some permanent movement is likely to occur by densification and shear distortion even without development of the sliding surface assumed by the Newmark model. These methods do not account for settlement due to volume change.

Limit-equilibrium analysis (using UTEXAS2, SLOPE/W, or a similar program) is used to determine the yield acceleration on potential sliding surfaces. The high-level, steady-state seepage condition is generally appropriate to use for the dynamic deformation, although other seepage conditions may need to be considered if the reservoir is usually low or may contain flood surcharge for long durations. **The yield acceleration should be calculated using a strength representation for each soil that is appropriate for *rapid* loading. However, some materials may progressively weaken during the course of the strong shaking, causing the yield acceleration to change.** The consolidated undrained strength is generally the most realistic for saturated materials unless they are dilative or extremely pervious (clean gravel or coarser). In reviewing older Reclamation reports, one may find that drained shear strength was assumed for saturated soils, with no consideration given to excess pore-water pressure developing during shaking. The results could be very unconservative, especially if the foundation contains liquefiable soils or normally consolidated clay. Unsaturated materials would usually require drained strengths, but if the degree of saturation is fairly high (so that air-filled voids occupy only a few percent of the volume), there can be high excess pore-water pressure.

Newmark-type analyses do not allow for permanent strain at stresses below the yield stress, but in laboratory shear testing, small permanent strain may occur at stresses as low as 80 percent of the yield strength. Therefore, for clayey materials, Makdisi and Seed (1977) recommended using strengths equal to 80 percent of the yield strength. That may be unnecessarily conservative in a situation where several tenths of a percent strain can be tolerated. For dense, dilatant material, it would be slightly conservative to use the drained strength. If the precise value of the settlement is an issue, the yield accelerations and deformations can be calculated using both actual and reduced strengths for comparison.

Seepage conditions assumed for analysis should include steady-state seepage with the reservoir filled to the top of active storage. Other loading conditions may also

need to be analyzed, depending on the typical operation of the dam in question. Movement on upstream sliding surfaces would generally be greater with lower water surfaces, although more settlement would have to occur in order to release the reservoir with it lower.

Preferably, failure surfaces involving the top fourth of the embankment, the top half of the embankment, and the full height of the embankment should be analyzed. The input for Reclamation's program SEIDA includes yield accelerations for all three of these failure surfaces. It may be appropriate to analyze both the upstream and the downstream slopes of the embankment. The sliding surfaces of primary interest are those that would directly affect the crest, rather than shallow slides that would cause movement only of the slope surfaces. Note that for the Bray-Travasarou analysis, the loading input is a free-field spectral acceleration, so analyzing a slide only in the upper half of the embankment may require a response analysis to find the spectral acceleration at the base of the potential slide.

Predicted deformations of less than 1 foot would ordinarily not be a threat to the dam, unless critical appurtenant features could be damaged or there are other special circumstances. Those circumstances could include an unreinforced concrete core wall, geometry that would be conducive to transverse cracking and internal erosion, such as abrupt changes in embankment height or small freeboard. For any embankment dam, estimated deformations exceeding 3 feet would raise concern about cracking and loss of freeboard. The impacts of movements that large must be carefully evaluated, and a site-specific Newmark analysis or nonlinear FDM analysis should be implemented to verify the results of the simplified analysis.

The Makdisi-Seed and Bray-Travasarou methods should not be used to verify the adequacy of a design or an existing dam if any of the following conditions exist:

- Earthquake magnitude, M_W, is 8 or greater.

- Available freeboard is 4 feet or less.

- Embankment or foundation materials may liquefy or be sensitive.

- There are features that could be damaged and cause dam failure, and precise estimates of deformation are needed to determine whether that would actually occur in a particular earthquake.

A higher level of analysis is generally needed if any of those conditions occur.

SEIDA generally cannot be used for analyzing movements of slides in the abutment or reservoir rim because SEIDA estimates the response of an embankment by approximating it as an elastic triangle resting on a rigid

foundation, using a Bessel series. This also affects its validity for embankments on thick alluvial foundations. Such cases often require site-specific Newmark deformation analyses with site response determined by FEM analysis.

13.9.3.1   Makdisi and Seed's Extension of Newmark's Method

Makdisi and Seed (1977) developed a simplified method for estimating seismic displacements of embankment crests by expanding on the work by Newmark. (It, too, is not applicable if liquefaction or sensitive clays are involved.) They produced a chart solution for predicting displacement based on "typical" earthquake records, normalized by the peak acceleration of the slide mass. The peak acceleration was estimated by modeling the dynamic response of the embankment as a Bessel-series approximation with strain-dependent elastic properties. The response of the embankment and foundation soil (if present) can cause acceleration of the dam crest to be much greater than the PHA at a bedrock outcropping or in foundation bedrock during the same earthquake.

The "displacement" calculated here is the amount of movement along the sliding surface. Depending on the geometry, it could be significantly different from the amount of freeboard that is lost to settlement.

In the early 1980s, Reclamation was performing initial reconnaissance-level Safety of Dams analysis on about 200 embankment dams and needed a simple method for evaluating dynamic deformation without extensive investigation or analysis. Reclamation personnel wrote the computer program, SEIDA, to allow rapid application of the Makdisi-Seed method (Adhya, 1982). The required inputs include the peak acceleration at the base of the embankment, the earthquake magnitude, the yield acceleration, and the elastic properties of the embankment. The Makdisi-Seed analysis can also be performed using the original charts by Makdisi and Seed, instead of SEIDA, although iterative calculations are required to find the peak acceleration of the dam crest, which is usually higher than the peak bedrock acceleration by a factor of 1.5 to 3. (A reasonable first approximation might be made using the Makdisi-Seed chart solution, assuming the peak crest acceleration is twice the peak bedrock acceleration. If the calculated deformations are minor, perhaps 1 foot or less, further deformation analysis may not be needed.)

The yield acceleration required as input for the Makdisi-Seed analysis must be calculated with shear strengths that are appropriate for rapid shearing; contractive materials generally require undrained strength. If there is potential for liquefaction, this method is not applicable. (Section 13.11 describes earlier practices at Reclamation. Some older Makdisi-Seed analyses found in the records may have used drained shear strengths where undrained shear strengths are required). This procedure may continue to be used for "order of magnitude" estimates, but precision should not be expected.

13.9.3.2   Bray and Travasarou's Extension of Newmark's Method

The Makdisi-Seed method is considered by some engineers to have been superseded by a newer procedure by Bray and Travasarou (2007), although, to date, Reclamation's experience with it is very limited. The Bray and Travasarou procedure is based on statistical analysis of a large number of numerical Newmark analyses with multiple sets of ground motions and slope-stability models. The input variables are yield acceleration, k_y, earthquake magnitude, M_W (again, as a proxy for earthquake duration), the fundamental period of the embankment, T_s, and the spectral acceleration for a period equal to 1.5 times the fundamental period, $S_a(1.5T_S)$. $S_a(1.5T_S)$ is used instead of PHA or $S_a(T_S)$ because the authors found that, statistically, it was the best measure of earthquake loading because of the effect of strain softening.

Bray and Travasarou's method provides two results: (1) the probability that practically no displacement would occur, and (2) if it would occur, an estimate of the displacement (less than 1 cm or 0.4 in). Strain softening, in this case, does not include liquefaction or remolding of sensitive soils.

This method would be cumbersome in hand calculations, but it can be implemented easily in a spreadsheet.

To date, Reclamation's experience with the Bray and Travasarou procedure is limited. One complication is that it requires the loading to be characterized by spectral acceleration at a period that varies from dam to dam, rather than PHA. That makes more sense physically, but hazard curves are not always available for spectral acceleration at the necessary period. In contrast, the Makdisi-Seed method requires the PHA, for which hazard curves are available for all Reclamation dams. Until Reclamation has more experience with it, the interim recommendation is that both methods be applied and compared any time a hazard curve is available for $S_a(1.5T_S)$. The Makdisi-Seed procedure may continue to be used for "order of magnitude" estimates, but precision should not be expected from either method.

13.9.3.3   Site-Specific Numerical Newmark Analysis

Site-specific Newmark analyses use recorded or synthetic earthquake ground motions and the characteristics of the embankment to calculate the permanent deformation as a function of time. The computer codes for the displacements require a dynamic response analysis to find the acceleration time history for the slide mass, and a slope-stability analysis to determine the yield acceleration and critical failure surface.

Historically, Reclamation used the slope-stability program UTEXAS2, with the Newmark deformation program DYNDSP, along with either SHAKE or QUAD4M for the dynamic response. (A utility called UTOD was used to convert UTEXAS2 output to DYNDSP input.) DYNDSP, written by Reclamation, can include variation in pore pressures and material properties with time. More

recently, Reclamation has used QUAKE/W and SLOPE/W, which together perform all three functions. Details of their use are not provided in this document; refer to the user's manuals. Other suitable programs may be available.

13.9.3.3.1 Failure Surfaces

The analysis should be made for failure surfaces that would cause movement of the dam's crest and have the potential to release the reservoir; both upstream and downstream surfaces should be considered. The elastic response of the dam embankment causes the accelerations to be larger at the crest than near the base of the embankment; for this reason, the failure surface with the lowest yield acceleration may not be the surface with the greatest potential for deformation. The analysis should, therefore, consider both the surface with the lowest yield acceleration (which typically involves the full height of the embankment), and one or more surfaces higher in the embankment. The need to analyze other surfaces should be evaluated based on the geometry of the dam, such as stabilizing berms, changes in zoning, and possible layers of weak material. The user must judge whether the critical failure surfaces indicated by stability analysis are realistic and relevant to disruption of the embankment crest.

13.9.3.3.2 Acceleration Time History

The acceleration time history for use in calculating deformation is preferably a mass-weighted average for the slide mass, obtained from 2D response analysis using QUAKE/W or QUAD4M. QUAD4M can calculate the stress history along a failure surface and convert it to a history of accelerations for the slide mass; this unique feature was written specifically for the purpose of Newmark analyses. Although the 2D analysis is preferred, a 1D analysis using SHAKE (Idriss and Sun, 1992) may be a reasonable approximation, particularly for preliminary analyses or if there is a thick soil profile between the embankment and bedrock (which fits better with the 1D assumption than with a dam on shallow bedrock).

As with the simplified solutions by Makdisi and Seed, and by Bray and Travasarou, the displacement calculated by SLOPE/W and QUAKE/W is movement along the slide surface. The vertical movement of the dam crest could be significantly smaller if the sliding surface is not steeply inclined at the top. If it is steeply inclined, the difference between the vertical movement and the movement along the sliding surface may be similar.

Deformation analysis by the Newmark approach assumes rigid-block motion of a single slide mass on a planar surface, whereas actual failure surfaces are commonly rotational or comprised of multiple blocks. Both upstream and downstream movements can contribute to settlement of the crest. Also, deformation may occur along any one of several potential slide surfaces at various times during the earthquake, as a result of strengths varying with position within the cross section (and possibly with time) and variable amplification of the ground motion as a function of the dam height. Slide surfaces at higher elevations in the dam may be fully contained by slide surfaces at lower elevations, thus isolating the upper slide surface from ground motions.

Regardless of whether it is site-specific or one of the simplified forms, a Newmark analysis must be regarded as an approximate indication of the size of the deformations, not a precise prediction.

Newmark analysis of an embankment with a liquefied foundation, or any slope with static FS only slightly greater than 1.0, can produce unrealistically large predicted displacements. If the analysis indicates dynamic displacements of tens or hundreds of feet for a stable slope, there may have been some violation of the assumptions of the program; the results may not be credible. However, if the post-earthquake static factor of safety is less than 1.0, flow sliding can cause displacements that large.

13.9.4   Nonlinear Finite Element/Finite Difference Deformation Analysis

With the advent of relatively inexpensive computing, it has become feasible to perform nonlinear finite-element or finite-difference analyses to model permanent deformations of earth structures, including the effects of generation of excess pore pressure in saturated soils. Numerous computer codes have been written, including OPENSEES, TARA, SWANDYN, PLAXIS, and FLAC. At present (2015), Reclamation uses FLAC almost exclusively, although no single program is universally preferred by the profession. Refer to the user's manual for each program, and to other publications on nonlinear analysis. To date, these analyses have had some success in reproducing the behavior in known cases of seismic loading in back analysis; however, they have not actually been tested in forward analysis of sites that were subsequently affected by major earthquakes to verify the prediction. These analyses should not be considered definitive predictions, but they can be quite useful for showing general trends in deformation and other behavior, and for evaluating sensitivity to variations in input assumptions. For a new dam or modifying an existing dam, risk considerations would generally indicate that a generous margin is needed in, for example, the amount of freeboard to be provided, rather than relying strictly on the results of deformation analysis.

13.10 Other Issues Affecting Seismic Safety of Embankment Dams

13.10.1 Embankment Cracking

Strong earthquake movements can cause cracking of an embankment, which can lead to failure if the water can flow through the cracks and erode the embankment or abutments. In 2010, Reclamation's All American Canal very nearly failed by internal erosion at a siphon structure following the M_W 7.2 Sierra El Mayor

Earthquake; only rapid action prevented the failure (Dewey and Palumbo, 2011). Rogers and Coleman Dams, both small concrete diversion structures, failed in the 1952 Fallon, Nevada earthquake, apparently because of erosion through cracks in earthfill closure sections between the concrete dam and the abutments, breaching them (Seed, Makdisi, and DeAlba, 1978). Differential settlements or strong earthquake motions parallel to the dam axis can cause transverse cracking (perpendicular to the axis) of the embankment crest by creating tensile strains. Motion perpendicular to the axis could also cause transverse cracking where embankment movements are out of phase with the movement of the abutments. Transverse cracking is most likely to occur at sharp bends in the embankment alignment, abrupt changes in the height of the embankment ("stairsteps" in the foundation), or where there is a "soft" inclusion in the embankment or foundation, such as a transition from a bedrock foundation to a soil foundation. Compacted embankment materials (other than clean, coarse-grained material) commonly display enough apparent cohesion (due to capillarity) to permit vertical cracks to remain open to a depth of tens of feet, if they are somehow created and not closed by subsequent shaking. This could create an open path for the flow of water, which could erode a breach in the embankment if there is not an adequate filter downstream to stop the movement of eroded particles.

Dynamic FEM/FDM analysis may provide some insight into potential locations for tensile or shear strains that would cause cracking. Three-dimensional analysis could directly model how abrupt changes in foundation materials, steep abutments, etc. affect the response and strains. Two-dimensional analysis (more readily available) would be less effective; however, if a number of cross sections are analyzed, it could help identify vulnerable areas if closely spaced cross sections respond strongly out of phase with each other or undergo very different amounts of settlement.

Longitudinal cracking (i.e., cracking parallel to the axis) can result from settlement of the shells or the material that they bear upon, from instability of slopes, or from dynamic yield with smaller movements. Purely longitudinal cracks would not, by themselves, threaten the safety of the dam, but could be a problem in association with other damage to the embankment, such as transverse cracks.

13.10.2 Damage to Appurtenant Features Within or Adjacent to the Embankment

Appurtenant features like spillways, outlet works, and penstocks can be damaged by shaking or by deformation of the embankment. This could potentially cause failure of the dam by exposing the embankment to erosive flow from the reservoir. Several potential failure modes are presented here, but analytical methods are not presented.

The walls of spillway chutes and crest structures often act as retaining walls for the adjacent dam embankment; many older walls were not designed for the earthquake loadings now considered possible at the site. Should a wall fail while the reservoir is near or above the elevation of the spillway crest, the embankment could be exposed to the reservoir, either as open-channel flow or as flow through transverse cracks if the wall is deflected without complete structural failure. This is more likely to be a problem with gated spillways because water is routinely stored tens of feet above the spillway crest. (The gates themselves and the piers that support them may also be vulnerable.)

The seismic analysis of retaining walls has historically used simplified methods to estimate the seismic loading, primarily Mononobe and Okabe's, which is an extension of Coulomb active force to include horizontal acceleration; and Wood's solution, which is based on elastic response of the soil against the wall. (Mononobe and Matsuo, 1929; Wood, 1973). There is some indication from laboratory experiments and field performance that these methods tend to produce conservative results (Al Atik and Sitar, 2009), but they may still be acceptable for small structures or where minor conservatism is not a problem. For major structures, the simplified methods have largely been replaced by dynamic FEM analysis. For details on implementing various methods of analysis for retaining walls, refer to Ebeling and Morrison (1992).

If an outlet works or spillway is constructed as a conduit through or at the base of an embankment, displacement of the embankment slopes could pull it apart longitudinally, exposing the embankment to flowing water. Damaged conduits or intake towers could also create new seepage paths that could allow internal erosion along the outside of a conduit, into it, or out of it, with the potential to cause internal erosion.

13.10.3 Settlement Due to Densification

If earthquake ground motions are sufficient to cause generation of excess pore pressures, there may be settlement due to consolidation, as the excess pore pressures dissipate. Loose, nonsaturated materials may also densify, causing settlement during the course of the earthquake. In very loose materials under high overburden stress, the volumetric strain could be as great as 5 percent, but smaller strains are more likely. Ishihara (1993) suggests a procedure for estimating the strain due to dissipation of excess pore pressure if using an upper bound of 5 percent is not sufficiently precise. Volumetric strains would usually cause much smaller settlements than shear strains would, but it is prudent to check how much settlement would occur from volumetric strain. This could be important for a modified embankment that has liquefiable material remaining under the embankment.

13.10.4 Fault Rupture in Embankment Foundation

If there is potential for fault rupture or structural folding in the dam foundation, it is necessary to assess the response of the embankment to the movement. The failure of Baldwin Hills Dam is thought to have resulted from aseismic fault movement that damaged the fragile asphalt membrane lining the reservoir, which led to failure by internal erosion (Jansen, 1980). Two small dams constructed directly over the San Andreas Fault held water at the time of the 1906 San Francisco earthquake; one failed and one did not. Possibly, the difference in behavior was because the one that failed had a steel outlet conduit through it. If embankment or foundation soils are disrupted by the movement, there is potential for failure of the dam by internal erosion, unless the damaged area is adequately filtered and drained by foundation or embankment materials. There is no simple procedure that can directly analyze this issue, although nonlinear FEM/FDM modeling may provide some insight into the behavior of the embankment. Sherard et al. (1974) and Bray (1990) summarize most of the available information and design approaches for dealing with foundation faults. Judgments are required regarding whether the disrupted embankment or foundation soils would be self-healing and prevent erosion in the cracks that could lead to a breach of the dam. Self-healing could result if cracks do not remain open to act as preferential seepage paths, if properly graded filters remain in place and block further movement of eroded particles, or if upstream material is washed into the cracks and plug them. Thin and/or brittle core materials would be the most vulnerable. Very wide protective drains and filters are important for controlling the seepage following the fault movement. Drainage would be necessary to relieve high water pressure caused by flow from the reservoir through the fault and damaged embankment,. There should also be sufficient weight of fill to prevent heave or blowout if the drains cannot fully relieve the pressure. Filters are required to prevent internal erosion into the drains. The filter and drainage zones need to be wide so that they would remain continuous with large fault offsets. All of these features were included in the modification of Reclamation's Lauro Dam, California, which was found to have an active fault in its foundation. Lauro Dam was also equipped with an automatic shutoff valve at the upstream end of the outlet works conduit, so that damage to the conduit would not release large amounts of erosive flow against the embankment.

13.10.5 Seiche Waves and Solitary Waves

Seiche waves are long-period waves caused by "sloshing" or oscillating of the reservoir within its basin. There is usually no visible surface wave. Instead, an observer would instead perceive the reservoir surface as remaining horizontal, but rising and falling away from its static level, while the opposite occurs on the other side of the reservoir. For an earthquake to cause significant seiche waves that could overtop the dam, it would likely need to be accompanied by either a large landslide, or coseismic movement of the reservoir basin (vertical fault

displacement within the reservoir, or tilting of the reservoir basin). The 1959 Hebgen Lake Earthquake caused the basin of Hebgen Lake to tilt away from Hebgen Dam. The initial movement of water was away from the dam (upstream), but three or four long-period waves poured over Hebgen Dam because the reservoir basin tilted. Because the tilt of the basin was upstream, the dam actually had more freeboard after the earthquake. The waves caused remarkably little erosion, although the dam was severely damaged by other mechanisms (USGS, 1964). Solitary waves and surges are fast-moving waves from a sudden disturbance of the reservoir. These can occur when water is displaced by a large landslide moving rapidly into the reservoir, as occurred disastrously at Vaiont Dam in Italy (Jansen, 1980), or when coseismic movement raises or lowers a portion of the reservoir. Reclamation has performed similar analyses for coseismic movement at Jackson Lake Dam in Wyoming, and Lake Tahoe on the California-Nevada state line (Dewey and Dise, 1987) (Older reports may refer to the computer program LSWAVE, developed by Reclamation (Pugh and Chiang, 1986), but it is no longer used.) More recently, Reclamation has hired consultants to model overtopping of Arthur V. Watkins Dam, Utah, using newer methods. There, the overtopping potential was compounded by the potential for large embankment settlement.

Although very uncommon, seiche waves 1 ft higher or more can be induced in a small or narrow reservoir by earthquake vibration alone. Both the 1964 Alaska Earthquake and the 2002 M 7.9 Denali Earthquake (also in Alaska) caused waves on Lake Union near Seattle that were large enough to damage houseboats (Barberopoulou et al., 2004). This would require strong ground motions with long duration and unusually long periods comparable to the natural periods of oscillation of the reservoir. Although possible, it is unlikely that waves occurring purely as a result of ground accelerations would be big enough to threaten the dam unless the freeboard was very small. Extensive analysis of reservoir bathymetry and ground-motion spectral characteristics is needed to predict the amplitude of waves caused by earthquake vibration.

The evaluation of overtopping by seiche waves or solitary waves needs to consider the possible reduction in dam crest elevation resulting from earthquake-induced deformation of the embankment and/or from coseismic movement.

13.11 Historic Bureau of Reclamation Practices for Seismic Analysis of Embankment Dams

The safety of every Reclamation dam is reviewed periodically, including review of previous analyses, which may have been based on versions of this design

standard chapter that are superseded by this one (Reclamation, 1989, 2001). Engineers need to understand the older work so that its conclusions can be evaluated and compared with modern practice. The descriptions of older practice that follow are for information only; they are not recommended for further use.

13.11.1 Deterministic Assessment of Dam Safety

The most important difference between current practice and Reclamation practice prior to the mid-1990s is the almost complete shift from standards-based deterministic analysis, to risk analysis. Formerly, each dam was required to withstand the maximum credible earthquake (MCE) for the site, regardless of how unlikely the MCE might be. If analysis indicated that it might not withstand the MCE, that was considered a dam-safety deficiency, and modification was required.

Typically, the Seismotectonics and Geophysics Group would identify MCEs from one or more sources. These sources could be the maximum magnitude an individual fault could produce, or they could be inferred from background seismicity. Multiple MCE sources were sometimes reported because, before doing the liquefaction or deformation analysis, it may not have been obvious which source would actually produce the most severe loading for a given structure. In liquefaction analysis, for example, a larger earthquake occurring farther away can be more severe than a smaller one located closer to the site, even if the peak horizontal ground acceleration (PHA) is not as high. This is due to the greater number of cycles of shaking expected from the larger magnitude. (Refer to section 13.6.2.3 for the magnitude scaling factor, MSF, which accounts for the greater duration of larger-magnitude earthquakes.)

Currently, in 2015, dam-safety decisions are guided, not by the response of the dam in the MCE, but by probabilistic risk analysis that considers the probability of a breach over the full range of potential loadings, and the probability of the loadings. (Risk-analysis methodology is not described here; refer to other publications, including the most recent versions of Reclamation's manuals for dam-safety risk-analysis.) To support the risk analysis, PSHA is performed, incorporating multiple sources and the full range of magnitude and A_{max} from each source (not just its MCE). This allows an annual probability to be associated with any level of earthquake loading; combining that with the probability of failure, given occurrence of each loading, allows calculation of the annual probability of dam failure, for comparison with other dams and with the public protection guidelines. The risk is sometimes dominated by earthquakes not much larger than the threshold because they are so much more probable than the extreme loadings.

13.11.2 Liquefaction Assessment

Liquefaction practice has evolved substantially since previous versions of this design standard chapter were published. Reclamation practice for assessing liquefaction potential has long been based primarily on updates of the simplified Seed-Lee-Idriss approach (Seed, Lee, and Idriss, 1969; Seed, 1987; Seed et al., 1985; Seed and Harder, 1990; NCEER, 1997). The NCEER report was of particular importance because it contained general consensus on what procedures constituted the state of practice and identified some areas where further development was needed. Updates made since 1997 have benefited from numerous additional case histories that have become available since the NCEER report. Specifics of the updates are provided in appendices of this chapter of Design Standard 13. Historically, the most commonly used index of density and cyclic resistance has been the standard penetration test (SPT), with the cone penetration test (CPT) and shear-wave velocity (V_S) being considered strictly secondary. The CPT has a greater place in Reclamation practice now, although its utility is still limited by the geology at many sites, particularly those with alluvium containing large amounts of gravel or cobbles.

Liquefaction is a component of some important seismic potential failure modes (PFMs). Probabilistic risk analysis of those PFMs requires liquefaction probability for the full range of possible earthquake loadings, not just liquefaction potential with the MCE. Therefore, Reclamation began using probabilities based on regression analysis of case history data, beginning with the early work by Liao et al. (1988) and, later, Youd and Noble (1997), Cetin et al. (2006), Idriss and Boulanger (2010), and Boulanger and Idriss (2014). Because of differences in methodology and updated data bases, probability estimates from different models can differ widely. Refer to appendices B, C, and E for current practice, based on SPT, CPT, and VS, respectively.

It was not universally recognized that typical published curves indicating the CRR as a function of in situ tests are not deterministic, even though they were often treated as such. The fact that the CSR is less than the CRR does not necessarily preclude liquefaction. Beginning with early versions by Seed in the 1970s, the CRR curves were actually intended to represent approximately 15 percent probability of liquefaction. Subsequent statistical analysis by Idriss and Boulanger (2010) showed that Seed's 1987 SPT-CRR curve was remarkably close to 15-percent probability, even with many more data added from later earthquakes. According to their model, the probability of liquefaction decreases to 2 percent with FS of 1.15 applied to the "deterministic" curve. (Cetin et al. [2004] concluded that the curve for 15-percent probability should pass through much lower values of CSR than indicated by Idriss and Boulanger and in earlier versions of the method.)

Cyclic stresses have most often been calculated by 1D equivalent-linear response using SHAKE, or by equation 4 with an earlier version of the r_d curves in

figure 13.6.2.1-1, which was based on numerous SHAKE runs. Strictly speaking, figure 13.6.2.1-1 and equation 4 are both for level ground, although the error diminishes somewhat with depth below the embankment. With computer programs for 2D FEM response analysis now readily available, there is less justification for 1D response analysis for cyclic shear stresses.

Equation 4 has been used with a value of A_{max} representing a bedrock outcrop, rather than a soil surface, which is incorrect and can be very unconservative because the soil tends to amplify the acceleration.

SPT blow counts and logs prior to about 2000 require scrutiny because drilling procedures were not standardized. In particular, some older data were measured in drill holes below the water table without an adequate depth of drill fluid or water to prevent heave or boiling at the bottom of the hole. Without fluid or water, unrealistically low blow counts may have been measured. Even later than 2000, equipment and procedures have not been fully standardized.

Section 13.7.2 above describes the use of criteria by Bray and Sancio (2006) to rule out liquefaction in fine-grained materials, based on the PI and the ratio of the water content to the LL. These criteria superseded an earlier set of criteria that was referred to informally as the "Chinese criteria" (Wang, 1979). The Chinese criteria indicated that liquefaction could be ruled out on the basis of high LL or a high percentage of particles smaller than 0.005 millimeter. However, it has since been shown that neither of those criteria successfully rules out liquefaction (Bray and Sancio, 2006). It is likely that the major differences between the two sets of criteria occur, in part, because Wang's data set was too limited. Both Wang (1979) and Bray and Sancio (2006) concluded that liquefaction would be precluded by a water content that is enough lower than the LL (provided that the water content is correct). Wang's criterion was less conservative, allowing water content as high as 90 percent of LL to preclude liquefaction, whereas Bray and Sancio limited it to 80 to 85 percent. Complications arise because the water content is generally measured for the whole sample, but the Atterberg limits are determined for the fraction finer than the U.S. Standard No. 40 sieve. Older analyses may not have compensated for that by adjusting the water content according to equation 11, or similar procedure, which would be unconservative. (It would also be unconservative to apply the water-content criterion to a sample that could have lost moisture in sampling and handling.)

13.11.3 Stability and Deformation Analysis

Prior to the widespread use of nonlinear deformation analysis in Reclamation, the typical practice for stability analysis was limit equilibrium analysis by a method of slices, most commonly Spencer's method in UTEXAS2, SLOPE/W, or an earlier program. Typically, the minimum acceptable post-earthquake static FS was 1.3; if this was not met, it was considered a dam-safety deficiency requiring corrective action. Higher FS were sometimes judged necessary if the duration of

shaking was expected to be long, or if the freeboard was small. Stability analysis was generally not required unless widespread liquefaction was expected to occur with the MCE.

With liquefaction (or other significant loss of strength) predicted for a large area of the embankment or foundation, post-earthquake static stability was analyzed, usually with residual undrained shear strengths in liquefied material, S_{ur}, from the correlation with SPT blow count by Seed and Harder (1990). For a few Reclamation dams, stability was analyzed using undrained steady state strength, S_{uss}, from very careful sampling and laboratory testing following a method described by Poulos, Castro, and France (1985). The Seed and Harder correlation is now generally acknowledged as somewhat conservative for dams because it does not allow for an increase in strength with the high overburden that occurs under the embankment fill (Seed, personal communication; Idriss and Boulanger, 2008). At present (2015), there is still no consensus in the industry, even for the correct format for S_{ur} correlations. The S_{uss} procedure, like any other laboratory method, is unable to capture all behavior of large masses of soil, including the effect of settlement and void migration within the liquefied deposit. This effect can create a loosened zone, or even a water film at the top of the liquefied soil. Refer to appendix F for current S_{ur} procedures, which rely primarily on correlation with penetration tests as indices of density.

Until the late 1990s, deformation analysis with liquefied materials was uncommon at Reclamation. Previously, deformation was usually analyzed by Newmark's sliding-block analysis (Newmark, 1965), in the form of either a numerical analysis with site-specific ground motions, or the simplified method by Makdisi and Seed (1977), based on the Newmark method. Makdisi and Seed's analysis was most often applied using Reclamation's computer program, SEIDA. Newmark and Makdisi-Seed analyses were usually performed with drained soil strengths, rather than undrained strengths appropriate for saturated soils in rapid loading. Calculated settlements rarely exceeded a few tenths of a foot, which is consistent with historic behavior of well-built dams. However, this was unconservative for some dams because of liquefaction potential or of fine-grained foundation materials with undrained strengths lower than their drained strengths. Strength assumptions should always be verified before relying on results of an older analysis.

Older reports may mention an approximate analysis of the movement of an unstable slope by analyzing the stability of the slope after some amount of deformation has occurred. (This was informally known as the "squashed dam" analysis.) It was done by postulating the configuration of the dam after deformation, then finding the static FS of the deformed embankment. Unless the calculated FS was above about 1.1 (to allow for the effects of momentum), additional movement could be expected. If the result was much higher than 1.1, the movement was likely over-estimated. In either case, the deformed section would have to be revised and analyzed again.

The squashed-dam procedure was used only occasionally, and it is no longer used at all, now that nonlinear deformation analysis is readily available; it is mentioned here for historic information only.

13.12 Seismic Design for New Dams

New dams are required to meet Reclamation's public protection guidelines in order to be accepted by the dam-safety program (Bureau of Reclamation, 2011). More specifically, the embankments must be shown to be reliably stable during and following a major earthquake, not subject to excessive deformation, and resistant to internal erosion resulting from embankment cracking or foundation fault movement. **A new dam should be designed so that changes in the state of practice, updated seismic hazard studies, and population increases would be very unlikely to raise the estimated risk to near or above the guidelines. Regardless of quantitative risk estimates, a new dam must incorporate defensive design measures and redundancy as required to ensure that its performance will clearly be adequate under the most severe earthquake loading that is plausible for the site.**

Adequate seismotectonic studies must be performed prior to final design so that valid seismic design parameters can be used in the design.

As applicable, the defensive measures should include:

- Removal or treatment of foundation materials that are of low strength or of insufficient density to preclude strength loss during plausible earthquakes.

- Shaping of the embankment foundation to minimize potential for cracks that could allow erosion. Shaping should remove abrupt changes in embankment height in the cross-valley direction ("stair steps" in the foundation) and, ideally, avoid having the foundation surface slope downstream. The foundation should slope no steeper than 2H:1V in the cross-valley direction, or 4H:1V downstream.

- Transition and drainage zones with gradations that are controlled by processing or careful selection to provide filter compatibility and adequate drainage capacity in case of cracking of embankment or foundation.

- A sand-and-gravel upstream crackstopper zone that can be washed into cracks by flowing water to help plug them, to provide additional "self-healing" capability. This concept was incorporated into embankment designs as early as the 1930s (for example, Coyote Dam in California), although its effectiveness has never been tested in the performance of an embankment with deep, open, transverse cracks. If a crackstopper is provided, there must also be a pervious downstream zone that is fine

enough to prevent the crackstopper material from being carried all the way through transverse cracks to the downstream face, where it would be ineffective.

- Generous thickness of the core, filters, and drainage zones. If the core is relatively thin (due to limited supply in borrow areas), it should be flared at the abutments to provide longer seepage paths where there is greater potential for cracking or erosion due to flow in fractured abutment bedrock. Plastic borrow material should be selected for the contacts for greater erosion resistance. It is best to make the core thicker throughout the length of the dam if the available borrow areas allow it, to provide an additional margin of safety against crack erosion.

  Controlled compaction of all embankment zones to high density, typically specified as a minimum density of 95 to 98 percent of the laboratory maximum density (ASTM D 698 12, D7382 08, or D4253 00 as appropriate), except for filters and gravel drains, as discussed below. For embankment materials containing fines, it may help to minimize cracking if the fill is placed slightly wetter than the optimum water content, rather than slightly dryer.

- FS for static slope stability under high-level,-steady-state seepage conditions at least 1.5.

- Generous freeboard, at least 5 to 10 percent of the embankment height (depending on the severity of design earthquake loading) and never less than 3 feet, as described in *Design Standard 13 – Embankment Dams*, Chapter 6, "Freeboard."

- Design of embedded structures, such as spillways and outlet works, to withstand earthquake loading without excessive deflection, with engineered filters and drains around them in case cracking does occurs. Embedded structures must be sited to minimize their impact on the performance of the embankment, so they do not promote cracking or create vulnerability to internal erosion.

- Treatment of potentially unstable slopes around the reservoir rim.

This list is based in large part on ICOLD (2001).

Good design practice for a new dam would address all plausible PFMs. For a new dam, redundant defensive measures can often be included for relatively little additional expense, compared to the cost of building the dam without them. For example, a thick filter may not cost much more than a thin one, if the additional cost of material is offset by savings on the cost per cubic yard from constructing it using larger equipment.

Filters should be designed according to *Reclamation's Design Standards No. 13 - Embankment Dams*, Chapter 5, "Protective Filters." For dams in general, but particularly for those in seismic areas, it is important that filters be able to deform without leaving open cracks. Open cracks are most likely in the upper part of a dam, where there is little overburden pressure to help close them. Therefore, filters should not contain more than 5 percent fines, in place, after compaction because fines promote capillary tension that could help cracks remain open in partially saturated filters. In addition, filters should not contain binding or cementing agents (such as salts on particle surfaces) or more than 3 percent mica, which readily breaks down into fines. Even microbes, notably iron-fixing bacteria, have been found to act as binding agents. Filters and gravel drainage zones should not be made too loose, so that they would be liquefiable, or too dense. Higher densities increase the potential for brittle behavior and cracking. Redlinger et al. (2012) and Bureau of Reclamation (2014) report experiments on the performance of cracked filters. One the important finding is that cracks in compacted sand filters cannot be relied upon to slump closed as soon as they are wetted by water in the cracks, except with very careful selection, processing, and placement. Also, if filters and drains are compacted too densely, their permeability can be impaired, particularly their vertical permeability, because overcompacting causes particle breakdown, which forms a thin, less-pervious layer at the top of each lift. No standard practice for filter density has been established at present, but the interim guidance is for compaction to at least 90 percent of the laboratory maximum density, but no more than 94 percent. Higher overburden stress would help close cracks, as would saturation during normal operation. It may be appropriate to use different compaction standards in different parts of the embankment, to minimize liquefaction potential in saturated portions, and to minimize cracking potential higher in the embankment where the filter may not get saturated in normal operation. Laboratory cyclic shear testing of material from the borrow area or processing plant may be informative for finding a balance between minimizing cracking and preventing liquefaction.

13.13 Remedial Measures for Existing Dams

It is not unusual for existing dams to require modification to improve their safety against seismic instability, deformation, and/or cracking. There may have been changes in the state of engineering practice, so that a previously unrecognized problem becomes apparent, or an updated seismotectonic study may find that the potential for loading is more severe than was recognized at the time the dam was designed. In general, upgrading existing dams is more complicated (and occasionally more expensive) than constructing new dams to meet the same standards or risk guidelines. Complication can arise from a number of conditions, including, but not limited to:

- The need to accomplish construction very quickly and/or without disrupting the water supply.

- A small working area that makes it difficult to use large construction equipment.

- Limited availability of suitable borrow materials, or borrow areas that require dewatering because they are within the reservoir.

- Difficulty of treating the embankment foundation due to a high water table.

- The need to excavate a major portion of the embankment or its foundation while there is water in the reservoir.

The design and construction methods must not unnecessarily increase the risk to the public downstream of the dam for the sake of expedience or economy.

In general, the modification concept should take a "holistic" approach, i.e., one that considers all potential failure modes together (not just the seismic modes). For example, if filtering of foundation seepage is required, that might be combined with excavation and replacement of foundation soil to create a "shear key" to support a berm that would buttress the downstream slope of the embankment against seismic instability.

Modifications of existing embankments for seismic safety could include:

- Foundation treatments and/or berms to improve the post-liquefaction stability of the embankment

- Crack-stoppers and filters to protect against internal erosion following cracking of the embankment resulting from shaking or fault movement in the foundation

- Widening of the embankment crest so that a portion of the embankment (usually the upstream slope) could slump or slide without causing a catastrophic release of the reservoir

- Filtered drains to lower the phreatic/piezometric levels in foundation or embankment

- Structural modifications of appurtenant structures such as spillway retaining walls

- Complete reconstruction of inadequate embankments or appurtenant structures

Appendix G summarizes current practice for improving seismic performance of existing embankment dams.

Nonstructural alternatives for achieving dam-safety objectives without actually modifying the dam exist, and may need to be evaluated as part of a Corrective Action Study:

- Temporary or permanent reservoir restriction, with an alternative water supply, if needed

- Early warning system

- Improved emergency action plan

- Relocating people at risk out of the area of potential flooding

13.14 References

Adhya, Kiran K. 1982. "SEIDA - A Computer Program for Simplified Earthquake-Induced Deformation Analysis of Homogeneous Embankment Dam." Bureau of Reclamation, Denver, Colorado.

Al Atik, Linda, and Nicholas Sitar. 2009. "Experimental and Analytical Study of the Seismic Performance of Retaining Structures." Pacific Earthquake Engineering Research Center Report No. PEER 2008/104.

Ambraseys, N.N. 1988. "Engineering Seismology," *International Journal of Earthquake Engineering and Structural Dynamics*, Vol. 17, No. 1, pp. 1-105.

Andrus, R.D., and K.H. Stokoe II. 2000. "Liquefaction Resistance of Soils from Shear-Wave Velocity," *Journal of Geotechnical and Geoenvironmental Engineering*, Vol. 126, No. 11, pp. 1015-1025.

Armstrong, R.J., and E.J. Malvick. 2014. "Comparison of Liquefaction Susceptibility Criteria," *Proceedings of the 34th Annual USSD Conference, United States Society on Dams,* Denver CO, pp. 29-37.

Barberopoulou, A., A. Qamar, T. Pratt, K. Creager, and W. Steele. 2004. "Local Amplification of Seismic Waves from the Denali Earthquake and Damaging Seiches in Lake Union, Seattle, Washington," *Geophysical Research Letters*, Vol. 31.

Bjerrum, L. 1973. "Problems of Soil Mechanics and Construction on Soft Clays," *Proceedings, 8th International Conference on Soil Mechanics and Foundation Engineering, Moscow*, Vol. 3, pp. 111-159.

Boore, David M. 2004. "Can Site Response Be Predicted?" *Journal of Earthquake Engineering*, Vol. 8, Special Issue 1, pp. 1-41.

Boulanger, R.W. 2003a. "Relating Kα to Relative State Parameter Index," *J. Geotechnical and Geoenvironmental Eng.*, ASCE 129(8), pp. 770-773.

Boulanger, R.W. 2003b. "High Overburden Stress Effects in Liquefaction Analyses," *J. Geotechnical and Geoenvironmental Eng.*, ASCE, 129(12), pp. 1071–1082.

Boulanger, R.W., and I.M. Idriss. 2004. "State Normalization of Penetration Resistances and the Effect of Overburden Stress on Liquefaction Resistance," *Proceedings, 11th International Conference on Soil Dynamics and Earthquake Engineering, and 3rd International Conference on Earthquake Geotechnical Engineering*, D. Doolin et al. (eds.), Stallion Press, Vol. 2, pp. 484-91.

Boulanger, R.W., and I.M. Idriss. 2014. *CPT and SPT Based Liquefaction Triggering Procedures.* University of California at Davis Center for Geotechnical Modeling, Report No. UCD/CGM.

Boulanger, R.W., M.W. Meyers, L.H. Mejia, and I.M. Idriss. 1998. "Behavior of a Fine-Grained Soil During Loma Prieta Earthquake," *Canadian Geotechnical Journal*, Vol. 35, No. 1, pp. 146-158.

Boulanger, R.W., and R.B. Seed. 1995. "Liquefaction of Sand Under Bidirectional Monotonic and Cyclic Loading," *Journal of Geotechnical Engineering,* Vol. 121, No. 12, pp. 870-878.

Bray, J.D. 1990. "The Effects of Tectonic Movements on Stresses and Deformations in Earth Embankments." Doctoral Dissertation, Department of Civil Engineering, University of California - Berkeley.

Bray, J.D., and R.B. Sancio. 2006. "Assessment of the Liquefaction Susceptibility of Fine-Grained Soils," *J. Geotechnical and Geoenvironmental Eng.,* ASCE 132(9), pp. 1165–177.

Bray, J.D., and T. Travasarou. 2007. "Simplified Procedure for Estimating Earthquake-Induced Deviatoric Slope Displacements," *J. Geotech. Geoenv. Eng.*, Vol. 133, No. 4, pp. 381-392.

Bureau of Reclamation, 1983. *DYNDSP – User's Manual - A Computer Program for Estimating Displacement of Rockfill Dams Due To Seismic Shaking.* Denver, Colorado.

Bureau of Reclamation. 1989. *Design Standards No. 13 – Embankment Dams,* Chapter 13, "Seismic Design and Analysis," Denver Office, Denver Colorado.

Bureau of Reclamation. 1998, 2001. *Engineering Geology Field Manual.* Volume I, Second Edition.

Bureau of Reclamation. 2001. *Engineering Geology Field Manual.* Volume II, Second Edition.

Bureau of Reclamation. 2007. *Evaluation of In Situ Methods for Liquefaction Investigation of Dams,* Research Report DSO-07-09. Prepared by William Engemoen.

Bureau of Reclamation. 2011. *Dam Safety Public Protection Guidelines - A Risk Framework to Support Dam Safety Decision-Making* (interim).

Bureau of Reclamation. 2014. *Large-Scale Filter Performance Tests – Results of "Crack-Box" Testing.* Research Report DSO-2014-05. Prepared by Ted Howard, Caleb Rudkin, and Peter Irey.

Cao, Z., T.L. Youd, and X. Yuan. 2013. "Chinese Dynamic Penetration Test for Liquefaction Evaluation in Gravelly Soils," *J. Geotechnical and Geoenvironmental Eng.,* 139, No. 8, pp. 1320-1333.

Castro, G., R.B. Seed, T.O. Keller, and H.B. Seed. 1992. "Steady-State Strength Analysis of Lower San Fernando Dam Slide," *Journal of Geotechnical Engineering,* ASCE, Vol. 118, No. 3, pp. 406-427.

Cetin, K.O., R.B. Seed, A. Der Kiureghian, K. Tokimatsu, L.F. Harder, R.E. Kayen, and R.E.S. Moss. 2004. "Standard Penetration Test-Based Probabilistic and Deterministic Assessment of Seismic Soil Liquefaction Potential," *J. Geotechnical and Geoenvironmental Eng.*, ASCE 130(12), pp. 1314–340.

Dewey, R.L., and K.M. Dise. 1987. "Fault Displacement Seiche Waves on Inland Reservoir and Lakes," *Wind and Seismic Effects: Proceedings of the 18th Joint Meeting of the U.S. - Japan Cooperative Program in Natural Resources, Panel on Wind and Seismic Effects.* National Bureau of Standards Publication NBSIR 87 3540.

Dewey, R.L., and D. Palumbo. 2011. "Near Failure of the All American Canal in Southern California Due to a 7.2 Magnitude Earthquake in April 2010," *Proceedings, 31st Annual USSD Conference.* United States Society on Dams, San Diego California, pp. 1437-1450.

Dobry, R., and T. Abdoun. 2011. "An Investigation into Why Liquefaction Charts Work: A Necessary Step Toward Integrating the States of Art and Practice" (Ishihara Lecture), *Proceedings, 5th International Conference on Earthquake Geotechnical Engineering.* Santiago, Chile, pp. 13-45.

Dobry, R., and L. Alvarez. 1967. "Seismic Failures of Chilean Tailings Dams," *Journal of the Soil Mechanics and Foundations Division*, ASCE, Vol. 93, No. SM6, pp. 237-260.

Ebeling, R.M., and E.E. Morrison. 1992. *The Seismic Design of Waterfront Retaining Structures.* U.S. Army Technical Report ITL-92-11, U.S. Navy Technical Report NCEL TR-939, U.S. Army Corps of Engineers, Waterways Experiment Station.

Edris, E.V., and S.G. Wright. 1992. *User's Guide: UTEXAS3 Slope Stability Package.* U.S. Army Corps of Engineers, Waterways Experiment Station Instruction Report GL 87 1.

Finn, W.D., D.J. Pickering, and P.L. Bransby. 1971. "Sand Liquefaction in Triaxial and Simple Shear Tests," *J. Soil Mechanics and Foundations Div.*, ASCE, Vol. 97, No. SM4, pp. 639-59.

Geo-Slope International, Ltd. 2014. *User's Manual for Geo-Studio 2012.* Calgary, Alberta.

Harder, L.F., Jr. 1991. "Performance of Earth Dams During the Loma Prieta Earthquake," *Proceedings: Second International Conference on Recent Advances in Geotechnical Earthquake Engineering and Soil Dynamics.* March.

Harder, L.F., Jr., and H.B. Seed. 1986. *Determination of Penetration Resistance for Coarse-Grained Soils Using the Becker Hammer Drill.* Report No. UCB/EERC-86-06, Earthquake Engineering Research Center, University of California, Berkeley.

Hudson, M.B., I.M. Idriss, and M. Beikae. 1994. *User's Manual for QUAD4M.* Center for Geotechnical Modeling, University of California - Davis.

Hynes-Griffin, M.E. 1987. *Seismic Stability Evaluation of Folsom Dam and Reservoir Project.* Technical Report GL-87-14. Report No. 1 - Summary Report. U.S. Army Corps of Engineers, Waterways Experiment Station, Vicksburg Mississippi.

Hynes, M.E., and A.G. Franklin. 1984. "Rationalizing the Seismic Coefficient Method." U.S. Army Corps of Engineers, Waterways Experiment Station, Miscellaneous Paper GL-84-13, Vicksburg, Mississippi.

Hynes, M.E., and R. Olsen. 1999. "Influence of Confining Stress on Liquefaction Resistance," *Proceedings, International Symposium on Physics and Mechanics of Liquefaction.* Balkema, Rotterdam, pp. 145-152.

ICOLD. 2001. "Design Features of Dams to Resist Seismic Ground Motion - Guidelines and Case Studies." Bulletin 120, International Commission on Large Dams, Paris, France.

Idriss, I.M. l999. "An Update to the Seed-Idriss Simplified Procedure for Evaluating Liquefaction Potential." *Proceedings, TRB Workshop on New Approaches to Liquefaction.* Publication No. FHWA-RD-99-165.

Idriss, I.M., and R.W. Boulanger. 2008. "Soil Liquefaction During Earthquakes," Monograph MNO 12. Earthquake Engineering Research Institute, Oakland, California.

Idriss, I.M., and R.W. Boulanger. 2010. *SPT-Based Liquefaction Triggering Procedures.* Report No. UCD/CGM 10/02, Center for Geotechnical Modeling, University of California - Davis.

Idriss, I.M., and J.I. Sun. 1992. *User's Manual for SHAKE91.* Center for Geotechnical Modeling, University of California – Davis.

Ishihara, K. 1993. "Liquefaction and Flow Failure During Earthquakes," *Géotechnique*, Vol.43, No. 3, pp. 351-415.

Itasca Consulting Group, Inc. 2014 *User's Manual for FLAC (Fast Lagrangian Analysis of Continua) Version 7.0.* Minneapolis Minnesota.

Jansen, R.B. 1980. *Dams and Public Safety.* U.S. Government Printing Office, Denver, Colorado.

Kammerer, A.M., R.B. Seed, J. Wu, M.F. Riemer, and J.M. Pestana. 2004. "Pore Pressure Development in Liquefiable Soils Under Bi-Directional Loading Conditions," *Proceedings, 11th International Conference on Soils Dynamics and Earthquake Engineering and 3rd International Conference on Earthquake Geotechnical Engineering,* Vol. 2, pp. 697-704, Berkeley, California.

Kayen, R., R.E.S. Moss, E.M. Thompson, R.B. Seed, K.O. Cetin, A. Der Kiureghian, Y. Tanaka, and K. Tokimatsu. "Shear-Wave Velocity-Based Probabilistic and Deterministic Assessment of Seismic Soil Liquefaction Potential," *J. Geotechnical and Geoenvironmental Eng.,* Vol. 139, No. 3 pp. 407-419.

Kuribayashi, E., and F. Tatsuoka. 1975. "Brief Review of Liquefaction During Earthquakes in Japan," *Soils and Foundations*, Vol. 15, No. 4, pp. 81-92.

Ladd, C.C. 1991. "Stability Analysis During Staged Construction," *J. Geotechnical Engineering,* ASCE Vol. 117, No. 4, pp. 538-615.

Ladd, C.C., and D. DeGroot. 2004. "Recommended Practice for Soft Ground Site Characterization: Arthur Casagrande Lecture," *12th Panamerican Conference on Soil Mechanics and Geotechnical Engineering*, June 23-25, 2003, Cambridge Massachusetts.

Lee, K.L., and A. Singh. 1971. "Relative Density and Relative Compaction," *Journal of Soil Mechanics and Foundations Division,* ASCE, Vol. 97, No. SM7, pp. 1049-1052.

Lekkas E. 2009. "Zipingpu Concrete Face Rockfill Dam Failures Caused by the 8.0R Earthquake on the 12th May 2008," *Geophysical Research Abstracts*, Vol. 11, EGU2009-7685, Chengdu, China.

Liang, L., J.L. Figueroa, and A.S. Saada. 1995. "Liquefaction Under Random Loading: Unit Energy Approach," *Journal of Geotechnical Engineering*, ASCE, Vol. 121, No. 11, pp. 776-781.

Liao, S.S.C., D. Veneziano, and R.W. Whitman. 1988. "Regression Models for Evaluating Liquefaction Probability," *J. Geotechnical Engineering Div.*, ASCE, Vol. 114, No. 4, pp. 389-411.

Lowe, John, III. 1988. "Earthfill Dams," *Development of Dam Engineering in the United States*. E.B. Kollgaard and W.L. Chadwick (eds.), Pergamon Press, New York.

Lunne, T., P.K. Robertson, and J.J.M. Powell. 1997. *Cone Penetration Testing in Geotechnical Practice*. Blackie Academic and Professional, London, UK.

Makdisi, F.I., and H.B. Seed. 1977. *A Simplified Procedure for Estimating Earthquake-Induced Deformations in Dams and Embankments*. University of California, Earthquake Engineering Research Center, Report No. UCB/EERC-77/19, Berkeley CA.

Miedema, D.G., and J.A. Farrar. 1988. "History and Investigation at Jackson Lake Dam," *Hydraulic Fill Structures*. Geotechnical Special Publication No. 21, American Society of Civil Engineers, New York, New York.

Mononobe, N., and M. Matsuo. 1929. "On the Determination of Earth Pressures During Earthquakes," *Proceedings, World Engineering Congress,* 9: 179-187.

Montgomery, J., R.W. Boulanger, and L.F. Harder, Jr. 2013. "Overburden Correction Factors for Predicting Liquefaction Resistance Under Embankment Dams," *Proceedings, United States Society on Dams*, Annual Meeting and Conference, Denver, Colorado.

NCEER. 1997. *Proceedings of the NCEER Workshop on Evaluation of Liquefaction Resistance, Salt Lake City, 1996.* National Center for Earthquake Engineering Research, Technical Report 97-0022.

Newmark, N.M. 1965. "Effects of Earthquakes on Dams and Embankments," *Géotechnique,* Vol. 15, No. 2, pp. 139-160.

O. Hungr Geotechnical Research, Inc. 2010. *User's Manual for Clara W, Slope Stability Analysis in Two or Three Dimensions for Microcomputers.* Vancouver, BC, Canada.

Olsen, R.S. 1997. "Cyclic Liquefaction Based on the Cone Penetrometer Test," *Proceedings, NCEER Workshop on Evaluation of Liquefaction Resistance, Salt Lake City, 1996.* National Center for Earthquake Engineering, Research Technical Report 97-0022.

Ordoñez, Gustavo. 2011. *User's Manual, SHAKE2000, A Computer Program for the 1-D Analysis of Geotechnical Earthquake Engineering Problems.*

Park, C., R. Miller, and J. Xia. 1999. "Multichannel Analysis of Surface Waves (MASW)," *Geophysics*, Vol. 64, No. 3, pp. 800-808.

Pillai, V.S., and R.A. Stewart. 1994. "Evaluation of Liquefaction Potential of Foundation Soils at Duncan Dam," *Canadian Geotechnical Journal*, Vol. 31, No. 6, pp. 951-966.

Plaxis bv, 2014. *User's Manuals for Programs PLAXIS 2D and 3D.* Delft, The Netherlands.

Poulos, S.J., G. Castro, and J.W. France. 1985. "Liquefaction Evaluation Procedure," *Journal of Geotechnical Engineering*, ASCE, Vol. 111, No. 6.

Pugh, C.A., and W.-L. Chiang. 1986. "Landslide-Generated Wave Studies," *Proceedings, Water Forum '86.* American Society of Civil Engineers.

Redlinger, C., C. Rudkin, D. Hanneman, W.O. Engemoen, P. Irey, and T. Howard. 2012. "Lessons Learned from Large-Scale Filter Testing," *Proceedings, 6th International Conference on Scour and Erosion,* Paris, France, pp. 2125-232.

Resendiz, D., M. Romo, and E. Moreno. 1982. "El Infiernillo and La Villita Dams: Seismic Behavior," *ASCE Journal of the Geotechnical Division*, Vol. 108, No. GT1, pp. 109-131.

Robertson, P.K., and R.G. Campanella. 1983. "Interpretation of Cone Penetration Tests, Parts I and II," *Canadian Geotechnical Journal*, Vol. 20, No. 4, pp. 718-745.

Robertson, P.K., D.J. Woeller, and W.D.L. Finn. 1992. "Seismic Cone Penetration Test for Evaluating Liquefaction Potential Under Cyclic Loading," *Canadian Geotechnical Journal*, Vol. 29, No. 4, pp. 686-695.

Robertson, P.K., and C.E. Wride. 1997. "Cyclic Liquefaction and its Evaluation Based on the SPT and CPT," *Proceedings, NCEER Workshop on Evaluation of Liquefaction Resistance, Salt Lake City, 1996*. National Center for Earthquake Engineering, Research Technical Report 97-0022.

Seed, H.B. 1979. "Soil Liquefaction and Cyclic Mobility Evaluation for Level Ground During Earthquakes," *Journal of the Geotechnical Engineering Division*, ASCE, Vol. 105, No. 2, pp. 210-255.

Seed, H.B. 1987. "Design Problems in Soil Liquefaction," *Journal of Geotechnical Engineering,* ASCE, Vol. 113, No. 8, pp. 827-845.

Seed, H.B., and I.M. Idriss. 1970. *Soil Moduli and Damping Factors for Dynamic Response Analyses*. University of California - Berkeley, Earthquake Engineering Research Center, Report No. EERC 70-10.

Seed, H.B., and I.M. Idriss. 1971. "Simplified Procedure for Evaluating Soil Liquefaction Potential*," Journal of the Soil Mechanics and Foundation Engineering Division,* ASCE, Vol. 97, No. SM9, pp. 1249-1273.

Seed, H.B., and I.M. Idriss. 1982. "Ground Motions and Soil Liquefaction During Earthquakes." EERI Monograph, Earthquake Engineering Research Institute, Oakland, California.

Seed, H.B., I.M. Idriss, and I. Arango. 1983. "Evaluation of Liquefaction Potential of Using Field Performance Data," *Journal of Geotechnical Engineering,* ASCE, Vol. 109, pp. 458-482.

Seed, H.B., K.L. Lee, and I.M. Idriss. 1969. "Analysis of Sheffield Dam Failure," *Journal of the Soil Mechanics and Foundations Division,* ASCE, Vol. 95, No. 6, pp. 1453-1490.

Seed, H.B., F.I. Makdisi, and P. DeAlba. 1978. "Performance of Earth Dams During Earthquakes," *Journal of the Geotechnical Division*, ASCE, Vol. 104, No. 7, pp. 967-994.

Seed, H.B., and W.H. Peacock. 1971. "Test Procedures for Measuring Soil Liquefaction Characteristics*," Journal of the Soil Mechanics and Foundations Division,* ASCE, Vol. 97, No. 8, pp. 1099-1119.

Seed, H.B., R.B. Seed, L.F. Harder, Jr., and H. Jong. 1989. *Re-Evaluation of the Lower San Fernando Dam.* U.S. Army Corps of Engineers, Contract Report GL-98-2, September.

Seed, H.B., K. Tokimatsu, L.F. Harder, and R.M. Chung. 1985. "Influence of SPT Procedures in Soil Liquefaction Resistance Evaluations," *Journal of Geotechnical Engineering,* ASCE, Vol. 111, No. 12, pp. 1425-1445.

Seed, H.B., R.T. Wong, I.M. Idriss, and K. Tokimatsu. 1986. "Moduli and Damping Factors for Dynamic Analyses of Cohesionless Soils," *Journal of Geotechnical Engineering,* ASCE, Vol. 112, No. 11, pp. 1016-1032.

Seed, R.B., and R.W. Boulanger. 1995. "Liquefaction of Sand Under Bidirectional Monotonic and Cyclic Loading," *Journal of Geotechnical Engineering,* ASCE, Vol. 121, No. 12, pp. 870-878.

Seed, R.B., and L.F. Harder. 1990. "SPT-Based Analysis of Cyclic Pore Pressure Generation and Undrained Residual Strength," *Proceedings of the Memorial Symposium for H. Bolton Seed,* BiTech Publications, Ltd.

Sego, D.C., P.K. Robertson, S. Sasitharan, B.L. Kilpatrick, and V.S. Pillai. 1994. "Ground Freezing and Sampling of Foundation Soils at Duncan Dam," *Canadian Geotechnical Journal*, Vol. 31, No. 6, pp. 939-950.

Sherard, J.L., L.S. Cluff, and C.R. Allen. 1974. "Potentially Active Faults in Dam Foundations," *Géotechnique*, Vol. 24, No. 3, pp. 367-428.

Singh, R., D. Roy, and S.K. Jain. 2005. "Analysis of Earth Dams Affected by the 2001 Bhuj Earthquake," *Engineering Geology*, Vol. 80, No. 3-4, pp. 282-291.

Stark, T.D., and I. Contreras. 1998. "Fourth Avenue Landslide During 1964 Alaskan Earthquake," *J. Geotechnical and Geoenvironmental Eng.*, ASCE, Vol. 104, No. 2, pp. 99-109.

Stark, T.D., and S.M. Olson. 1995. "Liquefaction Resistance Using CPT and Field Case Histories*," Journal of Geotechnical Engineering*, ASCE, Vol. 121, No. 12, pp. 856-869.

Stewart, J.P., A.H. Liu, and Y. Choi. 2003. "Amplification Factors for Spectral Acceleration in Tectonically Active Regions," *Bull. Seism. Soc. Am.*, Vol. 93, pp. 332-352.

Stokoe, K.H., II, S. Nazarian, G.J. Rix, I. Sanchez-Salinero, J.C. Sheu, and Y.J. Mok. 1988. "In Situ Testing of Hard-to-Sample Soils by Surface Wave Method," *Earthquake Engineering and Soil Dynamics II*, ASCE Geotechnical Special Publication No. 20, pp. 264-278.

Stokoe, K.H., II, S-H Joh, and R.D. Woods. 2004. "Some Contributions of In Situ Geophysical Measurements to Solving Geotechnical Engineering Problems," *Proceedings, International Conference on Site Characterization* (ISC-2). Porto, Portugal, September 19-22, 2004.

Swaisgood, J.R. 1993. "Historical Behavior of Embankment Dams During Earthquake," *Proceedings, Association of State Dam Safety Officials National Convention*, Kansas City Missouri.

Sy, A., and R.G. Campanella. 1994. "Becker and Standard Penetration Tests (BPT-SPT) Correlations with Consideration of Casing Friction," *Canadian Geotechnical Journal,* Vol. 31, No. 3, pp. 343-356.

United States Geologic Survey. 1964. *The Hebgen Lake, Montana Earthquake of August 17, 1959.* Geological Survey Professional Paper 435, U.S. Government Printing Office, Washington DC.

USSD. 1992. *Observed Performance of Dams During Earthquakes.* United States Society on Dams, Denver, Colorado.

USSD. 2000. *Observed Performance of Dams During Earthquakes*, Vol. II, United States Society on Dams, Denver, Colorado.

USSD. 2014. *Observed Performance of Dams During Earthquakes*. Vol. III, United States Society on Dams, Denver Colorado.

Wood, J.H. 1973. "Earthquake Induced Soil Pressures on Structures." Ph.D. Thesis, California Institute of Technology, Pasadena, California.

Wang, W. 1979. *Some Findings in Soil Liquefaction*. Water Conservancy and Hydroelectric Power Scientific Research Institute, Beijing, China.

Yokel, F.Y., R. Dobry, D.J. Powell, and R.S. Ladd. 1980. "Liquefaction of Sands During Earthquakes - The Cyclic Strain Approach," *Proceedings, International Symposium on Soils Under Cyclic and Transient Loading*, Swansea, England, pp. 571-580.

Yoshimi, Y., K. Tokimatsu, O. Kaneko, and Y. Makihara. 1984. "Undrained Cyclic Shear Strength of a Dense Niigata Sand," *Soils and Foundations, Japanese Society of Soil Mechanics and Foundation Engineering,* Vol. 24, No. 4, pp. 131-45.

Yoshimi, Y., J. Tokimatsu, and A.N. Ohara. 1994. "In Situ Liquefaction Resistance of Clean Sands Over a Wide Density Range," *Géotechnique*, Vol. 44, No. 3, pp. 479-494.

Youd, T.L. 1977. Discussion of "Brief Review of Liquefaction During Earthquakes in Japan," by E. Kuribayashi and F. Tatsuoka (1975), Vol. 15, No. 4, pp. 81-92, *Soils and Foundations*, Vol. 104, No. 1, pp. 82-85.

Youd, T.L. 1993. "Liquefaction-Induced Lateral Spread Displacement," U.S. Navy NCEL Technical Note N-1862.

Youd, T.L. 1997. "Seismic Factors for Use in Evaluating Liquefaction Resistance," *Proceedings, NCEER Workshop on Evaluation of Liquefaction Resistance, Salt Lake City, 1996,* National Center for Earthquake Engineering Research Technical Report 97-0022.

Youd, T.L., I.M. Idriss, R.D. Andrus, I. Arango, G. Castro, J.T. Christian, R. Dobry, W.D.L. Finn, L.F. Harder, Jr., M.E. Hynes, K. Ishihara, J.P. Koester, S.S.C. Liao, W.F. Marcuson, G.R. Martin, J.K. Mitchell, Y. Moriwaki, M.S. Power, P.K. Robertson, R.B. Seed, and K.H. Stokoe. 2001. "Liquefaction Resistance of Soils: Summary Report from the 1996 NCEER and 1998 NCEER/NSF Workshops on Evaluation of Liquefaction Resistance of Soils," J. *Geotechnical and Geoenvironmental Eng*., Vol. 127, No. 10, pp. 817–833.

Youd, T.L., and S.K. Noble. 1997. "Magnitude Scaling Factors," *Proceedings, NCEER Workshop on Evaluation of Liquefaction Resistance, Salt Lake City, 1996*, National Center for Earthquake Engineering Research Technical Report 97-0022.

Appendix A

Earthquake Loadings for Analysis of Embankment Dams

Co-Peer Review:

Ralph E. Klinger (signature)
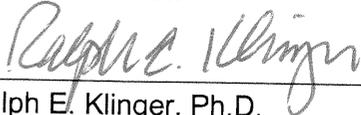
_5/12/2015_

Ralph E. Klinger, Ph.D.
Seismic Geologist, Seismology, Geomorphology, and
    Geophysics Group, 86-68330

Date

Contents

Figures

A.1   Introduction

This appendix of Chapter 13, "Seismic Analysis and Design," of *Design Standards No. 13 – Embankment Dams* provides a brief introduction to the earthquake loadings that may be required for analysis of embankment dams or that may be encountered in reports of earlier analyses or field performance. The required scope of seismotectonic studies for a specific dam depends on the analyses that are likely to be performed. Some analyses may require only very simple inputs, such as peak ground surface accelerations; others may require synthetic or modified earthquake ground-motion records tailored to a specific site.

In current Bureau of Reclamation practice, the Technical Service Center's Seismotectonics and Geophysics Group provides the required loadings for the analyses, including probabilistic seismic hazard analyses (PSHA), maximum credible earthquakes (MCE) (rarely), acceleration time histories, uniform-hazard response spectra (UHS), etc. Therefore, this appendix contains only descriptive information for the benefit of the engineering analyst, not the methodology for developing the loadings, which is covered by other publications.

At present (2015), Reclamation's dam-safety practice is primarily "risk-informed," which means that decisions are made with a consideration of probabilistic risk analysis that considers the annual probability of seismic loading (or other type of loading), the likelihood of dam failure should various levels of loading occur, and the consequences of dam failure. This risk-informed practice contrasts with deterministic analysis and decisionmaking, in which a dam is required to have, for example, some minimum factor of safety against slope instability when subjected to the MCE for the site. Therefore, *Design Standards No. 13 – Embankment Dams*, Chapter 13, "Seismic Analysis and Design," is intended primarily to guide geotechnical analysis in support of probabilistic risk analysis.

The characteristics of the dam and the expected use of the seismotectonic investigation; i.e., what analyses are expected, should be communicated to the seismologists as early in the process as possible. This will help to ensure that their work will meet the needs of the analysis without wasted effort or delays caused by adding more studies.

A.2   Products of Seismotectonic Studies

Depending on the level of analysis, seismotectonic studies for a given dam could include any or all of the following:

- Identification of seismogenic sources, both identifiable faults (which do not necessarily have surface expression but may have been identified through geophysical exploration or previous activity), or zones of

      seismicity without identified causative faults. This is the foundation
      for all other seismotectonic studies.

- Estimated MCEs for the site, generally expressed in terms of magnitude
  and distance. While these are generally no longer part of current
  Reclamation practice, this information may be encountered in older
  reports and other sources.

- Hazard curves that give the annual exceedance probability for values of
  the peak horizontal acceleration at the ground surface (PHA, also called
  PGA), or other parameter, such as the spectral acceleration (SA) for a
  particular response period, or the Arias intensity, which incorporates both
  the acceleration peaks and the duration of the peaks as an index of seismic
  energy at the site (Arias, 1970; Kramer and Mitchell, 2006).

- Uniform-hazard response spectra, showing the SAs associated with a
  given exceedance probability, plotted as a function of the period of
  oscillation. For embankment dams, UHS is primarily used to identify
  appropriate earthquake ground motions for a particular analysis.

- Earthquake ground-motion time histories associated with specific
  scenarios, such as rupture of some particular fault, or with some annual
  probability of exceedance, considering all seismogenic sources. These are
  required for numerical analysis of deformation and cyclic stresses.

- Identifying potential for coseismic fault rupture in the foundation of the
  dam or for displacement of the reservoir basin that could cause destructive
  waves.

Seismogenic sources can be either identified faults or other structural features, or
zones of seismicity without identified causative faults. Evaluation of fault sources
usually includes general geologic information, fault geometry (length, strike, dip,
and down-dip extent), style of slip (i.e., strike-slip fault versus thrust fault versus
normal fault), fault segmentation, and rate of slip. When feasible, the rate of slip
and activity of a fault are evaluated using paleoseismic studies, such as trenching
across fault traces, to locate and age-date soil horizons that have been disrupted
by fault movement, historic seismicity (including "microseismicity"), and surface
deformation data (global positioning system [GPS], geodetic surveys, etc.).
Source zones without identified fault sources are evaluated primarily from
statistical analysis of historic seismicity; however, if there is reason to suspect
the existence of a significant fault that is obscured by overlying strata, it can
sometimes be identified from a combination of historic seismicity, surface
deformation from aseismic fault creep, and geodetic measurements. Reclamation
has used geophysical data obtained from petroleum exploration by others to
clarify the geometry of faults and other structures.

Source characterization is a significant source of uncertainty in dam-safety
evaluation, especially in the western U.S., where relatively little is known about
active faults outside of major population centers. Reclamation dams are
frequently located in rural parts of the West, where there is only basic
understanding of fault activity and earthquake hazards. For dam safety risk
analysis, it is often necessary to gain a better understanding of earthquake hazards
than can be obtained from existing information. In fact, much of what is known
about earthquake hazards outside of population centers in the western U.S. was
developed for Reclamation's dam-safety program.

It can be tempting to simply default to conservative estimates for ground motions,
material properties, etc., instead of addressing the uncertainty. However, this can
lead to a design that is unnecessarily conservative, or a decision to modify a dam
that creates only modest risk. PSHAs sometimes address this by developing
16th- and 84th-percentile curves (or similar) for the annual probability of
exceedance for some index of loading, in addition to mean and median hazard
curves. This can be valuable for assessing the need for additional seismotectonic
studies. If, for example, calculating risk assuming the 16th-percentile loadings,
instead of the mean, gives a different overall outcome (such as whether an
existing dam should be modified), confidence in the result would not be very
high. Additional seismotectonic investigation may help clarify the situation and
increase confidence in the decision.

Ground-motion parameters can be developed for a specific scenario, such as the
MCE from a given fault, or in a probabilistic study that considers the frequency of
occurrence and magnitudes from all sources in the general area of the dam. The
most commonly used parameters for embankment dams are PHA, earthquake
magnitude, acceleration response spectrum, and acceleration time histories.
Acceleration response spectra (discussed below) are not used directly in analyses
of embankment dams the way they sometimes are in structural analysis. They
are, however, used to indicate the frequency content of ground-motion records to
determine whether a given record is appropriate for a dam site. PHA and
response-spectrum values can be expressed as point estimates for a single
earthquake scenario, or as hazard curves showing the relationship between
parameter values and annual probability of occurrence. Vertical accelerations are
frequently included in seismotectonic studies and numerical analysis, although
their importance for embankment dams is typically fairly minor compared to the
horizontal motions.

To estimate any ground-motion parameter for use in an engineering application,
it is necessary to have a clear understanding of the site geology and dynamic
characteristics, both shallow and deep. There are significant differences in
ground motions between rock and soil sites. It is important to perform the
calculations of ground motions using assumptions about site conditions that are
consistent with the engineering analyses. Furthermore, for numerical response
and deformation analysis, it is necessary to use acceleration time histories that are

consistent with the depth where the ground motions will be applied to the model. In other words, if the ground motions will be applied to a finite-element model at its base 50 feet below the ground surface, the input ground motions must be what would happen 50 feet below ground, not on the surface. Surface records can be adjusted numerically (deconvolved), but clear communication between the engineers and the seismologists is vital, so that all of them understand how the records will be applied in the numerical model.

A.3 Earthquake Magnitude

Earthquake magnitude is an index of the amount of energy released by an earthquake (Kanamori, 1983). On its own, magnitude indicates very little about the severity of loading at a particular site; however, when combined with the distance from the source to the site, it can be used to estimate other measures of loading, including the peak ground acceleration (horizontal and vertical) and SA. Magnitude correlates fairly well with the duration of strong shaking or the number of strong cycles of shaking, so it is used as a proxy for the number of cycles in liquefaction triggering analysis and in some simplified deformation analyses. Magnitude is generally abbreviated as "M," usually with a subscript to indicate how it was calculated (as described below).

The Richter scale (sometimes abbreviated M_L for "local magnitude") was the first practical method to quantify the overall energy release from an earthquake. Originally developed in the 1930s by C.F. Richter, the Richter scale is based on the response of a specific instrument (Wood-Anderson torsion seismograph) at a specific epicentral distance (100 kilometers [km]). It has no real physical meaning and is simply a rough index for comparing sizes of earthquakes. Richter magnitude is seldom used now (except in countries of the former Soviet Union), but the term "Richter scale" persists in the popular media, and occasionally in technical publications, even when other magnitude scales are actually being reported. The Richter scale is generally not useful for magnitudes above about 6.5 because the scale "saturates;" that is, increases in energy release do not produce consistent increases in the response of the Wood-Anderson seismograph. Hence, it cannot, for example, distinguish very well between 7.0 and 7.5. It was not intended to be used for earthquakes more than about 1,000 km away. Other magnitude scales have been proposed since then, based on the intensity of specific types of waves or on the perceived level of shaking at different distances. Most magnitude scales have been "calibrated" to coincide with Richter magnitude, to the extent practical, for consistency and ease of comparison.

The moment magnitude, M_W, is the preferred scale in most of the world because it has a physical basis and does not saturate at large magnitudes. It is based on the seismic moment, which is an index of the strain energy released by the earthquake.

The moment, M_O, is a function of fault area, fault displacement in the earthquake, and the shear modulus of the bedrock. M_W is a function of the seismic moment:

$$M_W = 2/3 \log(M_O) - 6.0 \qquad\qquad\qquad \text{Equation A1}$$

The seismic moment, M_O, is defined as:

$$M_O = \mu\ A\ s \qquad\qquad\qquad\qquad \text{Equation A2}$$

where μ is the shear modulus, A is the area of the causative fault (or of the causative segment), and s is the average displacement. (M_O has the same units as energy, dyne-centimeters, and it is roughly proportional to the energy released.) Equation A1 indicates that an increase of 1.0 in M_W corresponds to a 32-fold increase in energy M_O.

M_W can also be estimated from the Fourier spectra of recorded acceleration time histories, allowing comparison between magnitudes predicted from fault characteristics and magnitudes that have occurred.

For fault sources, the estimate of maximum magnitude is usually based on fault parameters, such as rupture dimension, and displacements in previous events. For source zones, analyses of historical data, physical constraints on rupture dimensions in features lacking surface expression, dimensions of zones of concentrated historic seismicity, and analogies to other regions are used. Maximum magnitude estimates should include estimates of uncertainty. Magnitude is used in selecting appropriate loadings for dam analysis (such as peak ground acceleration and acceleration time histories). Many simplified analyses of settlement and liquefaction potential use the magnitude as a proxy for the number of cycles of strong loading.

A.4   PHA and SA

The PHA is frequently an input in seismic analyses, including liquefaction triggering and dynamic deformation. (Peak vertical acceleration is seldom a major consideration for embankment dams, although vertical acceleration time histories are often included in response or deformation analysis.) Peak accelerations are predicted from empirical ground motion prediction equations (GMPE), also called attenuation curves, which give PHA (or other parameter) as a function of earthquake magnitude and distance from the site to the fault rupture surface. GMPEs are updated periodically as new earthquakes provide additional data. For the western and central U.S., the most recent GMPEs are provided by the Next Generation Attenuation West2 (NGA-West2) models (Bozorgnia et al., 2014). Different parts of the U.S. require different attenuation relationships; for some sites, it may be necessary to use more than one GMPE because it is not

always obvious which one should be used. For a given magnitude and distance, earthquakes in the eastern and central U.S. generally yield higher PHAs. Most of Reclamation's dams are located in the Rockies, or farther west, and would require GMPEs for the western U.S., and dams on the Great Plains usually require GMPEs for the central and eastern U.S. PSHAs for dams near the interface between the mountains and the plains may need to incorporate both (for example, those in the Colorado Front Range). Predicted ground motions also depend on the characteristics of the site, usually represented by V_{S30}, which is the time-weighted mean, shear-wave velocity in the top 30 meters (m) (98 feet [ft]). (The time-weighted mean is equal to 30 m divided by the travel time for a shear wave to travel upward through the top 30 m, rather than the mean velocity weighted by layer thickness.) Sites with soft bedrock or deep soil profiles may require geophysical investigations to determine V_{S30}.

The SA provides a general indication of how strongly a structure would respond to a particular earthquake motion. For a given earthquake record and a given period of oscillation, the SA is equal to the calculated peak acceleration of a one-degree-of-freedom oscillator driven by the acceleration record. For embankment dams, the SA is mainly used to select appropriate ground-motion records for dynamic response or deformation analysis, so they are realistic for the source and would excite the structure at the frequencies of greatest concern. (The SA has other uses in structural engineering.) Usually, the SA is calculated for a wide range of fundamental periods, ranging from zero to several seconds, and plotted as a function of period to obtain the response spectrum, which is unique to each earthquake record. In general, the more energy the record contains at a particular period of oscillation, the greater the SA will be at that period. If the earthquake record contains primarily long-period motion (for example, 0.5 second or longer), it would produce a greater response when applied to a structure with a similar period than it would when applied to a structure with a shorter period, like 0.05 second. For the special case of a rigid oscillator, whose fundamental period is zero, the SA is equal to the PHA of the earthquake record.

Like peak accelerations, SA values for fundamental periods other than zero can be estimated from magnitude and fault distance using empirical GMPEs. Most empirical attenuation relationships that are used to predict parameters like PHA and SA apply to either bedrock outcroppings or stiff soils. Additional calculations are required if the engineer needs the peak acceleration or other quantity at the surface of a soft soil, or at some depth below the surface. In particular, the Seed-Lee-Idriss simplified procedure for liquefaction potential requires PHA at the soil surface, not at a bedrock outcropping (NCEER, 1997). The difference is very important because the acceleration on a level soil surface is commonly 80 to 200 percent of what the same earthquake would produce on a bedrock outcrop. Nonlevel ground (a dam embankment, for example) can cause even greater amplification. The peak acceleration at the interface between

bedrock and the overlying soil would be somewhat lower than on exposed bedrock. Therefore, there needs to be clear communication on what location an estimate of a parameter like PHA or a ground-motion record is to be applied in the analysis, such as at a bedrock outcropping, 40 ft below the top of bedrock in the embankment foundation, etc. The specific needs of the investigation should be conveyed to the seismologists in advance, and the seismologists should explicitly label hazard curves and other products with the locations at which they are applicable.

A.5   MCEs

In earlier Reclamation practice, dams were typically evaluated for MCEs and required to withstand that loading. The MCE is literally the largest earthquake that could credibly be produced by an identified source (fault or fold), or by a zone of historic seismic activity. A dam that might not survive the MCE would have been considered deficient, and some sort of corrective action would be required. For each potential source, the peak acceleration and other parameters for the MCE were estimated by attenuation curves that are functions of distance from the source.

For an identified fault source, the MCE is usually determined by the dimensions and characteristics of the fault, and how far it could slip in a single event. Where the source is a zone of seismicity, rather than an identified fault, the MCE is sometimes defined by an annual probability of exceedance of 1/5,000 to 1/20,000 (with the precise value being somewhat arbitrary because the MCE has no probability associated with it). This is sometimes referred to as a "random" or "floating" MCE. A particular annual probability does not define one particular earthquake scenario, so the random MCE for a site could, for example, be a magnitude 5.5 earthquake within 20 km from the site, a magnitude 6.0 earthquake within 45 km, or a magnitude 6.25 earthquake within 70 km, all of which would have the same annual probability. Therefore, the random MCE for a site is often expressed as several pairs of magnitude and distance, and there can also be fault-related MCEs in the same analysis. It may not be obvious which of those earthquakes actually represents the worst loading for a particular structure. It depends on earthquake magnitude, distance from the site, the nature of the structure and its foundation, and the type of analysis being performed. For some analyses; e.g., liquefaction potential, the earthquake producing the highest peak acceleration is not necessarily the most severe loading, because larger magnitude earthquakes tend to produce more cycles of strong acceleration, even if the peak is lower. Sometimes, engineering analysis is required to determine which potential load case is most severe.

Typically, PSHAs provide hazard curves for outcroppings of bedrock or stiff soil. The peak acceleration on a soft soil surface or on a dam embankment can be

somewhat lower, or as much as double the acceleration on bedrock. Similarly, ground-motion time histories are usually developed for motion at the surface of a rock outcropping, although modern computational techniques permit development of acceleration or shear stress records that would apply at some depth in the bedrock or a thick layer of soils above bedrock, so they can be applied at the base of a response model (finite-element or finite-difference).

Although the "deterministic" MCE approach has been superseded in Reclamation's dam-safety practice, it is still commonly required among regulatory agencies and dam owners outside Reclamation; some have specific requirements for the level of conservatism in selecting the MCE ground motions, such as using the 84th percentile. Although the MCE is no longer part of typical Reclamation dam engineering practice, it is frequently referred to in older documents.

A.6   PSHA and Risk Analysis

In current practice at Reclamation, dam-safety decisions are generally based on the amount of risk a dam poses to public safety. For probabilistic risk analysis, it is necessary to know probabilities associated with different levels of loading, not just the maximum loadings considered possible at a site. This requires a PSHA, which yields curves of PHA values (and other parameters, such as 1-second SA) versus the annual probability of each value being exceeded. (Strictly speaking, these are frequencies of exceedance, rather than annual probabilities, but for practical purposes, they can be treated as probabilities for earthquakes of interest for dam safety.) PSHA is fundamentally an accounting method that combines earthquake recurrence information for all sources directly with earthquake energy-propagation models (attenuation curves). Figure A1 shows typical hazard curves, which give the mean annual probability that the peak ground acceleration or SA would exceed a particular value, along with confidence bounds. For example, the probability that the PHA would exceed 0.6 g (very severe loading) in any year is about 1.7×10^{-4} or 1/6,000, as indicated by the heavy dashed lines. The heavy red curve in figure A1 represents the sum of the hazards from a number of sources, with different activity rates, maximum potential magnitudes, and distances from the site. For this particular site, the great majority of the PHA hazard results from two major faults located nearby, each capable of producing earthquakes with magnitude M_W up to about 7 (the solid blue and black curves). Note that the summation occurs in the vertical direction, adding the exceedance probabilities for a given value of PHA (or other parameter), not in the horizontal direction.
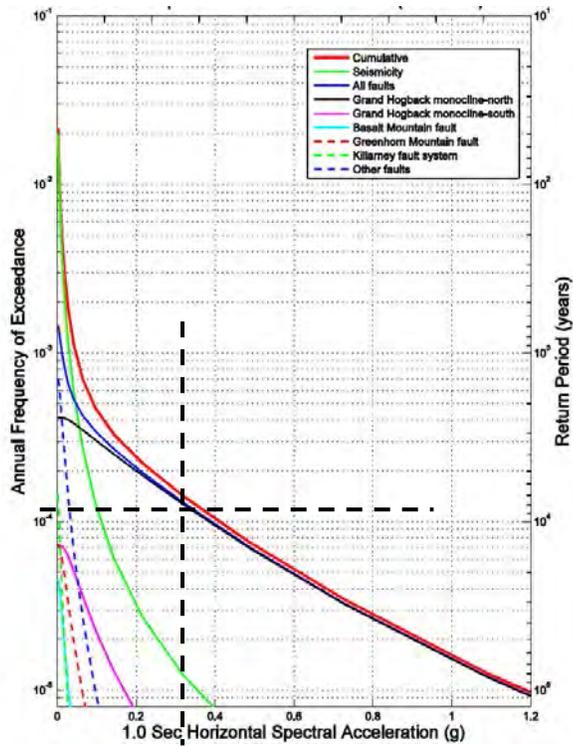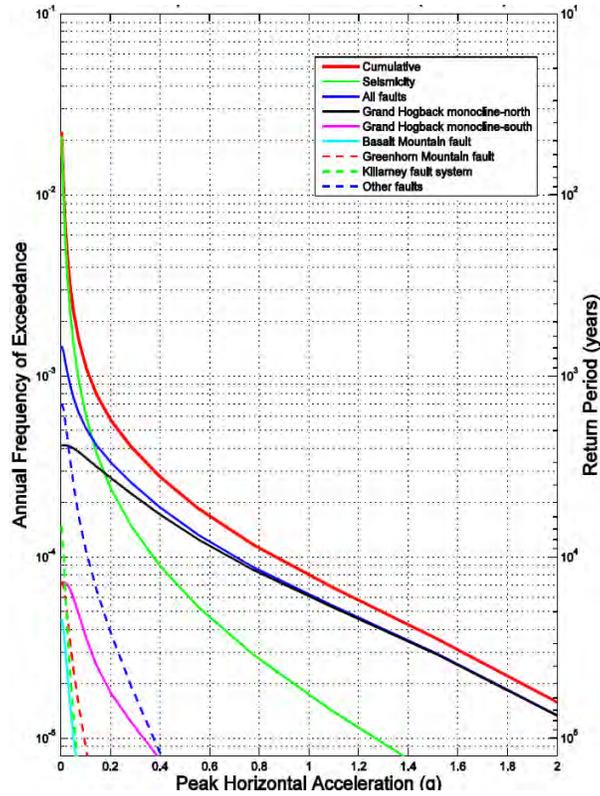
**Figure A1. Typical hazard curves giving
probability of exceedance for PHA and for
1-second SA.**

As mentioned above, the PHA does not, on its own, provide a complete description of the loading. For simplified liquefaction triggering analysis, one needs, at minimum, PHA at the ground surface and the earthquake magnitude, M_W. (The magnitude is used as a proxy for the number of cycles of strong motion because magnitude and duration correlate fairly well.) Numerical analyses of response and deformation require ground-motion records (time histories) with durations and frequency contents that are realistic for the earthquake source and the return period.

The widely used Seed-Lee-Idriss simplified method of liquefaction triggering analysis uses cyclic shear stresses estimated as a function of PHA and depth, via the factor rd, which is a function of depth. (See the main text of this chapter.) Therefore, a risk analysis based primarily on the simplified analysis may require hazard curves only for PHA (with some indication of the average earthquake magnitude to associate with a value of PHA). However, other analyses may require different indices of loading and, therefore, different hazard curves. For example, Bray and Travasarou's simplified deformation analysis (2007) uses the SA for a period equal to 1.5 times the fundamental period. Pseudostatic analysis of appurtenant structures, such as intake towers or spillway gate piers, may use the SA for the structure's fundamental period directly in the calculations. In these cases, the main index of loading in a risk analysis would be something other than the PHA.

Numerical analyses of response (including cyclic shear stresses) and deformation are sensitive to the frequency content of the ground motions; they require ground-motion records that are suitable for the specific source of the earthquake, including magnitude, distance, and style of faulting. Selecting suitable records therefore requires hazard curves for SA over a wide range of periods (further discussed below).

In contrast to embankments, concrete structures generally have shorter fundamental periods, and they are unable to tolerate as much momentary yield and permanent deformation as an embankment. Like concrete dams, appurtenant structures, such as spillway retaining walls, may have "brittle" failure modes, so yield needs to be avoided, unlike embankment dams where yield is expected to occur with fairly modest PHA values and can often be tolerated (within limits). Short-period hazard curves (including PHA) are required for stiff structures.

In seismic risk analysis of an embankment dam, the first entries of the event tree are commonly the earthquake loadings, although the first event can also be conditions that exist prior to the earthquake, such as reservoir level or foundation properties. Usually, the input loadings are either ranges or "bins" of PHA (or a related parameter) within which generally similar behavior is expected, or they are earthquake ground motions that could plausibly represent earthquakes with a particular return period.

If the risk analysis will be based on a simplified liquefaction analysis with the cyclic stress ratio (CSR) proportional to the surface PHA, the loading would be divided into PHA ranges with, to the extent practical, similar probability of liquefaction. The probability of each PHA range is simply the probability of exceeding the lower limit, but not exceeding the upper limit. If the range of interest is 0.3 to 0.5 g, figure A1 indicates the annual probability of a PHA in that range to be 3.9×10^{-4} minus 2.1×10^{-4}, or 1.8×10^{-4}.

If, instead, the risk analysis will be based on more detailed analysis, whether site response to calculate the CSR directly (rather than using the simplified equation with rd) or some type of numerical deformation analysis, the inputs would generally be ground motions to represent particular return probabilities. For example, the dam may have been analyzed with motions representing 1/500-, 1/1,000-, 1/5,000-, and 1/20,000-year loadings. In this case, the response or deformation using the 1/5,000-year earthquake might be assumed to represent all ground motions with return periods of 1/3,000 to 1/7,000 years. The probability of that range of loadings is also the annual probability of exceeding the lower limit, but not exceeding the upper limit. In this case, the load probability is 1/3,000 minus 1/7,000, or 2×10^{-4}.

The PSHA begins with identifying the sources, determining the recurrence characteristics of each source, and then applying empirical ground-motion prediction equations (GMPEs) to determine how events at each source would affect the dam site. The characteristics each source and the GMPEs are used to develop an individual hazard curve, giving the annual probability of exceedance for PHA or other parameter at the dam site contributed by each source. The individual probabilities are then summed as shown in figure A1.

In a region where no active faults have been identified, the earthquake hazard is based primarily on historic seismicity. Rates of occurrence are calculated from historic accounts and any available seismograph recordings. This can be complicated by the relatively short observation periods in the western U.S., as well as the relative lack of seismometers. In areas that were sparsely populated at the time of important earthquakes, there may be very few eyewitness accounts of the intensity of shaking. Recurrence rates are estimated from historic and recorded seismicity by statistical methods, although interpreting the statistics requires some judgment about site response and the PHA and M_W inferred from historic accounts, etc.

Where active faults have been recognized, the earthquake hazard is based on both historic seismicity and paleoseismicity. Recurrence intervals and the amount of movement from each event, and the variability associated with them, are best estimated from paleoseismologic trenching studies, in which the displacements from individual previous events are measured, and the timing of the events is determined by topsoil development, carbon dating, and other geologic techniques. Even with detailed paleoseismologic data, the uncertainty in frequencies and

magnitudes can still be very large. As in every other aspect of seismic analysis of dams, uncertainties in earthquake recurrence need to be estimated and documented for every seismotectonic study.

The value of PHA (or other parameter) having an annual probability of exceedance of 1/1,000, for example, is sometimes referred to as the "1,000-year PHA," and the "recurrence interval" or "return period" is said to be 1,000 years. These are both somewhat misnomers because they appear to imply that the ground motion would occur once every 1,000 years. The probability of the 1/1,000-year PHA being exceeded in a given millennium is actually 1-[(1-1/1,000)1000] or 0.63 (assuming each year to be an independent "trial," with no periodicity). While "recurrence interval" and "___-year earthquake" are convenient and familiar terms, they are sometimes misunderstood and need to be used carefully. Referring to the "1/1,000-year earthquake" may be less confusing.

Empirical GMPEs are available for both the PHA and the SA for longer periods, which allows hazard curves to be produced for both PHA and SA at longer periods that could be of importance for a dam. The hazard for the full range of periods of oscillation can be shown on a single plot showing the UHS for different return periods, including zero, which corresponds to the PHA. Each curve on figure A2 corresponds to the SA having a given exceedance probability, as a function of oscillation period. In effect, the PSHA has generated hazard curves for SA for periods of 0.01 to 5 seconds. The UHS curves are a plot of, for example, the 1/10,000-year value from each of those hazard curves. For embankment dams, the main use of UHS is in selecting ground motions for numerical analysis of response or deformation. The shape of the curves can vary with the characteristics of the source. For example, if the primary source is a large distant fault, the UHS would generally be higher at long periods, compared to local "random" seismicity of smaller magnitudes, even if the closer, smaller earthquakes would give higher peak acceleration.

The major benefit of the PSHA is that it combines the hazard from all potential sources to provide a more complete picture of the earthquake hazard for the dam site. However, many types of analysis require more than one parameter, so a unified PHA hazard curve cannot portray the probability for all "components" of the loading. For example, the simplified Seed-Lee-Idriss empirical liquefaction analysis (like the many methods that grew out of it) requires the earthquake magnitude as a proxy for the number of cycles of loading, in addition to the PHA (NCEER, 1997). However, a particular value of PHA or SA could result from a small, nearby earthquake, or a very large one distant from the dam site. Combining all of the earthquake sources into a single PHA hazard curve obscures the contribution from particular sources, and it may not be clear what magnitude to apply in the liquefaction analysis, or what duration of strong motion a record for deformation analysis should have. Therefore, it would be necessary to disaggregate the PSHA results into the contributions from the various sources.

Figure A3 portrays this in a three-dimensional plot of magnitude and distance in the horizontal plane, and relative contributions to the total hazard (exceedance probability) on the vertical axis. As shown in figure A3, the hazard is dominated by sources within 10 km of the dam (primarily represented by the solid blue and black curves in figure A1). It is also apparent that the hazard comes from earthquakes with a wide range of magnitudes. This information needs to be accounted for in the geotechnical and risk analyses because liquefaction potential and dynamic deformation are both strongly dependent on the number of cycles of shaking, not just the peak acceleration. The number of cycles is generally much larger with larger-magnitude earthquakes, and the frequency content tends to be different.
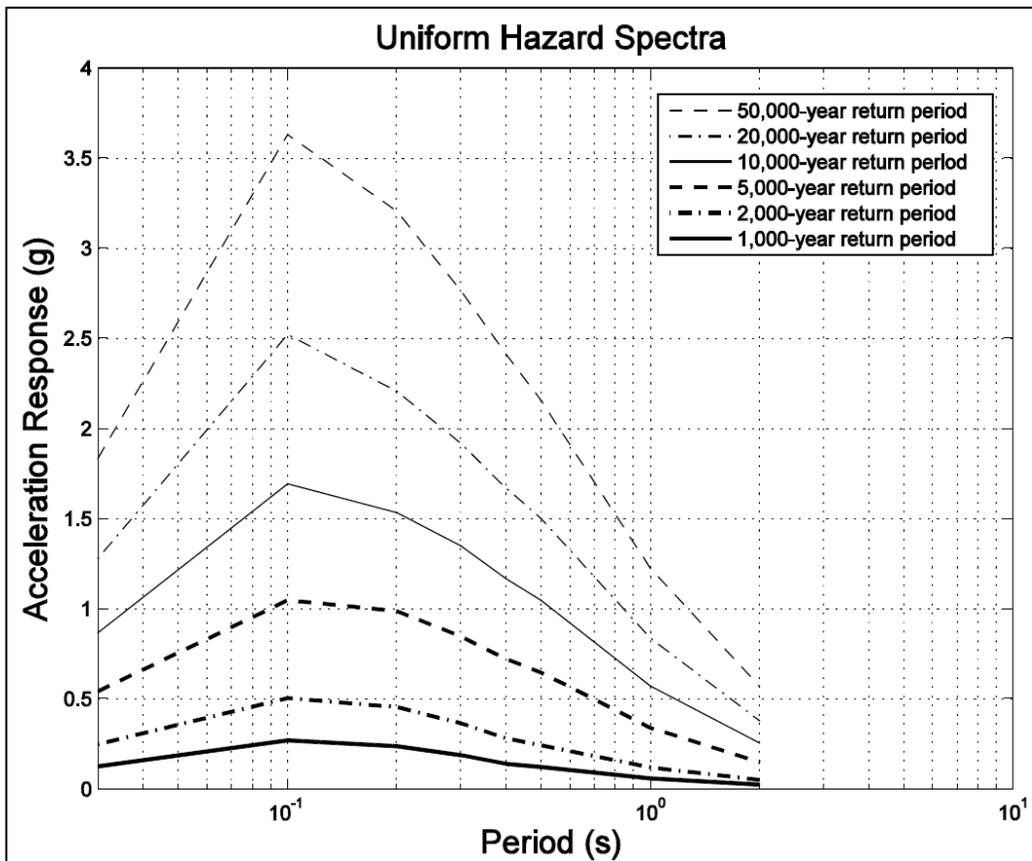
**Figure A2. Example UHS. Each curve indicates the SA with a particular
exceedance probability, plotted as a function of oscillation period.**
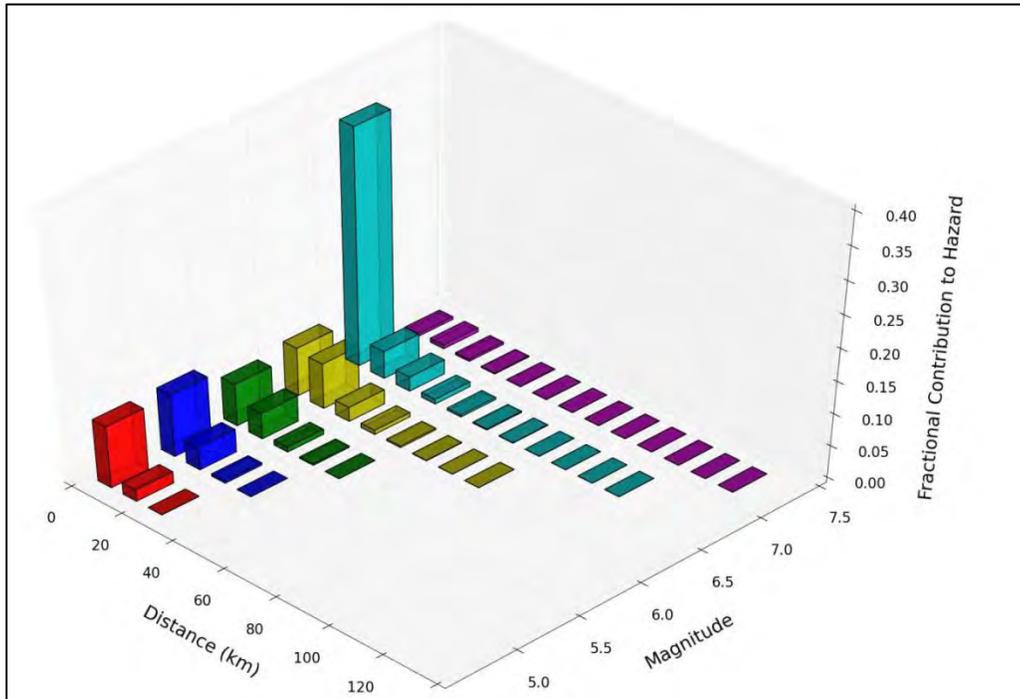
Figure A3. Example 1/10,000-year PHA hazard disaggregated to show relative contributions from different sources.

A.7   Earthquake Ground Motions for Response and Deformation Analysis

Analyses of dynamic response, cyclic stresses, and deformation may require more information than just peak acceleration and magnitude. The analyses may also require records of ground acceleration as a function of time, so that dynamic responses (accelerations, shear stresses and strains, deformation, etc.) can be calculated as functions of time. (Sometimes, ground motions are input as shear stress at the base of a finite-element or finite-difference model, rather than as acceleration, but the same considerations apply.) Ground motions can be developed for a specific scenario, such as the MCE or 1/5,000-year earthquake from a particular fault, or to represent ground motions with a particular probability of exceedance, considering the frequency of occurrence and magnitudes from all sources in the general area of the dam.

Deformation of a dam embankment is generally not very sensitive to high-frequency shaking with periods less than 0.2 second. Instead, it is much more sensitive to longer periods, such as 1 second. Beginning with a record that is rich in long-period shaking then numerically filtering out the portion with periods less than 0.2 second, the PHA could be reduced significantly

but there may not be much difference between the deformations predicted with the original and filtered records. If the PHA exceeds 0.2 g, most embankments would experience momentary yield and plastic deformation, which can typically, but not always, be tolerated, aside from any effect it would have on appurtenant structures. If the ground motion consists predominantly of very short periods, the duration of each occurrence of intermittent yield would be very short, and, therefore, the amount of deformation would be small. If the strong shaking predominantly consists of longer periods, the duration of each yield event and the permanent deformation could be much greater. There is also some effect from the elastic response of the embankment, which can magnify the acceleration, particularly if the record contains a large amount of energy near the fundamental period of the embankment. Thus, ground motion records must both be realistic for the earthquake sources, and be selected according to the hazard curves for the most critical periods for the dam. The critical period can be significantly different from the fundamental period of the embankment. Also, when response analyses are performed for liquefaction analysis, the computed CSR is strongly influenced by the long-period portion of a record's response spectrum, not just the PHA. For these reasons, PSHAs for embankment dams need to include hazard curves for parameters that reflect long-period shaking, such as 1-second SA, along with the PHA. Periods as long as 3 seconds may need to be considered in selecting ground motions for deformation analysis of a high dam.

Time histories for analysis can be existing strong-motion recordings or computed synthetic records. (Details of generating synthetic records and modifying existing records are not presented here because, at Reclamation, seismologists usually perform this work, rather than engineers.) Ground-motion time histories are selected with consideration of style of faulting, earthquake magnitude, source distance, and the specified return period, as well as the nature of the structure to be analyzed. A large embankment dam may respond most strongly to vibration with a period on the order of 1 second (depending primarily on its height and the stiffness and strength of the embankment materials). In contrast, a concrete dam might respond more to vibration with a period of 0.1 second. The response of soils is highly nonlinear, and the shear modulus decreases markedly with increasing strain, so the fundamental period at very low strains may have little relationship to how the dam responds under large accelerations with large strains. There is, unfortunately, no simple way to compare two acceleration records and determine which one constitutes more severe loading, without actually doing the response analysis and comparing results. Whether for a deterministic analysis with a design-basis earthquake or as input for a probabilistic risk analysis, a number of different plausible earthquake time histories need to be used for each scenario or return period.

Although the UHS is a useful tool for looking at the general severity of loading as a function of probability, it would not match the response spectrum for a particular recorded earthquake or earthquake scenario. Actual earthquake response spectra usually have one or two main peaks at particular oscillation

periods, with the remainder of the spectrum being lower than the UHS. The
1/1,000-year UHS is an envelope for all possible earthquake ground motions that
can be considered to have 1/1,000 annual probability of exceedance. A response
spectrum only needs to touch the 1/1,000-year UHS at one oscillation period to be
considered a 1/1,000-year loading. It is quite unlikely that an actual earthquake
would touch the UHS at numerous different oscillation periods.

Therefore, ground motions for analysis should not be forced to match the UHS for
the full range of periods because that would be unnecessarily conservative. For a
1/1,000-year earthquake, for example, that would require the ground motions to
match the 1/1,000-year PHA, the 1/1,000-year 0.1-s SA, the 0.2-s SA, the
1.0-s SA, etc. This is much less probable than an earthquake that fits the
1/1,000-year UHS in a small range of periods. At some sites, the short-period
portion of the UHS (including the PHA) is governed by small nearby earthquakes,
and the long-period portion is governed by distant, large-magnitude earthquakes.
Ground motions matching the whole UHS would, therefore, require simultaneous
occurrence of two earthquakes! The example disaggregation plot in figure A3
shows that the PHA hazard is distributed over a wide range of magnitudes, and a
response or deformation analysis would require ground motions representing two
or three different magnitudes, with the PHA probability distributed among them.
Whether for deformation analysis or liquefaction triggering, it is not always
obvious which source really governs the risk until the analysis is performed.
(This needs to be allowed for in budgets and schedules.)

When response analyses are required, to produce shear stress, deformation, etc. as
inputs for risk analysis, but suitable records for a particular earthquake scenario
do not exist, available records can be modified to fit the scenario. Simple
proportional scaling of recordings to match some specific parameter, such as peak
acceleration or spectral response at a particular period, should be avoided, except
when the adjustment is small, because the results can be unrealistic. There are
preferred techniques for numerically adjusting available records to match the
UHS at a particular oscillation period of interest. One such technique is the
conditional mean spectrum (CMS) (Baker, 2011). It is not always obvious which
period is most critical for a particular dam, so the preferred practice is to apply
CMS to several existing records, each with two or more potentially critical
oscillation periods. The resulting modified records are used in the response or
deformation analysis to determine the most critical oscillation period; subsequent
response and deformation analyses can then be focused on records matched to that
period. With nonlinear behavior expected for embankments, the most critical
period is often longer than the fundamental period of the embankment.

Typical Reclamation practice is for the TSC's Seismotectonics and Geophysics
Group to provide several sets of ground motion records for each return period
requested (with each set consisting of two horizontal components and the vertical
component). These records may all be adjusted to fit the UHS for one particular
oscillation period, or to fit several different periods, depending on the anticipated

behavior of the embankment and/or other structures. By design, each of these records is equally likely because each matches the UHS at one particular period or range of periods. It is, therefore, unnecessarily conservative to base a risk analysis only on the records and the polarity that give the worst results in response analysis. If only one or two out of six sets of records "tested" indicate severe distress to the dam, ignoring the results of the other records, which are equally likely, would cause the risk to be overstated by a significant factor. Carrying more sets of ground motions through the engineering analysis would significantly increase the labor cost, but that may be necessary so that the full range of results is available for the risk analysis. The "default" assumption in preparing project budgets and schedules should be that several ground motions will be used for each permutation of return period and material assumptions, not just the single record identified as the worst.

It is important that ground motions also fit the location at which they are applied to a numerical model. Typical ground-motion attenuation relationships and historic earthquake records are provided for bedrock outcroppings or the surface of stiff soil. However, in finite-element or finite-difference response and deformation analysis, the motions are usually input as records of acceleration or shear stress at the base of the model. This requires them to be numerically adjusted or "deconvolved" to find the acceleration time history that would occur at the depth of interest. Typically, this is done beginning with an outcrop record and using a simple response-analysis program like SHAKE to modify it. Refer to *Design Standard No. 13 – Embankment Dams*, Chapter 13, "Seismic Analysis and Design," Section 13.5.3, "Seismic Loading."

A.8   Required Scope of Seismotectonic Studies

There is no single scope of work that is universally applicable to all dams and all levels of analysis. The level of effort required depends on the seismotectonic setting of the dam, the nature of the foundation soils and embankment, appurtenant features, and the possibility of coseismic movement of foundation faults.

At minimum, a risk analysis that is based on simplified methods for liquefaction triggering and slope-stability analysis would require a hazard curve for PHA, and an indication of appropriate magnitudes to apply in the liquefaction analysis. As discussed above, it is not strictly correct to use a single value of magnitude for a single value of PHA, let alone for all values of PHA because the hazard comes from a range of magnitudes, although, in some cases, it may be a reasonable approximation to use an average magnitude without much loss of precision. However, in many other cases, it is necessary to distribute the disaggregated hazard between smaller, nearby earthquakes and larger, distant earthquakes with

different magnitudes applied in the liquefaction triggering analysis, and with different ground motions applied in response and deformation.

For nonlinear deformation analysis performed to support a probabilistic risk analysis, hazard curves are required for the full range of periods from 0 to 3 seconds, and possibly more. These hazard curves are needed to select or create ground motions that are appropriate to the magnitude, distance, and style of faulting for each source. It is suggested here that five or more sets of records be provided for each return period to be analyzed (each set consisting of two horizontal and one vertical). These records should be selected to match the UHS at oscillation periods selected for the particular dam under study. For two-dimensional analysis, this would create 20 combinations of horizontal and vertical motion, with 2 horizontal components from each of 5 earthquakes, and each horizontal component applied both upstream-downstream and downstream-upstream (different polarity). From these twenty, it may be feasible to identify two to four records that would portray the full likely range of results. Sometimes, one of the horizontal components is obviously much less severe than the other, and the effect of changing the polarity of a horizontal motion is typically small.

A.9   Summary

Reclamation's dam-safety program is largely guided by probabilistic risk analysis. In addition to knowing the behavior of dams under various levels of earthquake loading, this requires probabilities to be associated with the different levels of loading. Deterministic seismic hazard methodologies, such as the MCE, have been superseded by the PSHA in Reclamation's practice. The PSHA combines the annual exceedance probabilities for some measure of earthquake loading, such as the PHA, from all known seismic sources into unified hazard curves for different measures of earthquake loading, including the PHA and SAs for oscillation periods of interest. Depending on the level of analysis, the hazard curves may suffice, or they may need to be used in a more detailed analysis to develop suitable ground motions for numerical analysis of embankment response and deformation.

Even for simplified analyses of deformation and liquefaction potential, the relationship between PHA and probability does not provide enough information. The PHA hazard may require disaggregation, so that pairs of PHA and magnitude can be associated with both probability of their occurrence and probability of liquefaction if they do occur.

Earthquake records for numerical analysis must be appropriate for the structure, the seismic source, and the location at which the records will be applied to the numerical model. Records to represent earthquakes of a particular return period

should be selected according to the SA hazard for the critical oscillation period(s) that most affect the behavior of the dam. Therefore, the response spectrum of a suitable 1/10,000-year record would preferably meet the 1/10,000 UHS curve only at the oscillation period of main interest. The CMS is a technique for adjusting the UHS to create a target response spectrum that a suitable ground motion would resemble. The most important period(s) may not be the same as the fundamental period of the embankment, and it may not be obvious what the most important periods are without performing preliminary numerical analyses with different records. The duration of the ground motion must also be realistic for the source, because liquefaction potential and deformation are both more severe with more cycles of shaking. Hazard curves may, therefore, need to be disaggregated into the contributions from different earthquake magnitudes, because magnitude is a good predictor of the number of cycles. Finally, the selected records may need to be numerically deconvolved, so it can be applied to the model at some depth, rather than on an outcropping.

Changes in PSHA results over time reflect the constantly evolving understanding of earthquakes. In the western U.S., measurements and observations of newer earthquakes continually supplement the understanding of earthquake mechanisms and the resulting ground motions. In a similar way, understanding of prehistoric earthquakes is constantly changing, as new faults are discovered and studied. As more earthquakes are recorded with improving instrumentation, GMPEs and attenuation relationships will continue to evolve. Therefore, any given PSHA is considered a "snapshot in time" of the best available information. As new information becomes available, PSHAs may require adjustment to reflect the current state of knowledge.

A.10 References

Arias, A. 1970. "A Measure of Earthquake Intensity," R.J. Hansen (ed.), *Seismic Design for Nuclear Power Plants,* MIT Press, Cambridge, Massachusetts, pp. 438-483.

Baker, J. 2011. "Conditional Mean Spectrum: Tool for Ground-Motion Selection*," Journal of Structural Engineering*, Vol. 137, Special Issue: Earthquake Ground-Motion Selection and Modification for Nonlinear Dynamic Analysis of Structures, pp. 322-331.

Bozorgnia, Y., and 30 others. 2014. "NGA-West2 Research Project," *Earthquake Spectra*, Vol. 30, No. 3, pp. 973-987.

Bray, J.D., and T. Travasarou. 2007. "Simplified Procedure for Estimating Earthquake-Induced Deviatoric Slope Displacements," *Journal of Geotechnical and Geoenvironmental Engineering,* Vol. 133, No. 4, pp. 381-392.

Kanamori, H. 1983. "Magnitude Scale and Quantification of Earthquakes," *Tectonophysics*, Vol. 93, No. 3-4, pp. 185-199.

Kramer, S.L., and R.A. Mitchell. 2006. "Ground Motion Intensity Measures for Liquefaction Hazard Evaluation, *Earthquake Spectra*, Vol. 22, No. 2, pp. 413-438.

NCEER. 1997. *Proceedings of the NCEER Workshop on Evaluation of Liquefaction Resistance, Salt Lake City, 1996*. National Center for Earthquake Engineering Research, Technical Report 97-0022.

Appendix B

Assessment of Liquefaction Potential Using the Cone Penetration Test

Co-Peer Review:
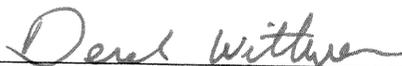
Derek T. Wittwer, P.E.
Manager, Geotechnical Engineering Group 4, 86-68314

5-8-15

Date

Contents

Figures

Figures (continued)

B.1   Introduction

B.1.1   General Considerations

This appendix of Chapter 13, "Seismic Analysis and Design," of *Design Standards No. 13 – Embankment Dams* describes empirical procedures for evaluating liquefaction potential and probability using the Cone Penetrometer Test (CPT), which is also referred to as the Electric Cone Penetrometer Test (ECPT). The procedures are based primarily on relating CPT data and cyclic loadings to historic ground performance (whether liquefaction occurred) at sites affected by earthquakes. The Standard Penetration Test (SPT) has been the workhorse of the Bureau of Reclamation's (Reclamation's) practice; however, due to a number of problems inherent in the SPT (lack of repeatability, slow production, cost, etc.) and greater experience with the CPT, the latter is gaining wider acceptance for analysis of liquefaction resistance at sites where it is suitable. (Many Reclamation dams have gravelly foundations where CPT may not be useful.)

Many factors affect a material's resistance to penetration by the CPT or other penetrometer, and its resistance to liquefaction under cyclic loading; simplifying assumptions have been made in the development of the empirical correlations. The user is encouraged to read the background literature and understand the basis and the limitations of the procedures used. General information on the CPT can be found in Lunne et al. (1997), and Robertson and Cabal (2014). For the use of CPT in evaluating liquefaction potential, see Moss et al. (2006), Idriss and Boulanger (2008), Boulanger and Idriss (2014), and Robertson and Cabal (2014). Like any other tool for assessing liquefaction potential, the CPT cannot be considered a "stand-alone" test from which a final conclusion can be made about seismic performance of a high-hazard dam (Bureau of Reclamation, 2007). Corroborating studies are almost always necessary. At minimum, soil samples are required to accompany the CPT data for classification and index properties.

Electric cone penetrometer specifications and test procedures are specified in American Society for Testing Materials (ASTM) D5778-12 (ASTM, 2012). In the standard form of the ECPT, a conical penetrometer is pushed into the ground at a steady rate of 2 centimeters per second (0.8 inch per second), stopping only to add additional rods to the string. The tip of the standard penetrometer is a 60-degree cone, with a projected end area of 10 square centimeters (cm^2) (diameter = 3.6 cm or 1.4 inches). (See figure B1.) The tip is connected to the body of the penetrometer by a load cell that measures the force required to push the cone. A cylindrical sleeve is located immediately above the tip of the standard penetrometer. The sleeve has the same diameter as the cone, and usually is 13.4 centimeters (cm) long, giving the sleeve a surface area of 150 cm^2. It too is connected to the body by a load cell, so that the friction on the sleeve can be measured. A longer sleeve or larger tip diameter is sometimes used when greater sensitivity is required in soft soils.
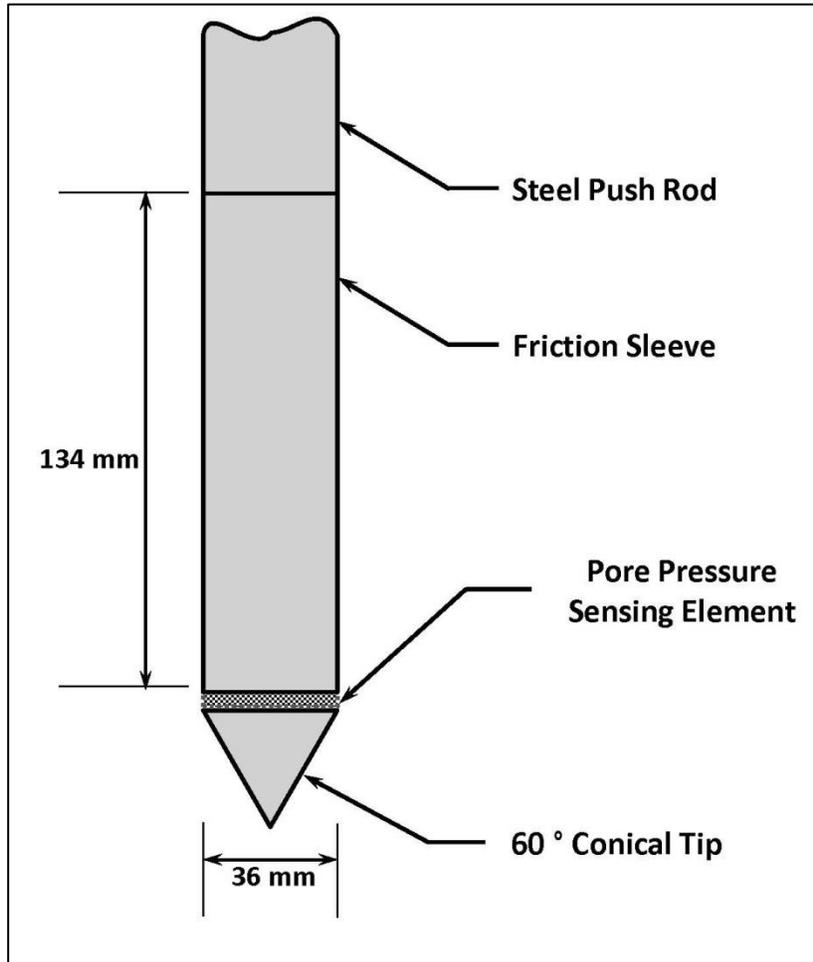
Figure B1. "Piezocone" cone penetrometer with pore-pressure measurement.

The penetrometer is often equipped with porous elements and a transducer to measure pore pressures during the push, in which case it may be referred to as a "piezocone" or CPTu. The penetrometer in figure B1 measures the pore pressure at the base of the cone, which is the most common configuration. This measurement is referred to as u_2, to distinguish it from u_1, measured on the face of the cone, and u_3 measured a small distance above the base of the cone. Typically, the load cells and pressure transducer are read and recorded by a computer data-acquisition system at intervals of 2 to 5 cm. Combined, the tip and sleeve measurements and u_2 measurements provide an **indication** of material type, sensitivity, etc. (It is only an indication, so drilling and sampling are still required.) The pore-pressure measurements also indicate material type and behavior, and they can be very useful for identifying layers of clay within coarser materials or layers of freer-draining material within low-permeability soils. Consolidation properties and in situ pore pressure can be estimated by stopping the push and observing the dissipation of excess pore-water pressure with time. Note that all procedures for assessing liquefaction potential from CPT (and other in situ tests) require the static effective overburden stress, calculation of which

requires the in situ pore-water pressure, either measured or calculated from an assumed piezometric surface. Often, there is a vertical seepage gradient, which means a single piezometric surface cannot be used for the whole embankment and foundation; CPT dissipation tests can be very helpful for determining piezometric conditions throughout the soil profile.

Prior to the development of the electric cone penetrometer, the mechanical "Dutch cone" penetrometer was used, but it is now considered obsolete. If mechanical-cone data from an old investigation are available, the measured tip resistance is usually similar to what the electric CPT would measure, but the sleeve has a different configuration, so the sleeve data are not comparable to ECPT sleeve-friction measurements. (Therefore, **tip data** from an older investigation using a mechanical cone could usually be substituted in a modern liquefaction analysis, but the **sleeve data** could not be substituted, which limits the value of the older data.)

CPT data are commonly reported in atmospheres (atm), tons per square foot (ton/ft^2), bars, or kilopascals (kPa). One atm = 2,116 pounds per square foot (lb/ft^2) = 1.058 ton/ft^2 = 1.033 kilograms per square centimeter (kg/cm^2) = 1.013 bar = 101.3 kPa.

The CPT tip resistance, q_c, provides an empirical indication of density and resistance to liquefaction. The measured resistance is normalized to a reference effective overburden stress, and then it is used in empirical correlations to predict the soil's ability to resist liquefaction. The earthquake loading is represented by the Cyclic Stress Ratio (CSR), which is the ratio of the average peak cyclic shear stress to the pre-earthquake effective overburden stress. The average peak is generally assumed to be 65 percent of the overall peak. Adjustments are made to the basic CSR for the effects of the number of load cycles (represented by the earthquake magnitude), in situ static stresses, etc. (also described in the body of Chapter 13, "Seismic Analysis and Design," of *Standards No. 13 – Embankment Dams)*. The soil's resistance to liquefaction is expressed as the Cyclic Resistance Ratio (CRR), which is the empirical maximum CSR for liquefaction to be considered unlikely. (Note that the empirical curves are not firm bounds on liquefaction potential; they are simply lines representing a low likelihood of liquefaction, as discussed in subsequent sections of this appendix.) Determination of the CSR is described in the body of chapter 13. The adjustment of CPT data is analogous to the familiar procedures for SPT presented in Appendix C, "Empirical Assessment of Liquefaction Potential Using the Standard Penetration Test," although the CPT test is more standardized and fewer adjustments are required. The representation of the earthquake loading by the CSR is identical to what is done for the SPT.

Numerous procedures for evaluating liquefaction potential using CPT data have been proposed, beginning in the early 1980s; these include Robertson and Campanella (1985), H. Seed and de Alba (1986), Olsen and Koester (1995), Stark

and Olson (1996), Robertson and Fear (1995), Robertson and Wride (1997), Idriss and Boulanger (2004, 2008), Moss et al. (2006), Robertson (2009), and Boulanger and Idriss (2014). Two of these procedures are presented here. One of them is Robertson's update of the procedure by Robertson and Wride (née Fear), prepared for the 1996 workshop on evaluation of liquefaction resistance. The workshop was sponsored by the National Center for Earthquake Engineering Research (NCEER), which is now known as the Multidisciplinary Center for Earthquake Engineering Research [MCEER]). The 1996 workshop was the basis for typical liquefaction practice for more than a decade afterwards. Robertson and Wride's procedure (abbreviated "RW") was designed to be deterministic; i.e., designed to provide the cyclic resistance ratio as a function of soil properties, with liquefaction essentially precluded by CRR greater than CSR (although it was later shown not to be deterministic, as discussed below). The second procedure presented here, by Boulanger and Idriss (2014) (abbreviated "BI"), is probabilistic, estimating the probability of liquefaction as a function of soil properties and earthquake loading. It is an update and extension of the earlier procedure by Idriss and Boulanger (2004), which also appears in Idriss and Boulanger (2008).

There are several reasons for including both procedures here. First, seismic risk analyses of embankment dams often require liquefaction probabilities, which the BI procedure provides. However, it has the significant drawback of requiring the fines content to be entered for each interval, in contrast to the RW procedure, which requires only the CPT data; it accounts for the effects of fines as a function of the sleeve friction. This makes it possible for large amounts of data to be processed very quickly, for identifying problem areas in the foundation, guiding the location of subsequent CPT soundings, and, possibly, providing the means to estimate fines content for use in the BI procedure for soundings without companion drill holes. However, Moss et al. (2006) found that the RW fines adjustment can overestimate the benefit from fines in some cases. To date (2015), Reclamation and the profession as a whole have greater experience with the 1997 RW procedure than with the 2014 BI procedure.

The CRR is conventionally defined as liquefaction probability of 15 percent, and Boulanger and Idriss refer to their 15-percent probability curve as corresponding to the CRR. The "deterministic" procedure, by Robertson and Wride, is not truly deterministic, in the sense of precluding liquefaction when CRR is greater than CSR. Although it was originally intended to be deterministic, a statistical analysis by Ku et al. (2012), using the expanded database that became available later, showed that the RW CRR curve corresponds to about 30-percent liquefaction. For the RW curve to be directly analogous to other CRR curves, i.e., 15-percent probability, a safety factor of about 1.2 would need to be applied.

For clean sands or sands with modest fines contents, at shallow depths, with M_W between 6.5 and 8.0, the CRR values predicted by the RW and BI procedures are generally similar for normalized clean-sand-equivalent tip resistance up to

100 atm. This is to be expected, because those are the conditions for most historic occurrences of liquefaction. CRR results from various procedures diverge from each other when extrapolating to soil properties or stress conditions that are not well represented in the data set, or are not represented at all. For example, when the fines content is high, or it is expected to be high from the sleeve friction, there are relatively few data to guide an empirical adjustment of CRR for fines.

In silty sands and in silts, the cyclic resistance is greater than in clean sand with the same tip resistance, so an adjustment is required. In the RW procedure, the adjustment is a multiplier that is a function of the tip resistance and sleeve friction, with a higher friction ratio indicating higher fines content and/or more plastic fines, which should give higher cyclic resistance for a given tip reading. The friction ratio and cyclic resistance are affected by both the percentage of fines and the nature of the fines, and the assumption is that the friction ratio allows empirical prediction of the effect of the fines. (Moss et al. included the friction ratio as an independent variable in the regression.) In contrast, the BI adjustment for fines is additive, and it is a function of the measured fines contents from companion drill holes, or fines contents estimated by correlation. Boulanger and Idriss caution that plastic fines may require a different analysis; for material with PI greater than about 7, they recommend using an approach developed specifically for clayey soils. It could be unnecessarily conservative to apply the BI procedure with plastic fines. Case history data (Moss et al., 2006) that became available after the RW procedure was published indicate that, where claylike behavior is suggested by high friction ratios, the RW procedure can be unconservative. The BI procedure appears to fit fairly well with case histories of materials with fines, and its calculations are straightforward and transparent. However, it has the major drawback of requiring the fines content to be input at each interval being evaluated. One of the primary reasons to use the CPT is to obtain a large amount of detailed subsurface information quickly and at lower cost than drilling. That advantage is lost if a drill hole is required next to each CPT sounding. Boulanger and Idriss (2014) suggest a general correlation to estimate fines content from Robertson's parameter, I_C, defined below, which is a function of tip and sleeve measurements. **However, that general correlation has a large amount scatter, so only a site-specific correlation should be used for Reclamation high-hazard dams.**

The recommended approach is to apply both BI *and* RW procedures for all CPT soundings that have companion drill holes, checking for agreement or disagreement between the RW and BI CRR results (recognizing that they correspond to about 30- and 15-percent liquefaction probability, respectively). If the results are not roughly in agreement, the reason for this should be investigated. The RW procedure is applied to all holes, with and without samples. It includes calculation of the soil behavior type index, I_C, which may correlate well enough with measured fines content for a particular site to provide a reasonable estimate of fines content for CPT soundings without companion drill holes. If it does, the BI procedure can be applied to all of the soundings, not just

those with companion holes. All other available indices of liquefaction potential, like the SPT or shear-wave velocity (V_s), should be included in the overall assessment of liquefaction potential.

An important limitation with all of the procedures is that they were developed from back analysis of limited data sets. Even the expanded databases used by Moss et al. (2006) and by Boulanger and Idriss (2014) included few data from depths greater than 20 feet, or with magnitudes outside the range of 6.5 to 8.0. The result is that, while uncertainty may be comparatively minor in forward analysis **for conditions similar to the case histories**, it becomes much greater when relationships are projected into regions with few or no data to constrain the relationships. Projection by simply extrapolating regression equations may not reflect the actual mechanics of soil and earthquakes. For example, the effect of high overburden stress on liquefaction probability may not be clear from field behavior because the range of stresses in the case histories is too narrow, or there are too many other variables in proportion to the number of data. While laboratory testing never strictly replicates field conditions, **trends** measured in controlled experiments can be informative. A controlled series of laboratory cyclic shear tests may be able to identify the trend much more precisely than the field data, which come from sites with widely different material properties, ground motions, overburden stresses, etc.

What follows is a simplified description of using empirical procedures for evaluating liquefaction potential and probability; it is not a complete survey of the topic. For detailed description, refer to Robertson and Wride (1997), Moss et al. (2006), Idriss and Boulanger (2008), Robertson (2009), and Boulanger and Idriss (2014).

B.1.2 Testing Program

CPT testing must be performed in accordance with ASTM D-5778-12 (ASTM, 2012). Reclamation has a 20-ton, electronic piezocone penetrometer vehicle that can perform this testing. Many contractors are also capable of good-quality CPT testing, and less can go wrong with the CPT test procedure than with the SPT. While pore-pressure measurements can be problematic, due to the difficulty of maintaining saturation of the porous element above the water table, they are not used directly in the liquefaction triggering procedure. They can, however, be very helpful in assessing material types, layering, and static piezometric conditions (with pushing halted to allow dissipation of excess pore-water pressure). The maximum testing depth is typically 100 to 150 ft, but testing can be performed to greater depths with special equipment; however, that may require drilling and either casing or backfilling with pea gravel, which would increase costs and slow the exploration. Not all sites are suitable for CPT; material with too much gravel or with cemented zones cannot be tested easily.

However, overlying material can be predrilled, so the CPT does not have to penetrate it to reach the layer that needs to be tested.

During field testing, CPT data can be reduced and plotted immediately after completion of each sounding. This allows the testing program to be monitored and decisions to be made regarding changing or adding test locations. The data from the testing program should include a summary plot, table of interpreted soils and engineering properties, and a digital data file for additional processing and interpretation. The records should also include all assumptions used for the field plots, including piezometric level, as well as the procedures and empirical parameters used for estimating material properties, etc. The field plots are typically based on assumed "default" correlations that may not be appropriate for the final analysis.

The CPT is a very useful complement to other liquefaction investigations because of its ability to rapidly indicate small-scale stratigraphy and show the areal extent of potentially liquefiable materials. The CPT collects data at intervals of 2 inches (actually 5 cm) or less, and sand layers as thin as 4 inches can be detected. Cone testing can be performed at much lower cost than SPT. It may be appropriate to perform a large number of CPT soundings before or concurrently with drilling, and use the CPT to guide the location of the drill holes. Although drilling is generally much slower and more expensive than CPT, soil samples are still necessary.

Because the CPT does not provide a soil sample, SPTs (or other form of sampling) are almost always performed at a site in conjunction with CPT. This usually requires mobilization of a drill rig to the site, in addition to the CPT rig, although under the right conditions, some CPT rigs, including Reclamation's, can perform direct-push sampling that is adequate for basic index properties (fines content, Atterberg limits). In some cases, undisturbed samples are needed. It is standard practice to have a number of locations at each site where CPT and SPT soundings are located very close to each other for comparison of penetration resistance, and comparison of the material types inferred from CPT against the actual material sampled by the SPT. It is especially important to check inferred classifications against sampling in "mixture" soils (i.e., coarse-grained soils with fines [clayey and silty sands, SC or SM] and fine-grained soils with sand [sandy silts s(ML) and sandy clays s(CL]). The actual grain-size distribution of the materials being evaluated needs to be tested, with particular attention paid to layering. (Layers **should not** be mixed for determining fines content.)

If the layering indicated by drilling and that from CPT do not agree closely, it is possible that the CPT sounding deviated from vertical by as much as 10 or even 20 degrees, which could cause the measured depth to be as much as 6 percent greater than the actual depth. Deviation is most likely to occur in gravelly soils, dense soils, or at sites that have been improved by in situ densification. Sometimes, layers that are cleaner or finer than the surrounding material can be

used as markers to establish the correct depth. It may also be that the stratigraphy really is different between the drill hole location and the CPT location, even if they are located very close to each other. Alluvium in meandering and braided streams often shows abrupt changes in material type, resulting from repeated erosion and deposition with changes in stream flow. Profiles of CPT data should be shown on cross sections through the site (along with SPT, geology, and other data), to make it easier to see trends, continuous weak layers, marker layers, etc.

The data base of liquefaction case histories is predominantly from quartzitic sands with hard particles. If compressible calcareous or micaceous sand particles are present, the tip resistance can be lower than in hard particles at the same relative density. This could cause the density to be underestimated (thereby indicating lower cyclic resistance) and/or cause incorrect soil classification by affecting the friction ratio. It is not clear, however, what the net effect would be on the determination of liquefaction potential. Soil samples need to be examined for the presence of these atypical materials, in which the empirical procedures may not work well. The geologic origin of the soil may provide an indication that compressible particles could be present. (Consult a geologist.)

With very thin layers, such as commonly found in hydraulic fills, the sleeve friction measurement may not be as meaningful as it is in other soils, even though the measurements are generally offset in the calculations, so they are taken at the same depth (instead of at the same time). Sampling is always required to verify classifications and fines adjustments made on the basis of friction measurements.

B.1.3 Selecting Representative Adjusted Tip Resistance Within a Layer

CPT tip resistance within a given layer is never completely uniform. In layers of concern for liquefaction, cone tip resistance values to represent the layer as a whole are selected from the measured values, considering horizontal and vertical variation, mode of soil deposition (for its effect on layer continuity), and the soil classifications indicated by CPT classification charts and nearby drill holes. Different researchers have based their procedures on different procedures of selecting the representative value. However, most procedures (including those discussed in this appendix) have used the average within the stratum that liquefied (or in the most susceptible stratum in the nonliquefaction cases), rather than the lowest tip resistance in the layer at each CPT sounding. The charts for liquefaction resistance are generally based on the **average,** normalized, clean-sand-equivalent tip resistance within the layer(s) that liquefied. In "forward analysis," it is not always clear which values should be included in a numerical average. The common practice of averaging only horizontally; i.e., averaging the lowest value in every CPT sounding (on the assumption that the overall strength is governed by an undulating surface that passes through the weakest intervals) can be unnecessarily conservative in a procedure that was originally developed

with averaging both horizontally and vertically. If the materials appear to be more randomly distributed, without much continuity, a conservative approximation of the average within the whole layer may be appropriate, such as the 33rd percentile. This judgment requires careful study of the CPT and other indices of density (SPT, V_S, etc.) in conjunction with the geology and geometry of the foundation. No single rule can cover all sites and all procedures. If the liquefaction analyses are inputs for risk analysis, a plausible range of **representative average values** is usually required, not just **statistics on the data set**. Determining which data to include in the average needs to consider the minimum liquefied area of the foundation required for instability or excessive deformation.

Again, CRR and liquefaction probability for a particular layer are not determined from the lowest adjusted tip resistance in the layer. In keeping with the development of the various procedures, they are associated with the *average* value. A spreadsheet or computer program that analyzes each CPT interval individually can be misleading by identifying intervals of low CRR or high probability that would not be identified as such if the average is considered. One cannot simply consider interval-by-interval output from the spreadsheet without grouping the intervals for averaging.

B.1.4 Equivalent Tip Resistance in Thin Layers

CPT tip resistance is influenced by soil several cone diameters below the tip. The tip resistance measured in sand that overlies softer material can be substantially lower than what would be measured if there were more of the same sand below instead of the softer material. As a result, thin, clean sand layers embedded in silt or clay are often misclassified as silty sands by classification charts that use tip resistance and sleeve friction, and the predicted liquefaction resistance may be incorrect (too low). Robertson and Wride (1997) provided a procedure to adjust for this situation in the NCEER volume on liquefaction assessment, which is described below. The computer program, CLiq, which Reclamation uses at present (2015), can perform this operation automatically (GeoLogismiki, 2014), but the results must be checked against soil samples, to the extent possible. Figure B2, from Robertson and Wride (1997), shows the adjustment for thin layers.
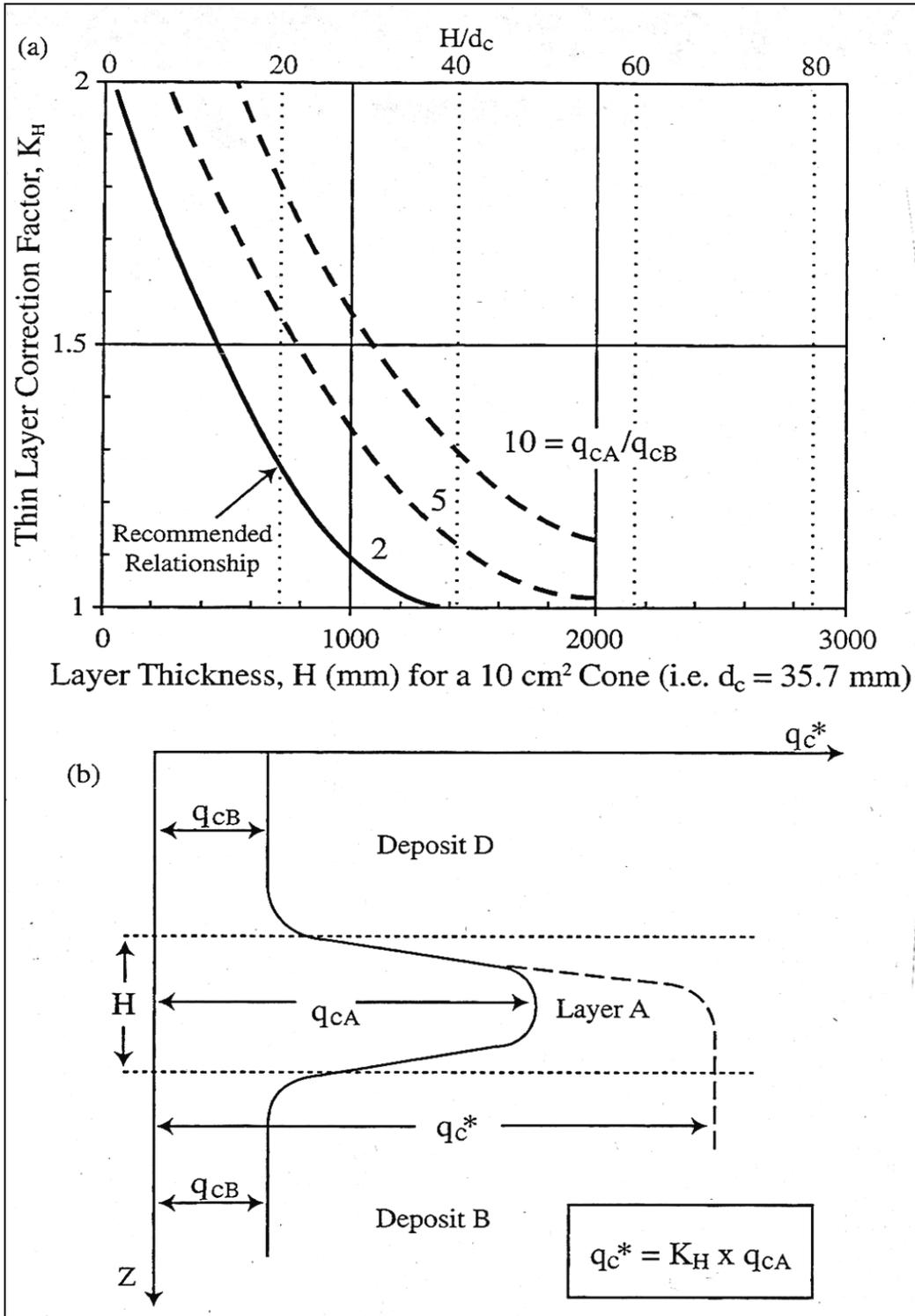
Figure B2. Adjustment of CPT tip resistance for thin sand layer overlying soft material, from Robertson and Wride (1997).

The adjusted tip resistance, q_c*, is calculated as follows, and then it is substituted for the actual measured q_c in the procedures outlined below for estimating liquefaction resistance:

$$q_c* = K_H \times q_c \qquad\qquad \text{Equation B1}$$

The correction factor, K_H, is shown in figure B2. It is a function of the ratio of tip resistances in the two layers (q_{cA} / q_{cB}), and the thickness of the sand layer (measured from the cone tip to the top of the softer layer below). Robertson and Wride (1997) recommended basing the correction on an assumed ratio q_{cA} / q_{cB} of 2.0 (solid curve), which can be approximated as follows:

$$K_H = 0.5 (0.036 \, H/d_c - 1.45)^2 + 1.0 \qquad\qquad \text{Equation B2}$$

where d_c is the cone diameter, and H is the layer thickness, in the same units, limited to $H < 40.6 \, d_c$. In most of the literature, those dimensions are expressed in millimeters (mm). The typical 10 cm^2 cone's diameter is 35.7 mm, but any consistent length unit can be used. If equation B2 is used with layer thickness H in feet, d_c is 0.117. This adjustment should be applied (or at least considered) for layers of sand less than 600 mm or 2 feet thick, if they overlie soft clay. As shown on Figure B2, measurements in layers up to about 6 feet thick (1,800 mm) could possibly be affected by a very soft underlying layer, although the NCEER recommended adjustment would have little effect in layers thicker than about 2 feet.

B.2 Updated Robertson and Wride Procedure for Assessing Liquefaction Potential)

B.2.1 General

This procedure for predicting liquefaction potential from CPT measurements follows the recommendations of Robertson and Wride (1997), with updates made by Robertson (2009) to fit with the greatly expanded data set that became available later. Prior to the 2009 updates, the RW procedure was adopted by the NCEER workshop as the preferred procedure. (The workshop proceedings included an alternative procedure by Olsen and Koester [1997], but it has not been widely used and is not presented here.)

The RW procedure is conceptually very similar to liquefaction potential analysis by the widely used Seed-Lee-Idriss procedure using the SPT. The tip resistance is normalized for the effects of overburden pressure to obtain Q_{tN}, and then it is multiplied by an adjustment factor K_C to account for the beneficial effect of

fines content, yielding Qq_{tNCS}, from which the CRR can be predicted. These calculations are detailed below.

Use of the RW procedure is limited to materials whose overall behavior is sandlike; i.e., clean sands, and silty sands and sandy silts with no or very low plasticity. Figure B3 below is a chart indicating general soil behavior as a function of the normalized tip resistance, Q_{tn}, and the normalized friction ratio, F_r (both defined below, in equations B3 and B5). The RW procedure is applicable primarily to materials located above and left of the dashed line labeled "$I_C = 2.6$," essentially just Zones 5, 6, and 7, and a small part of Zone 4. (I_C is also defined below, in equation B7.) Increasing I_C corresponds to increasingly claylike behavior and higher values of K_C, which is the multiplier applied to the tip resistance to account for the higher cyclic resistance with more fines. Originally, I_C greater than 2.6 had been proposed as a boundary separating liquefiable material from nonliquefiable clayey material. However, several examples of liquefied soils with higher I_C were identified subsequently, so the transition from sandlike to claylike materials is now considered gradual, between 2.5 and 2.7. If I_C is greater than 2.7, the cyclic resistance must be evaluated by methods for claylike soil, rather than the procedure described here for sandlike materials; between 2.5 and 2.7, it is less clear which type of behavior would occur, or if it would be somewhere in between. Both types of behavior need to be considered in this range.

The measured tip resistance, q_c is adjusted for the effect of excess pore-water pressure. At the base of the cone, just below the pore-pressure element in figure B1, there is a "shoulder," where the pore-water pressure acts on the base of the cone, reducing the measured tip resistance proportionately. This is corrected for by adding the resulting water force to the actual measured tip resistance:

$$q_t = q_C + u_2 (1 - a) \hspace{4cm} \text{Equation B3}$$

where a is the ratio of the net area of the cross section (total minus the area of the ring) to the total area of the cross section (typically 10 cm^2). The value of a is typically 0.70 to 0.85 and is provided by the manufacturer. Equation B3 requires valid measurements of u_2, but measuring u_2 relies on full saturation of the porous filter for the transducer (the dark band in figure B1). This is not always easy to achieve and maintain, particularly if the cone has to penetrate a large thickness of unsaturated soil before reaching the depth of interest. In pervious material (clean sand or sand with minor fines content), u_2 is likely to be small, and when necessary, it can be assumed to be zero, which would add a minor amount of conservatism. In soft clay or silt, the effect can be more important. When u_2 measurements are available, the calculations are done automatically by most CPT data-reduction programs.
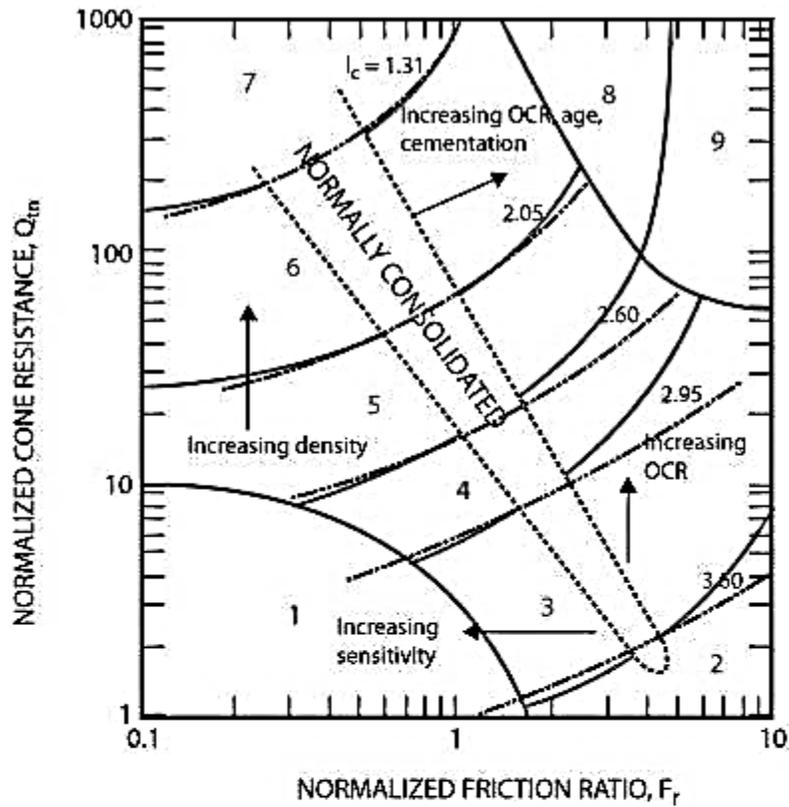
Zone	Soil Behavior Type	I_c
1	Sensitive, fine grained	N/A
2	Organic soils – clay	> 3.6
3	Clays – silty clay to clay	2.95 – 3.6
4	Silt mixtures – clayey silt to silty clay	2.60 – 2.95
5	Sand mixtures – silty sand to sandy silt	2.05 – 2.6
6	Sands – clean sand to silty sand	1.31 – 2.05
7	Gravelly sand to dense sand	< 1.31
8	Very stiff sand to clayey sand*	N/A
9	Very stiff, fine grained*	N/A

Heavily overconsolidated or cemented

Figure B3. Material classification chart. (Source: Robertson and Cabal, 2014)

Q_{tn} is the measured tip resistance (adjusted for u_2), normalized for the effect of overburden pressure:

$$Q_{tn} = C_N (q_t - \sigma_{vo}) / P_a \qquad\qquad \text{Equation B4}$$

where P_a is atmospheric pressure, and C_N is the normalizing factor:

$$C_N = (P_a / \sigma'_{vo})^n \qquad\qquad \text{Equation B5}$$

and F_r is the friction ratio, comparing the measured sleeve resistance with tip resistance:

$$F_r = [f_s / (q_t - \sigma_{vo})] \times 100\% \qquad\qquad \text{Equation B6}$$

C_N should be capped at 1.7 (which is relevant only very close to the ground surface). The exponent n is calculated as a function of the soil behavior type index, I_C:

$$I_c = [(3.47 - \log Q_{tn})^2 + (1.22 + \log F_r)^2]^{0.5} \qquad\qquad \text{Equation B7}$$

$$n = 0.38 I_C + 0.05 (\sigma'_{vo}/p_a) - 0.15 \qquad\qquad \text{Equation B8}$$

The value of n is limited to the range from 0.5 to 1.0.

It can be seen that Q_{tn} is a function of n, and n is a function of Q_{tn}, so it is necessary to iterate, beginning with an assumed value of n to find the initial value of Q_{tn}, using that Q_{tn} to find I_C and a new n, updating Q_{tn} with the new n, and so on, until adequate closure is reached. (Three iterations should usually suffice, although the spreadsheet program Excel can perform the iteration automatically to any desired level of convergence.)

With n established, the normalized tip resistance Q_{tn} and the clean-sand-equivalent (fines-adjusted) normalized resistance are calculated with C_N from equation B5. The coefficient K_C is the grain characteristic correction factor, often referred to as the "fines adjustment":

$$Q_{tn} = C_N q_C \qquad\qquad \text{Equation B9}$$

$$Q_{tn\,CS} = K_C Q_{tn} \qquad\qquad \text{Equation B10}$$

K_C is a function of I_C, as shown in figure B4 and equations B11a through B11d. If I_C is between 2.5 and 2.7, equation B11d would indicate a very high value of K_C, indicating very high resistance to sandlike **liquefaction** in soils that are not obviously sandlike or claylike from the CPT data. While that may be correct, it does not necessarily indicate high resistance to claylike **cyclic failure**. For preliminary analysis, it may be appropriate to limit the value of K_C to 2.0 or 2.5,

to reduce the potential that weak or liquefiable layers would be missed because of high K_C in the transition range of I_C. If the expected behavior depends on a high value of K_C, sampling is indicated. Refer to Section 13.7 of Chapter 13 for discussion of fine-grained and claylike soils.
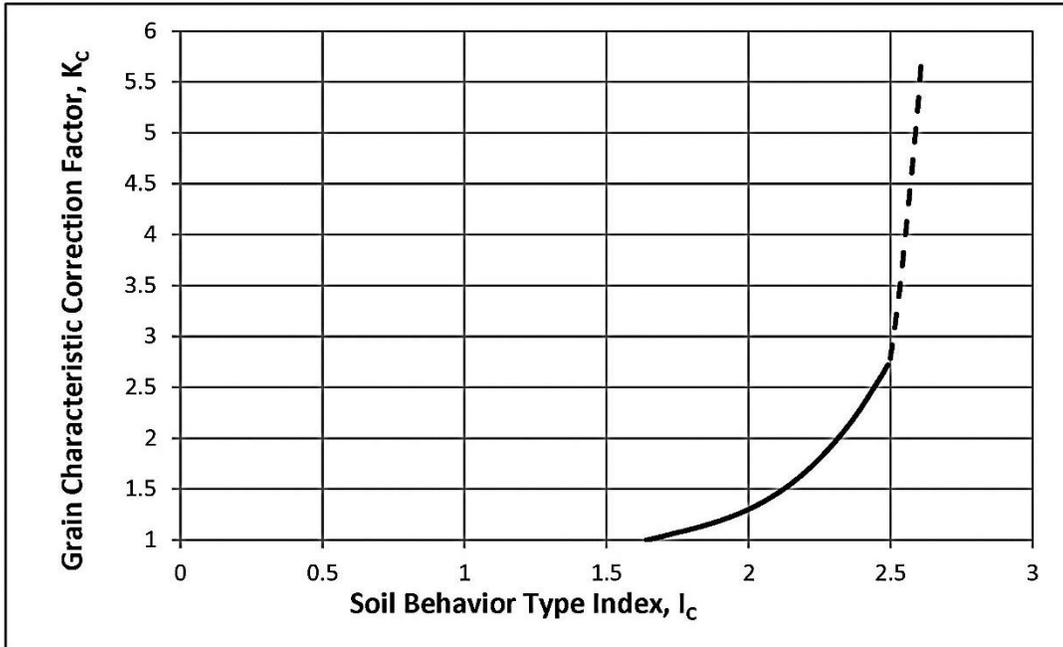
Figure B4. Grain characteristic correction factor, K_C, as a function of the Soil Behavior Type Index, I_C, based on Robertson (2009). Note that high K_C indicates high resistance to liquefaction, but not necessarily high resistance to cyclic failure of claylike soil.

In equation form:

If $I_C \leq 1.64$, $K_C = 1.0$ Equation B11a

If $1.64 \leq I_C \leq 2.5$, $K_C = -0.403\ I_C^4 + 5.581\ I_C^3 - 21.63\ I_C^2 + 33.75\ I_C - 17.88$

                                                                                                  Equation B11b

Except,

If $1.64 < I_C < 2.36$ <u>AND</u> F<0.5%, $K_C = 1.0$ Equation B11c

Robertson's relationship for K_C for higher values of I_C, equation B11d, becomes quite large as I_C increases above 2.5.

If $2.5 \leq I_C \leq 2.7$, $K_C = 6 \times 10^{-7}\ (I_C)^{16.76}$ Equation B11d

Again, great caution is required in using equation B11d, which is applicable to values of I_C corresponding to a transition between sandlike and claylike behavior. The very high value of K_C indicates very high resistance to sandlike liquefaction, but the resistance to claylike cyclic failure and resulting strain softening may not be high. Both sandlike and claylike behavior need to be considered for soils in this transition zone.

Finally, the cyclic resistance ratio, $CRR_{M=7.5,\sigma'=1}$, is determined from figure B5 or equations B12a and B12b. (Robertson and Wride actually referred to it simply as $CRR_{7.5}$; the more complete notation is used here for consistency with the rest of Chapter 13.)

If $50 < Q_{tnCS} < 160$, $CRR_{M=7.5,\sigma'=1} = 93*[Q_{tnCS} / 1,000]^3 + 0.08$ Equation B12a

If $Q_{tnCS} < 160$, $CRR_{M=7.5,\sigma'=1} = 0.833 [Q_{tnCS} /1,000] + 0.05$ Equation B12b
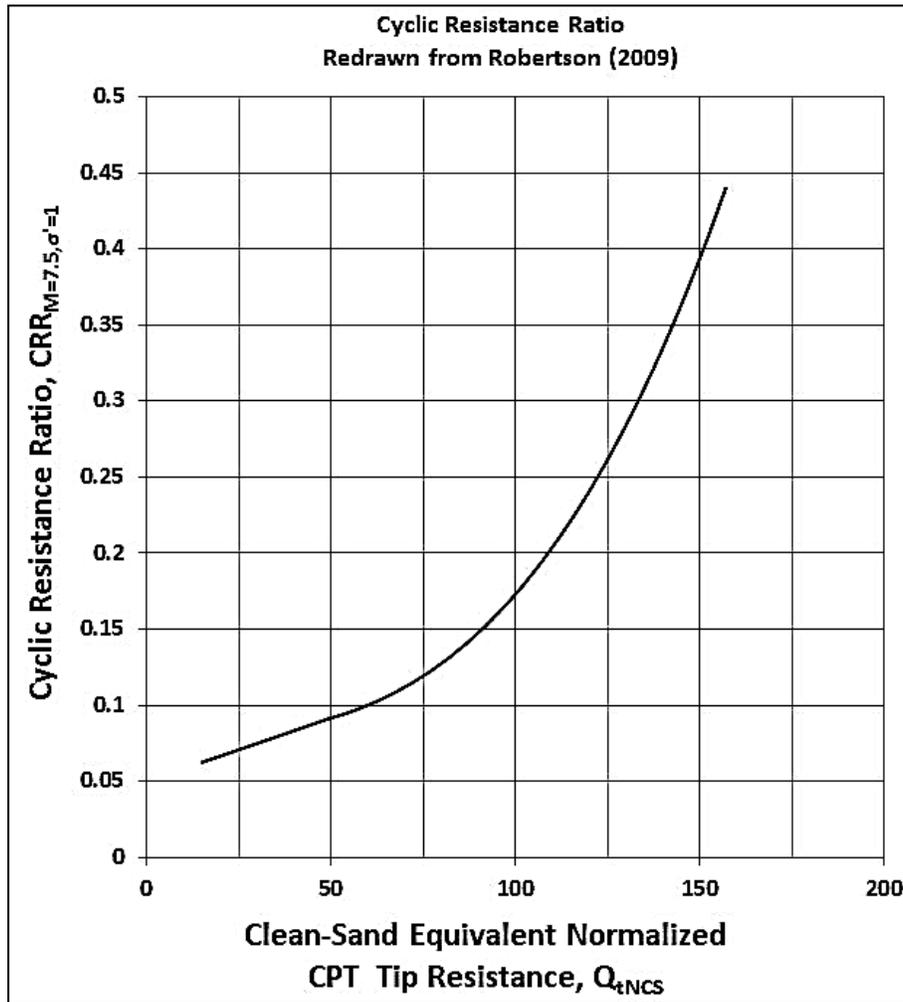
Figure B5. Cyclic Resistance Ratio, $CRR_{M=7.5,\sigma'=1}$, for M = 7.5, σ'_v = 1 atm.

The value of $CRR_{M=7.5,\sigma'=1}$, from figure B5 or equations B12a and B12b, is specific to the reference conditions: $M_W = 7.5$ and $\sigma'_{vc} = 1$ atm. The comparison between cyclic loading and cyclic resistance must be made between either the CSR and CRR for the specific conditions of the site and earthquake, or between the values adjusted to the reference conditions, i.e., $CSR_{M=7.5,\sigma'=1}$ and $CRR_{M=7.5,\sigma'=1}$. In general, the latter form is preferred, for consistency among projects, and to simplify calculation and presentation when more than one level of earthquake loading needs to be assessed, which is usually the case in probabilistic risk analysis. Determination of $CSR_{M=7.5,\sigma'=1}$ is described in Section 13.6.2 of Chapter 13.

Like most CRR relationships that are based on in situ testing, the CRR found from equation B12 or figure B5 is not considered a hard lower bound on the cyclic loading that could cause liquefaction. Although it was originally intended to be deterministic, Ku et al. (2012) concluded that this curve represents about 30-percent probability of liquefaction, based on a much larger database that became available after available. Other researchers have explicitly stated that their similar CRR curves are intended to correspond to liquefaction probability of about 15 percent. Lower probability of liquefaction requires a factor of safety applied to the calculated CRR.

The use of equations, instead of charts, to determine the various parameters allows for computer processing and plotting of the complete data profile with relatively little expenditure of time. Reclamation has used both Microsoft Excel spreadsheets and dedicated programs such as CLiq to reduce the data and determine liquefaction potential (GeoLogismiki, 2014). The program CLiq can apply several different procedures, including this one. However, as with any other program or spreadsheet, input assumptions must be checked to ensure that no errors have been made in entering units, depth to water table, etc., and that the empirical procedures(s) used are up to date. Also, the three-digit precision shown in the equations does not mean that the results are that precise!

As described in section B.1.3, this procedure (like most other procedures for CRR and liquefaction probability) was based on the **average** tip resistance in the layer in question, not the lowest tip resistance. A few scattered CPT intervals indicated by the program or spreadsheet to have low CRR do not necessarily mean that the deposit, as a whole, has low CRR.

The RW procedure is limited to soils that behave in the CPT as though they are predominantly sand. The limiting fines content (beyond which other procedures of assessing liquefaction potential are required) could be less than 20 percent with very plastic fines, or well over 60 percent if the fines are mostly coarse silt that barely passes the U.S. Standard No. 200 sieve (0.075 mm), which distinguishes

sand from silt. For plastic materials, refer to section 13.7 of Chapter 13, "Seismic Analysis and Design," of *Design Standards No. 13 – Embankment Dams.*

The RW procedure was developed using relationships for the mass participation factor (r_d), magnitude scaling factor (MSF), and overburden adjustment (K_σ) that are older than those presented in the main text of Chapter 13. To the extent practical, the use of any correlation in forward analysis should be consistent with the assumptions used in its development. However, for most of the case histories from which the RW procedure was developed, the differences would be fairly minor because of the depths (mostly between 5 and 30 feet) and the earthquake magnitudes that were involved (almost all between 6.5 and 8.0). For those conditions, all of the r_d, K_σ, and MSF relationships give values close to 1.0 (by definition), and there simply is not much potential for differences among the various curves. The RW CRR curve would not have looked much different had the newer r_d, K_σ, and MSF relationships been used in the back analysis. However, substantially greater differences can occur when those relationships are extrapolated outside the range of data, e.g., depth exceeding 30 to 40 feet, as it generally does beneath a dam, or earthquake magnitude less than 6.5.

B.2.2 Implementing the RW Procedure

The steps required to implement the RW procedure for assessing liquefaction potential of sand-like soils are shown as a flowchart in figure B6 (based Robertson and Cabal, 2007). The quantities q_C f_s, and σ_{vo}, can be measured in any consistent set of units because they all become dimensionless with normalization by atmospheric pressure, P_a, in the same units.

The RW procedure can be implemented using figures B4 and B5 for K_C and $CRR_{M=7.5,\sigma'=1}$ or with the equations above. The equations make it feasible to use a spreadsheet or a dedicated computer program, such as CLiq (GeoLogismiki, 2014), for processing and plotting the complete data profile, with relatively little expenditure of time. Reclamation has used both Excel spreadsheets and CLiq. These typically provide CRR interval by interval; however, recall that the RW relationship is based on averages within a layer, so individual intervals with low CRR do not necessarily mean CRR is low for the layer.

To reiterate, the RW equation for $CRR_{M=7.5,\sigma'=1}$ and figure B5 do not provide an absolute boundary on liquefaction potential. Instead, they represent conditions for which the probability of liquefaction is about 30 percent, with the probability dropping off quickly as $CSR_{M=7.5,\sigma'=1}$ decreases (Ku et al., 2012). (For $CSR_{M=7.5,\sigma'=1}$ greater than $CRR_{M=7.5,\sigma'=1}$, the likelihood of liquefaction increases, of course.)
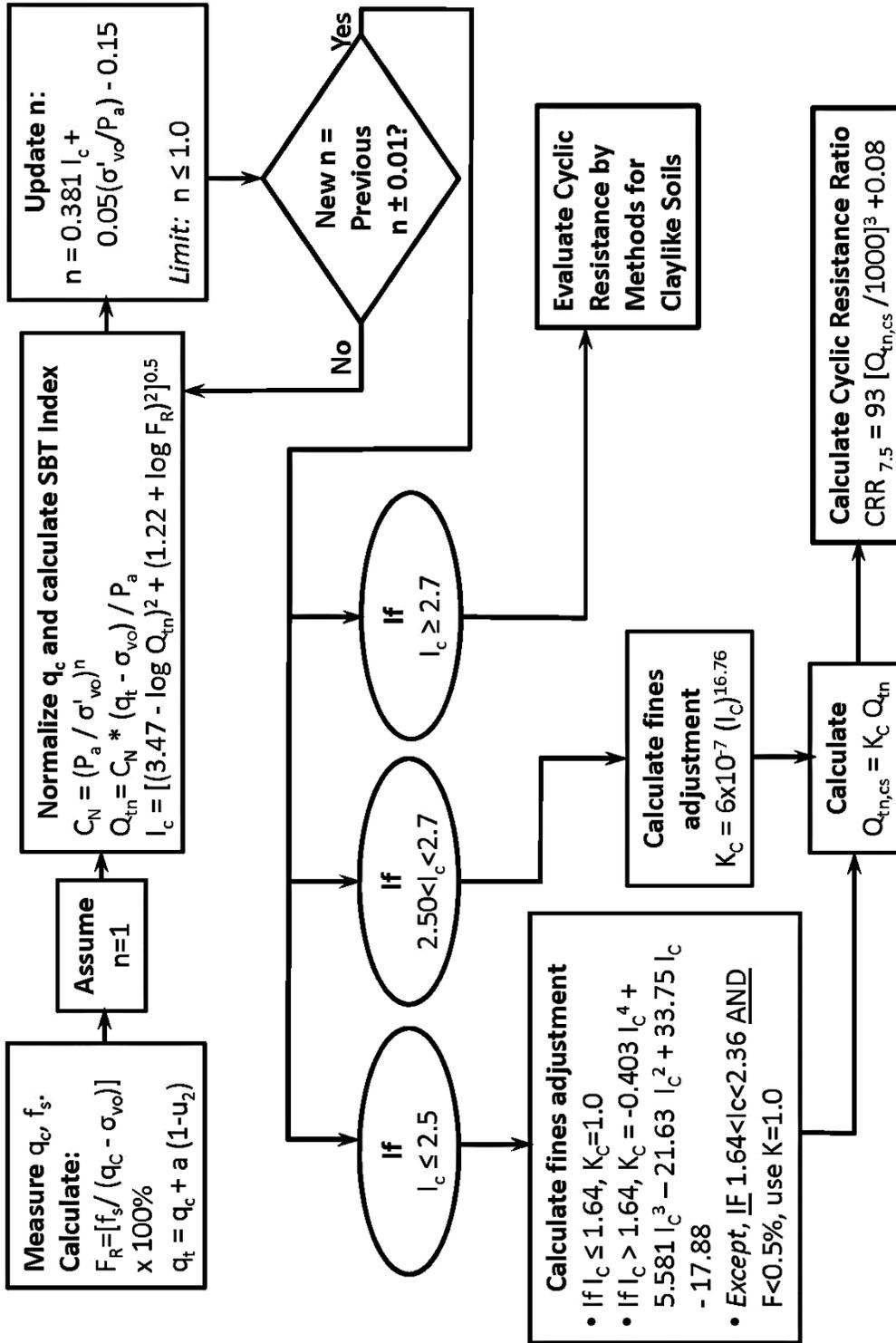
Figure B6. Flowchart for RW procedure (modified from Robertson and Cabal. 2014).

B.2.3 Details and Discussion

B.2.3.1 Soil Behavior Index, I_C

Soil behavior groups corresponding to different types of soil materials are divided according to cone tip resistance and sleeve friction, as shown on figure B3, from Robertson and Cabal (2014) (modified from Robertson and Wride, 1997). Initially, the group boundaries were drawn according to soil classification. Similar behavior would be expected from soils in the same location on the chart. It was noticed later that the boundaries were concentric circles (approximately), and it was proposed that the effect of grain sizes on liquefaction potential could be predicted by the radius. To allow automated soil classification and determination of $CRR_{7.5,cs}$, the soil behavior type index, I_C, was defined as the radius of the circle, easily calculated from Q_t and F_r. Increasing I_C corresponds to increasingly claylike behavior and, therefore, increasing resistance to liquefaction. Figure B4 shows the increase, in the form of the multiplier K_C that is applied to Q_{tn} to obtain $Q_{tn,cs}$.

The RW procedure is intended primarily for soils falling in zones 5, 6, and 7 of figure B3, which have I_C less than 2.6, rather than zones 1, 2, 3, and 4 ($I_C > 2.6$). (In zones 8 and 9, where Q_t and F are both high, the soil is stiff, probably clayey and overconsolidated or cemented, making liquefaction or high sensitivity unlikely.) A particular soil with I_C greater than 2.6 is **probably** not liquefiable, but Moss et al. (2006) show examples of liquefied soils with I_C significantly greater than 2.6. Moss et al. also point out that I_C was developed by correlation with soil classification, not with liquefaction resistance. Therefore, the relationship between I_C and liquefaction resistance is indirect, with general material properties predicted from I_C, and liquefaction resistance predicted from CPT tip resistance and material properties, as opposed to a direct relationship between cyclic resistance and CPT measurements.

Pore pressure response measured during the CPT sounding may provide corroborating information on material behavior. For example, a sudden spike of very high pore pressure coincident with low q_c would suggest a soft, clayey layer within denser material. While that layer may not be liquefiable, it could form an impervious layer that prevents drainage, thereby having an adverse effect on post-earthquake shear strength. (Refer to Appendix F, "Soil Strengths for Seismic Analysis.")

B.2.3.2 Portrayal of Results

For use by a risk-estimating team or other analysts, graphic portrayal of the results of liquefaction assessment are often the most effective means. One common format is shown in Figure B7. The analysis generates a profile of $CRR_{7.5,\sigma'=1}$. The seismic loading, $CSR_{7.5,\sigma'=1}$, can be plotted on the same profile for one or more selected earthquakes, making problem areas immediately apparent. In the profile, there will often be intervals where a clean-sand equivalent CPT procedure is not

applicable, such as gravel zones or fine-grained layers. To avoid confusion, CRR data should not be shown for those intervals.
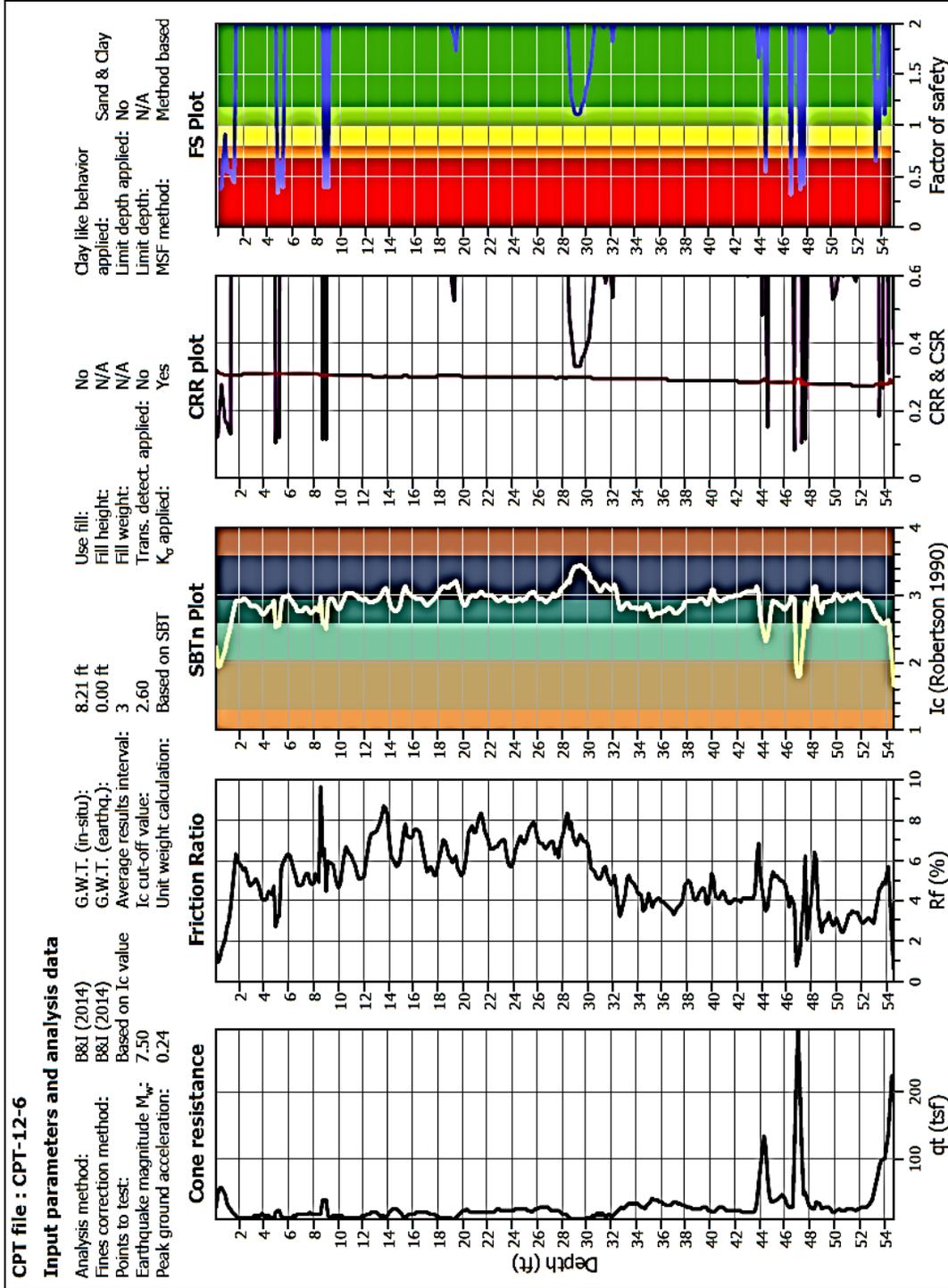

Figure B7. Portrayal of CPT liquefaction analysis as profile of CSR and CRR.

Another way of displaying the liquefaction evaluation is to plot the values of $(q_{c1N})_{cs}$, required to provide some value of CRR liquefaction for a given loading alongside the measured $(q_{c1N})_{cs}$. This portrayal is helpful in ground improvement studies where target values of penetration are needed.

It can also be useful to superimpose pairs of representative $(q_{c1n})_{cs}$ and $CSR_{7.5,\sigma'=1}$ on figure B5 for comparison with the curve of $CRR_{7.5,\sigma'=1}$, as shown in figure B8. In this example, pairs from different parts of the foundation are shown for two different levels of earthquake loading, showing a clear difference in expected behavior. In the 5,000-year earthquake, liquefaction would be expected in much of the foundation, in contrast with generally good behavior expected in the smaller one.
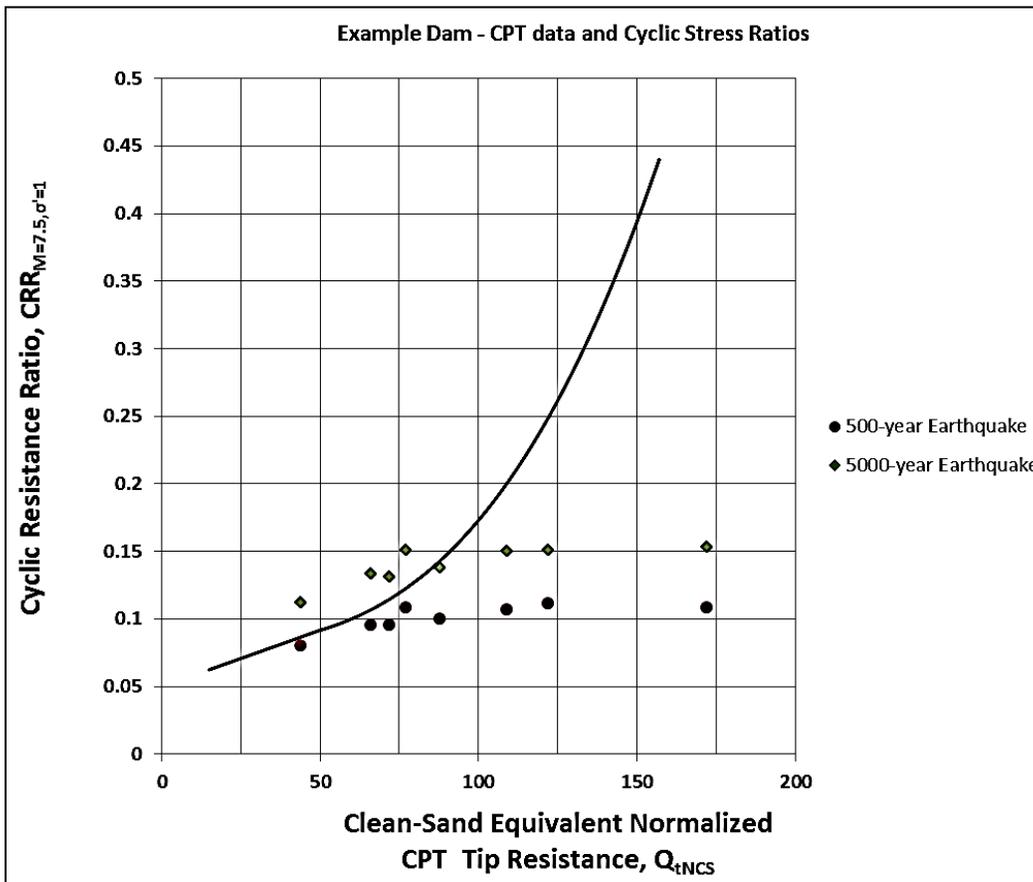
Figure B8. Example of CPT liquefaction results superimposed on Robertson-Wride CRR relationship.

Any report of liquefaction analysis should include references for the methodology, assumptions about piezometric levels, the basis for selecting representative values of q_{C1N} and other parameters from the data set, identification

of intervals where the thin-layer adjustment was applied, and the assumptions for the CSRs.

B.3   Boulanger-Idriss Procedure for Assessing Liquefaction Potential and Liquefaction Probability

In 2014, Boulanger and Idriss published a new study incorporating updated back analyses and a much larger database than Robertson and Wride had available (Boulanger and Idriss, 2014). Statistical analysis was used to estimate the probability of liquefaction, as well as to providing the conventional curve of cyclic resistance ratio, CRR. (In keeping with typical practice, CRR was defined to correspond to liquefaction probability of 15 percent, quite similar to the de facto value of 30 percent on the RW CRR curve.) The other major difference from the RW procedure is that the BI adjustment for fines is additive, and it is a function of the measured fines content in samples from companion drill holes, rather than being a multiplier based on the friction ratio.

Boulanger and Idriss state that, in sands, the difference is small between q_C, the measured tip resistance, and q_t, the tip resistance after it is adjusted for the effect of pore-water pressure acting on the shoulder of the cone. (See equation B3.) They recommend that the adjustment be made whenever u_2 data are available, although they use the notation "q_C" throughout, with the adjustment being implicit. Except in soft material with low permeability, the difference is fairly small, and it is conservative to neglect it.

B.3.1   Adjusting CPT Data to Reference Conditions

The adjusted cyclic resistance ratio, $CRR_{7.5}$, is a function of tip resistance q_C, normalized to the standard effective overburden stress of 1 atm, and adjusted for the effect of fines, to obtain the clean-sand equivalent value, q_{c1Ncs}. The value of q_{c1Ncs} is found by first converting the measured tip resistance q_c to atmospheres (1 atm = 2,116 lb/ft^2), then multiplying it by the empirical factor C_N (similar to Robertson and Wride's C_N, but slightly different in value) to find the normalized tip resistance that would be measured in that same sand at the same density, with an effective overburden stress of 1 atm.

$$q_{c1N} = q_{cN}* C_N \hspace{4cm} \text{Equation B13}$$

The value of C_N is found using equation B14 or figure B9.
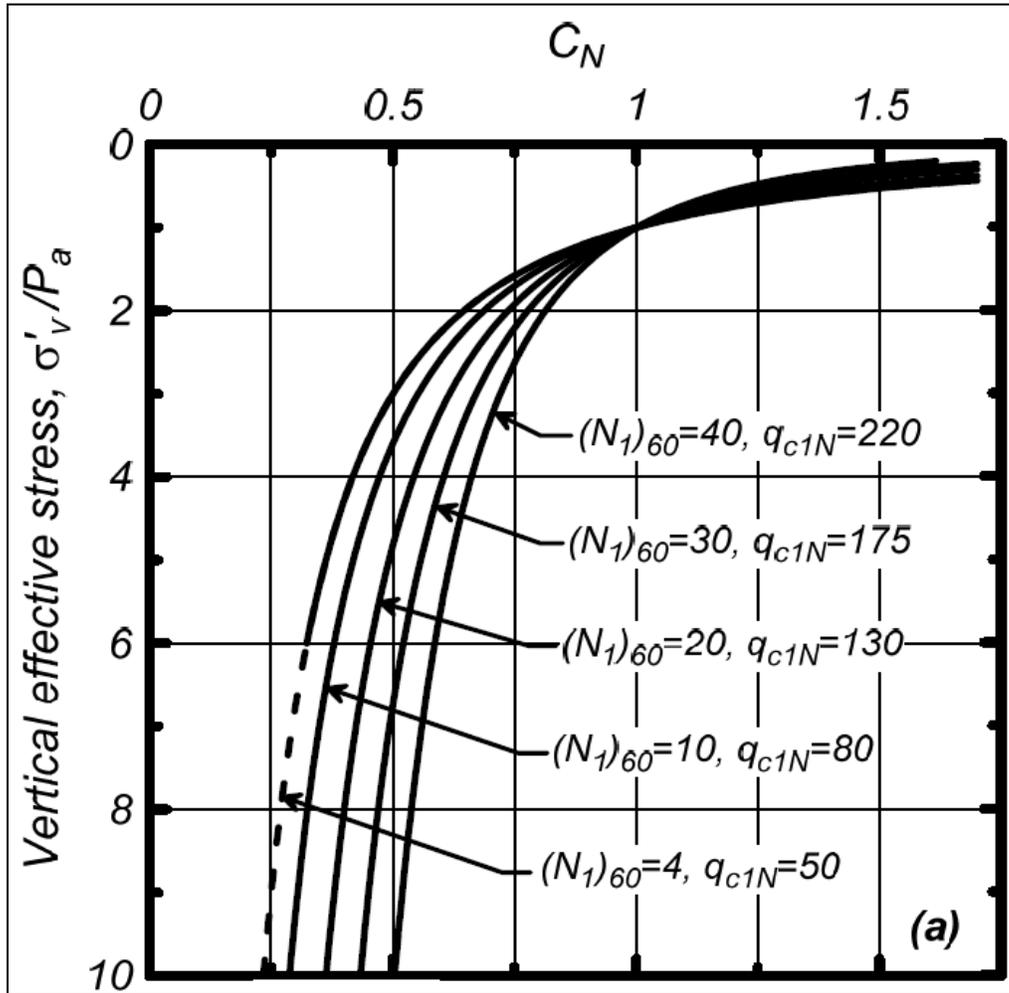
Figure B9. Factor for adjusting penetration resistance for effects of confining stress (Idriss and Boulanger, 2008).

$$C_N = \left(\frac{P_a}{\sigma'_{vc}}\right)^{1.338-0.249(q_{c1N})^{0.264}} \leq 1.7 \qquad \text{Equation B14}$$

C_N is a function of both overburden stress and q_{c1N}, effectively making it a function of itself. It is, therefore, necessary to find q_{c1N} iteratively, beginning by assuming some initial value for the exponent in equation B13, such as 0.7, and calculating C_N, which is then used in equation B14 to find an initial value of q_{c1N}. The calculated q_{c1N} is then used in equation B13 to find a new value of C_N, and so on, until q_{c1N} converges. This iterative calculation can be done automatically with the spreadsheet program Excel (by enabling iterative calculations), but it can also be done by handheld calculator, with adequate convergence likely to occur in two or three iterations.

To obtain the clean-sand normalized tip resistance, q_{c1Ncs}, an adjustment, Δq_{c1N}, is added to q_{c1N}; it is a function of fines content, FC, expressed as a decimal fraction, and normalized tip resistance, as shown in equation B15 and figure B10. (This is analogous to what Robertson and Wride called $(q_{c1N})_{cs}$, but the original notations were kept for both.)

$$\Delta q_{c1N} = \left(11.9 + \frac{q_{c1N}}{14.6}\right) exp\left(1.63 - \frac{9.7}{FC+2} - \left(\frac{15.7}{FC+2}\right)^2\right)$$

Equation B15
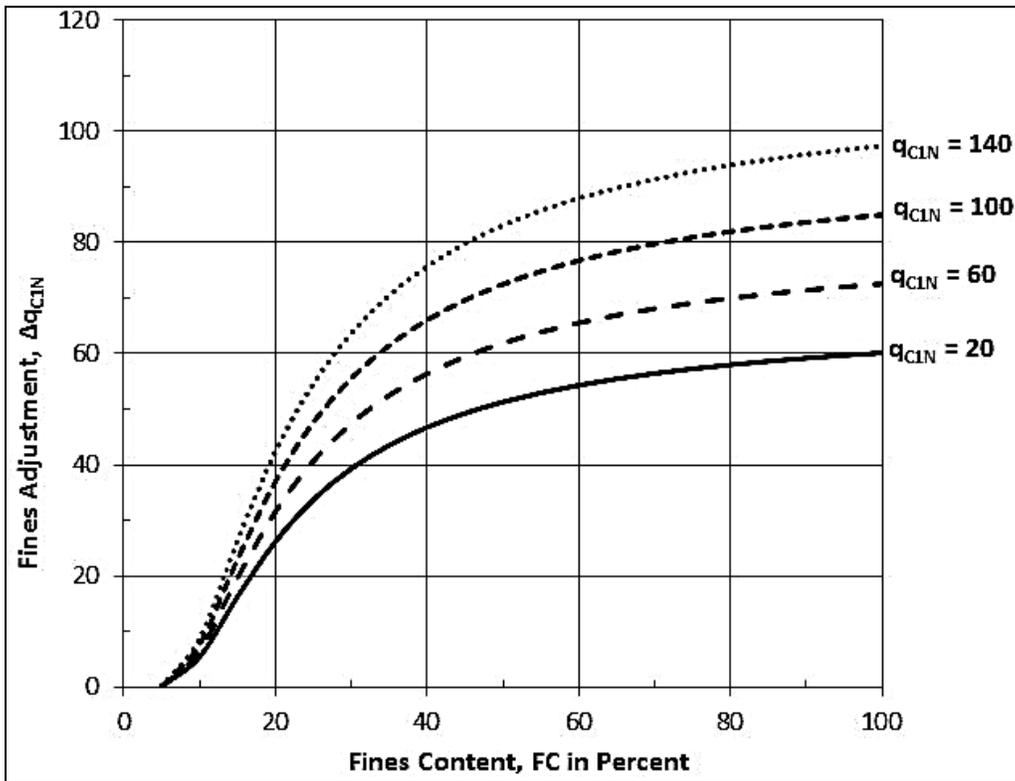
Figure B10. Adjustment for effect of fines (redrawn from Boulanger and Idriss, 2014).

B.3.2 CRR

Cyclic resistance is then assessed using figure B11 or equation B16. Because the CRR is defined to correspond to 15-percent probability of liquefaction, a factor of safety needs to be applied to CRR, if it is to correspond to some very low probability (approximating deterministic analysis). (As shown, these equations do not incorporate a factor of safety.) The factor of safety could be selected according to how much liquefaction probability can be tolerated; table B1 shows example values.
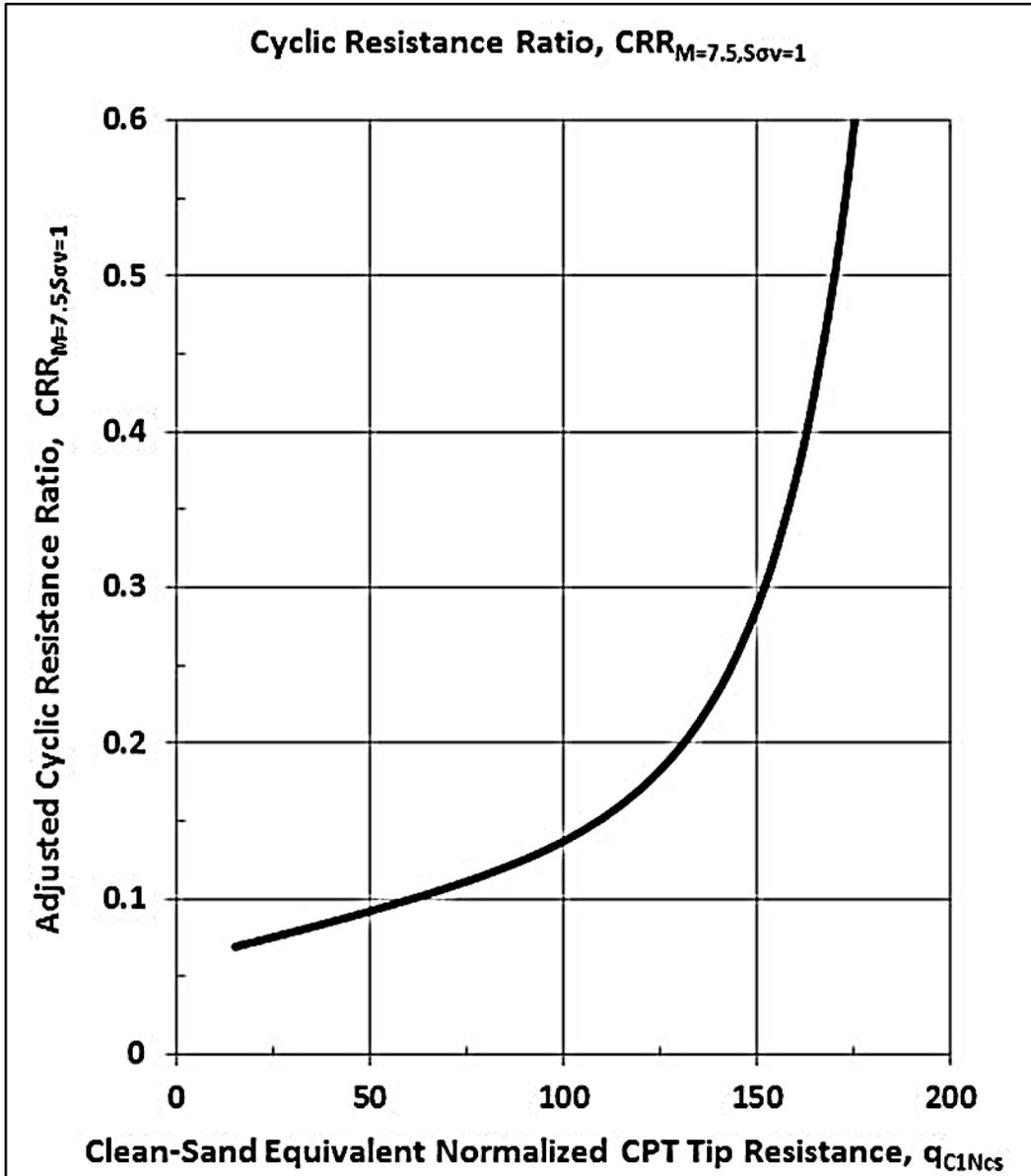
Figure B11. Cyclic resistance as a function of q_{c1N} (redrawn from Boulanger and Idriss, 2014). Curve applies to q_{c1N} in clean sand or clean-sand-equivalent q_{c1Ncs}.

$$CRR_{M=7.5,\sigma'_v=1atm} = \exp\left(\frac{q_{c1Ncs}}{113} + \left(\frac{q_{c1Ncs}}{1000}\right)^2 - \left(\frac{q_{c1Ncs}}{140}\right)^3 + \left(\frac{q_{c1Ncs}}{137}\right)^4 - 2.80\right)$$

Equation B16

Table B1. Factor of Safety and Corresponding Liquefaction Probability

Probability of Liquefaction (%)	Factor of Safety
15	1.0
5	1.15
2	1.25
1	1.3

B.3.3 Liquefaction Probability

Seismic risk analysis often requires an estimate of the probability of liquefaction occurring under earthquake loading. This can be obtained from equation B17 from Boulanger and Idriss (2014). Figure B12a, from the same publication, shows the results of equation B17 with case history data. Figure B12b shows the results of equation B17, replotted without the data but with additional curves liquefaction probabilities of 2 percent and 98 percent.

$$P_L\left(q_{c1Ncs}, CSR_{M=7.5\sigma'_v=1atm}\right) =$$

$$\Phi\left[-\frac{\frac{q_{c1Ncs}}{113}+\left(\frac{q_{c1Ncs}}{1000}\right)^2-\left(\frac{q_{c1Ncs}}{140}\right)^3+\left(\frac{q_{c1Ncs}}{137}\right)^4-2.60-\ln\left(CSR_{M=7.5,\sigma'_v=1atm}\right)}{\sigma_{\ln(R)}}\right] \quad \text{Equation B17}$$

The quantity inside the brackets is a function equal to the number of standard deviations that the adjusted cyclic resistance is above or below the adjusted CSR. The function $\Phi[x]$ is the standard normal distribution of x; its value is the probability that the loading exceeds the resistance. For programming in a spreadsheet, the mean of the quantity in brackets is zero. The quantity $\sigma_{\ln(R)}$ is the standard deviation on CRR for a given value of $(N_1)_{60cs}$, assumed to be constant for all values of $(N_1)_{60cs}$, and equal to 0.20. (In Microsoft Excel, $\Phi[x]$ is called NORMDIST.) Equation B16 is the inverse of equation B17, with $P_L(q_{C1Ncs}$ $CSR_{M=7.5,\sigma'v=1atm})$ set to 0.15.

Other models for liquefaction probability are available, most notably, Moss et al. (2006). However, the BI model was selected for this appendix because several newer case histories suggest that the Moss et al. procedure is somewhat unconservative at higher values of q_{C1Ncs}. Also, a question remains about whether smaller earthquake magnitudes and higher effective overburden stresses are well-enough represented in the data set that their effects on MSF and K_σ are fully accounted for by treating them as independent variables in the regression analysis, the way Moss et al. did. There were also some differences in the way some of the case histories were interpreted, including use of different r_d relationships.
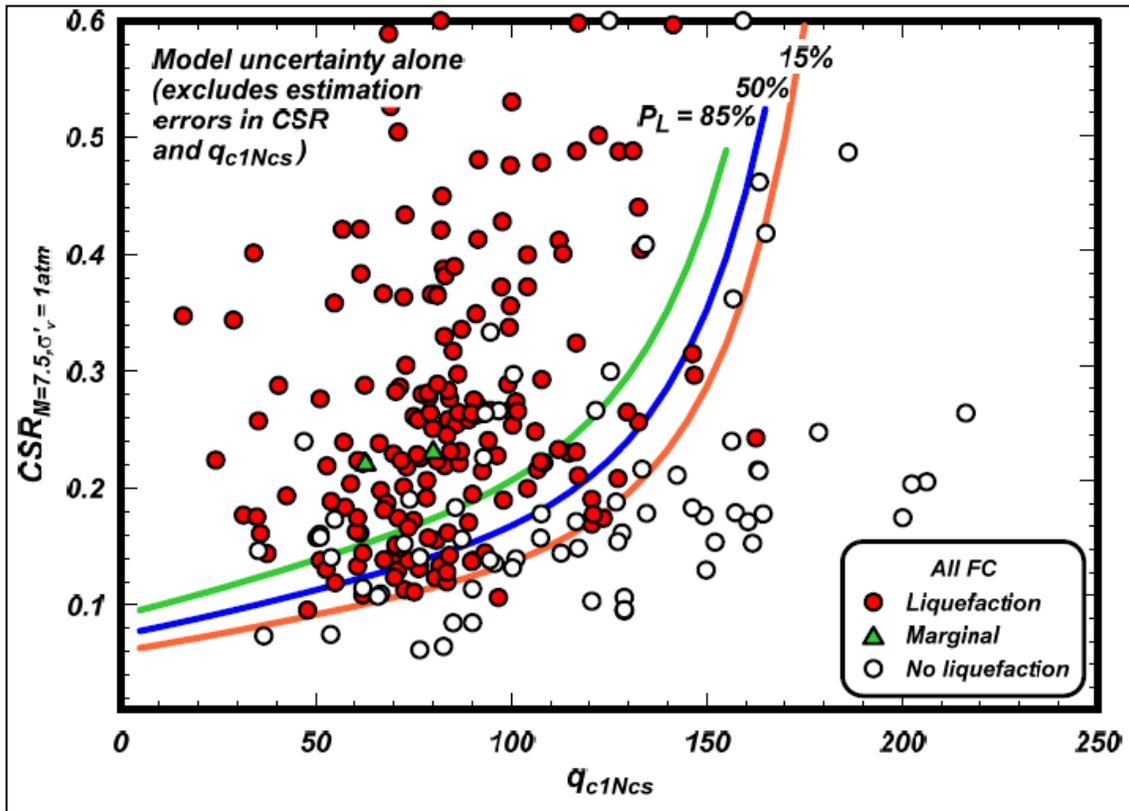
Figure B12a. Contours of equal liquefaction probability with case history data (Boulanger and Idriss, 2014). Red curve at bottom (15 percent) corresponds to cyclic resistance ratio, CRR$_{M=7.5,\sigma'v=1atm}$.
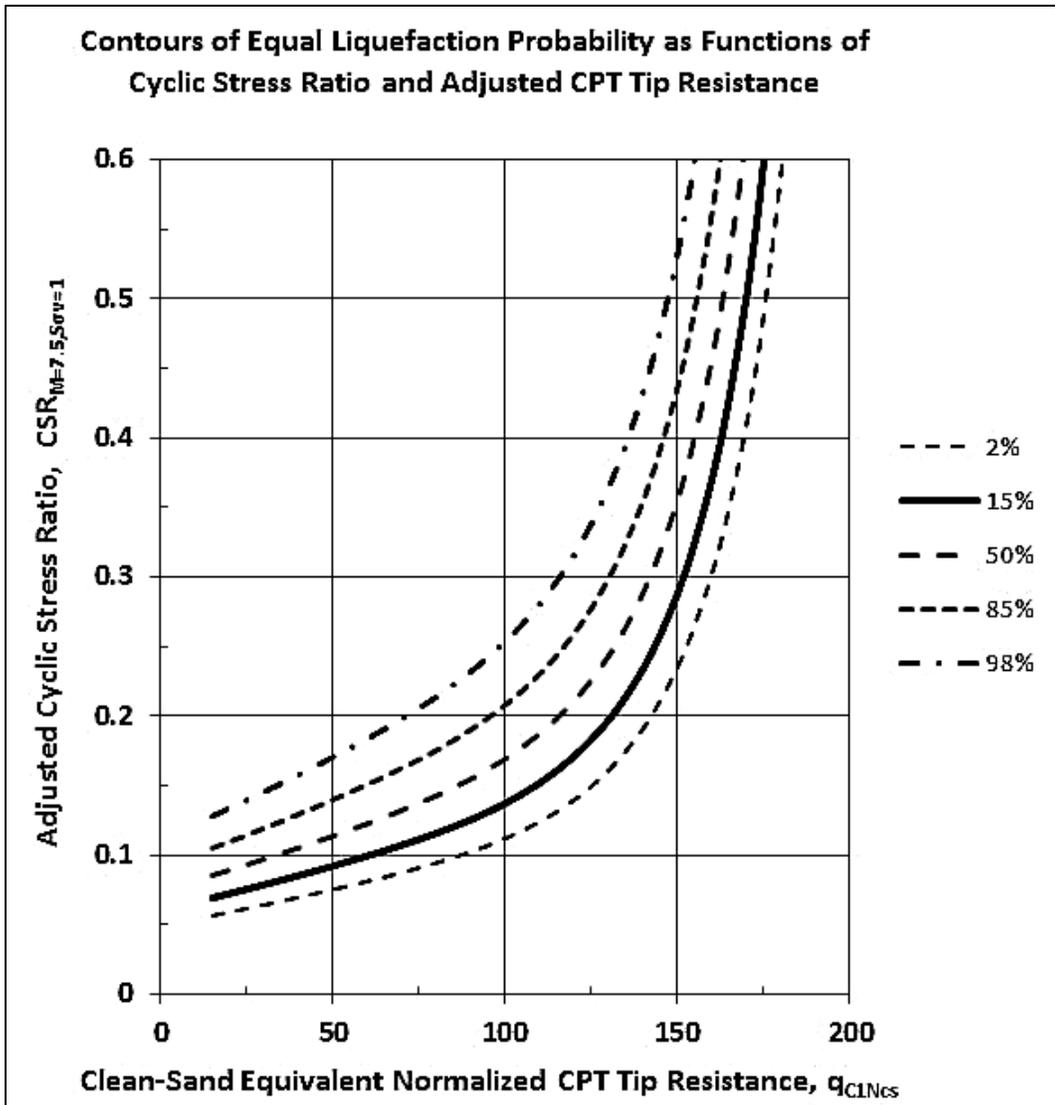
Figure B12b. Contours of equal liquefaction probability plotted without data for liquefaction probabilities of 2, 15, 50, 85, and 98 percent, based on Boulanger and Idriss (2014). Solid black line (15 percent) corresponds to cyclic resistance ratio, $CRR_{M=7.5,\sigma'v=1atm}$.

B.3.4 Details and Discussion

B.3.4.1 Updated rd

The BI procedure was developed using an updated r_d relationship that is magnitude specific (Idriss, 1999). Because the frequency content of earthquake ground motions and the amount of strain softening tend to vary with changes in earthquake magnitude, r_d also varies with magnitude, not just with depth. Additional variation in r_d with PHA or different shear-wave velocity profiles is

not accounted for. That would have been of minor consequence in the back
analysis of case histories from depths less than 20 feet, but it could be very
important in forward analysis with the potentially liquefiable layers being deeper.
For this reason, it is generally preferable to use site-response analysis with the
actual shear-wave velocities and ground motions that are appropriate to the site.
Also, dam foundations generally have significant horizontal static shear stresses,
which can have a major effect on liquefaction potential that is not accounted for
by r_d. (Refer to section 13.6.2.5 in the main text of Chapter 13, "Seismic Analysis
and Design," for determination of K_α.)

B.3.4.2 Adjustment for Fines Content

The effect of fines on liquefaction triggering is addressed by adding a term Δq_{c1N}
to q_{c1N}. to obtain q_{c1NCS}. With Δq_{c1N} depending on the actual fines content, the
BI procedure has the significant drawback of requiring a measured or estimated
value of the fines content for each interval being analyzed. In lacustrine
materials, where layering is expected to persist over greater distances, it may be
possible to project fines contents some distance away from the sampling hole, but
for Reclamation's dams (many located in hilly or mountainous terrain), this type
of foundation would be an exception, rather than the rule. For this reason, it is
recommended that both RW and BI procedures be used and compared for all
soundings with adjacent sample holes. Reasonably good correlation between
fines content and I_C at the site would suggest that the BI procedure can be applied
to the other CPT soundings, with fines estimated from the correlation. (The
correlation in Boulanger and Idriss [2014] has too much scatter to be applied at a
high-hazard dam without site-specific verification.) General consensus between
CRR values from the two procedures would enhance confidence in the BI
estimates of liquefaction probability.

B.3.4.3 MSF that Varies with q_{c1Ncs}

A simplification has been made here in regard to the MSF. In 2014, Boulanger
and Idriss proposed that MSF is a function not only of earthquake magnitude,
M_W, but also of the density, indicated by penetration resistance, q_{c1Ncs} or its
equivalent in SPT analysis, $(N_1)_{60\text{-cs}}$. In general, the greater the density, the more
MSF differs from a constant 1.0. However, that has not been incorporated into
Chapter 13, and the older relationship that does not vary with density has been
used. (Refer to section 13.6.2.3 of chapter 13.) With M_W equal to 6.0, the older
relationship makes MSF equal to 1.48. For the same M_W, the newer
relationship varies from about 1.1 in very loose sand to about 1.6 in dense sand.
The indication is that, with small M_W and loose to medium sand (q_{c1Ncs} up to
about 150 or $(N_1)_{60\text{-cs}}$ up to about 25), the older relationship is somewhat
unconservative, and it is conservative for higher q_{c1Ncs}. For M_W greater than 7.5,
this would be reversed. The effect that this refinement would have on
Reclamation's dams and risk analyses has not been evaluated.

B.3.4.4 Portrayal of Results

Results can be portrayed in the same format as for the RW procedure, either as profiles with depth for individual SPT soundings, or by superimposing pairs of q_{c1Ncs} and $CSR_{7.5,'=1}$ on figure B11 or B12b, instead of figure B5. Figure B13 shows pairs of q_{c1Ncs} and $CSR_{7.5,'=1}$ for various parts of a dam foundation and two different levels of earthquake loading with the curves of constant probability. This can be an effective way to help a risk-estimating team understand the likelihood of liquefaction and its sensitivity to loading and CPT data. In this example, liquefaction would be fairly unlikely, but still plausible with the 500-year seismic loading. With the 5,000-year loading, liquefaction is much more likely, having a probability of about 50 percent in some portions of the foundation.
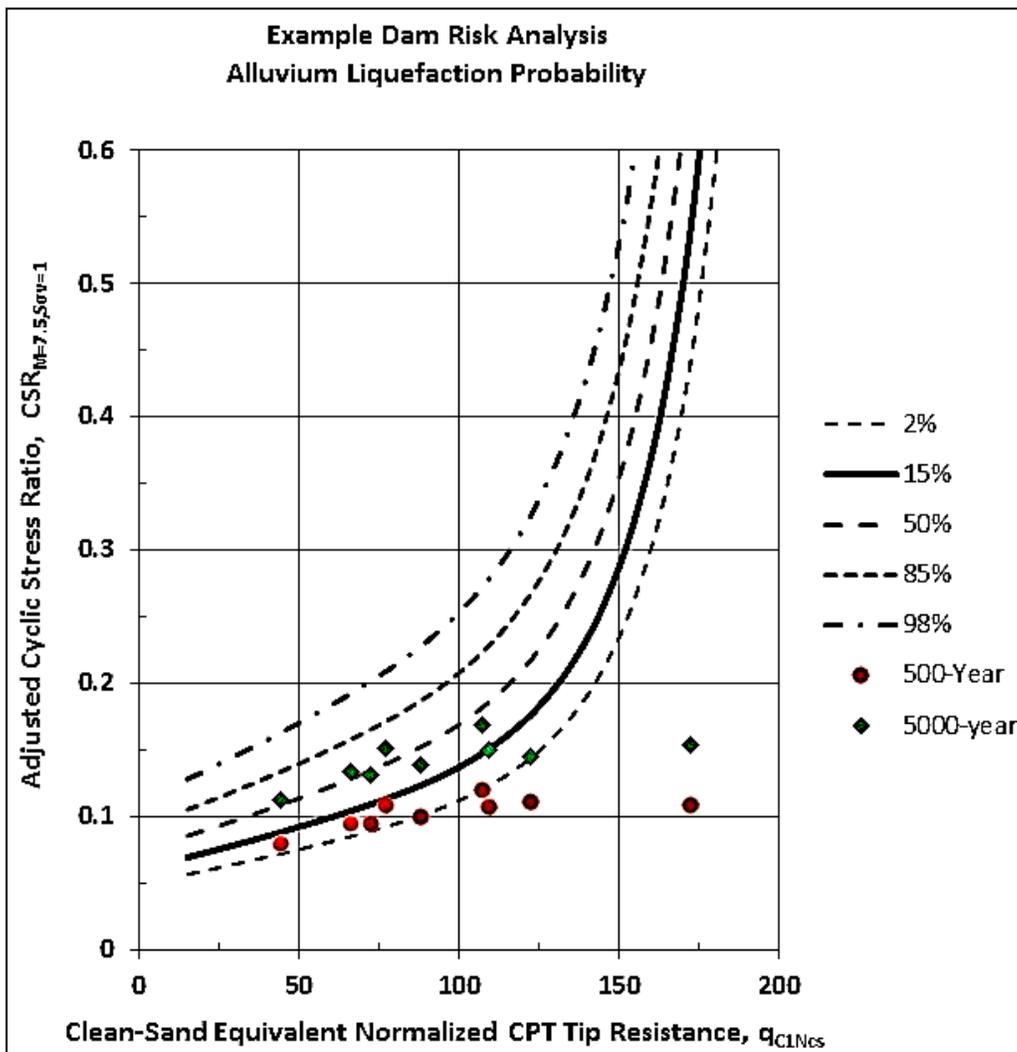
Figure B13. CPT data and CSRs superimposed on plot of liquefaction probability from BI procedure.

B.4 References

ASTM. 2012. "Standard Test Method for Performing Electronic Friction Cone and Piezocone Penetration Testing of Soil - Designation D 5778-12," *ASTM Annual Book of Standards*, Vol. 04.09, American Society for Testing and Materials, West Conshohocken, PA.

Boulanger, R.W., and I.M. Idriss. 2014. *CPT and SPT Based Liquefaction Triggering Procedures.* Report No. UCD/CGM. University of California at Davis, Center for Geotechnical Modeling.

Bureau of Reclamation. 2007. *Evaluation of In Situ Methods for Liquefaction Investigation of Dams.* Research Report DSO-07-09, prepared by William Engemoen.

GeoLogismiki. 2014. User's manual for the program CLiq. GeoLogismiki Geotechnical Software, Serres, Greece.

Idriss, I.M. l999. "An Update to the Seed-Idriss Simplified Procedure for Evaluating Liquefaction Potential." *Proceedings, TRB Workshop on New Approaches to Liquefaction.* Publication No. FHWA-RD-99-165.

Idriss, I.M., and R.W. Boulanger. 2004. "Semi-Empirical Procedures for Evaluating Liquefaction Potential During Earthquakes," *Proceedings, 11th International Conference on Soil Dynamics and Earthquake Engineering, and 3rd International Conference on Earthquake Geotechnical Engineering.* D. Doolin et al. (eds.), Stallion Press, Vol. 1, pp. 32-56.

Idriss, I.M., and R.W. Boulanger. 2008. *Soil Liquefaction During Earthquakes.* Monograph MNO-12, Earthquake Engineering Research Institute, Oakland, CA.

Ku, Chih-Sheng, C. Hsein Juang, Chi-Wen Chang, and Jianye Ching. 2012. "Probabilistic Version of the Robertson and Wride Method for Liquefaction evaluation: Development and Application," *Canadian Geotechnical Journal,* Vol. 49, pp. 27-44.

Lunne, T., P.K. Robertson, and J.J.M. Powell. 1997. Cone Penetration Testing in Geotechnical Practice. London, UK, Blackie Academic and Professional.

Moss, R.E.S, R.B. Seed, R.E. Kayen, J.P. Stewart, A. Der Kiureghian, and K.O. Cetin. 2006. "CPT-Based Probabilistic and Deterministic Assessment of In Situ Seismic Soil Liquefaction Potential," *J. Geotechnical and Geoenvironmental Engineering ASCE*, Vol. 132., No., 8, pp. 1032-051.

Olsen, R.S. 1997. "Cyclic Liquefaction Based on the Cone Penetrometer Test," *Proceedings of the 1996 NCEER Workshop on Evaluation of Liquefaction Resistance*.

Olsen, R.S., and J.P. Koester. 1995. "Prediction of Liquefaction Resistance Using the CPT," *Proceedings, International Symposium on Cone Penetration Testing*. Vol. 2, pp. 251-256, CPT 95, Linkoping, Sweden.

Stark, T.D., and S.M. Olson. 1995. "Liquefaction Resistance Using CPT and Field Case Histories," *Journal of Geotechnical Engineering*. American Society of Civil Engineers, Vol. 121, No. 12, pp. 856-869.

Robertson, P.K. 2009. "Performance Based Earthquake Design Using the CPT," *Proceedings, IS-Tokyo, International Conference on Performance-Based Design in Earthquake Geotechnical Engineering, from Case Histories to Practice,* Tokyo, Japan.

Robertson P.K., and K.L. Cabal (Robertson). 2014. *Guide to Cone Penetration Testing for Geotechnical Engineering*. Sixth Edition, Gregg Drilling & Testing, Inc., Signal Hill, CA.

Robertson, P.K., and R.G. Campanella. 1985. "Liquefaction Potential of Sands Using the Cone Penetration Test," *Journal of the Geotechnical Division of ASCE*, Vol. 111, No. 3, pp. 298-307.

Robertson, P.K., and C.E Fear. 1995. "Liquefaction of Sands and its Evaluation," *Proceedings, IS-Tokyo, 1st International Conference on Earthquake Geotechnical Eng*ineering, Keynote Lecture.

Robertson, P.K., and C.E. Wride (*née* Fear). 1997. "Cyclic Liquefaction and its Evaluation Based on SPT and CPT," *Proceedings of the 1996 NCEER Workshop on Evaluation of Liquefaction Resistance*.

Seed, H.B., and P. de Alba. 1986. "Use of SPT and CPT Tests for Evaluating the Liquefaction Resistance of Sands," *Use of In-situ Tests in Geotechnical Engineering*. ASCE Geotechnical Special Publication No. 6, pp. 281-302.

Appendix C

Assessment of Liquefaction Potential Using the Standard Penetration Test

Contents

Figures

Tables

C.1   Introduction

This appendix explains procedures for assessing the potential for soil liquefaction (the near-total loss of shear strength due to generation of excess pore pressure approaching the pre-earthquake effective stress) using the Standard Penetration Test (SPT). The procedures are based on correlations between a "catalog"" of liquefaction case histories, and the SPT and soil index properties. They were pioneered by the late Professor H. Bolton Seed and his coworkers at the University of California at Berkeley (H. Seed, Idriss, and Arango, 1982; H. Seed et al., 1985). Some portions of the procedure were updated in a 1996 workshop sponsored by the National Center for Earthquake Engineering Research (NCEER, 1997; Youd et al., 2001), and subsequently by Cetin et al. (2004) and Idriss and Boulanger (2008, 2010), and others.

Like any tool used to assess liquefaction or gather data for dynamic analysis, the SPT must be supplemented by other methods. For a high-hazard dam, a conclusion regarding seismic performance cannot be based on just one method of investigation (Bureau of Reclamation [Reclamation], 2007).

This appendix generally follows the procedure of Idriss and Boulanger (2010), with some exceptions made, where appropriate, to fit Reclamation's practice. Other procedures exist and can give significantly different results; most notably, the detailed regression model by R. Seed and coworkers at the University of California at Berkeley, which typically indicates lower resistance to liquefaction for a given combination of loading and SPT blow count (R. Seed et al., 2003; Cetin et al., 2004). The differences are due primarily to different interpretations of several critical sites (whether liquefaction occurred, which materials were actually liquefied), as well as somewhat different estimates of the cyclic shear stresses at a number of sites. Currently (2015), no consensus exists within the profession regarding which procedure is most "correct." The user of this chapter should be aware that newer developments could supersede the information contained in this appendix.

This appendix is intended only to lead the user through the mechanics of performing the SPT-based triggering analysis; it is not a complete discussion of the theory, background, and interpretation, for which many references are available. Cetin et al. (2004) and Idriss and Boulanger (2010) describe the development of the more recent procedures in greater detail.

Deviations in methodology from what is presented here should be documented, along with the rationale for the deviation, in addition to obtaining appropriate technical review and approval.

The results of a liquefaction triggering analysis based on SPT (or other test methods) are inherently imprecise and include a substantial amount of uncertainty. There are several reasons for this, including: (1) the SPT-based

liquefaction procedures are empirical, based on back analysis of field performance, with soil data of varying quality, and with the cyclic stresses for many cases estimated by very simplified means; (2) there are few case histories with stress conditions that closely match those in the foundation of a large dam, requiring extrapolation well beyond the range of available data; and (3) a number of simplifying assumptions are involved. This is further complicated by the strong influence of field procedures and equipment on the data. Also, the profession's interpretation of the database and its understanding of liquefaction in general are still evolving.

Forward analysis of liquefaction relies heavily on extrapolation from back analysis of historic cases that may not be similar to the soil conditions and earthquake loadings at the dam under study. For example, the database includes very few cases from earthquakes with magnitude M_W less than 6.0 (with magnitude being used as a proxy for the number of cycles of strong loading) or with effective overburden stress greater than 2,500 pounds per square foot (lb/ft^2). In contrast, dam-safety risk analyses must often include contributions to risk from small, nearby earthquakes with M_W less than 6.0 and overburden stresses that are many times larger than 2500 lb/ft^2. The database includes **no** cases with large static shear stresses on horizontal surfaces, as occur under embankment slopes, so it is necessary to extrapolate using a semi-empirical factor (K_α), which was based on theory and laboratory results, not on field behavior. Extrapolation is more reliable if it is guided by principles of soil mechanics or trends in related data, rather than if it is simply projection of data beyond the range of the data.

American Society for Testing of Materials (ASTM) standards cited in this chapter are all copyright protected by ASTM. They are numbered in the format "D1586-11," in which the last two digits are the year of the most recent revision. ASTM standards are regularly reviewed and updated, and there may be newer versions that supersede the ones cited here.

C.2 Material Characterization Using SPT

C.2.1 The SPT

The SPT blow count, N, is the number of blows of a standardized hammer required to drive a standardized, split-barrel sampler 1 foot (ft). The hammer weighs 140 lb and drops 30 inches onto a steel "anvil," which is attached to the drill rods by a threaded connection. The sampler has an outside diameter of 2 inches and an inside diameter of 1-3/8 inches. (See ASTM D1586-11 for details.) The sampler is driven a total of 1.5 feet for each test, with the blow count recorded for each 0.5 ft in typical practice. The first 0.5 ft is called the seating interval; blow counts are recorded there for comparison purposes, but they

are not used explicitly. The second and third 0.5-ft intervals together constitute the actual penetration test, and the sum of their blow counts is referred to as "N." For all Reclamation projects, field personnel should also record either the cumulative penetration after each blow, or the blows per 0.1 ft of penetration, to aid in recognizing and correcting for layering or gravel interfering with penetration.

The SPT blow count provides an empirical indication of resistance to liquefaction. The measured blow count is adjusted to account for the effects of test conditions and soil gradations that differ from the reference conditions, as described in this appendix. Then, it is compared with the blow count that would indicate sufficient density to resist liquefaction under the earthquake under consideration. In the simplified approach, the earthquake loading is represented by the Cyclic Stress Ratio (CSR) determined from site-response calculations, normalized for the effects of earthquake magnitude and in situ static stresses. Determination of CSR is described in Section 13.6 in Chapter 13. Different concepts are used in nonlinear coupled analysis, which predicts pore-pressure generation, along with the stresses and strains. However, such information is outside the scope of this appendix, and it is not presented here.

The blow count that is measured in the field depends not only on the density of the soil, but also, to a large extent, on the fines content, the effective overburden pressure, the efficiency of energy transfer from the falling hammer to the drill rods, and drilling methods, and, to a lesser extent, on other factors including the drill hole diameter.

In order for the SPT to provide a valid indication of liquefaction potential, the testing must occur according to consistent procedures, which are specified in ASTM D1586-11 (for SPT in general) and ASTM D6066-11 (which is specific to SPT for liquefaction assessment). Deviation from the testing standards can give misleading results. For example, tests performed without drilling fluid ("mud" or water) can give erroneously low blow counts because of heave and loosening of the bottom of the hole. The drill hole, therefore, needs to be kept full of fluid well above the water table. Particularly when dealing with older data, logs should be checked to verify that fluid was used, noting any intervals where it was not (or might not have been) used, which could bias the blow count to be too low. Any deviation from standard procedures should be documented, along with the results.

In addition to the careful attention to detail that is required to obtain good-quality data, attention is also required during drilling to avoid damage to the embankment. For example, when drilling through or beneath the impervious core of an embankment, it is necessary to monitor fluid pressures and return flows to ensure that pressures are kept small enough to prevent hydraulic fracturing, preferably not much greater than the static pressure from the drill fluid.

C.2.2   Gravelly Materials and Coarse Sand

If the soil contains gravel, especially gravel coarser than 3/4 inch (or large amounts of finer gravel), the SPT blow count may give an unrealistic picture of the density of the soil, due to gravel particles interfering with penetration of the sampler (which has an inside diameter of only 1-3/8 inch). It should be standard practice for all sites to record either the cumulative penetration after each blow, or the blows per 0.1 foot of penetration, not just the number of blows for each 0.5 foot. A cumulative plot of blow count against penetration that shows a sharp increase in slope may indicate that the sampler has reached material that is too coarse to enter the sampler without interference, the way sand would. In this case, one may be able to extrapolate the blow counts before the sharp increase to a full 1.0 foot to obtain a corrected blow count indicative of the first part of the SPT interval, as shown in figure C1. The absence of a sharp change in slope does not prove that there is not any gravel interference because there may have been gravel interference throughout the entire 1.5-foot test interval, in which case a high N value does not reliably indicate high cyclic resistance. (If N is low, despite the high gravel content, the cyclic resistance is likely to be low or very low.) Even with a sharp change in slope, making the correction does not guarantee a "correct" N value that accurately portrays the liquefaction resistance of the soil because there may have been gravel interference even before the change. These effects can only be judged properly with detailed descriptions of the samples, preferably including photographs. It is, therefore, important for personnel who log the samples to be fully aware of how the data and descriptions are to be used.

Field and lab descriptions of the sampled material are very important in determining whether a change in slope is due to a change in density, a change in material type, or oversize particles. Gravel adjustments should be made only when there is good reason to think that it is required, such as finding medium or coarse gravel in the samples, poor sample recovery with erratic blow counts, etc. **Any gravel corrections should be documented and highlighted in reports of the results .**

The bulk of liquefaction case-history data come from fine to medium sands, so the empirical curves for predicting liquefaction potential predominantly reflect the behavior of fine to medium sands. Coarse sands (even with no gravel) generally give higher N measurements than fine sands at an equivalent state condition, suggesting that **for a given value of N,** coarser sand is more susceptible to liquefaction (Skempton, 1986). This is supported **somewhat** by statistical analysis of liquefaction case histories (Liao, Veneziano, and Whitman, 1988). Therefore, conclusions based on penetration resistance in coarse sands could be slightly unconservative, but no procedure to compensate for this effect has been proposed to date.
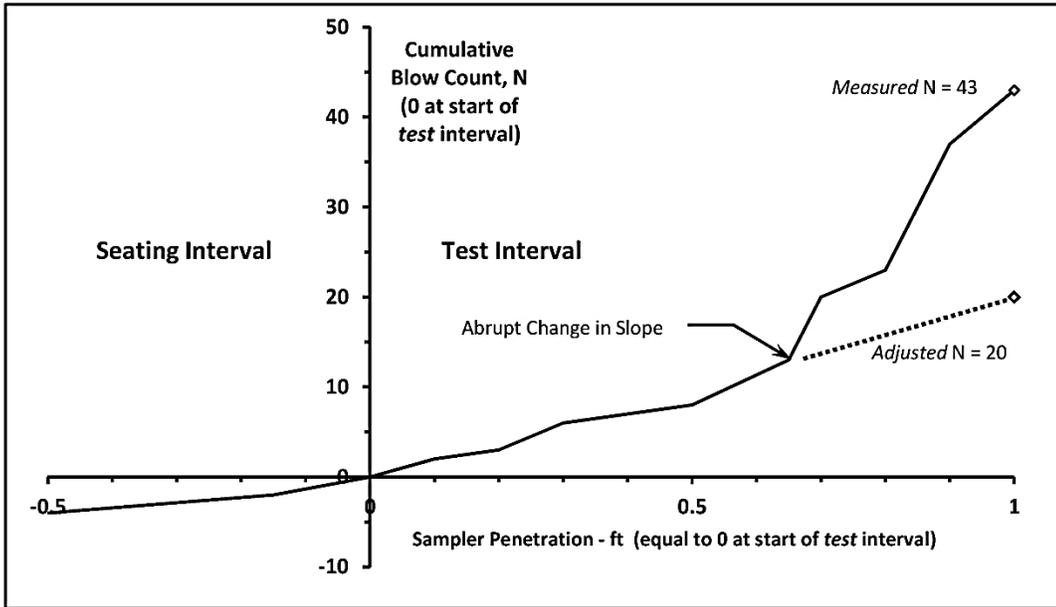
Figure C1. Correction of SPT blow count for apparent gravel interference. Check sample description, lab data, and recovery before applying correction.

When gravel is known to be present, other tests should be performed, such as the Becker hammer penetration test and the shear-wave velocity, along with the SPT, to assess liquefaction potential. (Use of the shear-wave velocity and the Becker test for liquefaction assessment are described in appendices, D and E of Chapter 13, respectively.)

C.2.3 Adjusting Blow Count to Standard Test Conditions

Standard penetration test blow counts are quite sensitive to the test procedure. It is, therefore, necessary to adjust the measurements to standard conditions before they can be used with correlations to predict liquefaction potential. The measured blow count is typically adjusted for test conditions by equation C1. The individual adjustments are discussed in sections C.2.3.1 through C.2.3.4

$$N_{60} = C_E \, C_B \, C_R \, C_S \, N \qquad\qquad\qquad \text{Equation C1}$$

where:

N_{60} is the SPT blow count adjusted for testing procedures.
C_E is the efficiency of energy transferred from the falling hammer to the rods divided by the "standard" value of 60 percent of the theoretical maximum

C_B is an adjustment to account for the effect of drill hole diameters larger than the standard (generally not used by Reclamation)

C_R adjusts for the effect that very short or very long rods have on transmission of energy from hammer to sampler,

C_S accounts for differences in blow counts between samplers used with liners or samplers without space for liners, and samplers with space for liners but used without liners

N is the field blow count (adjusted for gravel effects, if needed).

Once the blow count has been adjusted for the test conditions to obtain N_{60}, additional adjustments are applied to account for the influence of effective overburden stress and fines content on the behavior of the soil. This allows liquefaction probability or liquefaction resistance to be related to a single variable called the clean-sand-equivalent normalized blow count, $(N_1)_{60cs}$. These adjustments are described in sections C.2.3.5 and C.2.3.6 below, after the calculation of N_{60}.

C.2.3.1   Adjustment for Energy Transferred from Hammer to Sampler (C_E)

For liquefaction assessment, the SPT blow count must be adjusted to account for the amount of energy transmitted from the hammer to the sampler. Not all of the theoretical energy of the falling hammer (140 lb. x 30 inches) is actually transferred into the rods and sampler. Although mechanical trip hammers are now used on most Reclamation drill rigs, in the original form of the SPT, the hammer is raised by a rope that is wound twice around a constantly rotating, smooth, steel winch drum, known as the "cathead." The driller then throws slack into the rope, so that it can slip on the cathead and the hammer drops onto the anvil, before the rope is pulled tight around the cathead to lift the hammer again. This method was used by Reclamation until the early 1990s, and some other drillers still use it. Because of rope friction, hammer friction, wave reflections, etc., typically only 45 to 65 percent of the theoretical maximum energy is measured in the rods when the hammer is raised by rope and cathead. With the rope and cathead, even the best drillers show variation in drop height and energy transfer. This can vary in a single shift, depending on operator fatigue, condition of the rope or the cathead, and random variation from stroke to stroke. Mechanical hammers are, in general, preferred because they are more consistent than human drillers. They generally deliver more energy to the drill string because they do not have the friction from the rope on the cathead and the sheaves at the top of the mast. However, with some hammers, the drop height is sensitive to the rate of operation, and as much as 95 percent of the theoretical energy may be measured if the hammer operates too quickly. The operating speed must be consistent with the speed when the energy was being measured. Slower driving makes it easier to record penetration after each blow.

Energy measurements should be made using a pile-driving analyzer for any combination of drill rig and hammer being used. Preferably, the energy

measurement should be made with at least 35 feet of rods. (This is related to the short-rod correction discussed in section C.2.3.3.) Measurements are not necessarily required for each project, provided that operation of the hammer is consistent with the conditions during the measurements. Energy measurements are performed for all Reclamation rigs; previous measurements can be used for smaller projects if no changes have been made in the setup and the rigs are fully maintained. For larger projects, or if a contractor does the drilling, energy measurements should be made at the beginning of the project, regardless of whether the hammer being used is mechanical or the rope-and-cathead type. Reclamation's Technical Service Center, Materials Engineering and Research Laboratory can provide further assistance on energy correction for the specific hammer used. It is best to obtain energy measurements early in a test program so that equipment problems can be identified and corrected before drilling progresses very far. Testing should comply with ASTM D4633-10.

An energy delivery of 60 percent has been adopted as the standard to which all SPT measurements are normalized because that value is typical of common safety hammers lifted and dropped by rope and cathead (Youd et al., 2001). **Correct the raw or gravel-adjusted N value to an equivalent rod energy ratio of 60 percent using equation C1, using C_E from equation C2:**

$$C_E = (ER_i / 60) \hspace{4cm} \text{Equation C2}$$

where:

    ER_i is the measured drill-rod energy ratio for the hammer system used, expressed as a percentage of the theoretical maximum.

For example, if the energy delivered was 50 percent of the theoretical energy from a 30-inch drop of a 140-lb hammer), the measured blow counts would need to be reduced by multiplying by the ratio 50 percent / 60 percent to obtain N_{60}. Similarly, if the energy delivered was 70 percent, the measured blow counts would be increased by multiplying by the ratio 70 percent / 60 percent. If energies differ greatly from 60 percent, error could be introduced by correcting by a simple ratio. Note that a measured ER_i much greater than 60 percent results in a substantial increase as N is adjusted to N_{60}. An erroneously high energy ratio would create an unconservative bias, and equation C2 is not necessarily valid for energy ratios outside of a limited range. It is preferred that the hammer be operated so that ER_i is kept well below 90 percent, so that the energy adjustment is not so large and uncertain. (This should be stated in every Field Exploration Request.) If that is not possible because the testing is already done, it is reasonable to cap the value of ER_i used in equation C2 at 90 percent.

If no energy measurements are available (when analyzing SPTs from before energy measurements became common), the energy is usually assumed to have

been about 60 percent of the maximum for a "safety" hammer (in which the falling mass is a steel pipe surrounding the rod and anvil), and about 45 percent for a "donut" hammer (in which a compact 140-lb steel "donut" falls on an exposed anvil attached to the rods), although donut hammers were never commonly used by Reclamation. Due to the sensitivity of mechanical hammers to operation speed, no general recommendation like that can be made.

C.2.3.2   Adjustment for Borehole Diameter (C_B)

Reclamation standards for SPTs require a drill hole diameter of 4 inches, although it is sometimes necessary to use data from larger holes. It has been observed that larger holes tend to give slightly lower blow counts, and a correction factor C_B has been proposed to account for that (Skempton, 1986). However, the difference is fairly small, and the proposed factor is not supported by very many experimental data. **Therefore, C_B should be assumed to be 1.0 until it is better supported by research.** Neglecting the correction introduces minor conservatism.

C.2.3.3   Adjustment for Length of Drill Rods (C_R)

The energy must be further adjusted for the effects of short rods (less than about 33 feet) or very long rods (longer than about 100 feet). The adjustment is shown in table C1, from Youd et al. (2001). Idriss and Boulanger (2008, 2010) and Cetin et al. (2004) both used this same adjustment when developing their methods for identifying liquefaction potential. (Earlier versions of this chapter used $C_R = 0.75$ for all rod lengths less than 10 feet, and 1.0 for all lengths greater than 10 feet.)

Table C1. Energy Adjustment for SPTs at Large and Small Depths (Youd et al., 2001)

Rod Length in Feet (anvil to sampler)	C_R
0-10	0.75
10-13	0.8
13-20	0.85
20-33	0.95
33-100	1.0

The value of this adjustment depends to a small degree on the type of drill rod. Reclamation typically uses NW drill rods, which are somewhat heavier than A and AW rods that are more common outside of Reclamation for shallow holes; however, the difference is probably minor in the overall outcome of the analysis.

An additional minor adjustment is recommended to account for energy losses when the drill string is very long (exceeding about 100 feet) based on experiments with strain transducers and accelerometers attached along the rods. Some energy

is lost to friction, as well as slack and wave reflections at rod joints. When performing SPTs at large depths, the rod joints should be tightened with pipe wrenches, not just screwed together by hand, although there will still be wave reflections from each coupler even with the wrenches. **For depths exceeding 100 feet, rod energy should be reduced by 1 percent per 10-foot rod section beyond 100 feet** (Schmertmann, 1978; Farrar et al., 1998).

For example, assume that a conventional safety hammer (enclosed anvil), raised by rope and cathead, is being used to drive a sampler at a depth of 145 feet, with about 5 feet of drill rod sticking up above the ground level below the hammer's anvil. This hammer typically delivers an ER_i of 60 percent at middle depths; e.g., 30 to 100 feet. The drill rod energy ratio ER_i would then equal 55 percent, i.e., 60 percent minus 1 percent for each 10 feet below 100 feet. Thus, $(N)_{60}$ would equal (55 percent / 60 percent) x N. Note, however, that liquefaction analysis at such large depths requires extrapolation of field performance to depths and overburden stresses far greater than those associated with the case histories that the method is based upon, most of which occurred at depths of 25 feet or less. (Fortunately, at depths beyond 100 feet, the change in energy with depth is gradual enough that variation in the precise value of the reduction would not have a major effect on the adjusted blow count.) Possibly counteracting the energy loss in very long rods is the effect of the weight of the rods and the hammer assembly, which applies a large static force on the tip of the sampler. This has not been studied extensively, but it could bias blow counts to be "too low," which is one additional reason the SPT is far from a precise test.

In a spreadsheet, the combined energy adjustment for the effects of rod length can be approximated as:

If rod length = 5 to 33 feet:	$C_R = 0.009$ length $+ 0.7$	
If rod length = 33 to 100 feet:	$C_R = 1.0$	Equation C3
If rod length >100 feet:	$C_R = 1.0 - 0.001$ (length $- 100$)	

If the amount of "stickup" of the rods above the ground surface is not known, one can reasonably approximate the rod length by adding 5 feet to the depth. With a hole depth of 10 feet or more, the difference in C_R between assuming 3 feet of stickup and assuming 5 feet is minor. The exact value depends on the dimensions of the rods and the type of hammer; however, the variation in C_R with different rods and hammers is thought to be minor with respect to the other uncertainties in the analysis of liquefaction potential.

Full consensus does not exist within the profession regarding the short rod adjustment in Table C1. Daniel et al. (2005) concluded that the procedure most commonly used for calculating the energy that the hammer imparts to the rods is flawed, and they recommended that the use of C_R for short rods be discontinued. However, it was used by both Idriss and Boulanger (2008) and Cetin et al. (2004), and it had a significant effect in their back analyses, which involved soils mostly

within 25 feet of the surface. Conceivably, that would indirectly create a conservative bias in forward analysis of SPT data at greater depths, and little or no bias in shallow tests. Until this issue is resolved, C_R should be used for Reclamation dams.

If it is necessary to use SPT data to assess liquefaction potential at shallow depths, the uncertainties in the adjustments should be recognized and accounted for. The most common alternative method, the cone penetrometer test (CPT), does not share the problems of wave transmission in the rods, but interpreting CPT data does require the same normalizing factor C_N, which becomes very large and uncertain at low normal stresses. To confirm SPT or CPT estimates of cyclic resistance at small depths, or in place of them, it may be helpful and reasonably economical to make in situ density measurements by sand cone or nuclear density gauge in backhoe trenches, possibly with dewatering as needed to test below the water table. However, vertical effective overburden stresses under the dam are generally much higher than at the toe, so densities measured at the toe could be lower than those under the embankment.

C.2.3.4   Adjustment for Sampler Liner (C_S)

Accepted procedure for SPTs for liquefaction studies calls for either a sampler that meets the specifications of ASTM, and has an inside diameter (ID) of 1.5 inches and is used with a liner so as to have an effective ID of 1.375 inches, or has an actual ID of 1.375 inches. In either case, the drive shoe at the tip of the sampler has an ID of 1.375. Reclamation drill crews and those in foreign countries typically use the latter, but older Reclamation data or data from contract drillers **may** have been obtained with a 1.5-inch sampler without a liner. That way, there is a reduction in friction that causes the measured blow count to be 10 to 30 percent lower. The difference tends to be larger with higher blow counts, but the available data exhibit considerable scatter (Kovacs and Salamone, 1984).

If no liner was used in a sampler with space for one, the blow count should be multiplied by C_s following Youd et al. (2001). The value of C_S ranges from 1.1 if the adjusted blow count, $(N_1)_{60}$, is 10 or less, to 1.3 if $(N_1)_{60}$ is 30 or more; if $(N_1)_{60}$ is between 10 and 30, one can interpolate linearly. The correction factor C_S should be set equal to 1.0 (i.e., no change) if Reclamation performed the drilling, unless the drill log or other information specifically states that the drillers did not use a liner in a sampler with space for one. Erroneously applying C_S greater than 1.0 would, of course, be unconservative.

Note that this adjustment is circular, as is C_N to account for overburden pressure (below). This requires knowing the adjusted blow count in order to determine the adjustment factor. It is preferred that the adjustment be made iteratively, initially using all of the required adjustments with an assumed $(N_1)_{60}$, to find an updated $(N_1)_{60}$, then repeating the process once or more. (One iteration would probably be sufficiently precise, but the process can be programmed in a spreadsheet to perform more iterations with no more effort.)

Earlier versions of this chapter used a single value of 1.2 for C_S instead of it varying as a function of $(N_1)_{60}$. According to the current (2015) understanding of the SPT, this would be conservative if $(N_1)_{60}$ is greater than 20, and it would be unconservative if it is lower than 20.

If an important decision hinges on older data and the precise value of the liner correction, it may be more appropriate to perform additional drilling with SPTs in strict accordance with the most recent standards, including constant-diameter samplers, rather than rely on the correctness of this adjustment. New drilling programs should always specify liners or constant-diameter samplers to avoid the need to correct for the lack of liners. (This applies to the other adjustments for testing procedures as well.)

C.2.3.5   Normalizing to Standard Overburden Stress (C_N)

For a given density or void ratio, the adjusted SPT blow count, N_{60}, increases with increasing effective overburden stress, σ_v'. Hence, for the blow count to be representative of the density without dependence on overburden, N_{60} has to be normalized to what it would be in the same soil at a standard reference value of σ_v'. (The same principle applies to cone penetration tests and shear-wave velocities, as described in appendices B and D.) For this procedure, the standard effective overburden stress is 1 atm, or 2,116 lb/ft^2. Some other procedures, including earlier SPT procedures, use 2,000 lb/ft^2; but the difference is usually of little consequence.

Each N_{60} value is multiplied by the normalizing factor C_N, to obtain the overburden-adjusted blow count, $(N_1)_{60}$:

$$(N_1)_{60} = C_N * N_{60} \qquad\qquad\qquad \text{Equation C4}$$

C_N is a function of both overburden pressure and relative density, as represented by the *clean-sand equivalent* adjusted blow count, $(N_1)_{60cs}$, which is itself a function of both $(N_1)_{60}$ and fines content. This makes the calculations circular, requiring iterative calculation, beginning with an assumed C_N to find the initial estimate of $(N_1)_{60}$ from equation C4.

$$C_N = \left(\frac{P_a}{\sigma_{vo}'}\right)^{0.784-0.0768\sqrt{(N_1)_{60cs}}} \qquad\qquad \text{Equation C5}$$

where: σ_v' is the vertical effective stress at the test depth in the same units.

To begin, assume that the exponent in equation C5 is equal to 0.5 to get an initial estimate of $(N_1)_{60}$ from equation C4, then use equation C5 to obtain an "updated" C_N, go back to equation C4 to update $(N_1)_{60}$, and repeat until the results "close" with enough precision. (The adjustment for fines, to obtain $(N_1)_{60cs}$ from $(N_1)_{60}$, is presented below, in section C.2.3.6.) No more than two or three iterations should

be needed to achieve enough precision for this purpose, but the spreadsheet program Microsoft Excel can perform the iteration automatically until it closes within a very small tolerance.

C_N can also be found using figure C2 below; however, if many data are to be processed, it is more efficient to do it with equations C4 and C5 in a spreadsheet. (As with the equations, iteration may be required .)
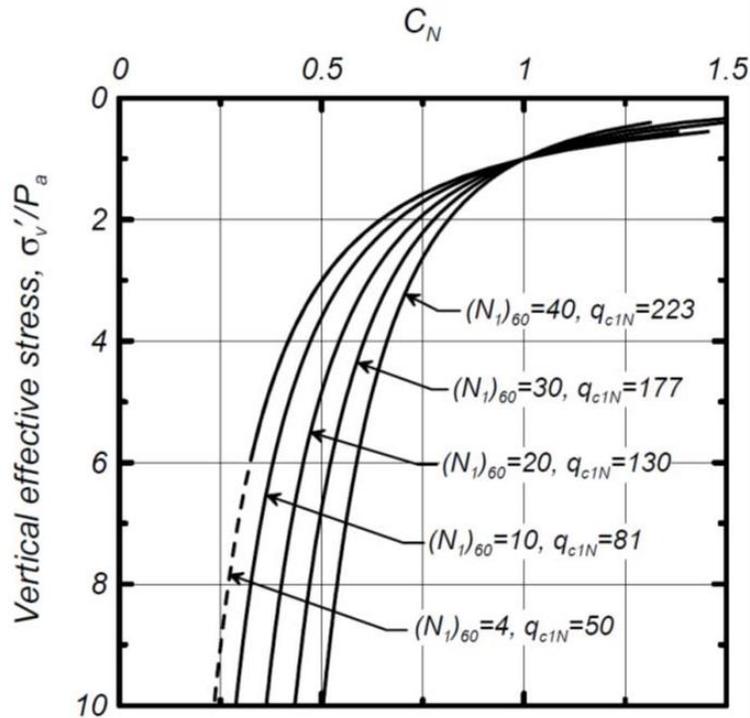
Figure C2. Overburden adjustment for SPT (Idriss and Boulanger, 2004).

Previous versions of Chapter 13 specified a constant exponent of 0.5, instead of an exponent that is a function of $(N_1)_{60}$, consistent with the National Center for Earthquake Engineering Research (NCEER) procedure (NCEER, 1997; Youd et al., 2001). This corresponds to the curve for $(N_1)_{60}$ of about 14 in figure C2. When the effective overburden stress is near 1 atm and/or $(N_1)_{60}$ is close to 14, the difference between assuming the exponent is 0.5 and using Equation C5 is very minor. In back analysis, to develop the various procedures, the difference would have had only minor effects because few of the case histories had effective overburden stress outside the range of 0.5 to 1.5 atm (1,000 to 3,000 lb/ft^2). Equation 5 is based on more extensive laboratory testing and theoretical considerations, but differences between its C_N predictions and those from the simpler version cannot be distinguished in field performance. The statistical analysis of back-analyzed case histories by Cetin et al. (2004) would show essentially no difference if it had been developed using equation C5 instead

of with a constant 0.5 for the exponent. However, in forward analysis of a dam foundation, where the overburden can be many times higher, the difference could be important. With an overburden stress exceeding 10,000 lb/ft^2 under a fairly high dam, the difference in $(N_1)_{60}$ can exceed 20 percent.

C_N should be limited to a maximum value of 1.7 and, in equation C4, $(N_1)_{60}$, should be capped at 46. Capping $(N_1)_{60}$ would have no effect on the outcome of a liquefaction analysis because blow counts that high indicate very dense material.

For determination of $(N_1)_{60}$, the effective stress should be calculated based on piezometric conditions *at the time of drilling*, as recorded on the drill log, or estimated from instrumentation and groundwater conditions. An important caution is that fluid levels on drill logs may not indicate the actual water table and piezometric surface, especially if drilling fluid is used. Unless the soil is fairly pervious, the level of the drilling fluid or clear water in the hole may not be in equilibrium with the groundwater outside of the hole, even if it is measured at the beginning of the shift after sitting all night.

C.2.3.6   Adjustment for Fines Content

For a given value of the adjusted blow count, $(N_1)_{60}$, liquefaction resistance increases with increasing fines content, FC, up to about 35 percent (Seed et al., 1982; Cetin et al., 2004; Idriss and Boulanger; 2010). As a standard, values of $(N_1)_{60}$ for material with more than 5 percent fines are adjusted to obtain the equivalent value for clean sand with the same cyclic resistance, $(N_1)_{60CS}$. **The adjustment is made by adding $\Delta(N_1)_{60}$ to $(N_1)_{60}$:**

$$\Delta(N_1)_{60} = \exp\ [1.63 + 9.7/(FC+0.01) - (15.7/(FC+0.01))^2] \qquad \text{Equation C6}$$

where FC is the fines content, expressed as a percentage (Idriss and Boulanger, 2010). The result is $(N_1)_{60CS}$, a single parameter that includes the effects of overburden stress and fines content, which can be used to predict cyclic resistance ratio or liquefaction probability for most nonplastic soils and some that are slightly plastic. The value of $\Delta(N_1)_{60}$ ranges from zero for fines contents less than 5 percent, to about 5.5 blows for fines contents of 35 percent or more. (For FC below 5 percent, it is assumed to be 5 percent in equation C6; above 35 percent, it is assumed to be 35 percent.)

Figure C3 shows the adjustment for fines in two forms: as the value of $\Delta(N_1)_{60}$, in the upper plot, and as a family of curves of Cyclic Resistance Ratio (CRR) $_{7.5}$ *versus* $(N_1)_{60}$ with different fines contents. In the lower plot, the curve labeled "≤5%" corresponds to $\Delta(N_1)_{60}$, so it is equivalent to the curve for the cyclic resistance ratio, $CRR_{7.5,\sigma=1,\alpha=0}$, as a function of the **clean-sand equivalent** adjusted blow count, $(N_1)_{60cs}$.

For consistency, it is preferred that the effect of fines be accounted for by adding $\Delta(N_1)_{60}$ from either equation C6 or the upper plot in figure C3, rather than

using the lower plot. The lower plot is shown here primarily to illustrate the effect of fines on cyclic resistance. In some earlier versions of *Design Standards No. 13 – Embankment Dams,* Chapter 13, "Seismic Analysis and Design," the fines adjustment was in the form of a multiplier applied to $(N_1)_{60}$ or as a family of curves of $CRR_{7.5}$ *versus* $(N_1)_{60}$ for different fines contents; the results are similar, however.
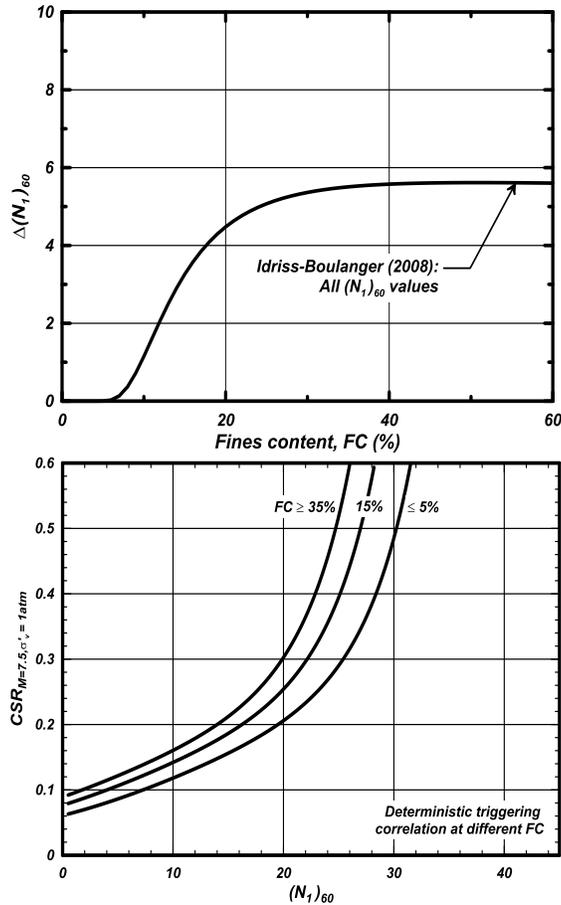
Figure C3. Adjustment of $(N_1)_{60}$ for fines content, to yield $(N_1)_{60cs}$ (Boulanger and Idriss, 2014).

If the fines are somewhat plastic, equation C6 and figure C3 may be conservative, but this is not easily quantified. Other researchers, notably Cetin et al. (2004), have found that fines produce less benefit than is indicated by equation C6 and figure C3.

This adjustment for fines content for determining liquefaction potential is **not** the same as the adjustment made to $(N_1)_{60}$ for empirical estimation of residual undrained shear strength of liquefied materials; for that, refer to appendix F.

C.3 Representative $(N_1)_{60\text{-cs}}$, Liquefaction Potential, and Liquefaction Probability

After $(N_1)_{60\text{-cs}}$, has been determined for each SPT interval, one must determine the representative value for the soil deposit under evaluation. For developing the relationships for liquefaction triggering, each case-history site was represented by the average value for the liquefied stratum, or for sites without liquefaction, for the layer judged most likely to be liquefied, based on blow counts and CSR. This same procedure should be followed in forward analysis, to the extent practical. It is not always obvious which values of $(N_1)_{60\text{-cs}}$ to include in the average. For liquefaction analysis in support of probabilistic risk analysis, it may be appropriate to identify two or more representative $(N_1)_{60\text{-cs}}$ values, and estimate their relative likelihoods. This can then be incorporated in the risk calculation model as either discrete or continuous probability distributions.

Once a representative adjusted blow count, $(N_1)_{60\text{-cs}}$, has been selected, liquefaction analysis can proceed in one of two ways:

(1) Probabilistically: calculating the probability of liquefaction under a given earthquake loading from $(N_1)_{60\text{-cs}}$, and the loading.

(2) Deterministically: using $(N_1)_{60\text{-cs}}$ to determine the CRR of the soil, or **vice versa,** finding the required value of $(N_1)_{60\text{-cs}}$ that is required to provide a particular value of CRR.

CSR is the ratio of the peak cyclic shear stress on a horizontal surface (averaged over the strongest cycles of earthquake loading) to the effective overburden stress. As described in detail in the main text of Chapter 13, it takes the form of :

$$CSR = 0.65\ \tau_{max}\ /\ \sigma'_v \hspace{3cm} \text{Equation C7}$$

where τ_{max} is the peak shear stress from the earthquake. The factor 0.65 accounts for the fact that most of the strong cycles of loading cause stresses smaller than the peak, so the average peak shear stress is roughly 0.65 times the maximum; this was originally included so that field performance could be related to laboratory testing with uniform stress cycles, and it has remained as part of the definition of CSR.

The CRR is the CSR that the soil is **expected to** withstand without occurrence of liquefaction; however, it is not **certain to** withstand it. CRR greater than or equal to CSR does not necessarily make liquefaction impossible or extremely unlikely. **The CRR corresponds to a likelihood of liquefaction of about 15 percent; it is**

not a deterministic boundary. Hence, a factor of safety must be applied to the loading to make the likelihood of liquefaction very small, as discussed later in this appendix.

In Chapter 13, CRR and CSR without subscripts refer to the cyclic stress and resistance ratios with the actual earthquake and overburden stress at the layer under analysis; with the subscripts, $CRR_{7.5,\sigma=1,\alpha=0}$ and $CSR_{7.5,\sigma=1,\alpha=0}$ refer to the stress and resistance ratios adjusted to reference conditions: level ground, 1 atm effective overburden stress, and earthquake magnitude 7.5. In equation form:

$$CSR_{7.5,\sigma=1,\alpha=0} = CSR / (K_\alpha \, K_\sigma \, MSF) \hspace{2cm} \text{Equation C8}$$

$$CRR_{7.5,\sigma=1,\alpha=0} = CRR / (K_\alpha \, K_\sigma \, MSF) \hspace{2cm} \text{Equation C9}$$

where K_α, K_σ, and MSF are adjustments for nonlevel ground, effective overburden stress that differs from 1 atm, and earthquake magnitude, which is used as a proxy for the number of cycles of strong loading. The adjustments are described in detail in the body of Chapter 13.

C.3.1 Probabilistic Liquefaction Triggering Analysis – General Discussion

Since the late 1990s, Reclamation's primary decision tool for dam safety is probabilistic risk analysis, which frequently requires estimates of the probability of liquefaction of a foundation soil or poorly compacted embankment under various loading conditions, along with the likelihood of subsequent events leading to failure of the dam under those loadings. The methods of estimating liquefaction probability are presented here, but their application in risk analysis is not addressed further; refer to Reclamation's most recent risk-analysis guidance.

A number of models have been developed to estimate the probability of liquefaction, beginning with the pioneering work by Liao et al. (1988). More recently, studies by Cetin et al. (2004) and by Idriss and Boulanger (2010), used expanded data sets and more detailed analysis of site response, effect of fines content, etc.; these have largely superseded the models of Liao et al. and other models in practice. Reclamation has used all three of the cited models in risk analyses.

The two newer models, Cetin et al. (2004) and Idriss and Boulanger (2010), abbreviated here as the "IB model," were both derived from statistical analysis of a large database of earthquake-affected sites with and without liquefaction. Cetin et al. included a large number of independent variables in the regression to predict liquefaction probability:

- CSR

- Fines content, FC,

- Earthquake magnitude, MW,

- Pre-earthquake effective overburden stress, σ_v'

- SPT blow count adjusted for hammer energy and overburden stress, but not for fines content, $(N_1)_{60}$.

In contrast with Cetin et al. (2004), the regression by Idriss and Boulanger used only two variables: the CSR adjusted for the effects of earthquake magnitude and effective overburden stress, $CSR_{7.5,\sigma=1,\alpha=0}$, and the equivalent clean-sand SPT blow count, $(N_1)_{60\text{-}cs}$. The effects of FC, M_W, and σ_v' were accounted for using equations C6 and C8, which came from other experimental and theoretical considerations (explained in Idriss and Boulanger, 2010). There are advantages to both models. Including FC, M_W, and σ_v' in the regression analysis explicitly means there is no need to assume a particular form or relationship for the effects of each, or assume that the effect of FC is constant for all values of $(N_1)_{60}$ and M_W, for example. The drawback is that the available database does not include cases that cover the full range of conditions likely to be found in practice, particularly for dams. For example, there are very few cases with σ_v' greater than 2,500 lb/ft^2, or M_W less than 6.0. Therefore, the regressed relationships need to be extrapolated for conditions where there are few or no data to constrain their position.

The two models differ greatly in their estimates of liquefaction probability for some combinations of loading and blow count, although they were developed from almost the same database of historic occurrence of liquefaction. For example, for a clean sand with $(N_1)_{60cs}$ equal to 10 (fairly loose soil), and a modest $CSR_{7.5,\sigma=1,\alpha=0}$ of 0.10, the Cetin et al. (2004) model indicates liquefaction probability of about 0.8, but the IB model indicates only 0.01. The primary reasons are the use of different r_d relationships in the back analysis of some case histories and different interpretations of several critical ones (whether or not liquefaction occurred, which materials liquefied).

The IB model was selected for Chapter 13 because of two concerns about the Cetin et al. (2004) model. First, the limited data set does not appear to constrain the effects of magnitude and effective overburden stress on the cyclic resistance very well, for small magnitudes and high effective overburden stresses. Hence, relationships based on mechanical considerations are preferred for extrapolating to small magnitudes and high overburden stresses, rather than statistical relationships. Second, liquefaction probabilities in the Cetin et al. model may have been affected by several sites that were treated as having been liquefied although the original source documents said

they were not; this appears to have caused the model to be overly conservative, particularly with low adjusted blow counts. Future research could supersede the IB model in practice.

The IB model is described below without detailed background information; for that, refer to Idriss and Boulanger (2010), and Boulanger and Idriss (2014).

C.3.2   IB Model for Probability of Liquefaction

The IB model was developed from statistical regression on only two parameters, $(N_1)_{60-cs}$ and $CSR_{7.5}$. The effects of fines in the soil, K_σ effects, and earthquake magnitude, etc. were assumed to apply deterministically, instead of being part of the regression. The calculation of probability for a given pair of $(N_1)_{60-cs}$ and $CSR_{7.5,\sigma=1,\alpha=0}$ is as follows:

$$P_L\big((N_1)_{60}, CSR_{M=7.5\ \sigma'_v=1atm}\big) = \qquad\qquad \text{Equation C10}$$

$$\Phi\left[-\frac{\frac{(N_1)60cs}{14.1}+\left(\frac{(N_1)60cs}{126}\right)^2-\left(\frac{(N_1)60cs}{23.6}\right)^3+\left(\frac{(N_1)60cs}{25.4}\right)^4-2.67-\ln\left(CSR_{M=7.5,\sigma'_v=1atm}\right)}{\sigma_{\ln(R)}}\right]$$

where the quantity inside the brackets is a function equal to the number of standard deviations that the adjusted cyclic resistance is above or below the adjusted CSR. The function $\Phi[x]$ is the standard normal distribution of x; its value is the probability that the loading exceeds the resistance. For programming in a spreadsheet, the mean of the quantity in brackets is zero. The quantity $\sigma_{\ln(R)}$ is the standard deviation on CRR for a given value of $(N_1)_{60cs}$, assumed to be constant for all values of $(N_1)_{60cs}$, and equal to 0.13

Figure C4 shows a family of curves in a space of $(N_1)_{60-cs}$ and $CSR_{7.5,\sigma=1,\alpha=0}$, with each curve corresponding to a fixed value of P_L. The curve for P_L equal to 0.15 corresponds to the cyclic resistance ratio ($CRR_{7.5,\sigma=1,\alpha=0}$), as it is generally defined. One can either use equation C10 to calculate P_L directly, or use figure C4, interpolating between curves to estimate P_L. Once it is set up, a spreadsheet can make the calculations easy and efficient. Extrapolating outside the curves for 0.15 and 0.85 is not recommended.
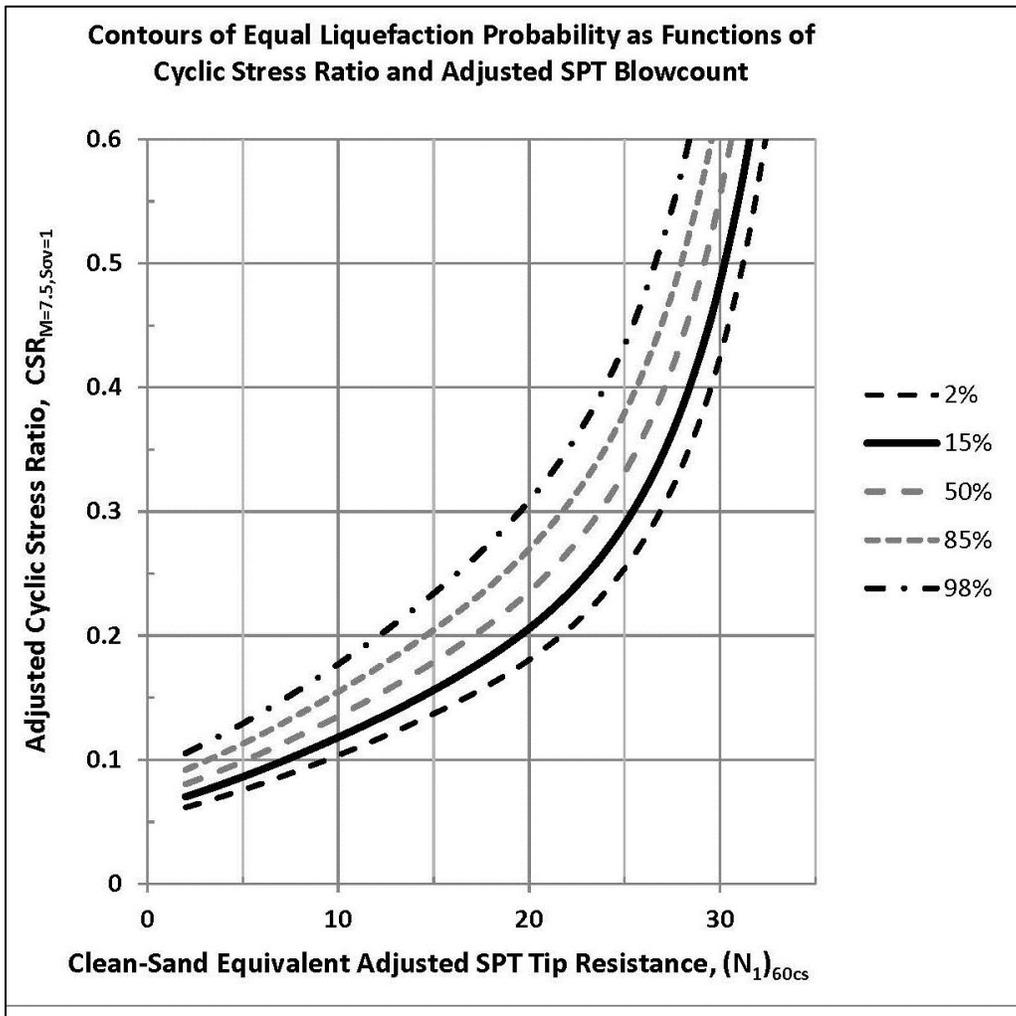
Figure C4. Probability of liquefaction by IB model (redrawn from Idriss and Boulanger, 2010).

C.3.3   Deterministic Analysis

In deterministic analysis, which might more accurately be called "pseudodeterministic analysis," dam performance is analyzed assuming the most severe potential loading (the Maximum Credible Earthquake [MCE], 10,000-year earthquake, or something similar), with generous factors of safety against liquefaction and instability, and sometimes with intentionally conservative assumptions about material properties and piezometric levels. If the structure meets all standards, such as maximum deformation and minimum factors of safety, it would be considered acceptable. This was the primary approach at Reclamation until the late 1990s, when dam-safety decision making became a

"risk-informed" process, comparing the annual probability and consequences of a breach against general guidelines about levels of risk and justification for corrective action. Although Reclamation dams are now generally evaluated using probabilistic risk analysis, Reclamation engineers may need to read and understand older reports or, possibly, to perform or review deterministic liquefaction triggering analysis for other agencies.

Most commonly, the comparison of demand and capacity is made in terms of $CSR_{7.5,\sigma=1,\alpha=0}$ and $CRR_{7.5,\sigma=1,\alpha=0}$, with a factor of safety applied as appropriate. It is possible and technically valid to make the comparison in other forms, such as CSR and CRR for the actual earthquake magnitude and static stress conditions, or between the required value of $(N_1)_{60\text{-cs}}$ for a given loading and safety factor and the actual value of $(N_1)_{60\text{-cs}}$. However, this requires very careful bookkeeping to ensure that all of the adjustments for CSR and N have been applied consistently and correctly.

The curve in figure C5 is used to find $CRR_{7.5,\sigma=1,\alpha=0}$ for a given value of $(N_1)_{60\text{-cs}}$ (Idriss and Boulanger, 2010). (The vertical axis is actually labeled "$CSR_{7.5,\sigma=1}$," but with a factor of safety of 1.0, CRR and CSR are equal to each other, so they are interchangeable for the purpose of this plot. "$\alpha=0$" is implicit.) For the plotted case-history data, the label on the vertical axis refers to the adjusted CSR that the soils experienced, with or without liquefaction, rather than the threshold value that could cause liquefaction. For an analysis to **be approximately** deterministic, a factor of safety must be applied to the loading, because with $CSR_{7.5,\sigma=1,\alpha=0}$ equal to $CRR_{7.5,\sigma=1,\alpha=0}$, (FS=1.0), there is about 15 percent probability of liquefaction. Alternatively, figure C5 can be used in reverse to find $(N_1)_{60\text{-cs-req}}$, the adjusted blow count required to provide $CRR_{7.5,\sigma=1,\alpha=0}$ equal to some value of $CSR_{7.5,\sigma=1,\alpha=0}$. A factor of safety would be applied to $CSR_{7.5,\sigma=1,\alpha=0}$ to find the blow count needed for some tolerable probability less than 15 percent. Table C2 relates liquefaction probability and factor of safety. Some agencies require at least 1.2, which would exclude all but one of the cases shown on figure C5.

Table C2. Factor of Safety and Corresponding Liquefaction Probability

Probability of Liquefaction (%)	Factor of Safety
15	1.0
5	1.1
2	1.15
1	1.2
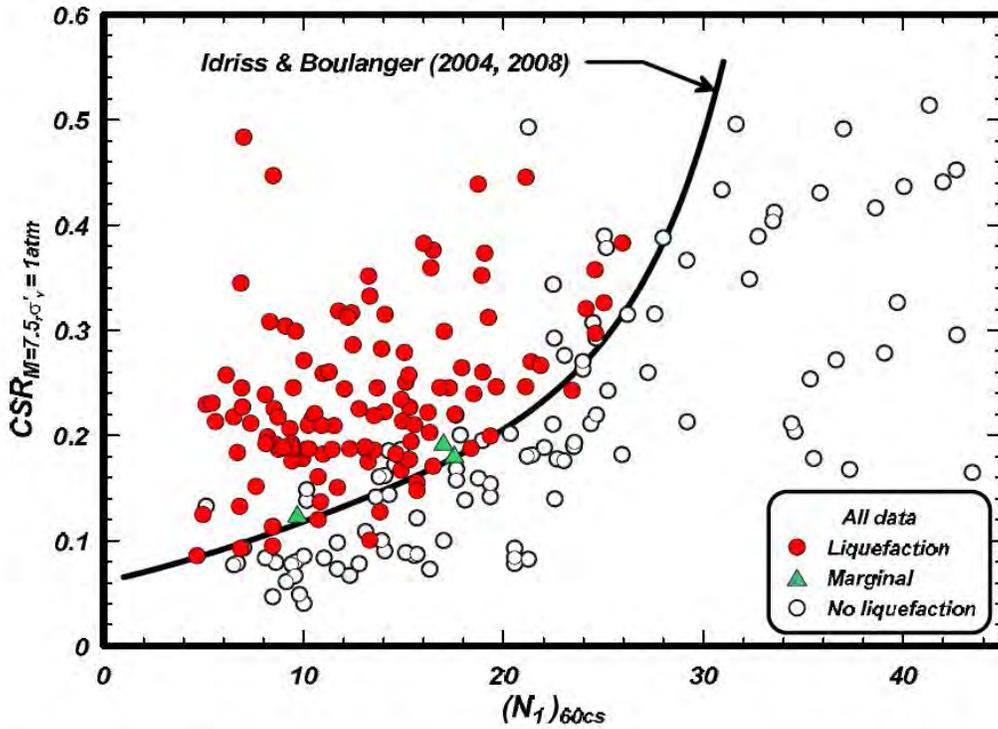
Figure C5. CRR as a function of $(N_1)_{60cs}$., for reference conditions of σ'_v = 1 atm, M = 7.5, and level ground (α = 0). Curve is equivalent to the one in figure C4 for P_L = 15% (Idriss and Boulanger, 2010).

In lieu of figure C5, $CRR_{7.5,\sigma=1,\alpha=0}$ can be estimated in a spreadsheet or other computer application using equation C11, from Idriss and Boulanger.

$CRR_{7.5,\sigma=1,\alpha=0}$ =   Equation C11

$\exp\{(N_1)_{60\text{-}cs}/14.1 + [(N_1)_{60\text{-}cs}/126]^2 - [(N_1)_{60\text{-}cs}/23.6]^3 + [(N_1)_{60\text{-}cs}/25.4]^4 - 2.8\}$

Equation C12, below, is the inverse of equation C11. It can be used to find the blow count required to provide some particular value of safety factor or liquefaction probability. As shown, it indicates the value of $(N_1)_{60\text{-}cs\text{-}req}$ for FS = 1.0 or liquefaction probability of 15 percent. If a lower probability of liquefaction is needed, substitute FS x $CSR_{7.5,\sigma=1,\alpha=0}$ for $CSR_{7.5,\sigma=1,\alpha=0}$ in the equation, with FS values suggested in table C2.

$(N_1)_{60\text{-}cs\text{-}req} = 342\ CSR_{7.5,\sigma=1,\alpha=0}^{1/4} - 108\ CSR_{7.5,\sigma=1,\alpha=0}^{1/3} -$ Equation C12

$85\ CSR_{7.5,\sigma=1,\alpha=0}^{1/2} - 11\ CSR_{7.5,\sigma=1,\alpha=0} - 107$

C.4 Uncertainty in Liquefaction Triggering Analysis Using SPT

Uncertainty in this analysis arises from several sources, including the model itself and the case-history data from which it was developed in back analysis; and in forward analysis, from the SPT blow counts at the site and their interpretation, and the predicted cyclic stresses.

The probabilistic approach addresses imprecision and variability in valid SPT results and cyclic stresses, but it does not account for uncertainty from bad drilling techniques, gravel interference, etc. It was developed from very carefully examined site data and response analyses. The user cannot ignore the quality of site data or cyclic-stress estimates, assuming that a probabilistic analysis can produce reasonable probability estimates from faulty inputs. If the model is applied to loading conditions that are far outside ranges of the historic data that would introduce additional uncertainty, regardless of how good the data and response analysis are.

Even with high-quality data, the model cannot be considered to provide a single "correct" value of liquefaction probability to apply in risk analysis. Significant variation in the liquefaction probability can be calculated with fairly modest variations in $(N_1)_{60\text{-cs}}$, CSR, static shear stress (K_α effects), etc. The user needs to consider how reasonably expected uncertainty in the input parameters would affect the resulting probability estimate. Ordinarily, the probability of liquefaction should be represented as a range of probabilities, rather than a single "best estimate."

SPT equipment and methods are still not completely standardized, and even new drilling needs to be checked for deviations from modern standard practice. (In particular, refer to ASTM D6066-11, which is specific to SPTs for liquefaction assessment.) While current Reclamation practice requires automatic hammers and strict adherence to ASTM D6066-11, older Reclamation data, and data from other sources, are more likely to have been obtained with different drilling techniques. The energy correction partially compensates for differences among hammers; however, even for a given hammer, there can be variation due to the condition of the rope (very new, very worn, wet, greasy, icy), the number of turns of rope on the cathead, the rate of operation of an automatic hammer, and human factors. The sampler may have been equipped with a "catcher" or "basket" to prevent the sample from slipping out; the resulting constriction may slightly elevate the blow count in moderately dense or dense soils. The bottom of the hole may have been heaved or loosened if there was no drill fluid or too little fluid to counteract the groundwater pressure. Particularly bad disturbance of the bottom of the hole can occur when the pilot bit is pulled out of a hollow-stem auger too

rapidly, so it acts as a piston and sucks soil into the bottom of the augers, loosening the soil. Disturbance by drilling or heave could result in blow counts that are lower than measurements taken under standard conditions. The drillers and field geologists need to make sure that standard practices are followed for new exploration, and engineers using the data are responsible for understanding how it was obtained.

The driller is human. With a rope and cathead to raise and drop the SPT hammer, one cannot expect that the energy transferred to the rods will be completely consistent from blow to blow or with other driller/hammer combinations. The height of drop inevitably varies, the amount of energy lost to friction of the rope on the cathead depends on the driller's technique, rods may be bent or not quite screwed together tightly, and the drill hole may deviate from plumb. All of these factors can cause the energy delivered to the split-barrel sampler to differ substantially from what is assumed in the analysis, or even from the previous test interval. This can, of course, affect the blow count. Mechanical hammers provide much greater consistency, but with some hammers, the drop and transferred energy vary with changes in the rate of operation (blows per minute), so precise control of the engine speed is needed, along with energy measurements. Refer to ASTM D1586-11 and to the owner's manual for each hammer. (Field personnel need to be aware of the issue of operation rate!)

The estimated CSR for a given level of earthquake loading is also both variable and uncertain. For example, for a given earthquake return period, there is variability because different earthquakes that would fit that return period can have different frequency contents. There is uncertainty because of the simplified response analysis and the assumptions about material properties.

C.5   References

Boulanger, R.W., and I.M. Idriss. 2014. *CPT and SPT Based Liquefaction Triggering Procedures.* University of California at Davis, Center for Geotechnical Modeling, Report No. UCD/CGM-14/01.

Bureau of Reclamation. 2007. *Evaluation of In Situ Methods for Liquefaction Investigation of Dams.* Research Report DSO-07-09, prepared by William Engemoen.

Cetin, K.O., R.B. Seed, A. Der Kiureghian, K. Tokimatsu, L.F. Harder, R.E. Kayen, and R.E.S. Moss. 2004. "Standard Penetration Test-Based Probabilistic and Deterministic Assessment of Seismic Soil Liquefaction Potential," *Journal of Geotechnical and Geoenvironmental Engineering,* Vol. 130, No. 12, pp. 1314-340. American Society of Civil Engineers.

Daniel, C.R., J.A. Howie, R.S. Jackson, and B. Walker. 2005. "Review of Standard Penetration Test Short Rod Corrections," *Journal of Geotechnical and Geoenvironmental Engineering,* Vol. 131, No. 4, pp. 489-497. American Society of Civil Engineers.

Farrar, J.A., J. Nickell, M.G. Allen, G.G. Goble, and J. Berger. 1998. "Energy Loss in Long Rod Penetration Testing – Terminus Dam Liquefaction Investigation," *Proceedings, Geotechnical Earthquake Engineering and Soil Dynamics III.* American Society of Civil Engineers, Geotechnical Special Publication No. 75, Vol. I, pp. 554-567.

Idriss, I.M., and R.W. Boulanger. 2004. "Semi-empirical Procedures for Evaluating Liquefaction Potential During Earthquakes," *Proceedings, 11th International Conference on Soil Dynamics and Earthquake Engineering, and 3rd International Conference on Earthquake Geotechnical Engineering.* D. Doolin et al. (eds.), Stallion Press, Vol. 1, pp. 32–56.

Idriss, I.M., and R.W. Boulanger. 2008. *Soil Liquefaction During Earthquakes*, Monograph MNO 12. Earthquake Engineering Research Institute, Oakland, California.

Idriss, I.M., and R.W. Boulanger. 2010. *SPT-Based Liquefaction Triggering Procedures.* Report No. UCD/CGM-10/02, University of California at Davis.

Kovacs, W.D., and L.A. Salamone. 1984. *Field Evaluation of SPT Energy, Equipment, and Methods in Japan Compared with the SPT in the United States*. Report No. NBSIR 84-2910, U.S. Department of Commerce, National Bureau of Standards.

Liao, S.S.C., D. Veneziano, and R.V. Whitman. 1988. "Regression Models for Evaluating Liquefaction Probability," *Journal of Geotechnical Engineering*, Vol. 114, No. 4, pp. 389-411. American Society of Civil Engineers.

NCEER. 1997. *Proceedings, NCEER Workshop on Evaluation of Liquefaction Resistance*. National Center for Earthquake Engineering Research, Salt Lake City, January 4-5, 1996.

Schmertmann, J. 1978. "Use of the SPT to Measure Dynamic Soil Properties? - Yes But ....!" *Dynamic Geotechnical Testing*. ASTM STP 654, pp. 341-355. American Society for Testing and Materials.

Seed, H.B., K. Tokimatsu, L.F. Harder, and R.M. Chung. 1985. "Influence of SPT Procedures in Soil Liquefaction Resistance Evaluations," *Journal of Geotechnical Engineering*, Vol. 111, No. 12, pp. 1425-1445. American Society of Civil Engineers.

Seed, H.B., I.M. Idriss, and I. Arango. 1982. "Evaluation of Liquefaction Potential Using Field Performance Data," *Journal of Geotechnical Engineering.* Vol. 109, No. 3, pp. 458-482. American Society of Civil Engineers.

Skempton, A.W. 1986. Standard Penetration Test Procedures and the Effects in Sands of Overburden Pressure, Relative Density, Particle Size, Ageing and Overconsolidation," *Géotechnique*, Vol. 36, No. 3, pp. 425-447.

Youd, T.L., I.M. Idriss, R.D. Andrus, I. Arango, G. Castro, J.T. Christian, R. Dobry, W.D.L. Finn, L.F. Harder, Jr., M.E. Hynes, K. Ishihara, J.P. Koester, S.S.C. Liao, W.F. Marcuson, G.R. Martin, J.K. Mitchell, Y. Moriwaki, M.S. Power, P.K. Robertson, R.B. Seed, and K.H. Stokoe. 2001. "Liquefaction Resistance of Soils: Summary Report from the 1996 NCEER and 1998 NCEER/NSF Workshops on Evaluation of Liquefaction Resistance of Soils," *Journal of Geotechnical and Geoenvironmental Engineering*, Vol. 127, No. 10, pp. 817–833.

Appendix D

Becker-Hammer Penetration Test for Gravelly Soils

Contents

Figures

D.1   Introduction

This appendix of Chapter 13, "Seismic Analysis and Design," of *Design Standards No. 13 – Embankment Dams* describes the Becker Hammer Penetration Test (BPT) as an index of density and liquefaction potential in soils that are too coarse for the Standard Penetration Test (SPT) or the Cone Penetration Test (CPT) to yield meaningful results. Because the diameter of the BPT penetrometer tip is much larger than that of the SPT sampler or the cone penetrometer, gravel-sized particles have much less effect on the BPT, whereas gravel contents greater as low as 15 to 20 percent can cause misleading results in the SPT. The BPT consists of driving a plugged steel casing into the ground using a diesel pile-driving hammer. The number of blows per foot of penetration is recorded and adjusted for driving conditions, then used with empirical correlations to estimate equivalent SPT N_{60} values. The BPT is performed with a Becker Drills, Ltd., model AP-1000 or B-180 drill rig, equipped with an International Construction Equipment (ICE) model 180, closed-end diesel hammer. The standard configuration uses 6.6-inch outside-diameter (OD), double-wall casing and a plugged "crowd-out" bit; the AP-1000 rig is preferred [1, 2].

Two methods for inferring equivalent SPT blow counts from BPT data have become established in practice [1, 3]; these are described below. However, a third method, called the iBPT [4], is now considered to be the state of the art for BPT interpretation. Although the Bureau of Reclamation (Reclamation) has no experience with it to date (2015), its use is strongly encouraged for any future BPT programs for high-hazard dams.

The BPT is rapid and economical to perform. Production can reach 500 feet per day. However, no sample is retrieved with the BPT, so other sampling, such as SPT or coring, is also required. (It is true that the Becker rig can be used to retrieve samples, but that requires a separate hole, and the samples are completely disaggregated because they are lifted out of the hole by compressed air and discharged through a cyclone. Even grain-size distributions on those samples would be suspect.) Another disadvantage is the uncertainty in interpretation of the data. Because the BPT is generally used to estimate equivalent SPT blow counts, significant uncertainty is introduced by that step, in addition to the uncertainty that exists in predictions of soil behavior from $(N_1)_{60}$.

The penetration resistance of soils is influenced by many factors, including soil type (grain-size distribution, plasticity of fines, particle sizes, particle shapes, and density), confining stress, the amount of energy delivered to the penetrometer tip, size and shape of the penetrometer, and friction on the sides of the penetrometer. The BPT is different from the SPT test in several ways, so one cannot expect consistent correlation between BPT and SPT data. Unlike the SPT, the BPT is not performed in an open hole with a diameter greater than the rod diameter, so there is substantial friction on the drill string, which greatly complicates the analysis. The BPT penetrometer tip is closed, also unlike the SPT sampler; this affects the

pattern of deformation around the penetrometer tip. In addition, in the same way that the SPT is adversely affected by large amounts of small to medium gravel, the BPT may give misleading results in soils containing boulders, cobbles, or possibly even large amounts of coarse gravel (larger than about 1-½ inches or 4cm).

The effect of fines on the relationship between Becker penetration resistance and liquefaction potential is not well established from experiments or field performance. It is usually *assumed* that the effect of fines is similar to what occurs with the SPT. Because the BPT does not provide a sample, it is necessary to estimate the fines content from nearby drill holes or to simply neglect the potential benefit of fines.

If a Becker drill is mobilized to a project for penetration testing, it can also be used for other tasks, such as installation of piezometers. This is not, however, a good method for any kind of geophysical testing related to soil density or stiffness, because an annulus of soil is densified around each Becker hole (though perhaps less so if an open crowd-in bit is used, instead of the BPT standard of a plugged crowd-out bit). The extent of densification is not known, so shear-wave velocities measured using Becker holes may not even be meaningful. It is also possible to use rotary drilling inside the double-wall Becker casing, for example, to socket inclinometers or piezometers into bedrock (by positioning a rotary drill rig over the top of the Becker casing). This is, of course, more expensive than standard BPT because of delays and the need for a second rig. (Becker rigs do not have rotary drilling capability.)

D.2   Equipment and Specifications

Becker drill rigs can be operated with a variety of equipment configurations, but for penetration testing, the standard testing setup as recommended by Harder and Seed [1] is as follows:

a. Drill rig: Becker Drills, Ltd., model AP-1000 rig

b. Hammer: ICE model 180 diesel hammer equipped with a blower that helps clear exhaust gases out of the combustion chamber between blows

c. Casing (rods):   168-millimeter (6.6-inch) outside diameter, double-wall

d. Drive bit: Crowd-out plugged bit

The correlation between BPT and SPT data proposed by Harder and Seed relies on strict adherence to the standard equipment configuration. Only if all four

conditions are met can the Harder-Seed method be used. Open-bit tests were found to be inconsistent and erroneously low relative to the closed-bit standard, so blow counts recorded during sampling with open bits and compressed air cannot be used (although consistently high, open-bit blow counts would likely indicate dense material). The older model B-180 and HAV-180 rigs equipped with the same ICE model 180 hammer were found to transfer about 50 percent more of the energy to the drill string than do AP-1000 rigs [1]. This factor has been tentatively confirmed by a limited number of energy measurements, but it is better to simply avoid the issue by specifying AP-1000 rigs only. In theory, the Sy-Campanella and iBPT methods [3,4] could work with any pile hammer, requiring only that conditions c. and d. be met. For example, British Columbia Hydropower has used an ICE 180 hammer on swinging pile leads suspended from a crane to allow drilling on an embankment slope without the need to construct a road [5]. However, all four conditions should be specified unless there is some unusual circumstance. (Some ICE hammers are labeled "Linkbelt.")

Although BPT testing can be performed without electronic data collection for the Harder-Seed method, BPT programs for Reclamation dams must include Pile-Driving Analyzer (PDA) measurements or, preferably, iBPT testing. Unfortunately, as of 2015, iBPT testing and analysis are available only through the University of California at Davis, where the iBPT was developed. This could be an issue for scheduling of work.

D.3   Assessing Liquefaction Potential Using the BPT

In soils containing significant amounts of gravel, measured SPT or CPT resistance may be misleadingly high, and there is potential for damage to CPT equipment. ("Significant" is not easily defined, but CPT equipment often cannot be advanced at all through thick gravel layers with more than about 30 percent gravel, depending on the size of the gravel and the density of the soil; misleading measurements may occur with gravel contents much smaller than that.) BPTs are rarely performed at the start of an investigation; instead, they are generally used after SPTs or CPTs have been attempted and found to be inappropriate because of too much gravel. BPT testing should generally not be relied upon as the sole basis for liquefaction evaluation. To the extent practical, it should be calibrated or verified by site-specific SPT-BPT correlation, or corroboration from shear-wave velocities or other predictor of liquefaction resistance.

The BPT blow count (or the blow count from any other dynamic penetration test) is a function of soil properties at the tip and the amount of energy that reaches the tip. The energy reaching the tip is governed by both the amount of energy that is

imparted to the drill string by the diesel hammer and the amount of energy that is lost to friction as the wave of compression propagates from the top of the drill string to the tip.

The diesel hammer does not provide a constant energy to the drill string. This is because the energy is dependent on combustion conditions, which are affected by fuel condition, air mixture, ambient air pressure, driving resistance, and throttle control. The ICE closed-end diesel pile hammer is equipped with a "bounce chamber" in which air is compressed by the rising ram after each blow; the air acts as a spring to push the ram back down for the next blow (unlike the more common open-ended diesel hammer, which uses gravity alone to return the ram). Measuring the bounce-chamber pressure provides an indirect measure of combustion energy. Figure D1, from Harder and Seed [1], shows how combustion energy affects the number of blows required for each foot of driving. The lower plot shows, as would be expected, that lower "raw" Becker blow counts, N_B, occur at any particular depth with better hammer performance. At a depth of 40 feet, the blow counts are 56, 26, and 10 for combustion efficiency curves numbered 1, 2, and 3, respectively. The upper plot shows three curves of Becker blow count, N_B, plotted against bounce pressure. Knowing blow count and bounce pressure, one can infer (roughly) how well the hammer is performing.

Because the BPT is not performed in an open drill hole, like the SPT is, friction along the drill string contributes to the driving resistance. The energy required to overcome the friction is, in effect, subtracted from the energy put into the drill string before the compression wave reaches the tip. At large depths, overcoming the friction can consume a large fraction of the energy from the hammer, so the amount of energy reaching the tip (and, therefore, the blow count) can be sensitive to fairly small variations in the friction. Sy and Campanella [3] attempted to account for this using a Pile Dynamics, Inc., PDA to estimate the friction. Harder and Seed's method was developed from testing relatively shallow soils, so the friction was a more minor issue.

The issue of rod friction can be addressed more directly by either measuring the energy that reaches the tip, at the tip, or by reducing the friction to the point that it has only a minor effect on energy transmission. In the most promising approach, called the instrumented BPT (iBPT), force and acceleration are measured at the **tip** of the drill string, in addition to the **top**, so the energy that reaches the tip can be determined more directly [4]. At this time (2015), Reclamation, and the profession as a whole, has little experience with iBPT. However, other agencies have used it, notably the Los Angeles (California) Department of Water and Power. In April 2015, BPT researchers and users of the BPT met in Davis, California, to discuss advances in BPT testing and procedures for liquefaction assessment of gravelly soils. The general consensus was that the iBPT represents the state of the art, and that it is the preferred method for major projects. For high-hazard Reclamation dams where liquefaction of gravelly soils could be important, the use of the iBPT is strongly encouraged. This is particularly true where casing friction

could be high (as it often is when testing below a compacted embankment) because high friction makes interpretation of BPT results more uncertain in the other two methods.
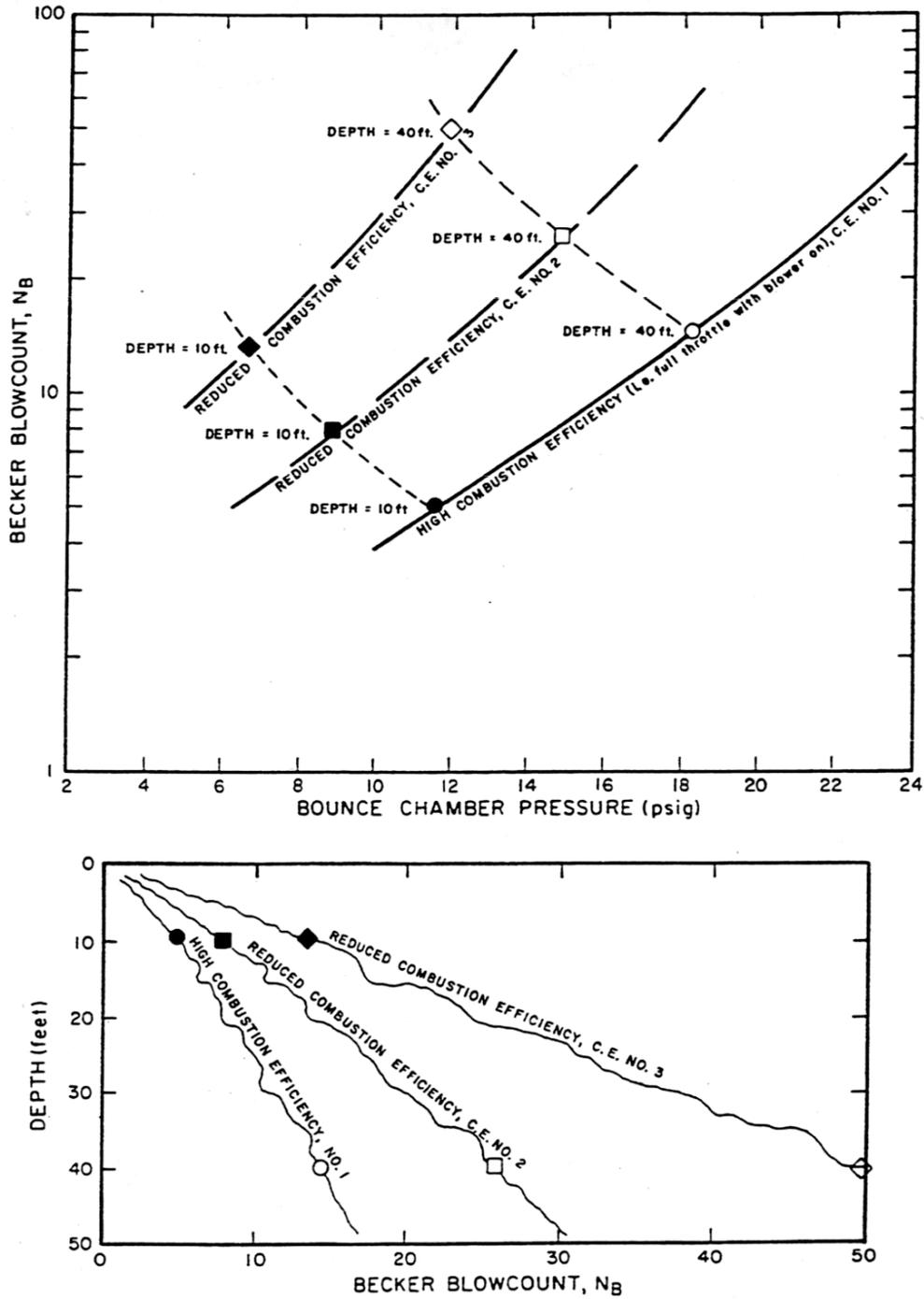

Figure D1. Influence of diesel hammer combustion efficiency on BPT blow count [1].

A "mud-injection BPT" has also been proposed as a way to eliminate the friction issue, using rods that are smaller in diameter than the 6.7-inch tip [8]. This creates a fluid-filled annulus around the rods, with the drilling fluid providing lubrication to keep the annulus open. There are a number of practical drawbacks, which include specialized equipment and the need to mix and dispose of the drilling fluid. The mud-injection BPT has been used very little in practice, and Reclamation has no experience with it.

BPT testing for liquefaction potential at Reclamation high-hazard dams must include either PDA measurements or, preferably, iBPT measurements. If iBPT is not available (due to difficulty scheduling iBPT data acquisition, for example), PDA measurements and the Sy-Campanella method may be used in its place. As of 2015, iBPT testing and analysis are available only through the University of California at Davis, where it was developed. On high-hazard dams, the Harder-Seed method is considered to be primarily for preliminary computations; for example, before the CAPWAP analyses needed for the Sy-Campanella method are available.

To the extent practicable, all BPT programs should include soundings close enough to SPT borings to verify that the BPT method(s) used agrees reasonably well with the SPT results in layers fine enough for the SPT to produce valid results.

D.4   Harder-Seed Method of BPT Interpretation

D.4.1 Description

The Harder-Seed method of interpreting the BPT uses measurements of bounce-chamber pressure as an indirect indication of the energy imparted to the rods by each blow. Figure D2 is used with the bounce-chamber pressure to adjust the blow count (as actually measured, with the actual combustion condition) to that which would be measured at a hypothetical constant combustion condition. The curve A-A represents the Becker hammer operated at near-maximum combustion efficiency (i.e., at full throttle with the hammer performing well). The actual blow count, N_B, and the measured bounce pressure are located on figure D2; from that point, the user then follows a path parallel to the nearest curve, down and to the right toward curve A-A. The blow count corresponding to the point where A-A is reached is called the corrected Becker blow count N_{BC}. When performing BPT, it is desirable to keep the hammer operating as near curve A-A as possible, so that the uncertainty introduced by the adjustment is kept to a minimum. (This also makes the testing proceed as quickly as possible.) Hence, the throttle should be kept wide open, and the blower should be operated

any time data are being recorded. (The driller may prefer to use a smaller throttle opening and/or operate without the blower at the beginning of driving, when the blow counts are smaller. If the blow counts required for analysis are near the surface, the driller should be informed of this and instructed to keep the throttle wide open. Any instances where full throttle and blower are *not* used should be recorded in the field notes.)
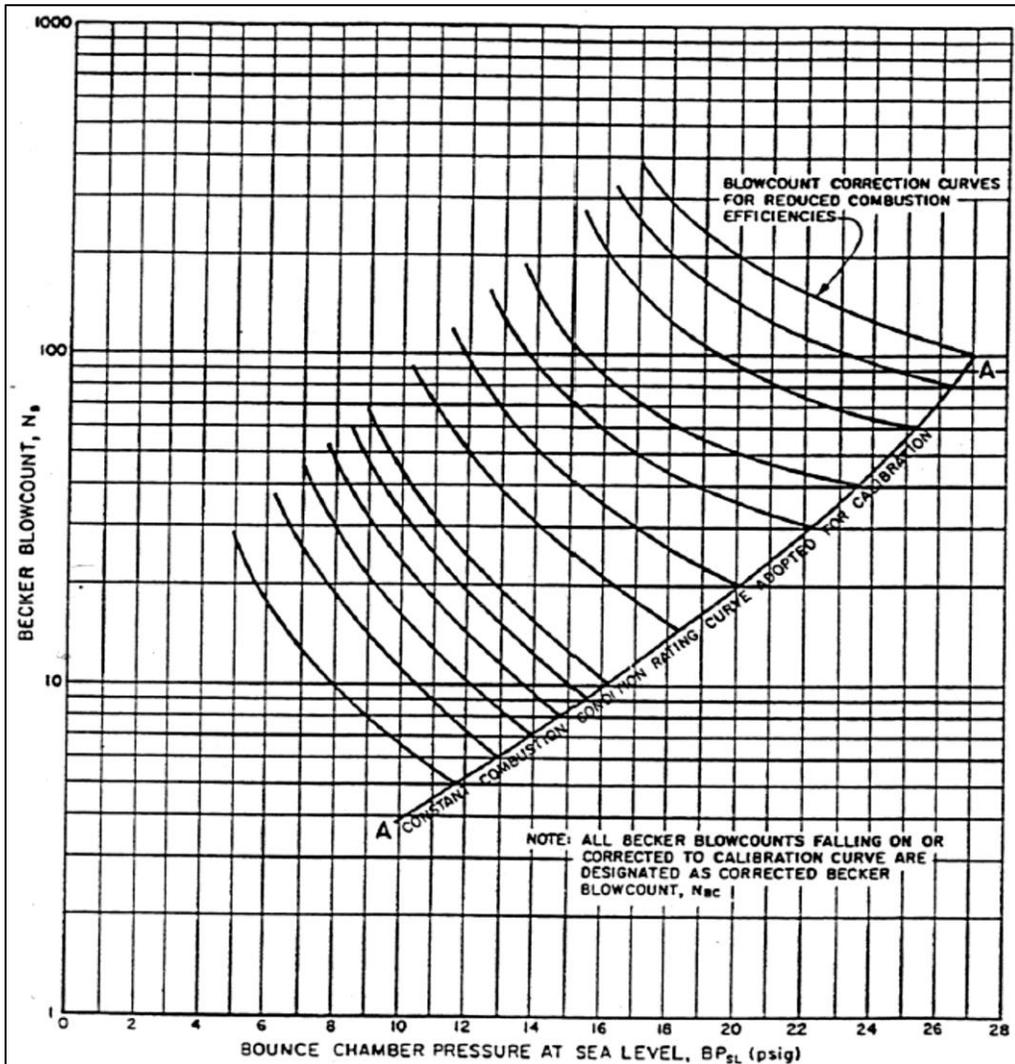

Figure D2. Chart for correcting blow count for hammer performance, to obtain N_{BC} [1].

In order to apply the adjustment in figure D2, the bounce chamber needs to be monitored continuously during testing. Reclamation has developed an electronic recording system specifically for this purpose. Information on this system can be obtained from Reclamation's Structural Behavior and Instrumentation Group [7].

The data can also be recorded manually using the pressure gauge provided by the hammer manufacturer, but the gauge reading is sensitive to the length of hose used to connect it to the hammer.

The corrected Becker blow count, N_{BC}, is then correlated to an equivalent SPT N_{60} value, according to figure D3 [2]. (The figure shows Harder and Seed's original correlation from 1986 [1], updated to include additional data.) The value of N_{60} so estimated is then adjusted by C_N for the effects of overburden stress (as described in Appendix C, "Empirical Assessment of Liquefaction Potential Using the Standard Penetration Test") to obtain the Becker-equivalent $(N_1)_{60}$, which can then be used in empirical correlations between $(N_1)_{60}$ and liquefaction resistance or post-liquefaction undrained shear strength. When possible, it is recommended that the curve of N_{BC} *versus* N_{60} be checked against site-specific SPT and BPT data. There is obvious scatter in the data in figure D3, some of which may result from variations in side friction among the different sites tested. Site-specific correlation may allow greater confidence in the results.
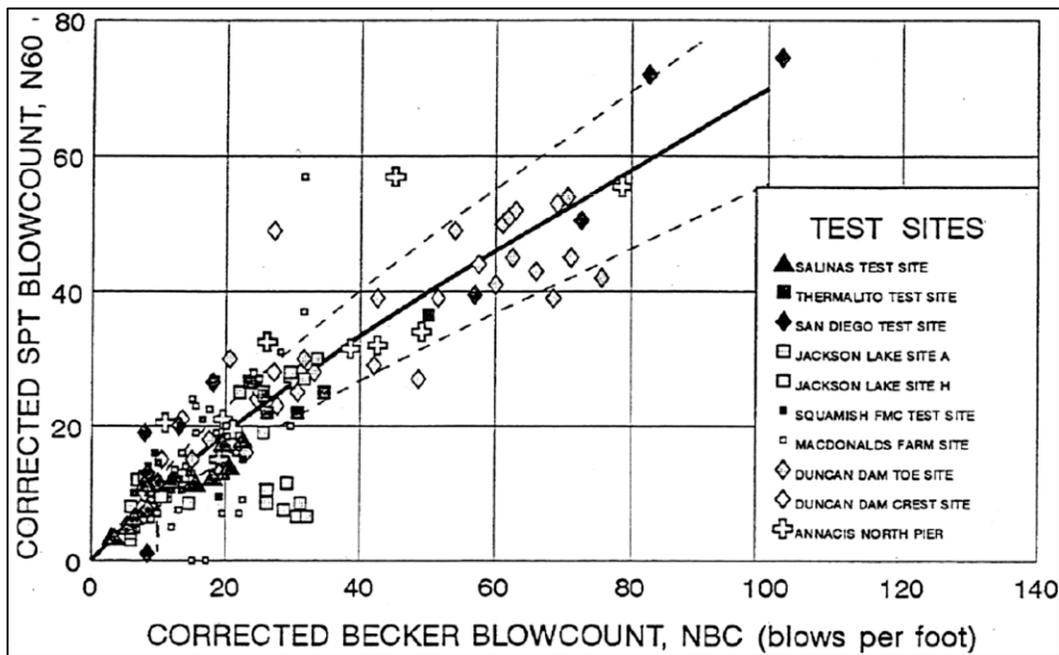
Figure D3. Correlation to estimate SPT blow count from corrected Becker blow count by Harder-Seed method [2].

If a B-180 or HAV-180 rig is used, instead of the AP-1000, the N_{BC} data would be adjusted by multiplying by the factor 1.5 to account for the difference in energy transmitted to the rods; however, this factor is supported by very few data, and it is better to avoid the whole issue by requiring the use of an AP-1000 rig. (The other two methods, Sy-Campanella and iBPT, should not be affected by the choice of rigs because the energy transmitted to the drill string is measured.)

The initial work by Harder and Seed [1] was based on comparison of SPT and
BPT testing at several sand sites in California, plus two gravelly sites in Denver,
Colorado, and at Mackay Dam in Idaho. The underlying assumption is that the
correlation developed for sands (where valid SPT results can be obtained) can be
used to predict the SPT blow count that would be obtained in gravel, if not for the
effect of the large particles interfering with penetration of the sampler. Even the
Becker blow count can be affected by cobbles or large amounts of coarse gravel
(larger than 1.5 inches in diameter). This, of course, introduces an additional
amount of uncertainty into the methods. Regardless of which method is used,
Becker data in deposits with numerous cobbles and boulders can greatly
overestimate the equivalent SPT N_{60} and liquefaction resistance. Therefore, it is
essential to have good stratigraphic information along with the penetration testing.

D.4.2 Implementation

The Harder-Seed method of interpreting BPT data is as follows:

1. Record the number of blows to drive BPT rods each foot of depth (N_B)
    and bounce-chamber pressure during that interval. Record driving
    conditions, and make note any time the drillers pull the rods back to
    loosen them up to reduce the driving friction, or to measure pullback
    friction for the Sy-Campanella method. It is not clear how much pulling
    and redriving would affect the blow counts, but they could be
    unrealistically low until the tip is actually past the previous maximum
    depth by some small amount. (Hence, it is necessary to track the amount
    of pullout and redriving very carefully.)

2. If, and only if, the Becker drill rig was model B-180 or HAV-180,
    multiply N_B by 1.5. (As discussed above, it is greatly preferable to avoid
    this question by requiring an AP-1000 rig.)

3. Adjust measured bounce-chamber pressure to sea-level conditions
    according to:

    $$BP_{SL} = BP (1 + 0.00003 \ A) + 0.00043 \ A \qquad \text{Equation D1}$$

    where A is the altitude in feet, and BP is the bounce-chamber pressure in
    pounds per square inch (lb/in^2) (gauge pressure). This formula is based on
    very limited data presented in reference [1], and it should be regarded as
    approximate. For elevations below 1,000 feet, this adjustment can be
    ignored.

4. On figure D2, locate the point where the coordinates are N_B and adjusted
    bounce-chamber pressure BP_{SL}. From that point, follow a path along or
    parallel to the nearest of the blow count correction curves to line A-A, the

Constant Combustion Condition Rating Curve. The value of N_B, where the path meets line A-A, is referred to as the corrected Becker blow count N_{BC}.

5. Enter figure D3 with the value of N_{BC}, and find the corresponding value of N_{60}, which is the estimated SPT blow count adjusted to the standard SPT hammer energy ratio of 60 percent, but without any adjustments for overburden or fines content.

6. Use the Becker-equivalent N_{60} in place of SPT N_{60}, as described in appendix C of this design standard for determining liquefaction potential, and in appendix F for estimating post-liquefaction shear strength.

This procedure can be implemented in a spreadsheet, using look-up tables in place of figures D2 and D3.

D.5 Sy-Campanella Method of BPT Interpretation

D.5.1 Description

The second method, proposed by Sy and Campanella [3], is more rigorous theoretically, although it is also more costly and time-consuming to implement because additional analysis is needed. Recognizing that friction on the rods may contribute a substantial portion of the driving resistance (unlike with SPTs, which-take place in a mudded hole), Sy and Campanella proposed using a Pile Dynamics, Inc., PDA to estimate rod (shaft) friction and hammer energy. For each blow, the PDA records force and acceleration at the top of the drill string as a function of time. From these, it calculates the energy each blow transmits to the drill string (referred to as ENTHRU). The PDA measurement of ENTHRU reduces concern about the performance of the hammer, effects of altitude, or loss of energy between the hammer and the rods. The recorded force and acceleration histories for selected blows are also analyzed using the computer program CAPWAP (Case Pile Wave Analysis Program) [9], which (among other things) separates the driving resistance contributed by the bearing capacity of the tip and by the side friction, R_S. (Like the PDA, CAPWAP was originally developed for analysis of driven piles.)

Sy and Campanella had SPT and BPT soundings performed adjacent to each other at several sites, with PDA measurements for the BPT. This allowed them to account for the amount of energy that would reach the tip of the drill string, rather than being lost to friction. They then developed a family of curves relating energy-adjusted SPT blow counts, N_{60}, to energy-adjusted BPT blow counts,

N_{B30},(which they actually called "N_{b30}"), explicitly accounting for the energy lost to friction. This is shown in figure D4, from Sy and Campanella [3]. Knowing BPT blow count, driving energy, and rod friction, one can use figure D4 to find the equivalent value of N_{60} that would have been measured without any effect from gravel interfering with SPT penetration. In addition to CAPWAP, friction can also be measured by pulling the rods out of the ground several feet, with a short instrumented section of drill rod that acts as a load cell.
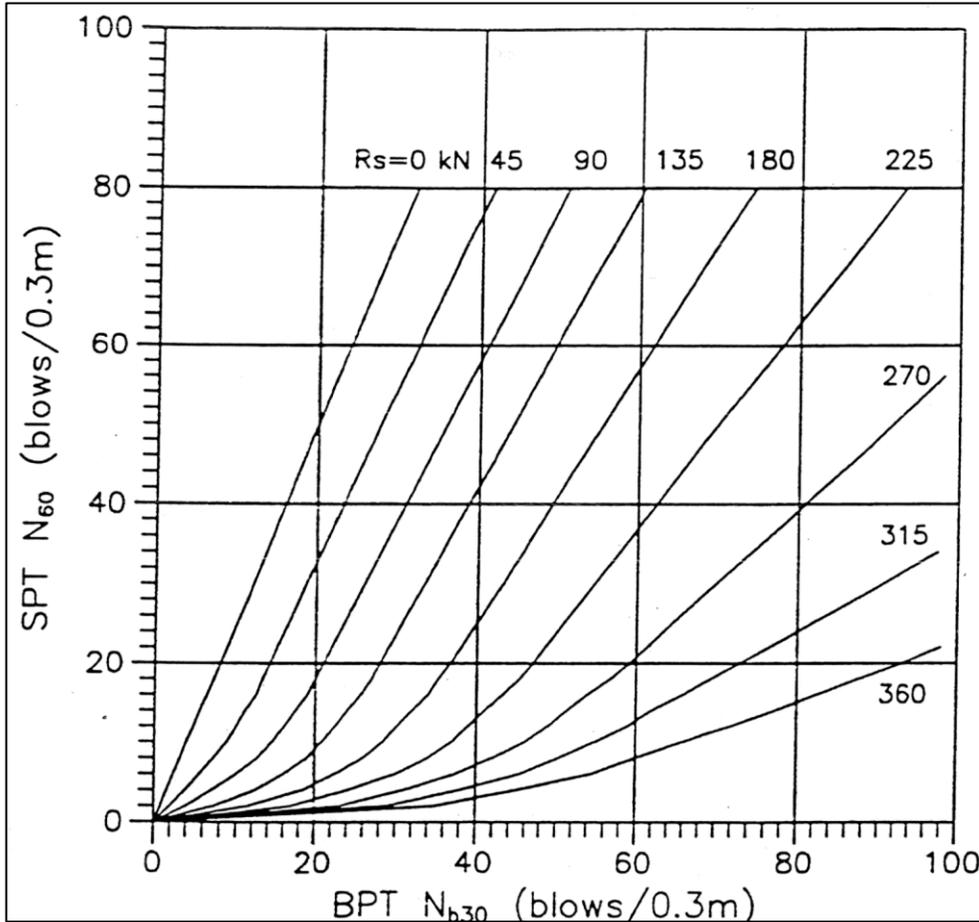
Figure D4. Chart for estimating equivalent SPT N_{60} from energy-adjusted Becker blow count [3].

At present (2015), Reclamation does not have a PDA or CAPWAP, so a contractor performs those analyses. As a consequence, the results may not be available immediately, and it is typical practice to use the Harder-Seed method to provide a "preview" to help in selecting the depths for CAPWAP analyses, as well as to provide a check on the reasonableness of the Sy-Campanella results.

In practice, two or more blows at different depths are selected from each BPT sounding for CAPWAP analysis. With interpolation, these yield a profile of side friction, R_S, *versus* depth. The equivalent SPT N_{60} is then estimated by the use of figure D4, from Sy and Campanella [3]. The figure contains a family of curves, each one corresponding to a different value of side friction. One simply enters the plot with the calculated N_{B30} and reads the equivalent SPT N_{60} from the applicable curve, interpolating between curves as required. The curves are labeled with side friction in kiloNewtons (kN). (1 kN = 225 lb).

The CAPWAP analyses should, at least in theory, eliminate concern about the effects of varying amounts of side friction on the blow count (although measuring the energy at the tip, as in the iBPT, greatly reduces the uncertainty in the energy). The primary drawback to Sy and Campanella's analysis is the need for PDA measurements and CAPWAP analyses. These substantially increase the cost of the testing program and slow the process of testing and interpretation, relative to the Harder Seed method. Also, the CAPWAP solution is not unique, and three different users could find three different friction values.

In addition to PDA analysis to determine the rod friction, it has become common practice to use a load cell to measure the force required to pull the rods periodically. Sy [10] suggests using the PDA to develop a site-specific correlation to estimate hammer energy from the bounce-chamber pressure, and then measuring the pullback force periodically. This allows the method to be used without actual PDA measurements and CAPWAP analyses for the remaining holes, but one must assume that the dynamic resistance as calculated by CAPWAP and the static pullback friction are equivalent. This is not exactly correct, and the assumption would introduce additional uncertainty into the predicted SPT blow counts.

D.5.2 Implementation

The Sy-Campanella method may be summarized as follows:

1. Record the number of blows, N_B, for each 1-foot interval of BPT driving. During driving, the PDA records time histories of force and acceleration for each blow, and calculates, among other things, the energy transferred to the drill string for each blow, referred to as ENTHRU. (The PDA is generally provided and operated by a consultant, working as a subcontractor of the driller to simplify the contracting process.) Also, record driving conditions and make note of any times the drillers pull the rods back to loosen them up to reduce the driving friction, or to measure pullback friction.

2. Adjust N_B to the standard driving energy, which is 30 percent of the ICE 180 hammer's rated energy of 8,100 foot-pounds (ft-lb), or 2,430 ft-lb, to

obtain N_{B30} (equation D2). This is analogous to adjusting SPT blow counts to 60 percent of the theoretical maximum to obtain N_{60}.

$$N_{B30} = N_B * ENTHRU / (0.3 \times 2{,}430 \text{ ft-lb}) \qquad \text{Equation D2}$$

3. Plot the pullback friction measurements (if any) as a function of tip depth. (This profile is the cumulative friction force from the surface to the tip, not the friction per unit area or unit length of rod.) Based on trends in these results and the depths with low blow counts, select tip depths for CAPWAP analyses. The depths should be selected considering the need to interpolate between CAPWAP values. Ideally, there would be one at the top of layer of interest and another at the bottom; in a very thick layer, there could also be one in the middle. Depths for CAPWAP tests should be at least 1 to 2 ft below the depth of a pullback test, to minimize any effects of disturbance caused by reversing the direction of movement of the drill string. The consultant will then select individual blows for CAPWAP analysis. CAPWAP analyses are labor intensive and fairly expensive, so there may be a practical limit to how many can be done in a BPT testing program.

4. Add the CAPWAP results to the plot of pullback friction measurements to obtain a profile of rod friction versus depth. If there are significant discrepancies between the two types of measurement, resolving them should include careful study of stratigraphy and the force-displacement behavior of the drill string during the pullback test. In resolving discrepancies, it **may** be appropriate to favor the CAPWAP results, in part because the Sy-Campanella method was developed using CAPWAP friction values. The pullback friction is not necessarily equal to the friction in driving because of dynamic effects and the reversal of the direction of the drill string's movement. Note that the friction measurement does not always increase monotonically with depth.

5. For each 1-foot interval, estimate R_S from the friction profile to determine which curve (or interpolated curve) to use in figure D4, interpolating between curves as needed. Use figure D4 with the adjusted blow count, N_{B30}, to find the Becker equivalent, N_{60}. The labels on the curves are in kilonewtons (kN). Note also that if the assumed friction is overestimated, the equivalent SPT blow count will also be overestimated; the difference may be important in a liquefaction assessment.

6. Use the Becker-equivalent N_{60} in place of SPT N_{60}, as described in appendix C of this chapter for determining liquefaction potential, and in appendix F for estimating post-liquefaction shear strength. N_{60} is the estimated SPT blow count adjusted to the standard SPT hammer energy ratio of 60 percent before any adjustments for overburden or fines content.

As mentioned above, if a site requires a large number of BPT soundings, it may not be necessary to have PDA measurements and CAPWAP analyses for all of them [10]. A correlation can be developed between bounce-chamber pressure and hammer energy that is specific to the site conditions (elevation, soils materials) and the specific BPT rig being used (hammer and rig characteristics). (This should include varying the throttle setting to get a wide range of energies.) Rod friction in each sounding can be measured using pullback tests each time additional rods are added or at other selected intervals. This would, in theory, provide all of the information needed to use the Sy-Campanella method without the PDA, albeit with the introduction of additional uncertainty. Note that, in some areas of figure D4, relatively small changes in R_S cause large changes in the predicted N_{60}.

Unless absolutely necessary, pullbacks should only take place before and after critical layers, not within them, because of the potential to invalidate important data by disturbance or make it difficult to interpret the profile of shaft friction.

D.6   Instrumented BPT (iBPT)

As of 2015, the instrumented BPT (iBPT) has been considered the state of the art for interpreting Becker hammer penetration tests [4]. It bypasses the issue of measuring and accounting for the friction on the drill string by making the energy measurements at the tip of the drill string. The standard BPT closed-end bit is replaced by a special bit that is instrumented with accelerometers and force transducers. As in the Sy-Campanella method, the BPT blow count is normalized to N_{B30} by proportion with the energy, but it is the tip energy, not the input energy from the hammer. Instead of using a family of curves like figure. The equivalent value of N_{60} is then estimated by a simple ratio with N_{B30}.

$N_{60} = 1.8\ N_{B30}$ Equation D3

This equation is essentially equivalent to the curve for $R_S=0$ in figure D4, although the slopes do not match precisely.

Details of the analysis are not provided here because the computations would all be done by the persons performing the data acquisition during the BPT testing.

Because it is a newly developed procedure, refinements may occur while this version of *Design Standards No. 13 – Embankment Dams*, Chapter 13, "Seismic Analysis and Design," is in use at Reclamation. All raw data should be stored safely, so they can be reanalyzed at a later date if necessary.

As of 2015, iBPT measurements and analysis are available only through the University of California at Davis, where the method was developed. This means that BPT field programs need to be scheduled far in advance.

D.7   Discussion of Methods

Several comparisons have been made between the Harder-Seed and Sy-Campanella approaches [3, 11, 14]. Figure D5 (from Sy, Campanella, and Stewart [11]) shows typical comparisons. As would be expected, the Sy-Campanella method tends to distinguish the high and low blow count zones better than the Harder-Seed method, which can mask these layers if the side friction is high [6, 11]. This is consistent with Reclamation's experience at Bradbury Dam and other sites.
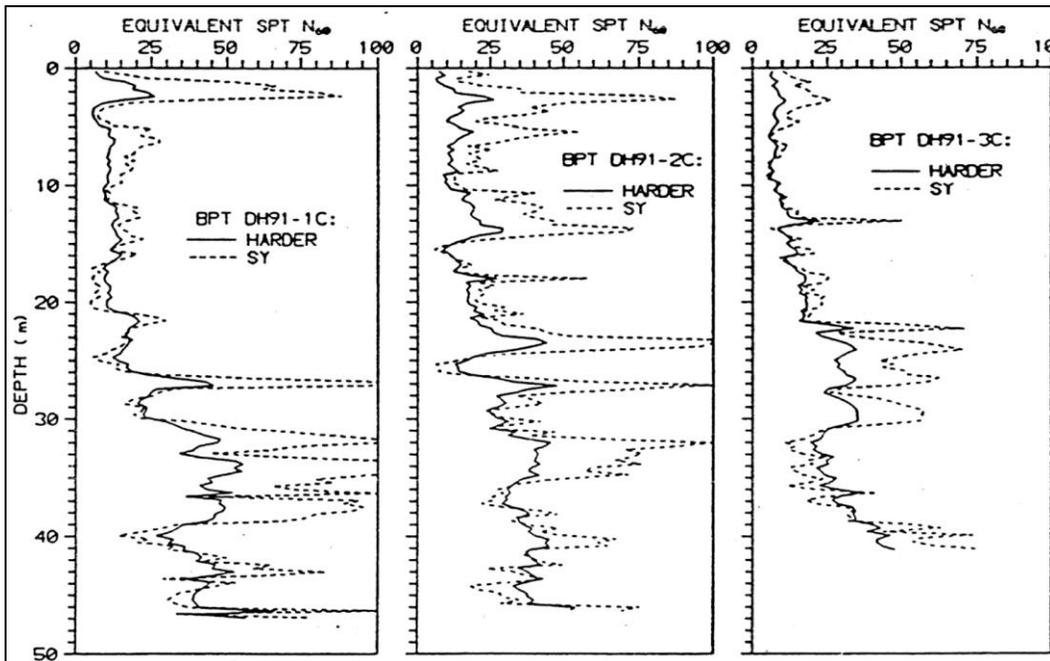

Figure D5. Comparison of predicted SPT N_{60} from different methods [11].

Lum and Yan [14] point out that the Harder-Seed method implicitly includes the effect of friction in the correlation. The friction is, in effect, a function only of the adjusted blow count, N_{BC}, and there is no way to explicitly account for variation in friction for a given blow count. The Harder-Seed correlation was developed from data at sites where the materials showed density generally increasing with depth. At a site where it is necessary to test looser alluvium below rolled embankment fill or dense alluvium, the actual friction may be substantially higher

than the implicit value. This would cause the correlation to overpredict the equivalent SPT blow count. At Terzaghi Dam, the Harder-Seed method consistently and markedly underpredicted the penetration resistance relative to the Sy-Campanella method in holes with high blow counts [11]. This resulted from unusually low rod friction, smaller than the friction implicit in the Harder-Seed method with high blow counts. Similarly, in denser materials at shallow depths, where there is little friction relative to the tip resistance, the Harder-Seed method could underpredict N_{60}. This apparently occurred at Reclamation's Deer Creek Dam in Utah, when shallow BPT soundings in the bottom of an excavation were used to determine whether it had to be made deeper [10]. One method indicated that the material left in place would be a problem, but the other did not. Sy concluded that the difference occurred because the material at the tip of the BPT was dense and gave fairly high blow counts at modest depths where there was not very much shaft friction.

In situations where shaft friction is likely to be high, such as driving through compacted fill overlying the material of concern, or in very deep deposits, the Sy-Campanella method is believed to be better at distinguishing low-density layers. Where very high resistance is expected, overlying material is sometimes predrilled to make it easier to reach the layer of concern. This can be done by drilling a hole with another rig and installing casing or backfilling with sand or pea gravel, or else predriving the BPT through the dense layers with an open bit and compressed air to remove the cuttings, pulling the drill string out, and replacing the open bit with a closed bit for the testing. The drillers may also pull the drill string up a few feet to loosen the adjacent material and then resume driving. These measures would not invalidate the Sy-Campanella analysis, because it uses using actual rod friction values determined from CAPWAP or pullback tests (once the tip is below the predrilled interval). However, the friction in predrilled holes or soundings driven through dense embankment fill may not be similar enough to that at the sites from which the Harder-Seed method was developed. If the friction is too high relative to those sites, N_{60} would be overpredicted, and the reverse would occur if the friction is too low. For example, the Harder-Seed analysis may not have produced reliable predictions of equivalent N_{60} for predrilled and cased BPT borings at Mormon Island Auxiliary Dam and Casitas Dam because of the essentially nonexistent friction [12, 13]. It is better to simply avoid the question of "too much" or "too little" friction by requiring iBPT or, at minimum, PDA measurements at every site.

As stated previously, it is recommended that the iBPT be used for high-hazard dams, and the PDA measurements and Sy-Campanella method should be used if the iBPT is not available. If a BPT rig is to be mobilized to a site, the additional cost of iBPT or PDA testing is not excessive, compared to the other costs of the investigation. It may not be necessary to have the PDA or iBPT onsite for every single BPT sounding. Once a number of instrumented soundings have been done, it may be possible to establish a site-specific correlation between bounce-chamber pressure and hammer energy. With that, and enough pullback

tests for the shaft friction, the Sy-Campanella method should be valid, albeit with greater uncertainty. At some sites, the Seed-Harder method may provide results that are similar enough to the iBPT or Sy-Campanella results that they can be used for the remaining soundings, provided that the overlying stratigraphy and shaft friction are similar. One could not, for example, use close agreement at the toe of an embankment to conclude that they would agree well under 100 feet of compacted fill. Pullback tests would still be required to verify that the shaft friction is similar among holes.

Sy and Campanella, Lum and Yan, and other investigations have reported success in interpreting data at alluvial soil sites by the Sy-Campanella method. However, Reclamation has had mixed experience with it to date. At some sites, agreement between Sy-Campanella method Becker-equivalent $(N_1)_{60}$ values and those from actual SPTs has been excellent, but at others, it has not. At Bradbury Dam, BPT was performed through the compacted embankment [6]. As would be expected, the Sy-Campanella method was generally more sensitive in distinguishing layers of loose material; however, some of the interpreted $(N_1)_{60}$ values were suspect because of an unrealistic friction value from CAPWAP. (This should serve as a reminder that any analytical result by Reclamation or external consultants needs to be treated with skepticism!)

The user of any method needs to be aware that substantial uncertainties exist both in the correlations to estimate the equivalent SPT N_{60}, and in the correlations to estimate soil behavior from the SPT blow count. Those uncertainties must be accounted for in dam-safety decision making, whether by an appropriate level of conservatism in deterministic analysis, or by allowing for a range of results in a probabilistic risk analysis.

D.8   Becker Drilling Programs

Testing dam foundations for liquefaction potential may require drilling well over 100 feet deep. The Becker drill rig is not ideally suited for this because a large depth of alluvium or compacted embankment fill can make it difficult and time-consuming to drive the BPT to the required depth. For this reason, Reclamation and others have occasionally predrilled holes with a larger diameter, to a few feet above the depths of greatest interest, using conventional drilling equipment or sonic drills. The hole generally needs to be cased or backfilled with loose pea gravel material, so that it will remain open. The Becker rig itself can be used to predrill, using an open bit and compressed air to lift the cuttings out of the hole (instead of the closed bit used for the actual penetration test). This would not eliminate the friction, the way predrilling and installing casing would, because the hole diameter created by predrilling is the same as the rod diameter, but it would greatly reduce the friction. **Drilling with compressed air must not occur in an embankment core or other location where cracking caused by compressed**

air could affect the safety of the dam. Reclamation generally does not allow
drilling with compressed air or foam in any part of an embankment, except
in specific circumstances with minimal potential for damage.

In most cases, BPT holes in dam embankments need to be backfilled with suitable
materials. If the iBPT instrumented tip has not been used, this can be done by
grouting through the BPT rods as they are pulled out. The "closed bit" can
actually be an open bit with a steel plug that can be knocked out and left in the
ground when the rods are pulled. In some cases, it may be more appropriate to
backfill with coarse sand or pea gravel because of concern about contaminating a
drain or filter zone with the grout. With the iBPT, it is not possible to backfill or
grout without completely removing the casing from the ground. If the hole is not
expected to remain stable long enough to grout it or backfill it, open BPT casing
can be driven into the hole to reopen it. It would then be retracted as the
backfilling or grouting progresses. This, of course, requires very careful attention
to any effect it might have on the safety of the dam, from leaving a hole open
temporarily or from suction created when the iBPT is withdrawn.

The Becker drill rig is quite large and heavy, so access can be problematic. The
capacity of any bridges that the rig has to cross should be checked, including
spillway bridges. Roads constructed for drilling may need to be wider than for a
typical soil drilling rig, and it may be necessary to make turns in the road more
gradual for the longer wheel base.

Reclamation does not have in-house capability for performing Becker drilling,
PDA measurements, CAPWAP analysis, or iBPT, so they must be contracted.
For the Sy-Campanella method, this process is made somewhat easier if the
consultant to do the PDA and CAPWAP work is hired as a subcontractor to the
drilling company, rather than being contracted directly by Reclamation. That
simplifies dealing with changes in schedule, unanticipated additional holes, etc.
Contracts should be explicit about which party will have responsibilities for
logging blow counts, recording bounce-chamber pressures, preparing final logs,
etc.

During testing, Reclamation should have either an engineer or a geologist on site
to record blow counts and bounce-chamber pressures, and to be sure that all other
pertinent details are documented. The field notes for each hole should include
any depth where pullback friction is measured, as well as any time the drillers pull
back the rods to reduce the friction; blow counts from redriving back to the
previous maximum depth are not valid, because the tip is pushing through the
void left by pulling back. (The same applies to blow counts in predrilled
sections.) The engineer or geologist will also be involved in decisions about
depths for pullback tests, adjusting the locations of BPT soundings, termination
depths, etc.

Reclamation's personnel on the site should have access to geologic cross sections and previous drill logs to help them decide where the pullback tests should occur. This should be discussed with the drillers prior to each hole, but all parties should be alert for unexpected conditions that would indicate a change in plans is needed.

Any BPT program should include soundings close to SPT borings, so that direct, site-specific comparisons can be made in materials that are fine enough for the SPT to produce valid results.

D.9   References

[1]   *Determination of Penetration Resistance for Coarse-Grained Soils Using the Becker Hammer Drill*, Report No. UCB/EERC-86-06, NTIS PB87 124210, L.F. Harder, Jr., and H.B. Seed, Earthquake Engineering Research Center, College of Engineering, University of California, Berkeley, California, May 1986.

[2]   "Application of the Becker Penetration Test for Evaluating the Liquefaction Potential of Gravelly Soils," L.F. Harder, Jr., Earthquake Engineering Research Center, College of Engineering, University of California, Berkeley, California, *January 4-5, 1996 NCEER Workshop on Evaluation of Liquefaction Resistance,* Salt Lake City, Utah, 1997.

[3]   "Becker and Standard Penetration Tests (BPT-SPT) Correlations with Consideration of Casing Friction," A. Sy and R.G. Campanella, *Canadian Geotechnical Journal,* 31(3): 343-356, 1994.

[4]   "Instrumented Becker Penetration Test for Improved Characterization of Gravelly Deposits," Mason Ghafghazi, Aravinthan Thururaijah, Jason T. DeJong, Daniel W. Wilson, and Richard Armstrong, *Proceedings, GeoCongress 2014,* American Society of Civil Engineers Geotechnical Special Publication No. 234, Atlanta, Georgia, pp. 37-46, 2014.

[5]   "Geotechnical Advances in BC Hydro's Dam Safety Program," K.Y. Lum, and S.J. Garner, *Proceedings, 49th Canadian Geotechnical Conference,* Vancouver BC, Canada, 2006.

[6]   "Liquefaction Potential and Post-Earthquake Stability, Bradbury Dam," Technical Memorandum No. BD-8313-2, Bureau of Reclamation, Technical Service Center, Denver, Colorado, 1995.

[7]   *Becker Drill Automated Data Recorder - Operations Manual*, J. Rosenfield, Becker Drill Study Team, Bureau of Reclamation, Technical Service Center, Structural Behavior and Instrumentation Group, Denver, Colorado, June 1995.

[8]   "Correlations of Mud Injection Becker and Standard Penetration Tests," A. Sy, and K.Y. Lum, *Canadian Geotechnical Journal*, Vol. 34, No. 1, pp. 139-144, 1997.

[9]   "Dynamic Determination of Pile Capacity," F. Rausche, G.G. Goble, and G.E. Likins, Jr., *Journal of Geotechnical Engineering*, American Society of Civil Engineers, Vol. 111, No. 3, pp. 367-383, 1985.

[10] "Deer Creek Dam, Utah, Review of Becker Blow Count Data," letter report prepared by A. Sy, Klohn Crippen, Ltd., Vancouver, BC, Canada, for Joe Prizio, Bureau of Reclamation, Technical Service Center, Denver, Colorado, 2005.

[11] "BPT-SPT Correlations for Evaluation of Liquefaction Resistance of Gravelly Soils," A. Sy, R.G. Campanella, and R.A. Stewart, *Static and Dynamic Properties of Gravelly Soils,* American Society of Civil Engineers, Special Publication 56, New York, New York, 1995.

[12] "Evaluation of Becker Hammer Soundings Performed at Mormon Island Auxiliary Dam in Conjunction with Upstream Remediation," prepared by L.F. Harder, Jr., Earthquake Engineering Research Center, College of Engineering, University of California, Berkeley, California, for the U.S. Army Corps of Engineers, Sacramento District, Sacramento, California, 1993.

[13] "Preliminary Evaluation of Becker Soundings Performed at Casitas Dam," prepared by L.F. Harder, Jr., Earthquake Engineering Research Center, College of Engineering, University of California, Berkeley, California, for Bureau of Reclamation, 1997.

[14] "In-Situ Measurements of Dynamic Properties and Liquefaction Resistances of Gravelly Soils at Keenleyside Dam," K.Y. Lum, and L. Yan, *Ground Failures Under Seismic Conditions*, American Society of Civil Engineers, Special Publication No. 44, pp. 221-240, 1994.

Appendix E

Assessment of Liquefaction Potential by Shear-Wave Velocity

Contents

Figures

# Tables

E.1   Introduction

Both liquefaction resistance and shear stiffness tend to increase with the density of a granular soil. One would expect, therefore, that liquefaction resistance would correlate (at least somewhat) with the shear-wave velocity, V_S, which is an indirect measure of the shear stiffness. In fact, Dobry and Abdoun [1] argue that this is precisely why liquefaction-resistance charts based on penetration resistance work at all; the higher stiffness of denser material makes it less likely for the soil to reach a critical shear *strain* for liquefaction to occur. Numerous studies have found such a correlation to exist and to be useful for assessing liquefaction potential [2, 3, 4, 5, 6, 7, 8, 9]. Relationships for estimating the probability of liquefaction from V_S have been published by Juang et al. [9] and Kayen et al. [8]. For dams, V_S is of greatest value where gravel and cobbles interfere with the Standard Penetration Test (SPT) and Cone Penetrometer Test (CPT) measurements. Measurements of V_S are often needed for ground response analysis, and it makes sense to take advantage of those same measurements for assessing liquefaction potential when it is practical, regardless of material gradation. However, the data requirements for the response and liquefaction analyses are very different, and it is not always practical to do so.

E.2   Measurement of Shear Wave Velocity, V_S

The preferred method for measuring shear-wave velocities is the cross-hole method, with one drill hole for the source and two drill holes with a receiver in each (depicted in figure E1). It is possible to do this test with two holes (one for the source and one for the receiver), but two receivers are the standard for Bureau of Reclamation (Reclamation) dams. Using two receivers allows better distinction between arrivals of direct waves (traveling horizontally through the same stratum from source to receiver), and arrivals of refracted waves (refracted into higher-velocity materials above or below the interval being tested, and able to "outrun" the direct wave). The resolution of cross-hole testing is good, allowing measurement in layers as thin as 2 feet [10]. Drill holes can deviate significantly from vertical; each hole should be surveyed, so that the actual distances between casings are known at every depth.

The down-hole method is less expensive to implement than cross-hole testing because it requires only one drill hole. The receiver is lowered into a drill hole, and the source is kept at the surface. The source is often a heavy wooden plank held tightly to the surface by the weight of a vehicle, and struck with a sledge hammer to create a shear wave. Down-hole testing is less precise than cross-hole testing because the wave path is longer, and it may traverse layers with very different V_S values and, possibly, multiple paths. It is also more likely to miss detecting a thinner low-V_S layer. The down-hole method is considered

acceptable; however, it is recommended for use only when cross-hole testing and other preferred methods (described below) are not practicable for reasons of site access, geology, scheduling, or cost.
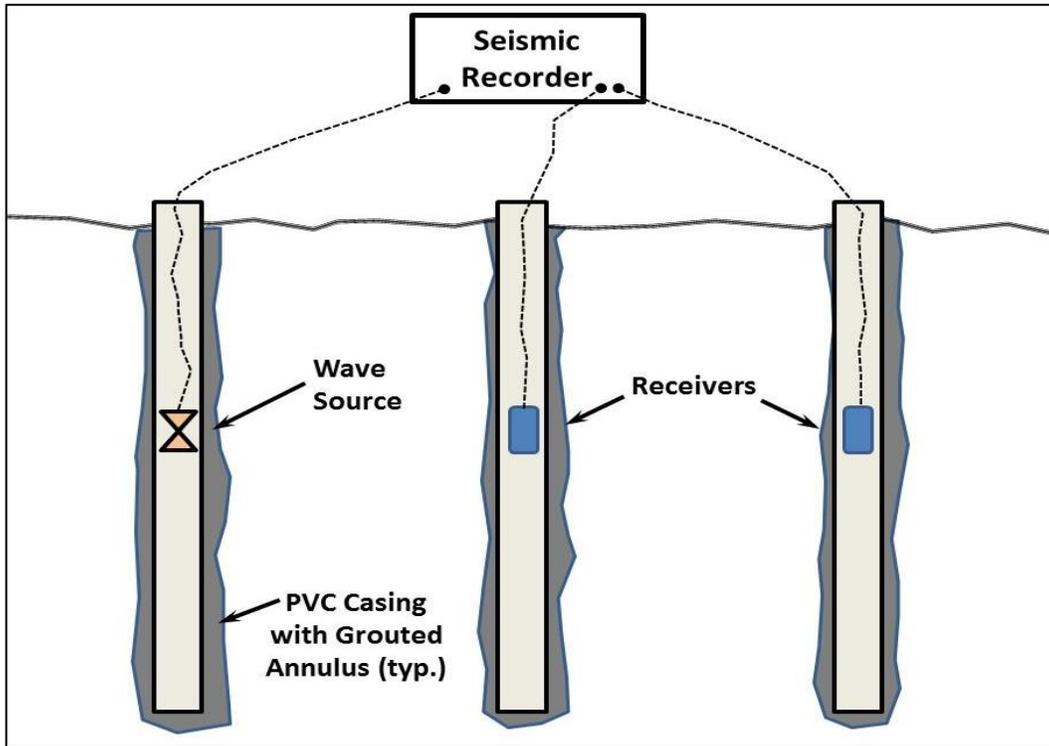
Figure E1. Cross-hole setup for measuring shear-wave velocity *in situ*.

The Seismic Cone Penetrometer Test (SCPT) is essentially a down-hole test, except that the receiver is incorporated into a cone penetrometer, instead of lowered down a drill hole. At selected depths, pushing of the cone is stopped briefly, while a wave is generated at the surface, commonly with a plank and a sledge hammer. In soils that are suitable for the cone penetrometer, this allows rapid, inexpensive data collection with no drilling required, and plots showing both CPT results and V_S on the same plot are generated automatically for comparison. This can be a very useful method, but it is desirable to have some cross-hole tests adjacent to SCPT soundings for verification at any site.

Multichannel Analysis of Surface Waves (MASW) is a surface method that has the advantage that drilling is not required [7, 11]. It uses an array of geophones along the ground surface and an energy source, such as a sledge hammer. Rayleigh waves recorded by the receivers are "inverted" to find the combination of depth, thickness, and shear-wave velocity of soil layers that make the motions predicted by response analysis match the recorded motions. Inherent in the analysis is the assumption that the layering is horizontal and uniform over a large

area; the length of the array needs to be at least four times the depth of testing. As a result, there are many sites where MASW is not usable. It is feasible to detect thin soft layers below stiff layers, but the resolution is not as good as with cross-hole measurements. An earlier method, Spectral Analysis of Surface Waves (SASW), uses a single receiver placed at varying distances from the source, which can be a sledge hammer or a vibrating shaker [12]. Typically, there are 6 shots in each direction, for a total of 12 shots. SASW is slower and more labor-intensive in the field because the source and receiver need to be moved after each shot. SASW also more difficulties with nonunique inversion solutions than MASW does, and it is more sensitive to noise from background vibrations [13]. SASW has generally been superseded in practice by MASW.

One newer development is a down-hole tool called the suspension logger, which can provide a high-quality V_S profile with a single fluid-filled drill hole [14]. It consists of a P-wave source and two sensors on a probe that is suspended in the drill hole (usually uncased) at the depths of interest. P-waves transmitted to the walls of the hole by the fluid are converted into S-waves that travel upward through the soil, generating P-waves within the fluid, which are then detected by the sensors. (Strictly speaking, these are Stonely waves, rather than S-waves, but the velocities of the two types are very similar.) In comparison with the down-hole test, it has better resolution and can be used at greater depths. Its vertical resolution is roughly 1 foot. Testing occurs in an uncased hole, supported by drill fluid, weighted if needed. Uncased drill holes in soil are vulnerable to collapse, particularly in the coarse-grained alluvial and glacial soils common at many Reclamation dam sites, so there is some risk of the hole collapsing and trapping the probe. The suspension logger is commonly used in stages as the drill casing is removed from the hole, retracting the casing to expose only as much of the soil as necessary for each V_S measurement. This reduces the risk of a damaged or lost probe, but the risk is not completely eliminated.

The selection of the V_S test method(s) for a particular site depends on the required accuracy and resolution of the measurements, whether a method is well suited to the site's geology, and the cost. In general, cross-hole measurement with three drill holes provides the best accuracy and resolution, followed by MASW and the suspension logger. Down-hole testing is less desirable, but SCPT down-hole testing can be very fast and economical, and it should be considered for any site where a CPT rig is to be used for other purposes.

Drill holes for V_S measurements need to be deep enough to allow the full length of the instruments to be lowered several feet below the depth of interest, plus an additional 2 feet at the bottom of each hole for sloughed material. For cross-hole testing, the holes should go 10 feet past the range of interest. With the suspension logger, the required depth of the hole depends on the design of the instrument. At present, Reclamation has a suspension logger that only requires 10 feet. If a contractor with another make and model may be doing the testing, the hole would need to extend as much as 33 feet past the depth of interest.

E.3 Determination of Liquefaction Potential

E.3.1 Normalizing V_S for Overburden Stress

The shear-wave velocity is a function of the shear stiffness and the mass density of the material:

$$V_S = (G/\rho)^{1/2} \hspace{4cm} \text{Equation E1}$$

where:

G = the shear modulus, and
ρ = the mass density (in slugs per cubic foot, kilograms per cubic meter, or other units consistent with the units of G).

(The density referred to is the total density, including the mass of the pore water.) For a soil at a given density, the shear modulus G varies approximately with the square root of the effective confining stress. Therefore, for a soil at a given relative density, the shear-wave velocity varies approximately with the fourth root of the confining stress. To allow direct comparison of shear-wave velocities measured at different overburden pressures, current practice is to normalize the velocity measured *in situ* to a reference effective overburden stress of 1 atmosphere (atm) (2,116 pounds per square foot [lb/ft^2]) analogous to normalizing standard penetration test blow counts to $(N_1)_{60}$. The normalized velocity is given by:

$$V_{S1} = V_{S\text{-measured}} * (1 \text{ atm} / \sigma_v')^{1/4} \hspace{3cm} \text{Equation E2}$$

(Older V_S analyses may normalize to an effective overburden stress of 1 ton per square foot, 2000 lb/ft^2, instead of 1 atm; in equation E2, the difference is inconsequential.)

Normalization of V_S simplifies comparison of velocities measured in the soil being studied with those measured at sites that have been subjected to large earthquakes, in order to predict the behavior of soil in an earthquake. For heavily overconsolidated materials, where K_0 can be substantially higher than 0.5, it may be necessary to use a different form of this equation [7].

(Shear-wave velocities are *not* normalized for other purposes, such as dynamic response analysis.)

E.3.2 Model for Estimating Cyclic Resistance and Liquefaction Probability

A number of empirical relationships have been developed to provide the Cyclic Resistance Ratio (CRR) as a function of V_{S1}, or the probability of liquefaction as a function of Cyclic Stress Ratio (CSR) and V_{S1}. Andrus et al. [3] have also developed a relationship for liquefaction potential based on peak ground-surface acceleration, instead of CSR. However, CSR is preferred because it more directly indicates the stress and strain the soil stratum experiences.) The model by Kayen et al. [8] provides both probability and CRR. It has been adopted for chapter 13 because it is based on a much larger data set than any previous study, and it lends itself well to probabilistic risk analysis, as well as deterministic use. (It may, however, be superseded as new data become available and the profession's understanding of liquefaction improves. The user of this chapter should be alert to such advancements and incorporate them into practice as appropriate.)

The Kayen et al. model is shown in simplified form in figure E2 from reference [8]. It shows contours of equal liquefaction probability as functions of normalized cyclic shear stress and shear-wave velocity. The quantity on the vertical axis, CSR*, is quite similar to what is called $CSR_{M=7.5,\sigma'=1}$ elsewhere in chapter 13 It is the CSR adjusted to the reference conditions, which are effective overburden stress equal to 100 kiloPascals (kPa) $\approx$ 1 atm, earthquake magnitude M_W equal to 7.5, and level ground, as defined in equation E3 below. The CRR for the reference conditions, CRR*, corresponds to the curve marked "15%" for liquefaction probability; it is also given by equation E4

$$CSR^* \approx CSR_{M=7.5,\sigma'=1} = 0.65\ \tau_{max}/\sigma_{vo}' / (MSF\ K_\alpha\ K_\sigma) \qquad\qquad \text{Equation E3}$$

$$CRR^* \approx \exp[(V_{S1}^{2.8011} / 1.88 \times 10^6) - 2.943)] \qquad\qquad \text{Equation E4}$$

CSR* and $CSR_{7.5,\sigma v'=1}$ are not exactly interchangeable. For CSR*, Kayen et al. used different Magnitude Scaling Factors (MSF) and K_σ relationships, so their notation is used here to distinguish it from $CSR_{7.5,\sigma v'=1}$ calculated with the Idriss and Boulanger [15] curves. However, the numerical difference between them is usually fairly small, so usually, little error would be introduced by using them interchangeably in forward analysis. Kayen et al. did not actually include K_α in the calculation of CSR* because all of their back-analyzed case histories, and most forward analyses (excluding dams), involve flat ground. It was included in equation E3 because of the importance of K_α for embankment dams.

The simplification that was made for figure E2 and equation E4 is that the effect of varying fines content on cyclic resistance has not been included. For a given V_{S1}, there is a small increase in cyclic resistance with increasing fines content, from 5 percent up to about 35 percent. Figure E2 and equation E4 were based on an assumed fines content of 15 percent. Therefore, no adjustment is made to V_{S1}

for fines, the way SPT or CPT data would be adjusted. Kayen et al. found that the error created by that simplifying assumption is minor, so that 15 percent can be used as a default value if the correct fines content is not known. (For calculating liquefaction probability with the more complete model, fines content is included explicitly, as described below.)
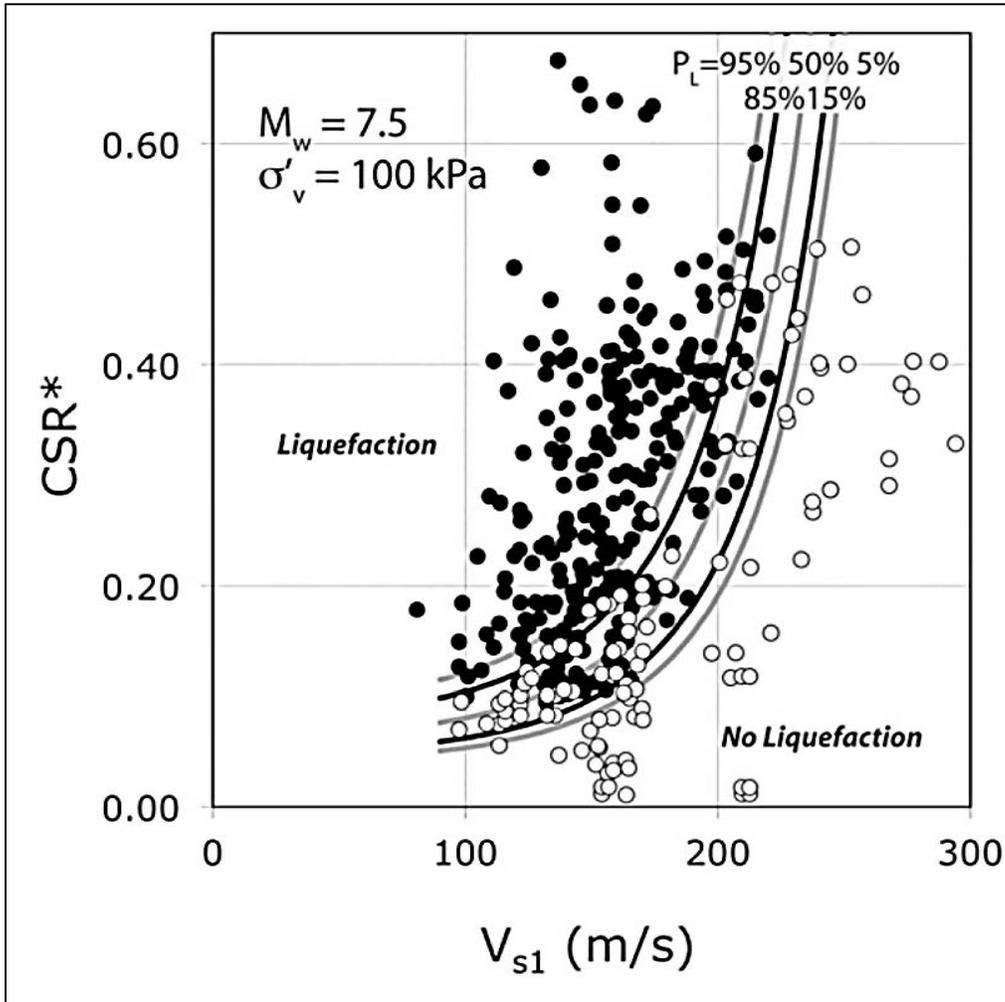

Figure E2. Liquefaction probability as a function of V_{S1} and adjusted cyclic stress ratio, CSR* [8].

Deterministic dam-safety analysis is generally no longer part of Reclamation practice, but the reader may need to understand older reports or work by others. In a typical deterministic liquefaction analysis, CSR* is compared with CRR*, with liquefaction considered unlikely if CRR* is greater. However, as conventionally defined, CRR* corresponds to liquefaction probability, P_L, of 15 percent, whether it is from SPT, CPT, or V_S. This much probability would generally not be accepted as "deterministic," so factors of safety are applied to

CRR*, depending on perceptions of uncertainties in the analysis and the consequences of liquefaction. Table E1 suggests safety factors, depending on the maximum acceptable probability of liquefaction for a particular application. For example, if P_L needs to be under 2 percent, a factor of safety of 1.3 would be needed. (These suggested values are based on Kayen et al.'s probability model, which is described below.)

Table E1. Required Factor of Safety to Achieve a Specified Value of P_L for Pseudo-Deterministic Analysis

Maximum Acceptable Probability of Liquefaction (percent)	Required Factor of Safety Applied to CRR* (equation E4)
15	1.0
5	1.2
2	1.3
1	1.4

The probability of liquefaction for a particular stratum can be estimated using equation E5 in a spreadsheet (preferred), or figure E2.

$$P_L = \Phi \left\{ -\frac{\left[(0.0073 \cdot V_{S1})^{2.8011} - 1.946 \cdot \ln(CSR) - 2.6168 \cdot \ln(M_w) - 0.0099 \cdot \ln(\sigma'_{vo}) + 0.0028(FC) \right]}{0.4809} \right\}$$

Equation E5

The function $\Phi[x]$ is the standard normal distribution of x, which is available in the spreadsheet program Microsoft Excel (the function NORMDIST with mean equal to zero and standard deviation equal to 1). The vertical effective overburden stress, σ'_{vo}, is expressed in kPa (1 kPa = 20.89 lb/ft^2).

Equation E5 explicitly includes the effects of earthquake duration and overburden stress on the cyclic resistance by making them independent variables. Therefore, CSR would not, in theory, be adjusted by the MSF and K_σ (as would be done when using the figure). However, there were very few cases in the data set available to Kayen et al. with σ'_{vo} greater than 150 kPa. Because of the lack of cases with high effective overburden, Equation E5 shows very little dependence on σ'_{vo}, compared with what is indicated by the K_σ equation and plot presented in the main text of this chapter. Recognizing this, Kayen et al. say that it is not applicable with σ'_{vo} greater than 200 kPa. However, as a reasonable approximation, one might use equation E5 with σ'_{vo}, set to 100 kPa, and apply K_σ to the CSR before it is put into equation E5. Figure E2 requires CSR*, which is CSR modified by both K_σ and MSF.

Equation E5 is applicable for fines contents between 5 and 35 percent; outside of that range, substitute 5 or 35 percent. If FC is unknown, Kayen et al. recommend assuming 15 percent. The uncertainty introduced by an error in FC would be minor compared to other uncertainties in the analysis. (Kayen et al. indicate that the difference in cyclic resistance between 5 percent and 35 percent fines is fairly minor, about the same as changing V_{S1} by 5 meters per second [m/s].)

Kayen et al. developed their correlation using a relationship for the mass participation factor, r_d (also called the stress-reduction coefficient) that is somewhat different from that shown in the main text of chapter 13 It is, in general, preferable to use any correlation consistently with the way it was developed. However, few of the case histories used by Kayen et al. were deeper than 20 feet, and most were much shallower, so differences among r_d curves from different publications would generally be minor (because r_d is identically 1.0 at the ground surface), and the back-analyzed CSRs would mostly differ by a few percent. In forward analysis, however, the r_d relationship is much more critical, and it is preferable to find CSR from site-specific, ground-response analysis.

In the equations for CRR* and liquefaction probability, the Kayen et al. model accounts for the effect of earthquake duration by including magnitude M_W as a variable in the equations. One caution, however, is that the data set included very few earthquakes with M_W outside the range of 6.5 to 8.0. For smaller earthquakes, this causes MSF to be significantly lower than the Idriss [16] MSF relationship in the main text of chapter 13. In forward analysis of liquefaction with M_W less than about 6, there would appear to be a small conservative bias, with respect to what would be predicted using the Idriss MSF. In most cases, but not all, this issue is minor.

E.3.3 Effects of Gravel

For a given value of V_S, a higher fines content indicates higher CRR*, empirically. By projecting that trend to coarser soils, or by applying theoretical arguments, one might expect that gravel could have the opposite effect of fines, causing this procedure to be unconservative. The data used by Andrus and Stokoe did not show that, however, and they tentatively concluded that the effect is minor. However, Rollins et al. [17] *did* find an effect from gravel. From the older, smaller data base, they concluded that for gravelly soils, the limiting value of V_{S1} could be higher, on the order of 230 m/s, instead of 200 m/s without gravel. The presence of gravel does not invalidate the use of the shear-wave velocities, but the findings of Rollins et al. [17] suggest that the measured shear-wave velocity may need to be reduced about 15 percent for use with figure E2 or with the equations, if the gravel content exceeds 10 to 20 percent.

E.3.4   Effects of Aging and Cementing

Figure E2 and equations E3 through E5 are for use in geologically young (Holocene) materials without cementation. It is well established that, in general, older soils are more resistant to liquefaction than younger soils. It has been proposed by Andrus, Stokoe, and Juang [7] that older soils are also more resistant even *for a given shear-wave velocity,* so the equations should be modified to account for that, with the adjustment depending on penetration testing. However, the supporting data are few, and the reverse situation could also be possible, if aged or weakly cemented sands would be stiff at small strains (giving high V_S) but still liquefiable under strong loading and shear strains that would break up the cementation or particle contacts. In the foundation of a dam, aging effects would possibly be destroyed by the increased overburden pressure, which could cause enough consolidation and rearrangement of particles that any weak cementation at particle contacts would be broken. This could affect both the overburden-adjusted shear-wave velocity and the CRR in a way that is not entirely clear. **At this time (2015), adjustment of V_{S1} for beneficial effects of aging is not recommended for high-hazard dams.**

E.3.5   Approach in Earlier Versions of this Design
Standard

The 1989 version of this chapter of *Design Standards No. 13 – Embankment Dams,* recommended that soils with measured shear-wave velocity (**not** normalized for overburden stress) exceeding 1,200 feet per second (ft/s) (366 m/s) can tentatively be considered nonliquefiable, and that those with V_S below 800 ft/s (244 m/s) be considered vulnerable to liquefaction [19]. With V_S between 800 and 1,200 ft/sec, additional information was considered necessary to determine liquefaction potential. Subsequently, a substantial body of case-history data has shown that is unnecessarily conservative; it has also been determined that the measured velocity needs to be adjusted for the effect of overburden stress (converting the measured V_S to V_{S1}). The 2001 "working draft" of chapter 13 used a curve by Andrus and Stokoe [6]; it generally indicated lower cyclic resistance, $CRR_{7.5,\sigma v'=1}$, compared to CRR* from Kayen et al. [8], for V_{S1} below 600 ft/s. However, Andrus and Stokoe's curve becomes nearly vertical at 700 ft/s, essentially ruling out liquefaction at higher velocities. The greatly expanded data set used by Kayen et al. includes cases of liquefaction with V_{S1} up to about 720 ft/s. Hence, the curve of CRR* (or 15 percent probability of liquefaction) is shifted to the right (higher V_S) relative to Andrus and Stokoe's curve.

E.4 Discussion

At present, Reclamation generally considers V_S a secondary tool used to support liquefaction assessments made by other means, rather than a primary tool to be used on its own. A risk-estimating team may be confronted with conflicting results, such as V_S indicating low probability of liquefaction, while the cone penetrometer indicates high probability. The team would have to judge the relative credibility of each test specifically for the site being studied. Often, the V_S results would be given less credibility, but there can be exceptions, such as when the results of other tests, e.g., the CPT, could be strongly affected by gravel.

Among the major sources of uncertainty in using V_S for liquefaction assessment is the fact that the behavior of soil during a liquefaction event is quite different from its behavior in the shear-wave-velocity measurement. With liquefaction, shear strains are large, and the structure of the soil is completely disrupted; in the V_S test, the stresses and strains are small, and the structure remains intact. There is no direct causal link between small-strain and large-strain behavior, so one would not expect to find that a single curve sharply divides liquefiable materials from nonliquefiable materials. Where side-by-side comparisons are available, V_S sometimes indicates higher liquefaction resistance than SPT or CPT, which could be a result of aging or cementation; Andrus et al. [7] have found reasonable agreement between V_S and penetration tests in uncemented young soils (less than 500 years old), but less agreement in older ones. This suggests that the small-strain behavior is affected more by aging than is large-strain behavior.

E.5 References

[1] "An Investigation into Why Liquefaction Charts Work: A Necessary Step Toward Integrating the States of Art and Practice," R. Dobry and T. Abdoun, *Proceedings, 5th International Conference on Earthquake Geotechnical Engineering – Ishihara Lecture,* Santiago, Chile, 2011.

[2] "Evaluation of SPT-, CPT-, and Shear Wave-Based Methods for Liquefaction Potential Assessment Using Loma Prieta Data," R.E. Kayen, J.K. Mitchell, R.B. Seed, A. Lodge, S. Nishio, and R. Coutinho, *Proceedings, Fourth Japan-U.S. Workshop on Earthquake Resistant Design of Lifeline, Facilities and Countermeasures for Soil Liquefaction*, 1992.

[3] "In Situ V_S of Gravelly Soils Which liquefied," R.D. Andrus, K.H. Stokoe, II, J.A. Bay, and T.L. Youd, *Proceedings, Tenth World Conference on Earthquake Engineering*, Madrid, Spain, 1992.

[4] "Shear Wave Velocity Measurements for Subsurface Characterization," A.L. Lodge, Ph.D. Dissertation, University of California at Berkeley, Berkeley, California, 1994.

[5] "Seismic Cone Penetration Test for Evaluating Liquefaction Potential Under Cyclic Loading," P.K. Robertson, D.J. Woeller, and W.D. Finn, *Canadian Geotechnical Journal*, Vol. 29, pp. 686-695, 1992.

[6] "Liquefaction Resistance of Soils from Shear-Wave Velocity," R.D. Andrus, and K.H. Stokoe, II, *Journal of Geotechnical and Geoenvironmental Engineering*, American Society of Civil Engineers, Vol. 126, No. 11, 2000.

[7] "Guide for Shear-Wave-Based Liquefaction Potential Evaluation," R.D. Andrus, K.H. Stokoe, II, and C.H. Juang, *Earthquake Spectra*, Vol. 20, No. 2, pp. 285-308, 2004.

[8] "Shear-Wave Velocity-Based Probabilistic and Deterministic Assessment of Seismic Soil Liquefaction Potential," R. Kayen, R.E.S. Moss, E.M. Thompson, R.B. Seed, K.O. Cetin, A. Der Kiureghian, Y. Tanaka, and K. Tokimatsu, *Journal of Geotechnical and Geoenvironmental Engineering*, American Society of Civil Engineers, Vol. 139, No. 3, 2013.

[9] "Probabilistic Framework for Liquefaction Potential by Shear Wave Velocity," C.H. Juang, C.J. Chen, and T. Jiang, *Journal of Geotechnical and Geoenvironmental Engineering*, American Society of Civil Engineers, Vol. 127, No. 8, pp. 670-678, 2001.

[10] *Resolution of Crosshole Shear-Wave Testing*, Research Report
No. DSO-04-10, Bureau of Reclamation, Dam Safety Office, Denver,
Colorado, 2004.

[11] "Multichannel Analysis of Surface Waves (MASW)," C. Park, R. Miller, and
J. Xia, *Geophysics*, Vol. 64, No. 3, pp. 800-808, 1999.

[12] "In Situ Determination of Elastic Moduli of Soil Deposits and Pavement
Systems by Spectral-Analysis-Of-Surface-Waves Method," S. Nazarian,
Ph.D. Dissertation, University of Texas at Austin, Austin, Texas, 1984.

[13] "A Comparison of Shear Wave Velocity Profiles from SASW, MASW, and
ReMi Technique," K.T. Tran, and D.R. Hiltunen, *Proceedings,
Geotechnical Earthquake Engineering and Soil Dynamics IV,*
Geotechnical Special Publication, American Society of Civil Engineers,
2008.

[14] "The Suspension P-S Velocity Logging Method," R.L. Nigbor, and T. Imai,
Geophysical Characterization of Sites, Technical Committee for
XIII International Conference on Soil Mechanics and Foundation
Engineering, Rotterdam, Netherlands, pp. 57–61, 1994.

[15] *Soil Liquefaction During Earthquakes*, I.M. Idriss, and R.W. Boulanger,
Earthquake Engineering Research Institute, Monograph MNO-12,
Oakland, California, 2008.

[16] "An Update to the Seed-Idriss Simplified Procedure for Evaluating
Liquefaction Potential," Publication No. FHWA-RD-99-165, I.M. Idriss,
*Proceedings, Transportation Research Board Workshop on New
Approaches to Liquefaction*, l999.

[17] "Implications of V_S - BPT $(N_1)_{60}$ Correlations for Liquefaction Assessment in
Gravels," K.M. Rollins, N.B. Diehl, and T.J. Weaver, *Proceedings,
Geotechnical Earthquake Engineering and Soil Dynamics III, Geotech.
Special Pub. No. 75*, American Society of Civil Engineers, Vol. 1,
pp. 506–517, 1998.

[18] "Some Contributions of In Situ Geophysical Measurements to Solving
Geotechnical Engineering Problems," K.H. Stokoe, II, Sung-Ho Joh, and
Richard D. Woods, *Proceedings, International Conference on Site
Investigation,* Porto, Portugal, 2004.

[19] *Design Standard No. 13 - Embankment Dams*, Chapter 13, "Seismic Design
and Analysis," Bureau of Reclamation, Dam Safety Office, Denver,
Colorado, 1989.

Appendix F

Soil Strengths for Seismic Analyses

Contents

Figures

Tables

F.1 Introduction

In order to analyze the stability or deformation of a dam during and immediately after an earthquake, it is necessary to estimate the shear strength to use for each material. This requires strength characterizations appropriate for the rapid, cyclic loading an earthquake imposes, and/or post-earthquake strengths that can be mobilized to maintain embankment stability once the strong shaking is over. The strength during the earthquake and the strength after it are not necessarily the same.

Embankment and foundation materials can be divided into three main categories:

1. **Dense, noncontractive materials that generate little or no excess pore-water pressure during cyclic loading.** This category includes most compacted granular embankment fills, as well as compacted clayey fill under low or moderate confining pressure. Clayey embankment core material under very high overburden stress may not fit this category. If the effective overburden stress is near or greater than the apparent preconsolidation stress induced by compaction, the fill may act like a normally consolidated or lightly overconsolidated clay. Coarse, clean materials that are free-draining relative to the short duration of earthquake loading can sometimes be included in this category, even if they are saturated and slightly contractive. A soil that does not liquefy in a particular earthquake does not necessarily fit in this category for that earthquake, if it would liquefy in a larger one. It would be at least somewhat contractive, so high excess pore-water pressure could develop in moderate earthquakes. Unsaturated materials can generally be assigned drained strengths, even if they are contractive, provided that there are several percent air voids, by volume.

2. **Liquefiable sandlike materials that undergo drastic loss of shearing resistance due to cyclic loading, with very high pore-water pressure.** This category includes loose clean sands, sand-gravel mixtures, and nonplastic to slightly plastic silts and silty sands. Usually, liquefaction is considered to involve excess pore-water pressure that is nearly equal to the initial effective stress, but under a steep slope, smaller pressures could reduce the effective stress and shear strength enough to allow instability.

   Liquefaction of sandlike materials is sometimes called "classic liquefaction" to distinguish it from softening of claylike materials, referred to as "cyclic failure." The difference between the two is due, in large part, to the greater potential for the claylike soil's skeleton to rebound with decreases in confinement, so the effective stress does not become nearly zero. The distinction is made in practice according to the fines content (FC) and the plasticity index (PI) [1, 2]. Boulanger and Idriss concluded

that for soils classified as "fine-grained" i.e., having more than 50 percent fines, claylike behavior would occur if the PI is greater than 4 to 7. For practice, Malvick et al. [2] suggest that if FC is less than 20 **and/or** PI is less than 7, the analysis should address classic liquefaction of sandlike soil. If FC is greater than 50 **and** PI is greater than 12, the analysis should address cyclic softening of claylike material. For other materials, the correct approach is less obvious; they recommend using both approaches, followed by additional in situ and laboratory testing, as needed to resolve conflicting results. It can be very instructive to have the engineers performing the analysis examine and handle the specimens.

Classically liquefiable soils may be subdivided into two subcategories, which are shown conceptually in figure F1:
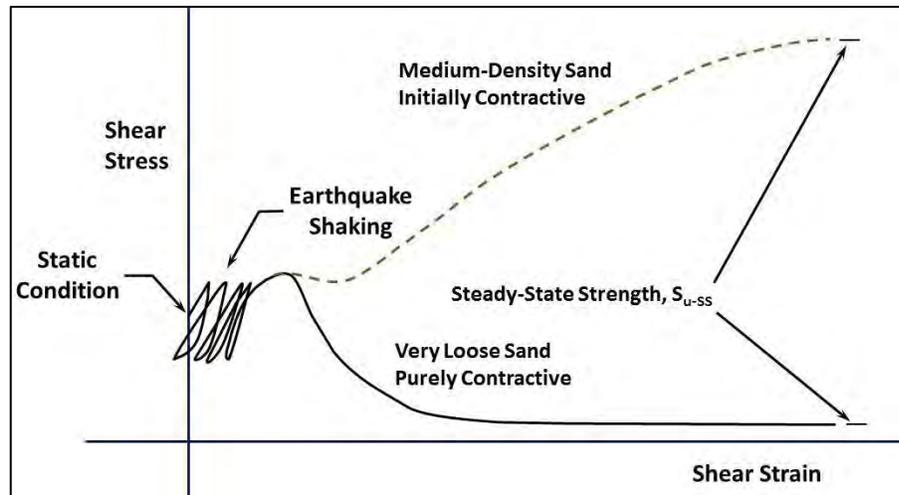
Figure F1. Comparison of stress-strain behavior of medium-density and very loose sand in undrained loading (conceptual).

a. **Purely contractive soils for which the loss of strength is practically complete once liquefaction has occurred.** The solid line in figure F1 shows stress and strain beginning with the pre-earthquake *in situ* stress condition. During the earthquake, excess pore-water pressure builds up, and the soil softens until its shearing resistance is greatly reduced. With increasing shear strain, the shearing resistance eventually flattens out at a lower value, which is referred to as the *steady-state strength*, S_{uSS}, or the *critical-state strength* (which is not necessarily the strength that can be mobilized in the ground for post-earthquake stability). Large deformations would occur if this value is less than the demand from gravity or dynamic loading. In sandlike soils, purely contractive behavior is most likely to be seen with clean-sand-equivalent adjusted Standard Penetration Test (SPT) blow counts, $(N_1)_{60CS-Sr}$, of 15 or less.

(The determination of $(N_1)_{60CS-Sr}$ is discussed below and in appendix C.)
Post-earthquake stability in the field is governed by the *residual
undrained shear strength*, S_r, which is related to the steady-state
strength, but it can be substantially lower. It is a gross-scale property of
the soil deposit that is affected by drainage, nonuniformity, and time.
Time is important because seepage from excess pore-water pressure can
reduce the shearing resistance in some locations, while increasing it
elsewhere. Highly sensitive clays can display similar stress-strain
behavior, even if they are not, strictly speaking, liquefiable.

b. **Soils that are initially contractive, but dilative at larger strains,
    which can cause an initial drastic loss of shearing resistance, but
    partial or full recovery after some amount of deformation** (the
    dashed line in figure F1). This behavior is sometimes referred to as
    "cyclic mobility" or "initial liquefaction with phase transformation and
    dilation." After several cycles of undrained cyclic triaxial or direct
    simple shear, the stress-strain plots typically show very low shearing
    resistance with strain near zero, followed by a rapid increase in
    resistance at several percent strain, when the material begins to dilate,
    reducing the pore-water pressure. The shearing resistance would
    eventually reach a constant value of S_{uSS} that is much higher than
    SuSS in the very loose soil. This behavior is most likely to occur in
    medium-density soils having $(N_1)_{60CS}$ between 15 and 30. The
    dilation at larger strains may or may not be sufficient to lower the
    excess pore-water pressure enough to restore stability of the
    embankment at the end of the earthquake. Even if the embankment
    is stable immediately after the earthquake, settlement after the
    earthquake can create a thin layer of loosened, weaker material at
    the top of the liquefied layer if there is not free drainage. This
    mechanism, called "void redistribution," is thought to have figured in
    the instability of hydraulic fills at Lower San Fernando Dam in
    California and Mochi-Koshi tailings dam in Japan, as well as in the
    failures of Ft. Peck Dam in Montana and Calaveras Dam in California,
    during construction. There could also be an adverse effect from
    intrusion of excess pore-water pressure from other liquefied materials
    in the minutes or hours after the earthquake. For these reasons, a
    distinction is made between SuSS and Sur, which is the strength in
    sustained loading, during which settlement and void redistribution
    might occur (described in section F.3).

3. **Contractive claylike soils that generate positive excess pore pressure
    in undrained shearing but, with the exception of very sensitive soils,
    do not undergo a drastic loss of shearing resistance like liquefied soils.**
    These soils can include normally consolidated to lightly overconsolidated
    foundation soils, hydraulic fills, and, possibly, rolled clayey embankment
    fills that are saturated and heavily loaded by overlying fill (so that they act

as if they are normally consolidated). Loss of shear strength can occur, although it would generally not be as drastic as in liquefaction; this is variously referred to in the literature as "strain softening" and "cyclic softening." For practice, Malvick et al. [2] suggest that these soils can be identified with some confidence by FC greater than 50 **and** PI greater than 12. Although not strictly classified as "fine grained," clayey sands often belong to this category because the fines tend to dominate the behavior. (If FC is less than 20 **and/or** PI is less than 7, sandlike behavior is expected; the remaining soils fall in a transition zone between claylike and sandlike behavior.)

Very sensitive clays or silts may behave very much like liquefied sand, but they are included with other fine-grained soils in the discussions below.

American Society for Testing and Materials (ASTM) standards cited in this design standard are all copyrighted by ASTM in West Conshohocken, Pennsylvania. They are numbered in the format "D1586-11," in which the last two digits are the year of the most recent revision. ASTM standards are regularly reviewed and updated, and there may be newer versions that supersede the ones cited here.

F.2 Strength Considerations for Dense Materials

These are materials of Category 1, described in section F.1.

It is usually reasonable to use the same strength parameters for these materials for dynamic loading as are used for static stability analysis.

Although a strongly dilative soil may generate negative excess pore pressure during shearing, making its undrained strength higher than its drained strength, strengths higher than the drained strength are unreliable and should generally not be used. If the negative excess pressure dissipates rapidly during or after the earthquake, or if it is diminished by cavitation or gas bubbles, the strength would be closer to the drained strength. Neglecting negative excess pore pressure in dense material could introduce conservatism, probably minor, in a dynamic deformation analysis (where there is generally not time for much seepage to occur). It could be unconservative to include benefit from negative excess pore-water pressure in post-earthquake stability analysis because seepage could cause the negative excess pressure to be lost soon after the earthquake, and cavitation or bubbles in the pore water could prevent negative excess pore pressure from developing in the first place.

Dense soils need to be distinguished from soils that are contractive but are not subjected to enough cyclic loading to cause liquefaction. The latter can still generate positive excess pore pressure, reducing their shearing resistance. In laboratory cyclic shear tests, large excess pore pressures can develop with factors of safety against liquefaction up to 1.4 or even greater [3, 4]. What happens then depends on several things, including the density (which governs whether the material is purely contractive or only initially contractive, with dilation at larger strains), the stresses and strains imposed after the pore pressure becomes high, and whether settlement and void redistribution can create a weakened layer following the earthquake. Marcuson and Hynes [3] suggested that the strength could be modeled as a friction angle that is reduced in proportion to the excess pore-water pressure that would be predicted by lab testing or other means. For moderate increases in pore-water pressure, this approach may be reasonable in medium-density material that is not purely contractive. (Laboratory tests are limited in the amount of shear strain that can be applied, but medium-density materials may recover some portion of their shear strength with larger strains, which may not have been accounted for in Marcuson and Hynes' analysis.) However, in a saturated, purely contractive soil, monotonic shear strain could result in a further increase of pore pressure.

Excess pore-water pressure in nonliquefied materials is not a simple problem to analyze. The logical starting point is to assess the sensitivity of stability and deformation to the strength of these materials, in order to determine how important it is to know. If quantifying this behavior is critical to a decision, a nonlinear numerical analysis that couples stress and strain with generation of excess pore-water pressure may be the most effective way to address the problem.

F.3 Strength Considerations for Nonplastic or Slightly Plastic Sandlike Soils That Could Be Liquefied by Cyclic Loading

These soils are materials of Category 2a, as defined in section F.1.

Because of their very low residual strengths, liquefied sandlike materials that would lose nearly all of their shear strength are often the most critical ones for embankment analyses, whether for dynamic deformations during the earthquake or for post-earthquake stability. They can also cause significant settlement due to consolidation (up to 3 percent volumetric strain), as excess pore pressure dissipates following an earthquake; however, for a dam embankment, the shear deformations are generally much more important.

Various authors have used different symbols for the post-earthquake, residual, undrained shear strength of liquefied soils; Chapter 13 (this chapter) uses S_{ur}, but S_r, $S_{u\text{-}liq}$, and $S_{u(liq)}$ are also found in the literature. A distinction needs to be made between S_{ur} and the related concept of "steady-state" strength, $S_{u\text{-}SS}$. S_{ur} is the post-earthquake strength that can be mobilized and sustained following an earthquake; it is a gross-scale phenomenon influenced by nonuniformity of materials and by seepage and settlement following an earthquake. The steady-state strength, $S_{u\text{-}SS}$, is also a post-liquefaction strength, but on the scale of laboratory specimens, with uniform properties throughout the specimen and throughout the duration of the test, and without drainage. It is, for a given soil, a function of void ratio only.

The strength that can actually be mobilized in a dam foundation or hydraulic fill to maintain stability or govern deformation can be significantly different from $S_{u\text{-}SS}$ because it is affected by nonuniformity in the materials and by changes in void ratio following an earthquake. Settlement of solids in the liquefied material, as the excess pore-water pressure dissipates, generally causes upward movement of water. This can create a thin layer of loosened soil, or even a film of water at the top of the liquefied zone [5, 6]. At any particular time and location in the slide, the shearing resistance is still equal to $S_{u\text{-}SS}$, but the value of $S_{u\text{-}SS}$ decreases when the void ratio increases, approaching zero if the top of the liquefied deposit is loosened enough. This has been demonstrated to govern the stability of slopes in centrifuge models [7, 8]. It was probably a factor in several of the historic seismic slope failures where instability occurred minutes to days after the earthquake, and in the failures during construction of Calaveras and Fort Peck Dams, both hydraulic fills that failed during construction. Formation of a loose layer is most likely to occur where a large thickness of loose, granular material is overlain by a less-pervious cap layer that prevents escape of the upward-migrating pore water. It can make the available shearing resistance for post-earthquake stability much lower than the shearing resistance available to resist dynamic deformation during shaking. Void redistribution is less likely to be a problem with thinner layers, higher densities, and higher clay contents. It is common practice to assume that a loosened zone *can* develop, unless a strong case can be made that conditions are not conducive. (In risk analysis, it is often appropriate to assign probabilities to each type of behavior.) The effect of void redistribution cannot be captured in a laboratory shear test.

Procedures for the evaluation of liquefaction potential and the characteristics of liquefied soils were first published in 1971 in two papers by Professor H. Bolton Seed and coworkers [9, 10]. Those publications discussed the definition and causes of liquefaction, and the types of soils that may be susceptible to liquefaction under earthquake loading. At that time, it was recognized that sandy soils may lose most or all of their strength (because of total or near-total loss of effective stress), but no method was proposed for estimating shear strength after liquefaction.

Subsequently, it was recognized that the post-liquefaction strength (S_{ur} or S_{u-ss}) can be greater than zero (substantially greater in medium-density soils), and a variety of procedures have been developed for estimating it. The methods are mostly based on strengths back-calculated from case histories of liquefaction and flow sliding [6, 11, 12, 13], or on laboratory undrained shear testing [14, 15, 16]. At this time (2015), no definitive guidance can be provided on the post-earthquake strength of liquefied soils, particularly for those of medium density (roughly speaking, those with adjusted SPT blow counts $(N_1)_{60-cs-Sr}$ of 15 to 30). There is no consensus in the profession at present, even about the most correct format for a correlation from case-history data, or on the ability of laboratory testing to replicate the strength of liquefied material in the field.

Although not common in practice anymore, laboratory triaxial and direct simple-shear tests have been used to estimate S_{ur} [14, 15, 16]. Unlike the empirical correlations described above, laboratory testing is tailored to the specific materials and stress conditions of the dam being analyzed. However, laboratory testing is far from being a definitive solution. Because S_{ur} is extremely sensitive to void ratio, it is necessary to obtain very high-quality undisturbed samples, and to account for the inevitable changes in void ratio during sampling, transportation, and preparation. In fact, for some major projects, samples have been obtained by freezing the ground with liquid nitrogen and coring the frozen mass, with thawing occurring only after the sample was in the triaxial shear device and the confining pressure had been applied. (This approach is limited to clean sands because drainage needs to occur during freezing to allow for the expansion of water as it freezes.) No matter how high the quality of sampling and testing, a laboratory test can only capture the behavior of one small "element" of the soil, a few inches in size, not the gross-scale behavior of a dam foundation where there are variations in density, gradation, plasticity, and confining stress, in addition to time-related effects like void redistribution and dissipation of excess pore-water pressure.

Under the present state of the art, S_{ur} is incompletely understood, and there is no consensus on the best methods for selecting values to apply in analysis. The analyst must consider and document the uncertainty in strength estimates so that dam-safety decisions are made with full awareness of the limitations and imprecision. In risk-based dam-safety analysis, it is usually necessary to consider a range of S_{ur}, the relative likelihood of different values, and how sensitive stability or deformations are plausible variation in S_{ur}. Often, however, uncertainty in the *strength* of liquefied materials (within typical limits) will prove unimportant relative to the *extent* of liquefied materials. For example, for a 100-foot-high embankment, it generally makes very little difference in the overall outcome if liquefied material in the foundation is assigned a strength of 50 pounds per square foot (lb/ft^2) or 150 lb/ft^2, whereas the outcome is quite sensitive to which portions of the foundation are assumed to be liquefied. Probability distributions on S_{ur} should include use of, or at least consideration of, multiple

approaches to portray the variability and uncertainty in the strength, and how they affect the quantification of risk.

F.3.1 Empirical Correlations with Penetration Resistance – General Discussion

The most commonly used method of estimating the strength of liquefied materials is correlation between penetration resistance (Cone Penetrometer Test [CPT] or SPT) and strengths back-figured from field performance (S_{ur}) [6, 11, 12, 13, 17, 18, and others]. These methods have two main advantages over actual strength measurements in the laboratory or in situ:

- First, empirical correlations with penetration resistance do not require extremely high-quality undisturbed sampling, transportation, and testing of materials that are easily disturbed by vibration and are quite difficult to set up in the test apparatus without further disturbance. The undrained shear strength of nonplastic granular soils is quite sensitive to small changes in void ratio.

- Second, they account (albeit crudely) for gross-scale behavior that cannot be measured in small laboratory samples. Redistribution or migration of voids probably had a major influence on the post-earthquake behavior of some slopes. The slides of both Lower San Fernando Dam and Mochi-Koshi Tailings Dam No. 2 occurred after the end of earthquake shaking. This was probably a result of settlement of soil particles and upward movement of pore water, increasing the void ratio, and decreasing the undrained strength in some portions of the material. Castro [19] has pointed out that pore-water pressure from liquefied zones can migrate into nonliquefied materials, causing their strength to be reduced as well. Also, the deformations that occur in flow slides may be concentrated in thin sheared zones [20]. The extremely large strains in the sheared zones (hundreds of percent) are likely to create a remolded soil structure that cannot be duplicated in laboratory triaxial or simple shear tests, which are limited to about 20 percent strain [21]. There is no way to measure these soil-mass behaviors with tests on small volumes of soil.

There are, however, a number of serious complications with using these correlations:

- First, there are only about 30 case histories on which to base a correlation, and those cases may not be directly applicable to the particular dam being studied. Among the 30 cases, the quality and level of detail of the available information are quite variable. Most of them involved liquefaction of fairly shallow layers, rather than material under 50 to 200 feet of overburden,

such as occurs in the foundations of large dams. At this time, there are
only six known case histories of flow sliding with initial effective
overburden stresses greater than 2,000 lb/ft^2, and all of them had SPT
$(N_1)_{60}$ values within the narrow range of 8 to 11, and clean-sand-equivalent
$(N_1)_{60\text{-cs}}$ values within the range of 10 to 14. Four of those case histories
were "static" failures of hydraulic fills or dumped fill, leaving only two
earthquake-induced slides with more than 2,000 lb/ft^2 of overburden (the
hydraulic fill of Lower San Fernando Dam and a loess slope in Tajikistan).
Few out of all the sliding case histories, and none of the high-overburden
cases involved alluvium. A larger data set might show greater variability.

- Second, because of the complexity of back-analyzing shear strength from
  slope failures and of determining the representative value of penetration
  resistance, there is not complete consensus among the various researchers
  on either strength or penetration resistance for some of the important case
  histories. In many cases, the $(N_1)_{60}$ or q_{c1} value was an estimate, rather than
  a measurement. Some of the strength estimates have uncertainties of
  ±50 percent or more. There is not even full agreement on the most correct
  format for a correlation. Should the blow count be adjusted for fines
  content? Should the correlation predict the value of the residual undrained
  shear strength, S_{ur}, directly, or should it predict a strength ratio, S_{ur}/σ_{vo}'
  (where σ_{vo}' is the pre-earthquake effective overburden stress)? Or, should it
  be a hybrid of those two approaches, one that lets the strength increase with
  increasing overburden, but not in direct proportion with it? It is generally
  accepted that, for a given $(N_1)_{60}$ or $(N_1)_{60\text{-cs}}$, there should be an increase
  with higher effective overburden stress, but the amount of increase is not
  settled (and it may not be consistent for all material types or densities).

- Finally, there is an important conceptual issue: The correlations are based
  primarily on shear strengths mobilized at very large strains during flow
  slides, which are not necessarily the same as the strengths that could be
  mobilized at smaller strains to *prevent* sliding or excessive deformation.

Post-liquefaction behavior is different in medium-density soils than in loose soils.
In medium-density materials (roughly speaking, those with clean-sand-equivalent
SPT blow counts, $(N_1)_{60\text{-cs}}$, greater than 15 or so, but less than 30), there may be
initial liquefaction, which means that very high excess pore pressures are
generated during cyclic loading, but the material tends to dilate with further
strain and recover its shearing resistance. At that point, the strength could
increase with time as excess pore-water pressure dissipates, but it is also possible
that void redistribution, as solids settle and water rises, would create a loosened
layer or water film. There are no known cases of flow sliding or large lateral
displacements with $(N_1)_{60}$ exceeding about 13, or $(N_1)_{60\text{-cs}}$ greater than 14.
That probably results from one or both of two causes: (1) the tendency of
medium-density materials to dilate and recover shearing resistance with larger
strains; and/or (2) there have been few good "tests" of steeply sloping ground or

large embankments with medium-density soils, sufficiently high earthquake loading to cause liquefaction, and the right stratigraphy to create a loosened zone or water film.

Based on laboratory undrained shear data from Duncan Dam in Canada, Fear [22] suggested that the strength of liquefied medium-density soils should rise very sharply with increasing penetration resistance just beyond the available data, which is consistent with the lack of slide case histories. This same conclusion has been reached by other researchers, and it is consistent with most correlations between penetration resistance and S_{ur}/σ'_{vo} or S_{ur}. Fear did not, however, recommend use of her extended curves for design purposes because of the lack of confirming case-history data. Idriss and Boulanger [23, 24] similarly concluded that the strength should increase rapidly, although they caution that void redistribution could severely reduce the strength that can be sustained after the earthquake is over. Hence, they present two different curves for S_{ur} as a function of CPT or SPT resistance, with one curve corresponding to the ideal situation where S_{ur} is not decreased ($S_{ur} \approx S_{uSS}$), and one curve for when void redistribution reduces it after shaking.

Clearly, extrapolation of strength correlations to densities greater than those in the known flow-slide case histories is not reliable; the analyst must allow for a very wide range of plausible results by considering, in particular, the possibility of loosening or a water film.

Robertson [25] analyzed penetration-resistance data and laboratory residual strengths using several techniques and found that there is no unique relationship between penetration resistance and residual strength that is applicable to all soils. He concluded that the S_{ur} - $(N_1)_{60}$ relationship proposed by H. Seed (a forerunner of figure F2) is purely empirical; it cannot be derived by any analytical method. Also, it indicates lower strengths than does laboratory testing. This is consistent with void migration affecting many of the case histories, and Robertson's conclusions would appear to apply to the other correlations as well.

Monotonic laboratory testing shows recovery of strength with further strain in materials with relative densities as low as 40 percent in direct simple shear, and as low as 20 percent in triaxial compression. For a given relative density, this tendency is stronger in triaxial compression, and weaker in triaxial extension; in simple shear (typically the dominant stress path) the behavior is intermediate between the other two. It should be recognized, however, that in postcyclic monotonic tests, the recovery of strength might not be as pronounced as in monotonic tests, and there may be potential for void migration and loosened zones, even in medium-density granular materials, if there is a looser zone below that could supply water to the zone in question. Again, laboratory tests cannot capture gross-scale behavior like void redistribution.

**At no time should one rely on an undrained strength that is higher than the
drained strength.** While higher undrained strength is possible, it would require
negative excess pore pressure resulting from dilation. The benefit of negative
excess pore pressure could be lost rapidly, due to dissipation or cavitation.
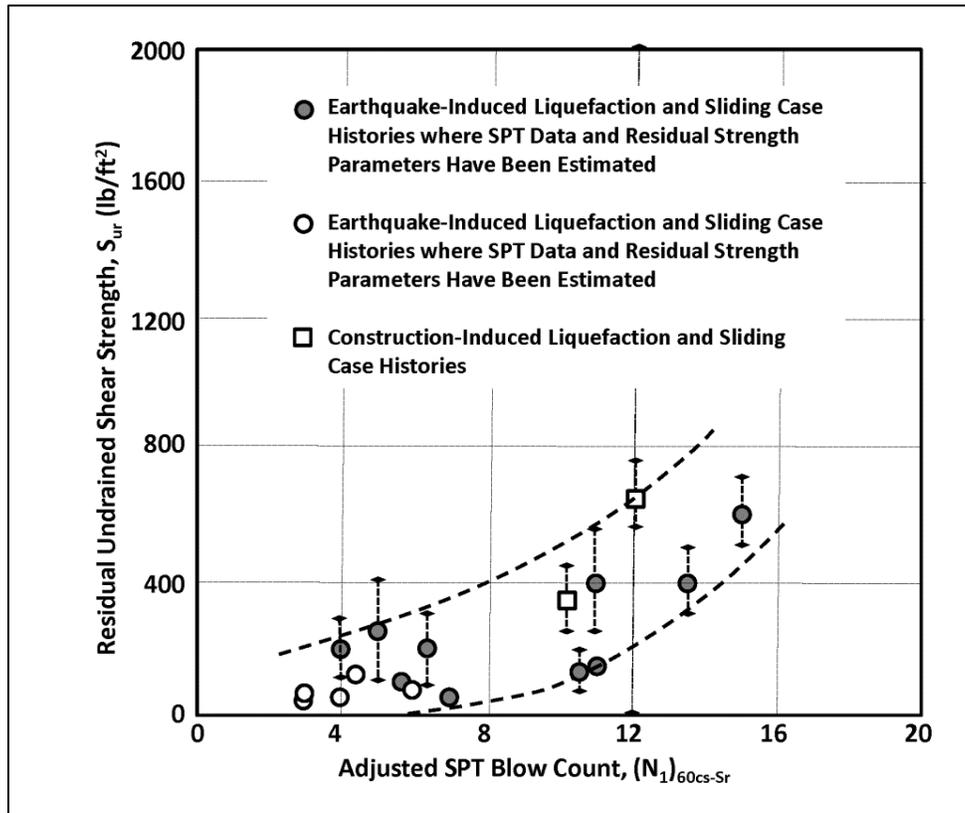

Figure F2. Residual undrained shear strength correlation with SPT (redrawn
from [11]).

Field investigation programs for assessing liquefaction potential generally include
numerous SPT or CPT data. Where those data are available, they provide an
important basis for estimating the residual undrained shear strength, even when
other approaches are used. Unless a deposit is extremely uniform, there will be
substantial variation among the data.

In liquefied foundation soil, the critical failure surface may follow the surface
with the lowest average shear strength through the liquefied zone, but not
necessarily do so. The critical failure surface depends on the geometry of the
dam and foundation, as well as the differences in strength among the various
materials. It is sometimes reasonable to assume that S_{ur} is a weighted average of
the strengths indicated by the lowest penetration resistance in each CPT sounding
or SPT drill hole, i.e., the "weakest link in the chain" at each location. That

assumption could, however, be unnecessarily conservative if the elevations of the weakest intervals are very different from hole to hole, or if there are geologic reasons why continuity of weak material should not be expected. In developing the correlations described here, the representative penetration value associated with a back-analyzed strength was defined as the mean for the material actually involved in the slide. In application, however, one is trying to *predict* behavior, rather than back-analyze what has already occurred, and it is not always obvious which data should be included in the averaging. It is frequently necessary to estimate a likely range of representative values for a particular soil deposit, rather than a single value.

The correlations described in this appendix (figures F2 through F4) below all show substantial "spread" in the range of back-analyzed strengths for a given SPT or CPT tip value. This spread does not necessarily cover the full range that needs to be considered in forward analysis of a particular dam because of the limited size of the data set and the fact that few of the case histories are directly relevant to a large dam embankment, with its high overburden pressure.

If a distinct, weaker layer can be identified, data from that layer should be considered separately from the material above and below it, even if it is part of the same general deposit.

One must also judge what horizontal area is to be included when determining the representative blow count. This is a function of dam geometry in three dimensions. If liquefaction were to occur only along a 10-foot-wide strip oriented upstream-downstream, instability of a large dam would be unlikely because shear resistance on the left and right sides of a slide mass (looking downstream) would help stabilize it. Any plausible slide would require liquefaction over a wider area. Similarly, instability requires liquefaction to occur under a significant portion of the embankment slope as measured upstream-downstream. While some general research has occurred on this subject, site-specific, three-dimensional deformation or stability analysis may be necessary.

In spite of these complications, correlations with penetration resistance remain the most widely used means (and often the only practical means) of estimating the shear strength. Several of these correlations are described below. Some of them predict the residual undrained shear strength, S_{ur}, as a direct function of the penetration resistance, but others predict a normalized shear strength or strength *ratio*, S_{ur} / σ'_{vo}, where σ'_{vo} is the effective overburden pressure prior to the earthquake. Newer work suggests that both approaches are simplifications; therefore, a hybrid approach has been proposed, in which S_{ur} is a function of both blow count and effective overburden stress, but not directly proportional to effective overburden [26, 27]. At present, there is no consensus on which format is more appropriate, although it is generally recognized that there should be *some* increase with increasing σ'_{vo} for a given blow count, even if it is not directly proportional. The great majority of the case histories involved low effective

overburden stresses. Under a large embankment, it is unnecessarily conservative to use a correlation between penetration resistance and back-calculated S_{ur} values without regard to overburden stress; the reverse may be true using back-calculated strength *ratios* from cases with low overburden.

Back-calculated strength ratios published by Olson and Stark [12] and by Idriss and Boulanger [24] do not appear to correlate very well with penetration resistance, although the correlation may improve somewhat if the cases with σ'_{vo} below about 1,000 lb/ft^2 are excluded [29]. (Under an embankment dam, σ'_{vo} is generally much greater than 1,000 lb/ft^2.) As noted above, however, that leaves rather few data, and the blow counts for those are all in a narrow range.

Laboratory data typically show an increase in liquefied strength with increasing consolidation stress, for a given soil at a given void ratio. However, they do not, in general, show direct proportionality at a given void ratio [30]. Considering only a small volume of liquefied soil (comparable to a laboratory test specimen), critical-state theory would argue *against* the strength-ratio approach, but it does not account for variation in properties over the large area of a dam foundation, or for void redistribution or other gross-scale behavior. Theoretical arguments can be made for the strength-ratio approach, considering nonuniformity of the deposit over a large area (so that not all of the area is purely contractive) and partial drainage or dilation in portions of the sliding surface. Considering the full set of case histories, the actual value of S_{ur} correlates with penetration resistance somewhat better than does the ratio S_{ur} / σ'_{vo}. Considering only the few cases with effective overburden stress greater than 1,000 lb/ft^2, strength ratios fit the data about as well as estimating S_u directly. This result suggests that normalization is most applicable to materials with higher overburden stress and higher blow counts. It would, therefore, seem most applicable to materials with $(N_1)_{60}$ greater than about 10, or with relative densities greater than about 50 percent. Many of the case histories with low blow counts were probably influenced by void redistribution that created a water film or very low-density zone that led to instability. If that same thing occurs in a large or medium-sized dam or its foundation, the strength is likely to be so low that the precise value would be unimportant to the stability; the extent of liquefied material is far more important.

Given the present state of knowledge, stability and deformation analyses to support risk analysis should include evaluating the influence that different strength approaches would have on the results. If the results of stability or deformation analyses are strongly sensitive to variation in S_{ur}, it would be appropriate to develop a probability distribution for S_{ur} considering the following:

- The estimators' confidence in different strength models
- Uncertainty and variability in SPT, CPT, or lab data
- Uncertainty in the results of each strength model

It is not, in general, sufficient to produce a "best estimate" value of S_{ur} to use for all analyses.

For calculating the overburden stress for normalizing the SPT or CPT tip resistance, use the piezometric level that existed at the time of testing. For estimating the residual undrained shear strength by a strength ratio, determine the effective overburden stress using the piezometric level that would exist at the time of the earthquake (which may not be the same).

F.3.2 Residual Undrained Shear Strength from Standard Penetration Test

F.3.2.1 Direct Prediction of Residual Undrained Shear Strength (Absolute Value)

Figure F2, originally from R.B. Seed and L.F. Harder [11], but with some later data added, presents a correlation between back-calculated residual undrained shear strengths, S_{ur}, of liquefied sands and sand-silt mixtures, and the equivalent clean sand SPT, $(N_1)_{60-cs}$, for each soil. The value of $(N_1)_{60-cs}$ is determined by adding an adjustment, $\Delta(N_1)_{60}$, based on fines content, to the actual value of $(N_1)_{60}$ (i.e., the raw blow count N, multiplied by the appropriate adjustments for overburden stress, hammer energy, and sampling conditions). (See appendix C for calculation of $(N_1)_{60}$.) Figure 2 has been used extensively by Reclamation and others since it was first published, although one of the developers (R.B. Seed) has indicated that work in progress will likely supersede it, particularly for cases with high effective overburden pressure [27].

The effect of fines on penetration resistance is accounted for using equation F1, first proposed by H.B. Seed [6] and later used by R.B. Seed and Harder [11]. The amount of adjustment is shown as a function of fines content in table F1. Penetration resistance is governed by both undrained shear strength and compressibility. Because fines, especially plastic fines, tend to make the soil more compressible, they reduce the penetration resistance associated with a given residual shear strength. Thus, a silty sand with a residual undrained strength of 300 lb/ft^2 would give lower SPT blow counts than a clean sand with the same residual strength. **Note that this adjustment for fines content is different from the one described in appendix C to obtain $(N_1)_{60-cs}$ for liquefaction triggering. This adjustment is applied in place of the adjustment in appendix C, not in addition to it.** It has also been suggested that one fines adjustment would suffice for both applications [31], or that no adjustment is needed at all [12, 18, 26].

$$(N_1)_{60-cs-Sr} = (N_1)_{60} + \Delta(N_1)_{60-Sr} \qquad \text{Equation F1}$$

Table F1. Adjustment to $(N_1)_{60}$ for Fines Content [6]

Fines Content (percent)	$\Delta(N_1)_{60}$
10	1
25	2
50	4
75	5

Note: This adjustment for fines is for estimation of S_{ur} only; the fines adjustment for liquefaction triggering is different. Refer to appendix C.

As described in appendix C, each SPT blow count is normalized for the effect of overburden stress by the factor C_N to obtain $(N_1)_{60}$. The C_N values used in developing figure F2 were not exactly the same as shown in appendix C. However, the potential error from using the one in appendix C is very small compared to all of the other uncertainties in the analysis.

About one-quarter of the data used by Seed and Harder came from "lateral spreads" or limited deformations that occurred during dynamic loading, rather than flow slides that occur under gravity loading, even after the earthquake motions have ceased. (Those data were not included by Idriss [32], Idriss and Boulanger [24], or Olson and Stark [12].) A study by Mabey and Youd [33] found that strengths back-calculated from lateral spreads are, on average, lower than those from flow slides in materials with similar penetration resistance. This may be because some lateral spreads are governed by a minimum strength (called the "quasi-steady-state strength") that is lower than the true residual (or critical state) strength that occurs at larger strains, such as would occur in a flow slide. It suggests that strengths back-calculated from lateral-spread case histories would be conservative if applied for determining post-earthquake stability of embankments. However, very large strains may have to occur before the full residual strength can be mobilized, possibly allowing significant damage to a dam embankment, even if actual instability does not occur. In this regard, it is of interest that Upper San Fernando Dam did not become unstable in the 1971 San Fernando Earthquake, but its downstream slope did move about 4 feet horizontally and 3 feet vertically. (This is the data point farthest right in figure F2.) The liquefied hydraulic fill was surrounded by a substantial thickness of compacted fill, which enabled the dam to remain stable after the earthquake and limited the strains, but not before the large displacement had occurred. In the 1994 Northridge Earthquake, the dam settled approximately another 1 foot.

The fines adjustment, $\Delta(N_1)_{60}$, is also an open question. The data are too few to support the adjustment on a purely empirical basis, and the adjustment proposed by H.B. Seed [6] was largely based on judgment. It should also be recognized that only two of the data points in figure F2 (Lake Merced and Lake Ackerman

banks) are actually from clean sand; the other data points are all from silty sands and one sandy silt (Mochi-Koshi tailings dam, with high fines content and blow counts near zero). Concerned that Seed's adjustment might overstate the benefit of fines, Baziar and Dobry [18] replotted the data without any adjustment for fines content and obtained a slightly tighter correlation. However, they did not include Mochi-Koshi in that plot because the SPT blow count was measured very soon after the earthquake, when excess pore pressures in the liquefied tailings may not have dissipated. The tailings dam was "active" at the time of the earthquake, and it is not certain that the pore pressure and consistency of the tailings were markedly different immediately before the earthquake. Some other data, including field Vane Shear Test (VST) measurements in materials with high fines contents [28], are at least compatible with the fines adjustment proposed by Seed. However, simplified statistical analysis shows that a slightly better correlation can actually be obtained with no fines adjustment, which may be influenced by the limited data set [29]. Compressibility of the soil is influenced by both the amount of fines and the nature of the fines, but the adjustment does not account for the latter. One would expect, *a priori,* that the nature of the fines would substantially influence the value of the correction. Certainly, caution is required in making large adjustments using table F1, especially if the fines are coarse silt with "bulky" particle shapes and little or no plasticity. Such materials would behave very much like fine sand and would not be expected to affect the penetration resistance in the same way as finer silt or clay. Seed [6] wrote "...Judgment is required in the use of the values since fines may differ in their characteristics and effects from one soil to another"; if all of the silt is coarse, it may not provide as much benefit as if it were finer and slightly plastic.

F.3.2.2 Residual Undrained Shear Strength Ratio from SPT

An alternative to figure F2 is a correlation that predicts the ratio of S_{ur} / σ'_{vc}, where σ'_{vc} is the pre-earthquake vertical effective stress. Such correlations have been proposed by Olson and Stark [12], Idriss and Boulanger [23, 24], and others. The primary difference is that Olson and Stark used the normalized blow count, $(N_1)_{60}$, with no adjustment for fines content, while Idriss and Boulanger used the *clean-sand-equivalent* normalized blow count, $(N_1)_{60cs\text{-}Sr}$, by adding an adjustment that increases with increasing fines content. (They used many of Olson and Stark's estimates of S_{ur}.) Only the Idriss and Boulanger correlation is presented here (figure F3) because Olson and Stark did not attempt to extrapolate strength ratios for blow counts greater than those in the historic cases, for which all of the $(N_1)_{60}$ values were less than 12. In embankment dam analysis, strengths associated with those low blow counts are generally too small for reasonable variation to affect the outcome. Only with $(N_1)_{60cs}$ greater than 12 or $(N_1)_{60cs\text{-}Sr}$ greater than 15 does the precise value of S_{ur} have much effect on the outcome. Therefore, with no case histories that include blow counts in the most important range for dam analysis, it is necessary to extrapolate.

If the post-liquefaction strength was governed by a water film or by the steady-state strength of material loosened by void redistribution uniformly over the whole slide surface, increasing pre-earthquake σ'_{vc} would have no effect. This is because the steady-state strength depends solely on the void ratio. However, the water film or loosening would not be uniform, and there may be some drainage and void migration. Some portions of a potential slide surface would be less contractive than others, or even dilatant, and would bear part of the overburden by effective stress that would, *on average*, be some percentage of the pre-earthquake effective overburden stress over the whole area. If so, the residual undrained shear strength, S_{ur}, would be proportional to pre-earthquake overburden, even if S_{uSS} is not. The strength-ratio approach assumes that the ratio with σ'_{vc} is a function of the adjusted penetration resistance from SPT or CPT, and that the same ratio applies to any value of σ'_{vo}. (In contrast, correlating S_{ur} directly with SPT or CPT assumes that the actual post-earthquake effective stress is a function only of adjusted penetration resistance, independent of the pre-earthquake effective stress, σ'_{vc}.)
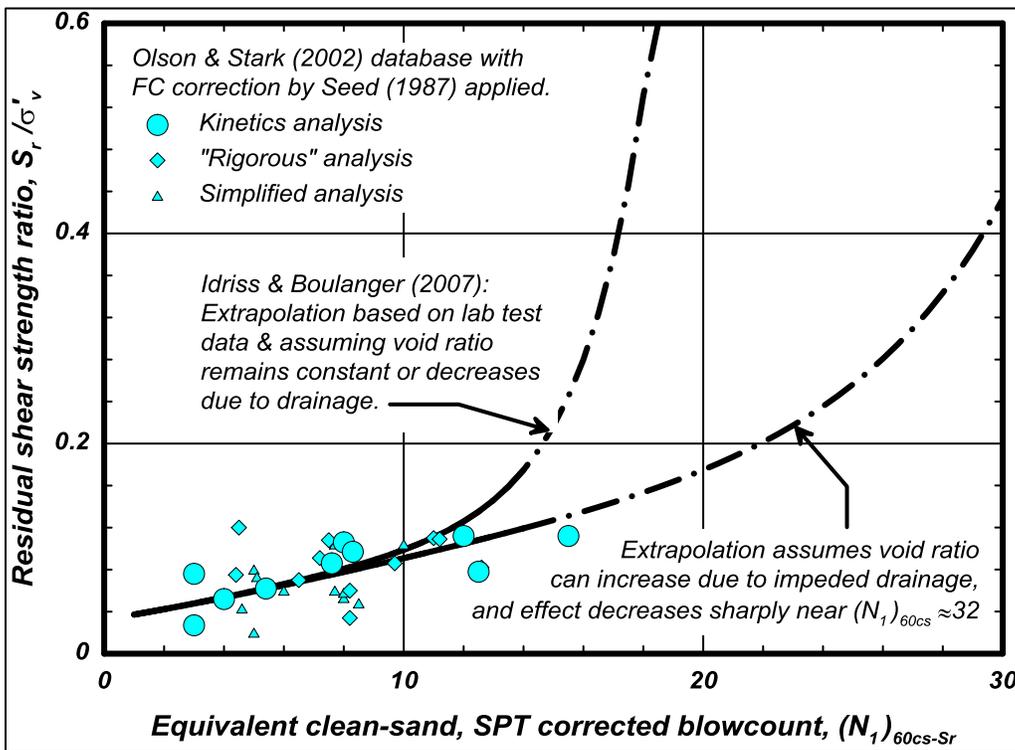

**Figure F3. Idriss and Boulanger [24] correlation for predicting residual
undrained shear strength ratio from SPT. Refer to table F1 for fines adjustment
(figure courtesy of Ross Boulanger).**

No clear correlation exists, in either figure F3 or Olson and Starks' equivalent figure, between increasing blow count and increasing strength ratio. Correlation

is somewhat improved if the case histories with effective overburden stress less than 1,000 lb/ft^2 are excluded, which drastically reduces the number of data available, as well as the range of blow counts. The data shown were not sorted to remove those with low overburden stresses; therefore, some of the highest ratios may not be relevant to a dam foundation with high overburden.

In figure F3, the curves have been extrapolated beyond the available field performance data on the basis of laboratory shear testing. They were not intended to be "best estimates" of S_{ur}. They are near the lower limits of the data and are the authors' recommendations for reasonably conservative values to use in a typical deterministic analysis. Stability and deformation analyses to support a risk analysis need to consider this and include the full reasonably likely range of behavior.

For large dams that apply high overburden stresses to their foundations, the strength-ratio concept would usually indicate higher strengths. However, it could be unconservative if strength ratios from field performance with low overburden stresses (the bulk of the case history data) are used in situations with high overburden stresses, such as the foundations of large embankment dams. Additionally, Idriss [34] has discouraged deterministic use of the "no void redistribution" curve in figure F3, except when a strong case can be made for free drainage at the top of a liquefying layer. With adjusted blow counts greater than 15, the difference between the two curves becomes very large, and it could make the difference between good and bad performance of the dam. **For risk analysis, it is often appropriate to consider the relative likelihood that the upper or lower curve would apply (or values in between), specifically for each dam and site geology. In addition, consider whether a direct-strength or hybrid approach to S_{ur} would be more nearly correct.** Future research may clarify the appropriate model.

Olson and Stark concluded that influence of fines content is minor, and examination of their data seems to support that conclusion. Idriss and Boulanger used the fines adjustment shown in table F1, the same as Seed [6] and Seed and Harder [11]. As stated above, the adjustment was based largely on theory and judgment because not enough field data exist to quantify it.

Similar to the Seed and Harder [11] correlation presented in section F.3.2.1 above, C_N values for developing figure F3 were slightly different from those in appendix C. Again, however, any error introduced is minor in comparison with other uncertainties.

As mentioned earlier, if piezometric levels vary with fluctuation in the reservoir level, the strength ratio is applied to the effective stress that would exist immediately prior to the earthquake (which may not be the same as it was at the time of testing). The latter is used only for adjusting the raw blow count N for effective overburden stress to obtain $(N_1)_{60}$.

F.3.3   Residual Undrained Shear Strength from Cone Penetrometer Test

Cone-penetrometer tip resistance can also be used to estimate post-liquefaction shear strength, S_{ur}. Cone tip resistance is usually normalized to a standard overburden pressure of 1 ton/ft^2, 1 atmosphere, 1 bar, 1 kgf/cm^2, or 100 kilopascals (kPa) (which are all essentially equal within the level of precision for this sort of measurement), and made dimensionless, as is described in appendix B for liquefaction triggering analysis. The resulting value, referred to as q_{c1N}, is analogous to $(N_1)_{60}$, in that it is a dimensionless index of density that is independent of the overburden stress. For general information on CPT test procedures and analysis, refer to Lunne, Robertson, and Powell [35] or Robertson and Cabal [36].

At present (2015), there is no published correlation that predicts the residual undrained shear strength, S_{ur}, directly from the CPT tip resistance (analogous to figure F2), but at least three correlations have been published that predict the residual undrained strength *ratio,* S_{ur} / σ'_{v0} [12, 13, 24]. They are essentially analogous to figure F3 for the SPT, except that only Idriss and Boulanger, and Robertson, incorporated a fines adjustment. Olson and Stark's correlation uses the tip resistance adjusted for overburden pressure, but not for fines.

None of the three correlations clearly fit the available data better than the others. Idriss and Boulanger's correlation (figure F4) was selected for this appendix for two main reasons:

(1) First, Olson and Stark did not extrapolate their relationship beyond the available data to values of q_{c1n} (without fines adjustment) greater than 60, so it does not provide any guidance for the most important values of q_{c1n} or $q_{c1ncs-Sr}$ for embankment dams. For a dam of even modest height, strengths and strength ratios associated with the historic flow slides are all so low that their precise value is immaterial to the performance of the dam. The important range is where the penetration resistance is too low to prevent liquefaction, but high enough that reasonable variation in S_{ur} could affect the outcome. With a fines adjustment, the important range of $q_{c1ncs-Sr}$ is roughly from 100 to 180.

(2) Idriss and Boulanger provide extrapolated curves for situations, both with and without void redistribution, even though there are no known case histories of flow slides with $q_{c1ncs-Sr}$ greater than 90. (The extrapolation was based on laboratory testing and theoretical considerations.) The absence of flow slides with $q_{c1ncs-Sr}$ greater than 90 suggests that void redistribution has not played an important role in those materials historically, but it may have done so for looser materials. In forward analysis, analysts and risk estimators should generally consider the

strength both ways and assess the likelihood that void redistribution would occur, case by case, unless it is obvious that free drainage would be inhibited by layers of lower permeability.

The piezometric level used for adjusting the cone tip resistance for effective overburden stress is the one that existed at the time of testing, which may be different from what it would be at the time of an earthquake. The latter is used for calculating the strength from a strength ratio.

F.3.3.1   Idriss and Boulanger Strength Ratio Correlation

Figure F4, from Idriss and Boulanger [24], shows S_{ur} / σ'_{v0} as two functions of the clean-sand-equivalent normalized CPT tip resistance, $q_{c1n\text{-}cs\text{-}Sr}$. The lower of the two curves is for sites where there is potential for void redistribution to create very weak loosened zones. The other curve is for sites where drainage at the top of a liquefied layer is able to prevent formation of a loosened zone.. As in the case of figure F4, Idriss does not encourage the use of the upper curve, unless a strong case can be made for drainage at the top surface or other mechanism to prevent a loosened zone [34]. (It may, however, be appropriate to use both curves in a probabilistic analysis, with relative likelihoods assigned to each.)
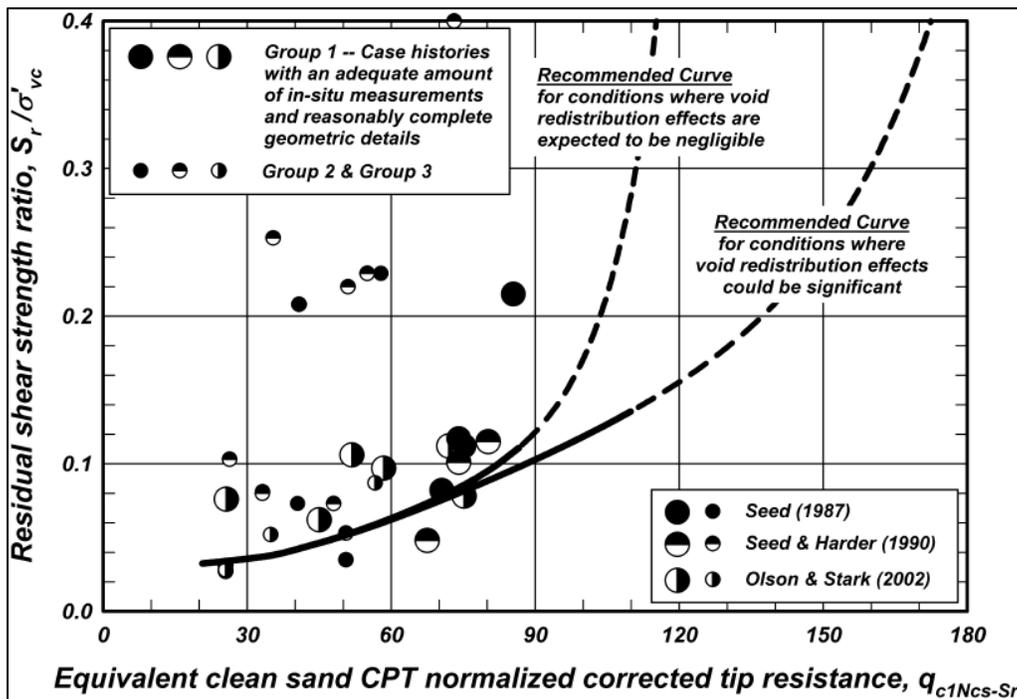

Figure F4. Idriss and Boulanger [24] correlation for S_{ur}/σ'_{vo} from CPT, for use with effective overburden stresses up to about 8,000 lb/ft^2.

The procedure for adjusting the measured tip resistance to obtain $q_{c1n\text{-}cs\text{-}Sr}$ is the same as described in appendix B to obtain $q_{c1n\text{-}cs}$, except for using a different fines adjustment. Once q_{c1n} has been calculated, the clean-sand equivalent normalized tip resistance (on the horizontal axis in figure F4) is found by adding an adjustment to account for the beneficial effect of fines for a given value of q_{c1n}:

$$q_{c1n\text{-}cs\text{-}Sr} = q_{c1n} + \Delta q_{c1n\text{-}cs\text{-}Sr} \hspace{3cm} \text{Equation F2}$$

The adjustment is taken from table F2, below, which is analogous to table F1. This value of $\Delta q_{c1n\text{-}cs\text{-}Sr}$ is specific to estimating residual undrained shear strength; it is different from the adjustment used to analyze liquefaction triggering with the CPT. Unfortunately, it requires one to know the fines content for each interval. Boulanger and Idriss [37] suggest a general correlation for predicting fines content from CPT tip resistance and friction ratio (in the form of the behavior type index, I_c,) but the data come from many sites with different material types, and the scatter in the data is substantial. One should use measured fines contents, or at least a site-specific correlation between measured fines contents and some parameter related to material characteristics, such as I_c. It is possible that more than one correlation would be needed for one site because of varying material types.

Table F2. Adjustment to qc1n-cs-Sr for Fines Content

Fines Content (percent)	$\Delta q_{c1n\text{-}cs\text{-}Sr}$
10	10
25	25
50	45
75	55

Similarly to figure F3, figure F4 provides one curve for sites where there is potential for redistribution of voids to create a weakened layer at the top of the liquefied material, and one curve for sites where free drainage would prevent formation of a loosened layer. These curves are not intended to be "best estimates" of S_{ur}. They are near the lower limits of the data and are Idriss and Boulanger's recommendations for reasonably conservative values to use in a typical deterministic analysis. The definition of the curves needs to be considered in risk analysis and in stability or deformation analyses to support a risk analysis. The data shown were not sorted to remove the ones with low overburden stresses, and some of the highest ratios may, therefore, not be relevant to the foundation of a dam embankment.

The piezometric level used in adjusting the cone tip resistance for effective overburden stress is the one that existed at the time of testing, which may be different from what it would be at the time of an earthquake.

F.3.3.2 Other Approaches

There are two other possibilities for estimating S_{ur} from CPT data: using the normalized tip resistance, q_{c1N}, to estimate an equivalent $(N_1)_{60}$ for use with figure F2, or using the CPT sleeve resistance directly as an approximation of the residual strength of the material, as suggested by Lunne, Robertson, and Powell [35].

No correlation has been published to relate S_{ur} directly to q_{c1N}, and while one could convert q_{c1JN} to an equivalent $(N_1)_{60}$, and use that with figure F2, it would require two empirical correlations to be applied in series (q_{c1N} to $(N_1)_{60}$, then $(N_1)_{60}$ to S_{ur}), compounding the uncertainties in each. That could, however, be a useful quick check on other estimates, and it does not depend on the currently controversial assumption that S_{ur} should be normalized by the effective overburden stress. An estimate of the equivalent $(N_1)_{60}$ from q_{c1N} would need to have the fines adjustment $\Delta(N_1)_{60}$ added to it to obtain $(N_1)_{60-cs}$ for use with figure F2. Typically, q_{c1N} is about 4.5 to 5.0 times $(N_1)_{60}$ for clean sand, so that a normalized tip resistance q_{c1N} of 60 would be roughly equivalent to a normalized blow count $(N_1)_{60}$ of about 12 or 13. The factor tends to be smaller in silty sands (about 3.5 to 4.0) and silts (as small as 3.0).

While appealing for its simplicity, the sleeve measurement cannot account for void migration or other gross-scale effects; its use should be limited to providing a quick check on other methods, possibly as an upper bound. The CPT sleeve resistance provides a rough measurement of the remolded or residual undrained strength of a soil if the permeability is not high enough to allow rapid dissipation of excess pore-water pressure. For the strength of liquefied materials, its use should be limited to materials with a significant amount of fines (perhaps 40 percent or more) to inhibit rapid dissipation of excess pore pressure. Even then, it should be considered a quick check on other methods because, as with any method where the strength is being *measured*, rather than back-figured from field performance, it could overestimate the actual strength if there is potential for void migration to create a loosened zone or water film at the top of the layer. Precise measurements may not be possible if the strength is very low compared to the range of the CPT sleeve load cell.

F.3.4 Field Vane Shear Tests

For soils that are suitable for the VST, the measured post-peak (remolded) strength from VST can provide a rapid, inexpensive indication of the residual or remolded undrained shear strength. Clayey silts, silty clays, and low-plasticity

clays can be liquefiable if low enough in plasticity. (Even without liquefaction, they may be sensitive, so that large earthquake-induced strains would cause a major reduction in shear strength.) Limited data from Charlie et al. [28] show reasonable agreement between VST remolded strength and the SPT-based correlation in figure F2 in silty sands. Also, VST measurements in liquefied fine tailings at Mochi Koshi, Japan, shortly after the earthquake that caused the slope failure [38], agreed well with the strength back-calculated by Seed [6]. The use of VST to determine S_{ur} of sandlike materials is not common, but its use can be considered when the materials are suitable, i.e., having sufficient fines content to minimize drainage, little or no gravel, and few interbeds of weaker material. Reclamation's Technical Service Center laboratory, in Denver, Colorado, is equipped to do field VST.

The shearing resistance mobilized by the VST after several full rotations provides a more direct indication of S_{ur} than do other *in situ* tests, and it has the advantage over laboratory testing that the VST can be run at extremely large strains, comparable to those in actual flow slides. The strength of soils is almost always anisotropic. Most of the resistance to rotation of the vane comes from shearing along the cylindrical vertical portion of the surface sheared in the test, but potential sliding surfaces are commonly closer to horizontal than to vertical. Thin, weak layers would, in effect, make the strength of the soil mass highly anisotropic. Unless the vane is almost completely within a weak layer, the lower strength would not be detected. The CPT is superior in that regard because the data are recorded every 2 to 5 cm. For static stability and bearing capacity, the VST strength of clayey soils is usually adjusted by an empirical factor (e.g., Bjerrum [39]). This compensates for the effects of anisotropy, strain rate, and the fact that the sheared surface at peak torque can differ significantly from the cylinder that is generally assumed. Charlie et al. [28] did not include an adjustment of this sort.

For estimating S_{ur}, the test must be run with sufficiently high rotation rate that the sheared soil is essentially undrained during the course of the test, and enough rotation must occur to ensure that the material has reached its residual strength. For guidance on testing, refer to ASTM D-2573-08. Note, however, that rotation rates higher than those specified by D-2573-08 may be needed to minimize dissipation of excess pore-water pressure during shearing; dissipation could cause the VST to overpredict the S_{ur}. (CPT pressure dissipation tests may provide some guidance on rotation rates.)

Because residual strengths are generally small, the VST device should be equipped with slip couplings, so rod friction can be measured and adjusted for.

Like any other measurement of S_{ur}, VST cannot account for effects of void migration or other gross-scale effects, so it is probably best to consider VST as providing a "soft" upper bound on S_{ur}, to corroborate other methods, such as correlation of S_{ur} with penetration resistance. Weakening by void migration

becomes less likely with increasing fines and plasticity, but it could be very important for cohesionless sands and silty sands. Because of the mechanics of yield in the VST, and strength anisotropy and other behaviors of clayey soils, the peak strength from the VST in clayey soils is generally adjusted by an empirical factor that is based on case histories of slope failures. A different adjustment may be needed for residual strength measurements, but none has ever been established. Like any other test, the VST measurement cannot be considered a true direct measurement of the residual undrained shear strength. In strongly anisotropic soils, the measured torque is largely controlled by the vertical cylindrical portion of the sheared surface around the vane.

F.3.5   Laboratory Strength Testing for Liquefiable Granular Soils

This section provides background information only, not detailed description of undisturbed sampling and laboratory shear testing for liquefied granular soils.

Several procedures have been proposed for estimating the post-liquefaction residual undrained shear strength using laboratory testing [14, 16, 40]. All of them involve recovery of "undisturbed" samples of the material in question and undrained cyclic or monotonic shear testing. Cyclic laboratory tests can be used to simulate the buildup in pore-water pressure experienced during earthquake loading, and to evaluate the corresponding decrease in strength. The same general behavior can sometimes be observed in undrained monotonic tests, although monotonic tests do not provide any indication of the number of cycles of a given stress that is required to initiate liquefaction. Tests on reconstituted samples are important in research and may also be useful for determining general *trends* in behavior for a specific site, even if they cannot be considered direct measurements of S_{uss} or S_{ur}. Good examples of their use are provided by Pillai and Salgado [15], and by Castro et al. [41]. Sampling and testing can be very expensive, which is one reason their use is not common for assessing liquefaction potential and post-earthquake residual undrained shear strength.

As discussed in earlier sections of this appendix, laboratory shear tests on small volumes of material cannot account for soil-mass behaviors, such as void redistribution and nonuniformity, and strains in common laboratory devices are limited to values far below those that occur in flow slides. For that reason (in addition to the cost), laboratory procedures for assessing the post-liquefaction undrained shear strength are not frequently used, and they are not included in this appendix. They may, however, be useful occasionally for understanding the behavior of foundation materials at the site, as long as their limitations are recognized and documented.

No sample is truly undisturbed, and sampling, handling, and consolidation of loose, nonplastic to slightly plastic soils prior to testing generally lead to densification. Compared to the drained friction angle, for example, undrained shear strength is very sensitive to minor changes in density. Laboratory testing must include procedures to minimize and account for disturbance. The process of retrieving a sample from the ground inevitably results in some disturbance, no matter how careful the drillers are. The confining stress on the sample is relieved by drilling and sampling, and the sample rebounds as a result. Because the measured residual strength is very sensitive to void ratio, interpretation must account for changes in void ratio during sampling and reconsolidation, and their effect on residual strength.

The steady-state shear strength determined in laboratory tests, S_{uss}, is quite sensitive to the stress path; direct simple shear and triaxial extension tests generally give strengths that are substantially lower than triaxial compression tests. (This is not the same as the residual undrained shear strength that can be mobilized in the field, S_{ur}, which can be significantly lower than S_{uss}.) Some soils that are initially contractive then become dilative in monotonic triaxial compression tests can be purely contractive in simple shear or triaxial extension [30, 42]. By theory, the critical-state or steady-state strength should be independent of the type of the stress path. The difference between theory and measurement may be because the strains in laboratory tests are not sufficient for the soil to truly reach the steady state or critical state in all types of tests. Although the load path in most stability analyses on embankment dams with liquefied foundations is a combination of compression, simple shear, and extension, the simple shear test is thought to best approximates the "average" load path. (The resistance to liquefaction in laboratory cyclic tests also depends on the type of test.)

Recognizing that laboratory samples are never truly undisturbed, the steady-state procedure was developed to explicitly account for the effects of disturbance [14, 19, 41]. Samples are taken from the zones judged most likely to liquefy, based on penetration resistance, shear-wave velocity, and/or soil type. Every effort is made to minimize disturbance and changes in void ratio during sampling, shipping, and testing, and the changes that do occur are tracked very carefully. Each sample is tested in undrained monotonic triaxial compression to determine its laboratory steady-state strength at large strain. A suite of tests is also run on remolded composite (mixed) samples of material from the same deposit at different void ratios to determine the slope of the steady-state line, i.e., the curve of steady-state strength *versus* void ratio. It is then assumed that the slope of the steady-state line is similar throughout the deposit, with only the position of the steady-state line varying from point to point due to minor variations in grain-size distribution. The in situ steady-state strength at each sample location is estimated by adjusting the laboratory strength for the changes in void ratio during sampling and testing, assuming the same slope of undrained strength *versus* void ratio.

The steady-state method is difficult to implement properly, and it is not widely used in practice at this time (2015). However, this procedure was used for several Reclamation dams in the 1980s, and the results may be encountered in older reports.

F.4 Strength Considerations for Nonliquefiable Claylike Materials

These are Category 3 materials, as described in section F.1.

F.4.1 General Concepts of Undrained Shear Strength

The behavior of saturated, normally consolidated or lightly overconsolidated claylike soils under dynamic loading is generally governed by their undrained shear strength. Depending on the situation, this could be the peak shearing resistance in monotonic loading, the resistance to yield in repeated cycles of loading, or the monotonic resistance at very large strain after the soil has been subjected to numerous cycles of smaller strains (post-cyclic monotonic strength). In the event that a sensitive clay is subjected to very large strains, the analysis may even need to consider the remolded strength of a sensitive clay subjected to very large strains. The applicable shear strength(s) depend on the expected amount of shear strain and the sensitivity of the soil, and the strength of the soil can degrade during the course of the earthquake. There is not always a single "correct" representation for a given situation; risk analysis may, therefore, have to include nonzero probabilities for more than one type of undrained strength, or undrained strength that evolves from peak, to post-peak, to remolded during the course of an earthquake.

For many materials, the undrained shear strength can be assessed by the same methods that are used to assess the strength for monotonic loading. Among these methods are SHANSEP (Stress History and Normalized Soil Engineering Properties) (Ladd and Foott [43] and Ladd [44,45]), in situ measurements, and/or an adaptation of the Duncan, Wright, and Wong [46] method of estimating strength for rapid-drawdown stability of submerged slopes.

The initial yield accelerations for dams with clay foundations should be calculated using peak undrained strengths. It is common for the yield acceleration to be much smaller than the ground motion possible at the site, and it may decrease with softening of the clay during the course of the earthquake. This does not necessarily mean that large deformations would occur, however. Depending on

the severity of loading (peak acceleration and duration of shaking) and the stress-strain behavior of the clay (peak and post-peak strengths, and the amount of strain required to degrade the strength), the deformation is usually limited to intermittent small deformations. Momentary yield during the stronger cycles of loading would be expected to cause some settlement and deformation in shear, but typical clays are capable of undergoing strains of 5 percent or much more without large decreases in shearing resistance.

Large-magnitude earthquakes typically cause many cycles of loading, which can cause enough remolding and strength degradation that the strength at the end of the earthquake is somewhat lower, or even much lower than the strength at the beginning of the earthquake. This is of particular concern with subduction-zone earthquakes possible in the Pacific Northwest.

The term "cyclic failure" is used to indicate yield and permanent strain of claylike soils, but it should not be confused with slope failure or severe strain softening. In laboratory testing, cyclic failure may be defined to mean yield with strains as small as 3 percent, which is far different from failure of a slope because clays can usually withstand much larger strain without severe loss of strength. Some publications have recommended that strengths be reduced by 20 percent in deformation analysis because permanent strains begin to accumulate with cyclic stresses as low as 80 percent of the monotonic yield strength. However, this general recommendation is not included here, because the permanent strains prior to yield are probably too small to compromise the safety of an embankment dam. Exceptions could occur if appurtenant structures are embedded in the embankment, if the freeboard is unusually small, or in other circumstances.

Sensitive clays, however, can be drastically weakened by modest amounts of strain, unlike typical clays. Some clays are sensitive enough that their remolded strength is not sufficient to maintain static stability of a dam embankment at the end of an earthquake. Apparently, clay sensitivity played a major part in the Fourth Avenue landslide in Anchorage during the 1964 Alaskan Earthquake; the slide moved much farther than it would have with typical insensitive clay [1, 47, 48]. It slide was one of very few known examples of earthquake-induced, large deformations associated with sensitive clay. There is little information available from either field performance or laboratory testing to indicate how rapidly the decrease in shearing resistance occurs with slide displacement. At present (2015), there is no simple or precise way to predict the amount of displacement required to shear the soil past the peak strength, through post-peak (softened) strength, to the remolded strength. Field VST may provide a qualitative indication (by how quickly the shearing resistance drops with increased rotation after the peak), but the strains cannot actually be measured with VST. As a general rule, the more sensitive the soil, the smaller the strain required to cause large reductions in shearing resistance. The foundation clay in the Alaskan example was moderately

sensitive (sensitivity ≈ 4), and the reduction from the peak strength was estimated to begin with less than 1 foot of deformation, with remolded strength reached after less than 10 feet. Comparable case histories are rare, and this one may not be typical of the behavior of clays in general.

Reclamation has applied these concepts to B.F. Sisk Dam in California, Scoggins Dam in Oregon, and Arthur V. Watkins Dam in Utah. The latter is of interest because of the sensitivity of some clayey foundation soils.

A comprehensive study by Boulanger and Idriss [1] addressed cyclic failure and liquefaction of fine-grained soils in a framework similar to that used for liquefaction triggering in granular soils. The effect of sloping ground and high static shear stress (high α) is accounted for in their analysis by K_α, analogous to K_α in liquefaction triggering analysis. (The coefficient α is the ratio of static shear stress to effective normal stress on a horizontal plane.) For clays, however, the value of K_α is always less than 1 (indicating that α is never beneficial in preventing cyclic failure), and it drops rapidly below 1.0 with increasing α. With high α, as exists under an embankment slope, the ground acceleration required to cause cyclic failure, as predicted by the analysis by Boulanger and Idriss is similar to that predicted for the yield acceleration by a simple pseudostatic slope stability analysis using conventional undrained shear strength. Hence, details of the Boulanger and Idriss analysis are not presented here.

In determining undrained shear strength, one must consider the effect of stress rotation, i.e., changes in the orientation of the principal stresses during shearing from their orientation during consolidation. For example, for a given preconsolidation pressure, an anisotropically consolidated, triaxial compression test (major principal stress in the same direction as in anisotropic consolidation) gives higher shear strength than shearing in simple shear (principal stresses rotated 45 degrees or more). In turn, simple shear gives a higher strength than shearing in triaxial extension (principal stresses rotated 90 degrees). In the foundation of a dam loaded by large horizontal accelerations, the stress path would most closely resemble simple shear. Along a steeply inclined shear surface in the core of an embankment, the stress path would more nearly resemble triaxial compression (with anisotropic consolidation).

F.4.2 Stress History and Normalized Soil Engineering Properties

SHANSEP is a system for characterizing the strength of saturated clayey materials by undrained strength ratios, S_u / σ'_{vo}, where S_u is the undrained strength, and σ'_{vo} is the effective overburden stress [43, 44, 45]. The value of the ratio depends on the material, its overconsolidation ratio (OCR), and the stress path, as shown in equation F11:

$$S_u / \sigma'_{vo} = S(OCR)^m \qquad\qquad \text{Equation F11}$$

where S is the strength ratio for normally consolidated conditions, and m is an exponent that accounts for the relatively small decrease in undrained shear strength as the effective overburden stress is removed from a normally consolidated clay, making its OCR greater than 1.0. S varies with the stress path and rotation of principal stresses. For the peak strength in monotonic simple shear, S is typically between 0.20 and 0.26, with higher and lower values measured in triaxial compression and triaxial extension, respectively. The exponent m is typically 0.7 to 0.9.

Clay in the foundation of many dams is normally consolidated (OCR = 1.0) under the downstream slope because of the weight of the dam. However, farther upstream, the soil may be normally consolidated when the reservoir is empty, but become lightly overconsolidated when the reservoir is high (OCR as high as 1.9). The higher reservoir increases the pore-water pressure and decreases the effective stress, increasing the OCR. If upstream portions are assumed to be normally consolidated when the reservoir is full, the results can be unnecessarily conservative. At a very high OCR, the undrained strength can be greater than the drained strength, in which case the drained strength should be used; the higher undrained strength requires negative excess pore-water pressure, which cannot be relied upon. Values of OCR can be obtained from oedometer (one-dimensional) consolidation tests and from analysis of stress history and settlement records if they are available. (It is also possible to estimate OCR roughly using the CPT, but it requires some assumptions.) The values of S and m are best obtained from laboratory shear testing of undisturbed samples tested with precisely controlled (and, therefore, precisely known) preconsolidation pressures and OCRs. These may include anisotropically consolidated triaxial compression, triaxial extension, and direct simple shear tests. Field VST and CPT can be very helpful in determining the value of S or S_u in material with low OCR (in conjunction with oedometer tests to determine the preconsolidation pressure). If direct simple shear testing is not readily available, it may be reasonable to assume the DSS strength ratio is halfway between the values from triaxial compression and from triaxial extension, or slightly lower.

SHANSEP provides a useful framework for organizing and combining all available in situ and lab strength measurements with in situ stress history, so they can be used to create a unified strength model for an entire deposit of clayey material, rather than looking at it point by point. For examples of application, see references [44] and [45] by Ladd. Strength data, whether as S_u or normalized as S_u / σ'_{vo} (or both), should be plotted on geologic cross sections for selecting values to put into analyses and for documentation.

F.4.3 In Situ Testing

The VST provides a fairly direct measurement of both peak and remolded strengths of fine-grained materials, and it, therefore, provides a good indication of sensitivity. Refer to ASTM D2573-08 for test procedures. Peak strengths from the VST are ordinarily adjusted downward because of differences between stress and strain conditions in the test and those in static slope stability [39]. The high strain rates in the VST can cause the measured shearing resistance to be higher than the "static" strength. High strain rates would also occur during earthquake loading, so applying the typical adjustment may create a conservative bias in dynamic deformation analysis. However, at the end of the earthquake, the embankment needs to be statically stable, so there would be no benefit from high strain rates; the adjustment is, therefore, required in analyzing post-earthquake stability.

The CPT provides an indirect measurement of the peak undrained shear strength, S_u. The cone tip resistance, q_t is governed by the undrained strength and the overburden stress. The strength can be estimated from equation F12:

$$S_u = (q_t - \sigma_v) / N_{kt} \hspace{3cm} \text{Equation F12}$$

where q_t is the measured tip resistance, σ_v is the total overburden stress, and N_{kt} is an empirical factor that can vary between about 10 and 20 [36]. The value of N_{kt} depends on a number of factors, including sensitivity of the clay and the type of test the correlation was referenced to. Considering that the most relevant reference test would usually be undrained direct simple shear, which generally gives lower peak strengths than undrained triaxial compression, and that there can be some degradation of strength from repeated loading, it would be appropriate to use only N_{kt} values of 16 to 20, unless a site-specific testing program (referenced to appropriate lab or in situ tests) shows that a lower value can be used (giving higher values of S_u).

The CPT sleeve resistance in clayey materials is roughly equal to the remolded shear strength, but the CPT does not provide a post-peak or softened undrained shear strength that is intermediate between the peak and remolded strengths. Furthermore, the remolded strength may be too small for the sleeve load cell to provide a precise measurement. When it is feasible, VST is likely to provide a better measurement of post-peak and remolded shear strength.

Correlations do exist for estimating the peak strength of clays from the SPT blow count [49, 50]. However, their use is not encouraged because of imprecision and inconsistency among the various correlations (resulting, in part, from the different strength tests they are referenced to, and from differences in SPT equipment).

F.5 Conclusions and General Recommendations

As described in this appendix, embankment and foundation soil materials fall into three main categories for estimating their shearing resistance for use in dynamic deformation and post-earthquake stability analyses. These are: (1) nonliquefiable granular materials, (2) liquefiable materials, and (3) nonliquefiable fine-grained materials. The considerations for the first and third groups are fairly similar to considerations for monotonic shear strengths of the same materials. The exception to that is that fine-grained materials may need post-peak or remolded undrained strengths if the yield acceleration would be exceeded enough during the earthquake to cause very large strains.

The second group, liquefiable granular and fine-grained soils with little or no plasticity, is of greatest concern for dam safety, but it is the most difficult group for which to quantify shear strength for seismic analysis. Currently available methods to estimate their post-earthquake undrained shear strength all have substantial drawbacks and uncertainties. None of them provides a precise, direct measurement of the strength that could be mobilized to resist instability or deformation. Precision is simply not available, and for a given set of foundation data (SPT results, water contents, etc.), the plausible range of post-earthquake strengths is generally rather wide. However, this does not necessarily result in a wide range of predicted deformations or factors of safety; if the liquefied materials are very weak relative to the dynamic or static applied stresses, doubling or tripling the strength may have a proportionately very small effect on the overall resistance to shearing.

There are, of course, transitional materials for which the most correct category and method of estimating the shear strength may not be obvious. In those cases, it is generally necessary to apply procedures for any category that could apply. For a probabilistic analysis, the full range of reasonably likely values needs to be considered, recognizing the uncertainty both in the choice of soil category and in the results of the methods used within each category. Stability and deformation analyses to support a probabilistic study should be focused on determining the sensitivity of the results to strength assumptions. Laboratory shear testing can be helpful in characterizing the behavior of the material qualitatively, although often it cannot produce a precise measurement of the shear strength that could be mobilized in situ.

Even if the soil category is obvious, prudent practice for probabilistic or deterministic analysis requires consideration of historic precedents from liquefaction and flow-slide case histories. While recognizing that the available data are far from exhaustive and that their interpretation is not an exact science, strong technical justification is required for use of strengths that are substantially

outside the profession's range of experience. Because of the many sources of uncertainty, it may be appropriate to design new dams or modifications using a value considerably below the "best estimate." In probabilistic risk analyses, it is usually necessary to consider reasonable ranges of strength values and their influence on stability and deformation, rather than simply defaulting to conservative values.

The level of investigation should be tailored to the potential benefit. More extensive investigations are justified when there is potential for cost savings in a design to be greater than the cost of the investigation, and or especially when more investigation could lead to a decision not to modify an existing dam.

This appendix does not include any detailed guidance on coupled nonlinear analysis that includes generation of excess pore-water pressure with shaking and changes in strength with pore-water pressure. At present (2015), the state of practice for coupled analysis is still rapidly evolving.

References

[1] R.W. Boulanger and Idriss, I. M., *Evaluating the Potential for Liquefaction or Cyclic Failure of Silts and Clays,* Report No. UCD/CGM-04/01, Center for Geotechnical Modeling, Department of Civil and Environmental Engineering, University of California, Davis, 2004.

[2] "An Approach to Evaluating the Potential for Dynamic Strength Loss of Soils at Dam Sites," Erik J. Malvick, Richard J. Armstrong, Kristen M. Martin, and Phu L. Huynh, *Proceedings, 34th Annual United States Society on Dams Conference,* San Francisco, California, April 7-11, 2014.

[3] "Stability of Slopes and Embankments During Earthquakes," W.F. Marcuson, and M.E. Hynes, *Proceedings, American Society of Civil Engineers/Pennsylvania Department of Transportation Geotechnical Seminar,* Hershey, Pennsylvania, 1990.

[4] *Liquefaction of Soils During Earthquakes*, Report No. CETS-EE-001, National Research Council, Committee on Earthquake Engineering, Washington DC, 1985.

[5] "On liquefaction," R.V. Whitman, R. V., *Proceedings, 11th International Conference on Soil Mechanics and Foundation Engineering,* San Francisco, CA, A.A. Balkema, pp. 1923–926, 1985.

[6] "Design Problems in Soil Liquefaction," H.B. Seed, *Journal of Geotechnical Engineering,* American Society of Civil Engineers, Vol. 113, No. 8, 1987.

[7] "Water Film in Liquefied Sand and Its Effect on Lateral Spread," Takeji Kokusho, *Journal of Geotechnical and Geoenvironmental Engineering*, Vol. 125, No. 10, pp. 817–826, 1999.

[8] "Simulations of a Centrifuge Test with Lateral Spreading and Void Redistribution Effects," R. Kamai, and R.W. Boulanger, *Journal of Geotechnical and Geoenvironmental Engineering,* Vol. 139, No. 8, pp. 1250-1261, 2013.

[9] "Simplified Procedure for Evaluating Soil Liquefaction Potential," H.B. Seed, and I.M. Idriss, *Journal of the Soil Mechanics and Foundations Division,* American Society of Civil Engineers, Vol. 97, No. SM9, September 1971.

[10] "Test Procedures for Measuring Soil Liquefaction Characteristics,"
H.B. Seed, and W.H. Peacock, *Journal of the Soil Mechanics and
Foundations Division,* American Society of Civil Engineers, Vol. 97,
No. SM8, August 1971.

[11] "SPT-Based Analysis of Cyclic Pore Pressure Generation and Undrained
Residual Strength," R.B. Seed, and L.F. Harder, Jr., *Proceedings,
H. Bolton Seed Memorial Symposium,* Volume 2, British Columbia,
Canada, May 1990.

[12] "Liquefied Strength Ratio from Liquefaction Flow Case Histories,"
S.M. Olson, and T.D. Stark, *Canadian Geotechnical Journal,* Vol. 39,
No. 3, pp. 629-647, 2002.

[13] "Evaluation of Flow Liquefaction and Liquefied Strength Using the Cone
Penetration Test," Peter K. Robertson, *Journal of Geotechnical and
Geoenvironmental Engineering,* American Society of Civil Engineers,
Vol. 136, No. 6, pp. 842-853, 2010.

[14] "Liquefaction Evaluation Procedure," S.J. Poulos, G. Castro, and
J.W. France, *Journal of Geotechnical Engineering,* American Society of
Civil Engineers, Vol. 111, No. 6., 1985.

[15] "Post-Liquefaction Stability and Deformation Analysis of Duncan Dam,"
V.S. Pillai, and F.M. Salgado, *Canadian Geotechnical Journal,* Vol. 31,
No. 6, pp. 967-978, 1994.

[16] "Liquefaction and Flow Failure During Earthquakes," K. Ishihara,
33rd Rankine Lecture, Géotechnique, Vol. 43, No. 3, pp. 351-415, 1993.

[17] *Residual Strength of Sand from Dam Failures in the Chilean Earthquake of
March 3, 1985*, Report No. UCB/EERC-87/11, P. de Alba, H.B. Seed,
E. Retamal, and R.B. Seed, Earthquake Engineering Research Center,
Oakland, California, 1987.

[18] "Residual Strength and Large-Deformation Potential of Loose Silty Sands,"
Mohammad H. Baziar, and Ricardo Dobry, *Journal of Geotechnical
Engineering,* American Society of Civil Engineers, Vol. 121, No. 12,
pp. 896-906, 1995.

[19] "On the Behavior of Soils During Earthquakes - Liquefaction," G. Castro,
*Soil Dynamics and Liquefaction, Developments in Geotechnical
Engineering 42,* Computational Mechanics Publications, pp. 169-204,
1987.

[20] "Instrumented Laboratory Flowslides," J.D. Eckersley, *Géotechnique*, Vol. 40, No. 3, pp. 489-502, 1990.

[21] Participant Written Summary, Pedro de Alba, *Preliminary Proceedings, National Science Foundation Workshop on Post-Liquefaction Shear Strength of Granular Soils,* Urbana, Illinois, April 17-18, 1997.

[22]   "In-Situ Testing for Liquefaction Evaluation of Sandy Soils," Catherine E. Fear (Wride), Ph.D. Dissertation, University of Alberta, Edmonton, Alberta, 1996.

[23] "SPT- and CPT-Based Relationships for the Residual Shear Strength of Liquefied Soils," I.M. Idriss, and R.W. Boulanger, *Proceedings, 4th International Conference on Earthquake Geotechnical Engineering,* Thessaloniki, Greece, 2007.

[24] *Soil Liquefaction During Earthquakes*, Monograph MNO-12, I.M. Idris, and R.W. Boulanger, Earthquake Engineering Research Institute, Oakland, California, 2008.

[25] "Evaluation of Residual Shear Strength of Sands During Liquefaction from Penetration Tests," Peter K. Robertson, *Proceedings, 43rd Canadian Geotechnical Conference,* Vol. 1, Laval University, Quebec City, Quebec, Canada, p. 257-262, 1990.

[26] "An Empirical Model for Estimation of the Residual Strength of Liquefied Soil," S.L. Kramer and C-H Wang, in press, 2015.

[27] Personal communication, R.B. Seed, 2013.

[28] "Measurement of Post-Liquefaction Shear Strength from Piezovane™ Field Tests," W.A. Charlie, T.J. Siller, and D.O. Doehring, *Preliminary Proceedings, National Science Foundation Workshop on Post-Liquefaction Shear Strength of Granular Soils,* Urbana, Illinois, April 17-18, 1997.

[29] "On the Use of Empirical Correlations for Estimating the Residual Undrained Shear Strength of Liquefied Soils in Dam Foundations," Paper No. 4.26b, D.R. Gillette, *Proceedings, 5th International Conference on Recent Advances in Geotechnical Engineering and Soil Dynamics,* San Diego, California, 2010.

[30] "Factors Affecting the Apparent Position of the Steady-State Line," Michael F. Riemer, and Raymond B. Seed, *Journal of Geotechnical and Geoenvironmental Engineering,* American Society of Civil Engineers, Vol. 123, No. 3, pp. 281-288, 1997.

[31] "Undrained Shear Strength of Liquefied Sands for Stability Analysis," Timothy D. Stark, and Gholamreza Mesri, *Journal Of Geotechnical Engineering,* American Society of Civil Engineers, Vol. 11, No. 11, pp. 1727-1747, 1992.

[32] "An Update to the Seed-Idriss Simplified Procedure for Evaluating Liquefaction Potential," I.M. Idriss, *Proceedings, TRB Workshop on New Approaches to Liquefaction,.* Publication No. FHWA-RD-99-165, l999.

[33] "Development of a Correlation Between Residual Strength and $(N_1)_{60}$ for Lateral Spreads in Natural Materials," Mathew A. Mabey, and T. Leslie Youd, *Preliminary Proceedings, National Science Foundation Workshop on Post-Liquefaction Shear Strength of Granular Soils,* Urbana, Illinois, April 17-18, 1997.

[34] Personal communication, I.M. Idriss, circa 2009.

[35] "Cone Penetration Testing in Geotechnical Practice," T. Lunne, P.K. Robertson, and J.J.M. Powell, Blackie Academic and Professional, London, England, 1997.

[36] "Guide to Cone Penetration Testing for Geotechnical Engineering," P.K. Robertson, and K.L. Cabal, Gregg Drilling and Testing, Inc., Signal Hill, California, 2007.

[37] *CPT and SPT Based Liquefaction Triggering Procedures, Report No. UCD/CGM-14/01*, R.W. Boulanger, and I.M. Idriss, University of California at Davis, Center for Geotechnical Modeling, Davis, California, 2014.

[38] "Liquefaction of Mine Tailings in the 1978 Izu-Ohshima-Kinkai Earthquake, Central Japan," Shegeyasu Okusa, So Anma, and Hiromu Maikuma, *Proceedings, 7th World Conference on Earthquake Engineering,* Istanbul, Turkey, Vol. 3, pp. 89-96, 1980.

[39] "Problems of Soil Mechanics and Construction on Soft Clays," Laurits Bjerrum, *Proceedings, 8th International Conference on Soil Mechanics and Foundation Engineering,* Moscow, Russia, Vol. 3, pp. 111-159, 1973.

[40] "Liquefaction and Postliquefaction Behavior of Sand," Y.P. Vaid, and J. Thomas, *Journal of Geotechnical Engineering,* American Society of Civil Engineers, Vol. 121, No. 2, pp. 163-173, 1995.

[41] "Steady State Strength Analysis of Lower San Fernando Slide," G. Castro, R.B. Seed, T.O. Keller, and H.B. Seed, *Journal of Geotechnical Engineering,* American Society of Civil Engineers, Vol. 118, No. 3, pp. 406-427, 1992.

[42] Participant Written Summary, Peter K. Robertson, *Preliminary Proceedings, National Science Foundation Workshop on Post-Liquefaction Shear Strength of Granular Soils,* Urbana, Illinois, April 17-18, 1997.

[43] "New Design Procedure For Stability Of Soft Clays," C.C Ladd, and R. Foott, *Journal of the Geotechnical Engineering Division,* Vol. 100, No. GT7, pp. 763-786, 1974.

[44] "Stability evaluation during staged construction (22nd Terzaghi Lecture)." C.C. Ladd, C.C. (1991). *J. of Geotech. Eng.*, Vol. 117, No. 4, pp. 540-615, 1991.

[45] "Recommended Practice for Soft Ground Site Characterization: Arthur Casagrande Lecture," C.C. Ladd, and D. DeGroot, *12th Panamerican Conference on Soil Mechanics and Geotechnical Engineering,* June 23-25, 2003, Cambridge Massachusetts, 2004.

[46] "Slope Stability During Rapid Drawdown," J.M. Duncan, S.G. Wright, and K.S. Wong, *Proceedings, H. Bolton Seed Memorial Symposium,* Volume 2, British Columbia, Canada, May 1990.

[47] "Fourth Avenue Landslide During 1964 Alaskan Earthquake," T.D. Stark, and I.A. Contreras, *Journal of Geotechnical and Geoenvironmental Engineering,* Vol. 124, No. 2., pp. 99-109, 1998.

[48] "Evaluating seismic risk in engineering practice." I.M. Idriss, (1985). *Proceedings, 11th International Conference on Soil Mechanics and Foundation Engineering,* San Francisco, CA, Vol. 1, Balkema Publishers, The Netherlands, 255-320.

[49] "Soil Mechanics in Engineering Practice," K. Terzaghi, and R. Peck, John Wiley and Sons, Inc., New York, New York, 1967.

[50] "Correlation of Field Penetration and Vane Shear Test for Saturated Cohesive Soils," Laboratory Report No. EM 586, Bureau of Reclamation, Denver, Colorado, 1960.

Appendix G

Improving the Seismic Resistance of Existing Dams

Contents

Figures

Figures (continued)

G.1 Introduction

This appendix provides a general overview of remedial measures and soil improvement methods that may be useful for improving the earthquake performance of embankment dams and the Bureau of Reclamation's (Reclamation) experience with these methods. Verification of foundation improvement, which can be a time-consuming and costly part of the remediation process, is also discussed, as is analysis of proposed modifications to demonstrate adequacy of designs.

The potential failure modes most commonly addressed by embankment dam modifications are

- Very large settlement due to post-earthquake instability (gravity-driven) and/or dynamic deformation from strong shaking, causing overtopping of the dam, typically a result of liquefaction of the foundation or poorly compacted embankment

- Internal erosion through cracks caused by shaking, possibly exacerbated by liquefaction and large deformations, or by the presence of structures within the embankment

- Structural failure of spillway walls or other structures within or adjacent to the embankment

The first two potential failure modes are covered here; spillway retaining walls are addressed in other publications. Less commonly seen are potential failure modes resulting from sensitive clays or fault rupture in dam foundations.

Instead of modifying an existing embankment, one can completely remove it, improve the foundation as needed, then reconstruct the embankment more or less within its original footprint. Reclamation did this for Jackson Lake Dam, located in Grand Teton National Park in Wyoming, in part because the original embankment consisted of loose hydraulic fill, but also because it did not require taking any additional land from the national park to build stability berms. Removing the dam required almost completely draining the reservoir, with loss of benefits during construction for both water deliveries and recreation.

G.2 Stabilizing Embankment Slopes

Stabilizing the slopes of an existing embankment against dynamic deformation (driven by shaking) or post-earthquake instability most commonly involves foundation treatment, to create a strong "shear key" of nonliquefiable material within the foundation, and placement of a berm over the key to buttress the slope

of the dam and increase the strength of the key (by increasing the vertical effective stress). Most of the seismic modifications that Reclamation has constructed have incorporated this concept, including those for Casitas (California), Bradbury (California), Scofield (Utah), Steinaker (Utah), and Cold Springs (Oregon). Both downstream and upstream slopes can be stabilized this way, but the former has been much more common at Reclamation dams. The key is usually formed of densified soil or of soil-cement, but a few other approaches have also been used. Deciding which approach to use is based on the nature and depth of the materials to be treated or replaced, working conditions at the site, and safety of the dam during construction.

As a general rule, performing soil improvement as closely as practical to the centerline of an existing embankment would minimize the overall volume of soil needing improvement and the volume of borrow material needed for the berm. On the other hand, working farther from the centerline would generally reduce the amount of excavation required to reach the material needing treatment, and reduce the working depth for in situ treatments. Working on the downstream side of the embankment, excavation farther from the centerline may create less concern for the safety of the dam during construction, which could reduce the required amount of dewatering or reservoir restriction. The optimum location of the treatment would depend on site and embankment geometry, embankment and foundation material properties, groundwater conditions, seepage through and beneath the embankment, locations of appurtenant structures, selected foundation improvement method, and reservoir operations. For example, at Bradbury Dam in California, the area available between the embankment and the spillway stilling basin was limited, which forced the foundation treatment (excavation and replacement) to occur farther upstream, necessitating removal of a portion of the embankment shell. This required extensive dewatering, excavation stability analysis, and monitoring during construction to ensure reliable performance during construction. See figure G1.
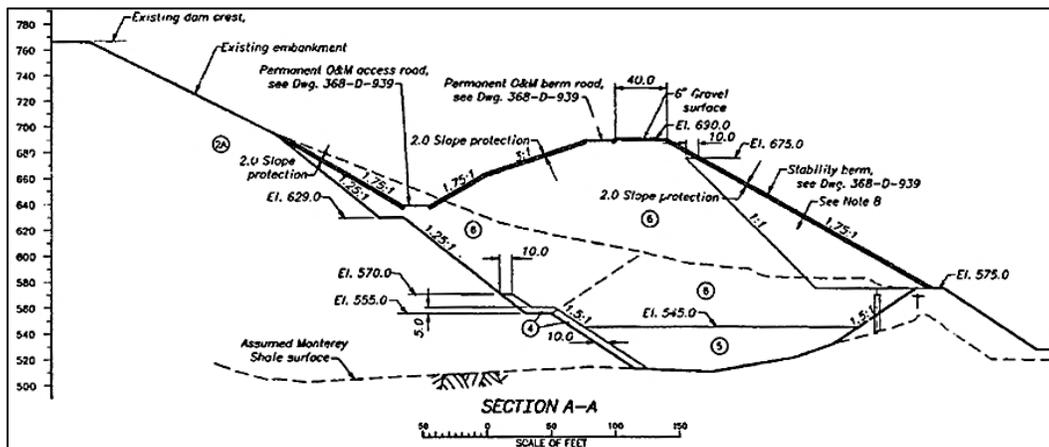
Figure G1. Stability berm and earthfill shear key with filter, Bradbury Dam, California.

Finally, the design and specifications must provide for safety of the public and workers during construction, in addition to reliable performance in the design earthquake. This generally requires excavation stability analysis, dewatering, and monitoring, and it may also be necessary to alter reservoir operation during construction.

The level of analysis required to show that a modification design is adequate varies from case to case. The absolute minimum would be post-liquefaction stability analysis, which might be acceptable if the earthquake magnitude and duration were small (so there would be little additional shaking after liquefaction and drastic loss of strength in the alluvium), and the freeboard was generous (so that moderate deformations could be tolerated). In other cases, it is more appropriate to perform detailed deformation analysis using finite-element method (FEM) or finite-difference method (FDM) computer programs, multiple sets of ground-motion records, and possibly coupled numerical analysis, modeling the development of excess pore pressure during the course of the earthquake. Where the liquefied material is confined to a narrow valley, it may be valuable to use three-dimensional (3D) analysis that accounts for the potential benefit of shear resistance on the sides of a slide mass, not just on its base.

It may also be necessary to analyze the condition of the dam at various stages of modification construction for both constructability and safety against a catastrophic release of water that would threaten workers and the downstream public. For example, if foundation treatment requires excavation at the toe of the dam, it must be shown that all the slopes are stable with reasonably foreseeable seepage conditions (requiring analysis of seepage and the dewatering system). An excavation or dewatering system could create an unfiltered exit point for seepage, which could cause failure by internal erosion. In areas of high seismicity, one may also need to show there is not significant risk of a catastrophic breach caused by an earthquake occurring during construction.

G.3   Foundation Improvement

A number of case histories have shown acceptable seismic performance of improved soils, in contrast to poor performance of adjacent, unimproved soils [1, 2, 3]. However, in many of those cases, the level of earthquake shaking was well below the full design loading. In addition, there are no case histories available that can provide a direct comparison of dam embankment performance during strong earthquake shaking, with and without foundation treatment. Therefore, it is important that the effectiveness and suitability of the soil improvement methods described herein continue to be reevaluated as new performance data and construction experiences are acquired.

The methods discussed here are not all-inclusive. To the extent practicable, the various methods have been described using generic names because equipment and terminology vary worldwide. Some methods can be, and often are, used in combination with others to meet the seismic remediation goals of a given project. Other features, such as stability berms, drains, and filters are used in conjunction with foundation improvement methods to ensure the integrity of an embankment during strong earthquake shaking.

The reader desiring greater detail on methods of in situ foundation treatment should refer to the state-of-the-art report contained in *Ground Improvement, Ground Reinforcement, Ground Treatment — Developments 1987-1997* [4]. Most of that publication is still current (2015). In addition, Iowa State University maintains a Web site that describes many soil improvement techniques and examples of their use: http://www.geotechtools.org.

Reinforcing a dam foundation is somewhat different from other typical applications in several ways. First, the treated zone must be able to resist high horizontal forces during and after the earthquake. Pervasive weak layers within the treated zone, or at the contact with the stronger material below it, could allow sliding. Because the embankment imparts a large driving force for slope instability, the treatment needs, not only to limit deformation during the earthquake, but also to maintain slope stability until excess pore-water pressure from shaking and consolidation have dissipated. For dams, the consequences of instability or excessive dynamic deformation can be severe, so a high degree of confidence in the treatment is required.

Foundation reinforcement (as opposed to relatively uniform improvement of the foundation's properties by densification) often requires complex structural analysis, rather than just limit-equilibrium stability analysis, or deformation analysis that treats the reinforced soil as a single material. In particular, slender, stiff elements within the soil (e.g., shear walls created by deep soil mixing [DSM]) require structural analysis methods to account for bending, buckling, tensile stresses, and complementary shear stresses on column interfaces. Cemented materials are brittle and not strain-compatible with loose or soft soils; they would generally fail at strain levels much less than the strain required to mobilize the strength of the soil. In dynamic response, the stiffer elements would need to resist most of the force caused by shaking, without severe breakage. Reclamation would, therefore, not use a composite shear strength based on averaging the properties of disparate materials like liquefied soil and soil-cement. In general, it is necessary to either densify the soil throughout the foundation, or construct reinforcement in the form of massive blocks that would not be affected by bending or buckling, and which might still be able to provide shearing resistance if cracked. Even though stone columns are not brittle, they provide little benefit in stiffening or strengthening the soil unless they actually densify it.

Any method of foundation treatment requires verification that the required improvement has been achieved. If the treated area must resist high horizontal forces, such as under the slopes of a dam embankment, thin horizontal layers of untreated material could allow sliding, whether within the treated zone or at the contact with the stronger material that underlies it. (This is less of an issue for other applications, where the loading is primarily vertical, or where the lateral forces are smaller. For in situ treatment, construction of a test section can demonstrate the feasibility of a particular method for a particular site and aid in the final design and contracting for the treatment.

Test sections are strongly encouraged for any in situ treatment method, both to verify that a particular method will work at the site, and to optimize the design for cost and construction duration. Depending on the situation, the test section may be a separate contract, executed prior to the actual modification construction, or as part of the modification contract if its primary purpose is to "fine tune" the construction program. A test section can be of great benefit to both Reclamation and the contractor. A good example is the modification of Salmon Lake Dam with stone columns to densify the potentially liquefiable foundation soils. Test sections were constructed in two areas: one with particularly high fines contents, and another of particularly low blow counts, which were the materials expected to be the most difficult to treat effectively. At each test section, a large amount of subsurface had been collected prior to treatment, so that material properties before and after treatment could be compared. Figure G2 shows verification testing in progress with Standard Penetration Test (SPT) and Cone Penetrometer Test (CPT) at one of the test sections, while stone column construction continues at the other test site (at far right). The viability of stone columns at the site was verified, and the spacing, size, and construction sequence were established, along with the benefit of wick drains and their layout within the pattern of stone columns. At other sites, test sections have shown that a particular treatment method would not be effective, saving millions of dollars on a modification that would not work. As at Salmon Lake, test sections can target areas that are thought to be difficult to treat, such as finer-grained units or where the soils are particularly loose or soft. It is preferable to have a large amount of in situ data, such as SPT and CPT, at the test sections prior to treatment for "before and after" comparison. Verification is discussed further in section G.3.7.

Figure G2. Verification testing with SPT and CPT to confirm sufficient densification by Stone Column Construction at Salmon Lake Dam. Stone column equipment appears at the far right side of the photograph.

G.3.1 Excavation and Replacement

The simplest of methods is to excavate any loose, potentially liquefiable foundation soils and replace them with well-compacted, nonliquefiable materials. Usually, the backfill can include part or all of the excavated material, placed and compacted to a denser state. Figure G1, above, provides an example. When site conditions permit it, this approach has a number of advantages. Because the work can be done with conventional earthmoving equipment, such as hydraulic excavators, scrapers, dump trucks, and compactors, there is no need for specialized equipment. The foundation for the key fill is exposed in the excavation, so it can be inspected, sampled and tested as necessary, and prepared, eliminating uncertainty about whether the improved key material actually extends all the way to the stronger material below, without a weak layer being left in place. Conventional embankment construction control can be maintained over the replacement materials, greatly reducing the cost and uncertainty in verifying adequate compaction. In contrast, verification of in situ treatments can be difficult and expensive by requiring drilling and sampling and/or some form(s) of in situ testing that indirectly indicates density. Reclamation dam-safety modifications that incorporated excavation and replacement include Bradbury, Casitas, Cold Springs, Deer Creek, O'Neill, Pineview, and Rye Patch Dams.

Excavation and replacement are generally used in conjunction with a berm to
stabilize embankment slopes. The berm performs two functions: (1) buttressing
the embankment slope, and (2) increasing the vertical effective stress within the
earthfill key, which increases its shearing resistance. Filter and drain elements
can also be incorporated into both the backfill and the berm as the foundation and
structure are rebuilt to help control seepage and prevent internal erosion in normal
operation or due to earthquake-induced cracks. Including filters and drains is far
more difficult with in situ treatment, so seepage may need to be addressed by
other means, such as upstream cutoffs or downstream relief wells.

Generally, compaction of the replacement material is specified as a minimum of
95 to 98 percent of the laboratory maximum density (the "D value"), or somewhat
less in filter materials that need to deform without cracking. (On some projects,
compaction has been controlled by an equivalent relative density, although that is
no longer recommended because control by D value is easier and just as
effective.) While high excess pore-water pressure can occur in dense fill under
cyclic loading, that would not likely persist at large strain, so the shearing
resistance that can be mobilized is comparable to the drained strength.

Excavation and replacement are usually most cost effective when treating soils at
relatively shallow depths (up to perhaps 70 feet) and on the downstream side of a
dam. At greater depths, or on the upstream side of a dam where dewatering and
unwatering could be difficult, in situ methods that do not require excavation may
be more economical. Even at greater depths, if the potential earthquake loading is
very severe and a very high degree of reliability is required (because of high
likelihood of earthquake loading and large population at risk downstream),
excavation and replacement may be the most viable approach because, among
other reasons, it yields a key that can deform plastically (not in a brittle way), and
its properties are well controlled and well understood. Managing construction for
an excavate-and-replace operation can also be less complex than for in situ
improvement methods because the adequacy of construction is obvious almost
immediately from conventional sand cone tests.

At two of Reclamation's dams, concrete was used as the replacement material. At
Rye Patch Dam in Nevada, the modification contractor determined that it was
faster and more economical to use lean concrete for the narrowest part of the key
in the bottom than to backfill with compacted soil materials (Figure). The
remainder of the key was conventional earthfill with a filter and a drain. For the
downstream side of Mormon Island Auxiliary Dam (MIAD) in California, there
was a limited working area and concern for static and seismic safety of an open
excavation at the toe while water is stored in the reservoir. The working area
between the toe of the dam and a highway limited the top width of an excavation
and the upstream-downstream width of a berm, so it was not possible to make an
earthfill key that was wide enough to provide adequate stability. Instead, the key
was constructed as a concrete block. Because open excavation was thought to
create excessive risk in that situation (considering geology and the large

population at risk), the key was constructed in sections no longer than 150 feet, with the vertical excavation supported by braced, reinforced secant-pile walls (figures G4a and G4b) . Dewatering wells were built into the secant piles by installing steel pipes within the wall, and then drilling through the pipes into the material below. Although it was complex to design and build, this supported excavation allowed for completion of the project without undue risk to the public or the need to restrict operation of a critically important reservoir, and it turned out to be no more expensive than in situ treatments. However, it did create additional analytical issues, including overturning stability of the concrete block and the effect that it might have on seepage.
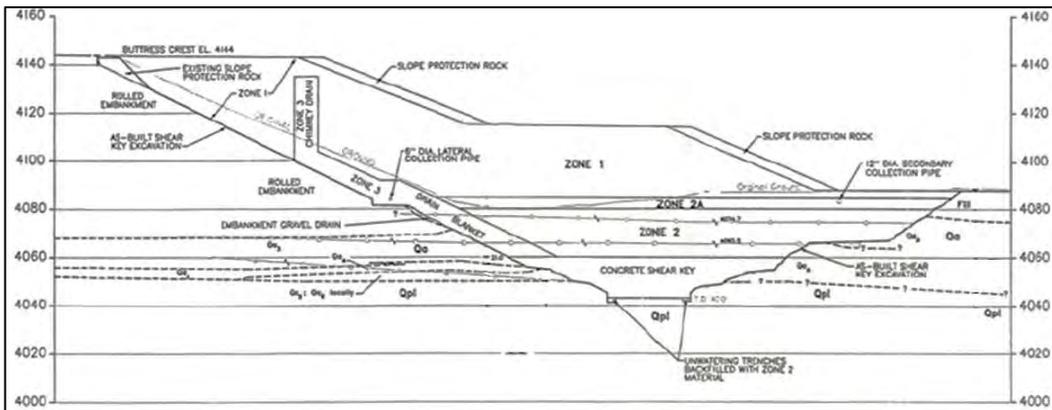
Figure G3. Partial concrete shear key, Rye Patch Dam, Nevada.
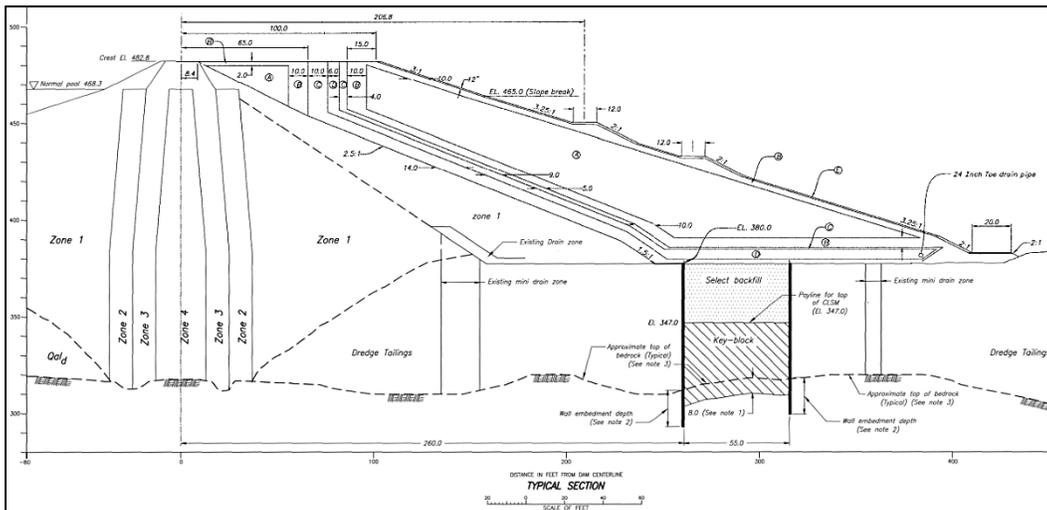
Figure G4a. Section of the concrete key block for seismic modification MIAD, Folsom, California.

Figure G4b. Excavation bracing for the key block at MIAD, Folsom, California (2011).

The feasibility and the cost of excavation and replacement are governed by a number of considerations, which are summarized below:

- What are the groundwater conditions at the site? Because groundwater affects the stability of cut slopes and the embankment during construction (thereby affecting public safety), dewatering is generally necessary. Dewatering is also generally required to permit excavation and fill placement "in the dry." The need for dewatering can impact reservoir operations, excavation geometry, and the timing of construction. Some form of seepage cutoff may also be needed. At Bradbury Dam, for example, the key excavation took place in a narrow area between the embankment and the stilling basin. The stilling basin would have been a major source of groundwater recharge for the dewatering system to work against. The solution was a soil-bentonite cutoff wall excavated to bedrock under bentonite slurry [5]. At Pineview Dam, both a retaining wall (consisting of soldier piles and lagging) and dewatering were required to fit the excavation into the area available at the toe of the dam. Figure G5 shows a dewatering bench with header pipes halfway down the slope, and construction of the wall system.

Figure G5. Pineview Dam excavation, dewatering bench, soldier piles, and lagging (2003).

- If work is required on the upstream side of the dam, the cost of cofferdams, loss of reservoir storage, and/or diversions may be prohibitive, and dewatering could be more difficult. It is also possible that dewatering of low-density foundation materials could cause settlement of the embankment.

- Are the site and foundation materials suitable for a large excavation? It may be difficult, or even infeasible, to treat enough area by excavation and replacement at small, constricted sites, especially if the depth of excavation is great. Typically, excavation slopes are no steeper than 1.5H:1V (horizontal:vertical), which means that, for a given width of the key at its invert, the top of the excavation gets wider by at least 3 feet for every 1 foot of depth, unless the sides of the excavation are shored, as at Pineview Dam (figure G5). Without adequate dewatering, or with weak soils, cut slopes might need to be much flatter than 1.5:1. Even with shoring, some dewatering is generally necessary for good working conditions. The excavation layout also needs to consider equipment access for excavation, cleanup, and fill placement. Greater efficiency can be obtained if the site allows gentle slopes and gradual turns on haul roads, and if it permits the equipment to enter the excavation on one side and exit on the other side without turning or backing. In figure G5, it can be seen that steep ramps were required at Pineview Dam, because of the constraints of the site, and that the trucks had to back into the excavation. At MIAD, cranes had to be

used to lower equipment to the bottom of the key-block excavation. Adequate stockpile areas are necessary for all excavated material that will be used as backfill for the key excavation or to construct a berm. If material cannot be reused, perhaps because it cannot be dried enough for proper compaction, a disposal site would be needed.

- What are the properties of the excavated materials? They would influence the design of the dewatering system and the allowable steepness of cut slopes. In addition, the properties of the excavated materials would determine whether they can be used as compacted fill in the improved foundation or in the berm. If not, material from borrow areas would be needed. Drying may be required for material from below the water table before it can be placed as fill; it may not even be practical if the excavated material contains many fines, especially if the fines are clayey.

- What impact could excavation have on the safety of the dam during construction? Clearly, a major excavation at the toe of a dam requires attention to both slope stability and seepage in both the design stage and in monitoring during construction. Seepage is an issue for both excavation stability and internal erosion because an open excavation, or even a dewatering well, could create an unfiltered exit point for internal erosion of soil from the dam or foundation. Monitoring would require some combination of piezometers, observation wells, inclinometers, surface measurement points, shear strips, and, of course, frequent visual monitoring. Construction specifications must spell out contractor requirements for recordkeeping, backups for dewatering equipment, monitoring of slopes and dewatering, etc. In a highly seismic area, it may also be appropriate to analyze the open excavation for seismic stability with, for example, 100- or 500-year ground motions, accounting for potential beneficial effects from dewatering and adjusting the designs of excavation and dewatering as needed.

G.3.2 Surface Compaction Methods: Dynamic Compaction and Rapid Impact Compaction

Dynamic compaction (DC), also known as heavy tamping, surface-impact compaction, and deep dynamic compaction, can be a relatively low-cost method for increasing the density of granular foundation materials [4, 6, 7, 8]. It has been used by Reclamation at Steinaker and Lost Creek Dams in Utah, Jackson Lake Dam in Wyoming, and on the upstream side of MIAD in California.

Steel-and-concrete weights, typically weighing 5 to 35 tons, are repeatedly dropped from a height of 40 to 120 feet in a grid pattern over the area to be treated (figures G6a, G6b, and G7). The resulting craters are backfilled as needed, and

the weight is dropped again. The weights are dropped in a predetermined pattern and sequence until adequate density is achieved at depth, usually in two or three phases with "rest periods" between phases to allow time for settlement and dissipation of excess pore pressures to occur. The working surface needs to be compacted with rollers after dynamic compaction has been completed because the surface is disturbed and loosened by the impacts. Following compaction, there is usually a gradual increase in strength and stiffness with time (as indicated by penetration resistance and shear-wave velocity).

Figure G6a and G6b. Dynamic compaction at Jackson Lake Dam.

Figure G7 shows a typical DC pattern (Steinaker Dam, Utah). First, in order to permit drainage of pore water from the alluvium as it was being compacted, wick drains were installed to a depth of 30 feet over the entire treatment area, spaced 5 feet apart in both directions. Then, dynamic compaction was performed on a 25-foot grid in phases to allow some dissipation of pore-water pressure for more effective compaction. The weights were dropped first at the primary points designated by circles on the figure, and then at the secondary points, marked by squares, after the primary compaction was completed and some dissipation of

excess pore-water pressure had occurred. Finally, the tertiary phase of
compaction was performed at the center of each square of the grid pattern
(triangles).
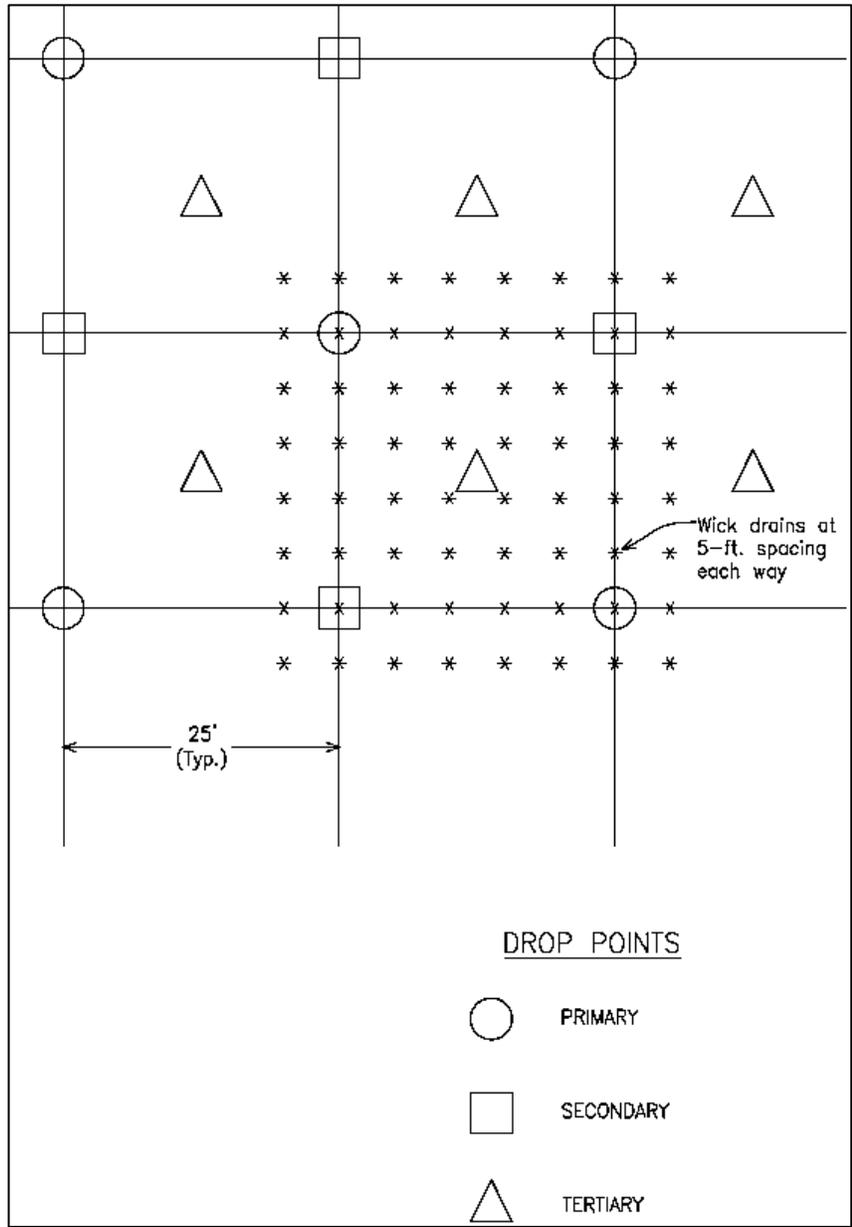
**Figure G7. Layout of impact points and wick drains for dynamic
compaction at Steinaker Dam.**

DC treatment requires the soil to undergo a reduction in porosity very quickly. If
the voids are filled primarily with water (practically incompressible), the soil must
be very pervious so that the water can escape. If it is feasible to actually

desaturate the foundation material with pumped wells, that would make it easier to compact because air is so much more compressible than water. Unless the water table is far below the surface, the excess pore pressures can cause upwelling of water onto the ground surface, and a free-draining gravel pad may be required to provide a firm, dry working surface. For the DC at Steinaker Dam, well points and pumped dewatering wells were found to be important, in addition to the wick drains in figure G7, because the foundation soil contained small amounts of silt, and its permeability was limited. These drainage features improve the dissipation of excess pore pressures generated during compaction by shortening the seepage path and lowering the water table within the treated zone.

Dynamic compaction is generally most useful at sites with large areas to be treated, and with high groundwater tables or other condition that would make excavation and replacement more difficult. The materials to be treated must be sufficiently pervious that they can drain freely or be dewatered. This would require that the fines content is fairly low, and that the fines have no plasticity or very low plasticity.

Although improvement has reportedly been achieved at depths as great as 49 feet, the effective depth of treatment is usually limited to 30 to 35 feet, even with very large equipment [4]. This is consistent with Reclamation's experience when DC was used to stabilize the upstream slope of MIAD. One reach of the dam was founded on tailings from placer mining of gold; the tailings were a somewhat chaotic mixture of sand, gravel, and cobbles with varying amounts of fines. Where bedrock was less than 35 feet below the working surface, compaction was successful. In another area, with deeper bedrock and higher fines content in some of the deepest tailings material, it was not very effective. In all of the treated area, the shear-wave velocity showed significant increases over several years after compaction.

When compaction is required at large depths, so that heavy weights and large drop heights are needed, modified cranes or purpose-built machines are generally used; these machines are usually owned by specialty contractors. Typical cranes can be used when the desired depth of treatment is small (less than about 20 feet), so the weights and drop heights are smaller. However, cranes are typically not designed to withstand repeated sudden releases of large weights, and they are subject to much more wear and tear than in normal use; as a result, they are not often used for dynamic compaction anymore.

The depth of effective treatment depends on foundation material types, groundwater conditions, site geometry, weight drop patterns, equipment, drainage provisions, and equipment sequencing. A rough estimate of the depth of treatment can be obtained from Ménard's equation:

$$D = n \, (WH)^{1/2} \hspace{5cm} \text{Equation G1}$$

where D is the depth in meters, n is an empirical coefficient, W is the weight in
metric tonnes, and H is the drop height in meters. The value of n ranges between
0.3 and 0.8, averaging about 0.5 in granular soils [9]. It is lower with finer
material, and in soils containing significant amounts of clay, the method is simply
not effective because the permeability is too low for the pore water to escape.
The depth of effective treatment decreases for sites having soil horizons with high
silty fines contents (greater than 20 to 30 percent) unless wick drains or other
drainage features are installed.

There is a similar surface-compaction technique, called rapid impact compaction
(RIC), that is more suitable than DC for small areas (due to lower mobilization
costs) or for working near structures that could be damaged by vibration from the
very large impacts from DC [10, 11]. RIC uses repeated blows from a drop
hammer mounted on the boom of a hydraulic excavator. The hammer typically
weighs 5 to 9 tons and drops about 4 feet onto a 5-foot-diameter steel "shoe,"
rather than directly on the ground surface. The hammer can provide 40 to
60 blows per minute. Successful (and cost-effective) compaction has reportedly
been achieved to depths of 25 feet or more, although 16 to 20 feet is more
commonly reported. To date (2015), Reclamation has not used RIC, but it may be
useful on future projects that require compaction of granular soils at modest
depths.

Verification of compaction is generally done with *in situ* tests of penetration
resistance and sometimes shear-wave velocities. Caution is required in
interpreting the tests because of two effects: (1) an increase in K_0 from
compaction, which tends to increase the penetration resistance shear-wave
velocity for a given density and effective overburden stress; and (2) delayed
increase in penetration resistance and shear-wave velocity with time after
treatment.

The potential for adverse effects on embankments and any adjacent structures
from vibrations or material displacement should be considered when evaluating
deep dynamic compaction as a foundation improvement method.

G.3.3 Vibrocompaction and Stone Columns (Vibroreplacement)

Loose foundation materials can sometimes be densified at low to moderate cost
by inserting a vibrating tube or probe into the foundation at predetermined depths
and patterns, and then backfilling the resulting holes with sand and/or gravel.
This can take two forms: **vibrocompaction** and **vibroreplacement** [4, 12]. The
two forms are distinguished from each other by the amount of backfill used.
Figure G8 shows a typical stone column rig.

With vibrocompaction, the vibrating probe is used simply to shake the surrounding material, so that it will settle into a denser state, sometimes liquefying it locally. Depending on the overlying soils, inserting the probe may require only vibration, but drilling and water jetting may be needed if the water table is low or the overlying soils are denser. The resulting holes are backfilled with sand and/or gravel, but there is no attempt to intrude the backfill into the foundation soil. (In this regard, it differs from vibroreplacement.)

Figure G8. Bottom feed stone column equipment at MIAD in Folsom, California.

If, instead, gravel is introduced into the foundation during the compaction process and the gravel is compacted by the probe, the process is referred to as **vibroreplacement** or **stone columns**. Rather than simply vibrating the surrounding material to densify it (then backfilling), vibroreplacement involves compaction of the gravel as it is placed in the hole. The compaction of the gravel forces it radially outward, intruding into the foundation soil somewhat and, more importantly, compacting it by the radial compression, in addition to the effects of vibration and settlement under gravity. The gravel is introduced either through the annulus around the probe ("top feed") or through the probe itself ("bottom feed"). The probe is repeatedly withdrawn and inserted at the point of treatment to maximize foundation improvement. Columns are typically constructed in triangular or rectangular grid patterns, at center-to-center spacings of 6 to 12 feet.

The columns are generally 3 feet or greater in diameter. Smaller diameter columns on closer spacing have also been used. The volume of gravel put into the hole is much greater than the volume of the hole made by the probe.

The effectiveness of vibrocompaction or vibroreplacement is very dependent on material type, the depth of treatment, hole spacing, vibration levels, and pore-pressure response during treatment. The materials most easily treated are those having less than 15 percent fines, and effectiveness of treatment decreases with increasing fines content. It may not even be possible to treat saturated materials with more than about 25 to 35 percent nonplastic fines, or with lesser amounts of plastic fines, because of their low permeability. This was demonstrated by Reclamation's experience at Scofield Dam in Utah, where stone columns achieved very good compaction in sandy layers with few fines, but poor results in a low-permeability silt layer, as indicated by SPT blow counts. In addition to not densifying well, soft fine-grained layers may simply be displaced by the gravel, resulting in significant quantity overruns if the soft layer is very thick, which occurred at both Scofield and MIAD.

Performance of vibrocompaction (or vibroreplacement) in finer materials may be improved by vertical wick drains among the vibrocompaction columns to allow the pore water to escape more easily. Prior to the actual construction of the modification of Salmon Lake Dam in Washington, Reclamation used a test section to determine the necessary spacing and size of the columns and the need for wick drains. (See figures G9a through G9c.) The treatment was successful, even though the foundation soil was somewhat less pervious than is ideal, but only because the drains were installed. It is typical practice to allow rest periods between phases of treatment in a particular area, so that excess pore pressure can dissipate. Figures 9a and 9b show the treatment in section and plan view with wick drains among the columns.
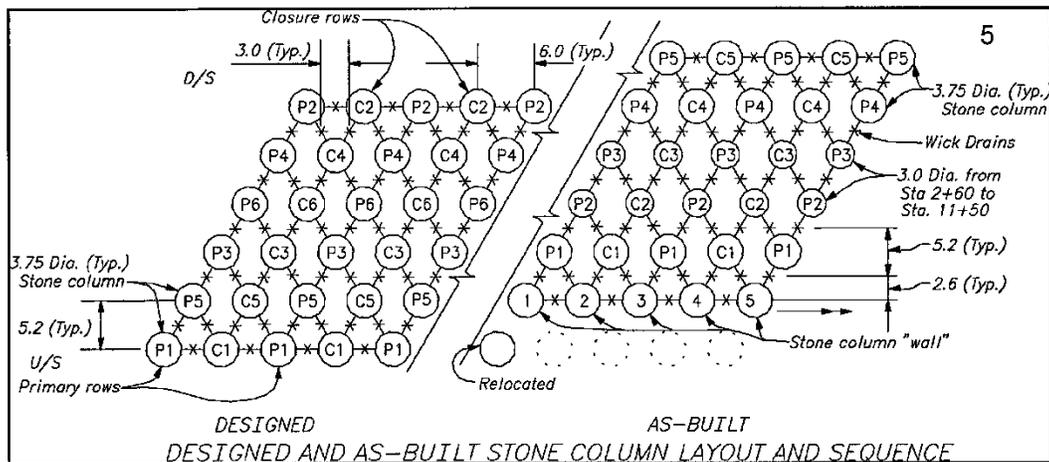
Figure G2a. Stone columns and overlay, Salmon Lake Dam, Washington.
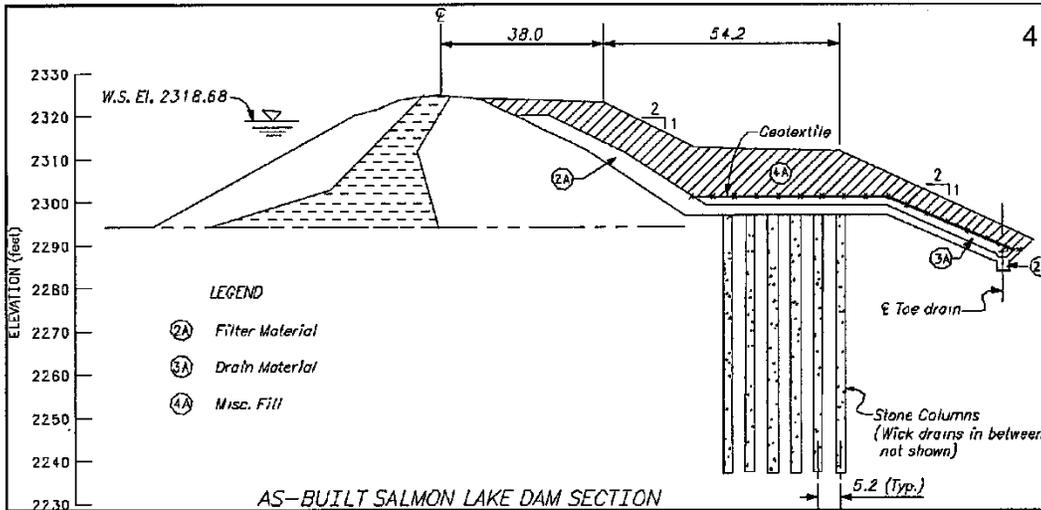
Figure G2b. Layout of stone columns and wick drains for treatment of Salmon Lake Dam foundation, Washington.

Figure G9c. Wick drains discharging water during stone column installation, Salmon Lake Dam, Washington.

Densification is usually verified by in situ testing (SPT, CPT, etc.) at the centers of the open areas among the columns, on the assumption that the least densification would occur there. As with other densification measures, stone

columns tend to increase K_0, which somewhat complicates the interpretation of in situ test results.

During construction, densification is monitored qualitatively by the amperage drawn by the electric motor that provides vibration. As column installation approaches "refusal," the maximum amount of gravel that the ground will accept, the amperage increases sharply. If this does not occur, it most likely means that densification is not being achieved, and softer material is simply being displaced. Even if refusal does occur, that does not, on its own, demonstrate that adequate compaction has been reached; it is only a "relative" measure that indicates further vibration will not improve compaction very much.

Improving a dam foundation is different from treating a foundation under a building because the treated zone under a dam must be able to resist very high horizontal forces during and after the earthquake. This requires good densification, not only "on average" throughout the treated zone, but also without leaving weaker, untreated zones within the treated zone or at the contact with the stronger material below it. If the underlying material is soil, the treatment can sometimes be extended down into it, but good contact may be harder to achieve if it is bedrock.

Introduction of sand or gravel may improve the vertical permeability and drained shearing resistance of the treated zone somewhat, although that is difficult to quantify, and it may not be reliable. One cannot assume that the permeability of the columns would be much better than that of the surrounding material, which can intrude into the column (as has been observed when stone columns have been excavated). In order for drainage to actually prevent liquefaction, or at least mitigate it, a large volume of water would need to drain from the foundation very rapidly, which is simply not a realistic expectation with stone columns with finer material intruding into them.

At least in theory, the greater shear stiffness of the material in the compacted stone columns would help to reduce the cyclic shear strain in the surrounding material, helping to prevent liquefaction, even in material that was not successfully densified by installing the stone columns. However, unless the weak layer is thin compared with the column diameter, the benefit would be minor because the columns would behave as slender elements with essentially no bending stiffness. Because the material in stone columns generally has high density and high friction angle, it has been suggested that they would also improve the post-liquefaction shearing resistance of foundation layers that have not been successfully densified. Their benefit for that situation would likely be small and difficult to quantify (again, because the columns are slender). The strength and stiffness of the gravel are dependent upon the effective stress within the columns, which could be very low if they are surrounded by weak, liquefied material with very high excess pore-water pressure. To resist lateral forces, each column would need to be completely continuous within the weak layer, and there

would need to be high effective stresses within the column. With significant shear deformation (tilting or offsets in the column), the axial force that provides the vertical effective stress needed for shearing resistance on horizontal surfaces is likely to be lost. Unless the thickness of the weak layer is small compared to the diameter of the columns (analogous to a direct shear test), they cannot be expected to provide significant resistance to lateral loads. Even with thin layers, the analysis would need to allow for gaps or undersized columns, and for intrusion of excess pore-water pressure or liquefied foundation soil into the columns. **For a layer that has not been successfully densified by column installation, it is incorrect and potentially very unconservative to analyze the stiffening and reinforcement provided by stone columns by assuming a simple area replacement ratio.** In fact, slender elements (stone columns or thin soil-cement walls or columns) within low-strength material may not provide much stiffening or reinforcement at all [13, 14].

Stone columns are commonly (and successfully) used in fine-grained material as reinforcement to resist settlement under *vertical* loads; there, they act as axially loaded columns of relatively stiff, strong material that bear a large percentage of the overburden. Small gaps or flaws in the columns would have fairly minor effects on settlement under vertical loading. This is inherently different from using the columns to resist lateral loading, where gaps or flaws in a column could render it useless. For creating a shear key, stone columns are considered to provide densification, not reinforcement. The difficulties described here do not affect the viability of stone columns for resisting *vertical* forces.

Vibro-compaction or vibro-replacement methods using water or, to a lesser extent, dry placement with a high water table can have substantial containment and/or cleanup costs during construction. It may be necessary to handle large quantities of mud and turbid water, depending on the methods employed, foundation and column materials, groundwater conditions, and site surface characteristics.

G.3.4   Other Compaction Methods

G.3.4.1   Blast Densification
Blasting to densify loose soil is mentioned here as a possibility for granular soils that are too deep to be treated easily by other means [2, 4, 12]. It is not a technique that would be applied at very many existing dams, although it was used at Seymour Falls Dam in British Columbia [15]. Explosive charges in deep drill holes can densify loose soils by shock waves and vibration, causing limited liquefaction, displacement, and remolding; this leads to settlement and higher density in the treated soils as the excess pore-water pressure dissipates. This can be relatively low in cost, compared to other treatment methods at large depths, provided that the required density is not particularly high and uniformity is not

critical, as verification could prove difficult. Near or beneath existing embankments or structures, blasting would generally not be appropriate because of the real or perceived potential for damage, unless other options were impractical. At Seymour Falls, the zone to be treated was about 35 feet below the invert of the core trench. Blast densification is more likely to be considered for a site where the existing embankment is to be removed completely and replaced, or prior to construction of a new embankment. The best documented case is blast densification prior to construction of Jebba Dam in Nigeria, with the goal of minimizing settlement [16]. This case is also of interest because, after blasting, SPT blow counts were initially lower than before, but they rose quickly and continued to rise for months after blasting, long after excess pore-water pressure would be expected to have dissipated. Blast densification has also been used for nonplastic mine tailings and hydraulic fill.

Narin van Court and Mitchell [17] proposed techniques for predicting the performance of blast densification.

G.3.4.2   Compaction Grouting

Compaction grouting uses low-slump grout (usually 0 to 2 inches in the slump-cone test for concrete) injected under high pressure to form a series of grout bulbs that radially displace and compact loose foundation materials between and adjacent to the bulbs [3, 4, 12, 18]. The process is fairly simple, consisting primarily of drilling or driving the grout pipe into the ground and using a high-pressure concrete pump to force the grout into the layer to be treated. When the soil to be treated contains a significant amount of silty fines, compaction grouting can be more effective than vibratory methods because the soil is sheared and compressed more slowly, so the permeability does not have to be as high for the displaced pore water to escape. The grout is generally silty sand with a small amount of Portland cement, but it does not always contain cement. It may simply be silty sand, with enough silt and water to make the mixture deform plastically under high pressures, and enough sand to develop internal friction. With no cement in the grout, it does not harden, so the area can be regrouted later to achieve additional densification if needed. Also, verification of treatment is easier without cement in the grout mixture because it can be done by conventional penetration testing.

The maximum depth of treatment with compaction grouting is limited only by the cost of drilling. However, shallow treatment can be problematic. Successful treatment has been reported as shallow as 5 feet, but there is potential for surface heave and less effective treatment if there is not enough overburden stress; the injected grout can simply lift the overlying soil instead of radially compressing it.

At present (2015), Reclamation has no experience with compaction grouting for dam foundations, although others have used it. For example, Baez and Henry [18] describe successful treatment of the foundation of Pinopolis West Dam in South Carolina.

The cost of compaction grouting, when compared to other methods of foundation improvement, is moderate to high. Compaction grouting becomes more economical, relative to other methods, when treating identifiable thin lenses or layers, where overlying layers are already competent and do not require treatment, or for treating small volumes adjacent to structures.

G.3.4.3   Compaction Piles

Small-diameter piles can be driven by standard methods to densify soils through vibration and displacement. They can be left in place or removed and the remaining hole backfilled. Backfilling can be accomplished by using a "pile" that is actually a casing with a driving shoe that can be opened. After it has been driven, the shoe is opened, and backfill material is poured in as the casing is withdrawn. The casing is repeatedly driven and withdrawn to form the piles and densify the foundation materials.

This method of soil improvement is relatively high in cost; therefore, it is limited to sites where small volumes of soil are to be improved, and other methods like excavation and replacement are not practical. Reclamation has not used compaction piles for improving a dam foundation to date (2015).

G.3.5 Cementing Methods

A variety of methods have been developed for mixing the soil with Portland cement or other cementing agents in situ to create soil-cement that is much stronger than the soil in its natural condition. Reclamation has employed two cementing methods: deep soil mix walls (Jackson Lake Dam, Wyoming) and jet grouting (Wickiup Dam, Oregon).

For a dam foundation or shear key, the soil-cement can take the form of shear walls oriented upstream-downstream, rectangular lattices or "honeycomb" shapes of interconnected soil mix walls, or massive blocks. The resulting material is stiff and strong, but brittle. Suzuki [19] provides useful data on the mechanical properties of soil-cement created in situ using Portland cement. Analytical issues for soil-cement are discussed below.

G.3.5.1   Jet Grouting

Jet grouting uses high-pressure, high-velocity jets of Portland cement grout (slurry), water and/or air to "erode" the foundation material and mix it with the cement grout (Figure G3). The result is soil-cement mixed in place to replace the weak foundation soil. Jet grouting can be used to construct columns of soil-cement in a wide variety of foundation material types (gravel, sand, silt, and low-plasticity clays) [4]. Experience at Reclamation and the U.S. Army Corps of Engineers (USACE) projects suggests that it works best in nonplastic material

with few cobbles and little coarse gravel. It did not work well at a test section at MIAD with its foundation consisting of loose placer tailings with gravel, cobbles, and boulders. Too many "shadows" of untreated foundation remained around the large particles. Individual jet-grout columns cannot be expected to provide high resistance to lateral forces, but they can be overlapped to form shear walls or, preferably, massive blocks of soil-cement. Overlapping columns can also be used to create a seepage cutoff.
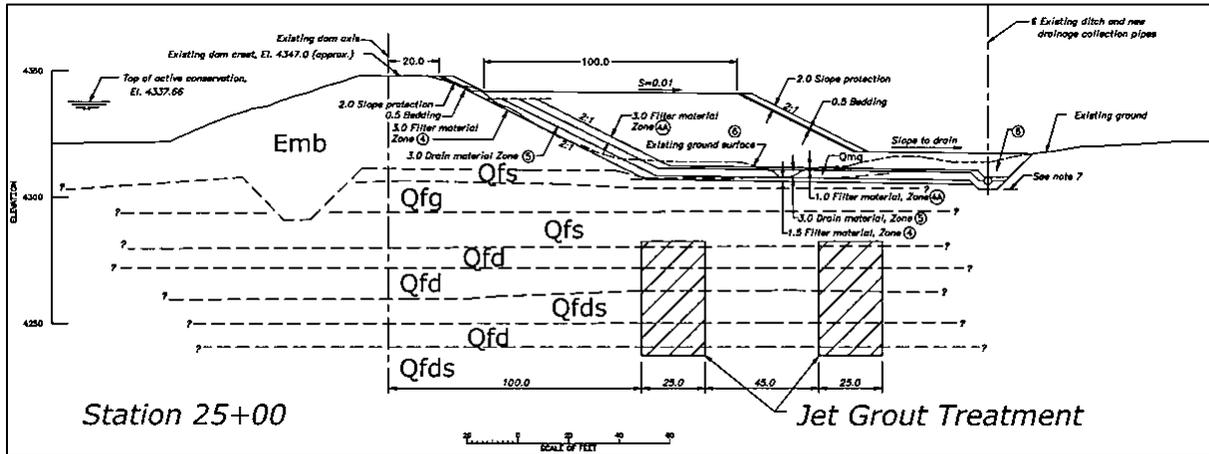
Figure G3. Jet grout rig, Wickiup Dam modification, Oregon. Note the high-velocity jets of Portland cement grout.

At Wickiup Dam in Oregon, much of the foundation consists of liquefiable, loose, nonplastic silt. Reclamation used jet grouting to create massive blocks of soil-cement under the embankment slope for sliding resistance (figure G11). As indicated by the strong and continuous drill core recovered from the foundation, the results were excellent. In the extensive list of jet-grouting projects in reference [4], there were no examples of jet grouting for mitigation of liquefaction potential as of 1997. Instead, jet grouting had been used primarily for underpinning, seepage barriers, and support for tunneling and excavation. Wickiup Dam may have been the first application of jet grouting for mitigating liquefaction under a dam.

When properly constructed, the soil-cement created by jet grouting has high compressive strength and fairly high shear strength, but little tensile strength. Therefore, the bending strength of an individual column is low, which needs to be accounted for in the embankment stability and deformation analyses. Analyzing foundation reinforcement created by jet grouting and other cementing methods requires a structural approach. For Wickiup Dam, the jet-grout blocks were designed to be sufficiently massive so that, if cracked, they could be assumed to act like dense gravelly soil. In individual columns or relatively thin walls, this assumption would not be valid.

Figure G11. Jet-grout blocks in the foundation of Wickiup Dam.

A portion of the grout-soil mixture returns to the surface along the annulus around the drill rods, which can be a significant drawback. In its liquid state, it needs to be contained and kept away from streams and wetlands. Once hardened, the waste grout needs to be disposed of; that can be a significant drawback unless the material is suitable for use as fill for the stability berm or other embankment. Another drawback is the risk of fracturing the embankment core or foundation material by injecting liquids and air at very high pressures. At one site, this caused air to bubble up in the reservoir 50 feet from the grout hole [20].

The cost of jet grouting can be relatively high, compared to other foundation improvement methods, depending on the design goals of foundation remediation and the distribution and type of materials to be treated. It is most likely to be the preferred method only when conditions are poor for excavation and replacement, and the soils to be treated are too fine for in situ densification. For reinforcing the foundation of a dam against lateral forces, it is necessary to have high strength on horizontal surfaces. For this reason, it is important to ensure that the treatment is vertically continuous. Removal of the mixing tool at a rate that is too high could cause gaps that would create horizontal planes of weakness in the treatment, as could layers of plastic clay or other strong material that prevents the jetting from reaching the designed column radius. Verification of the integrity of jet grouting by coring and, possibly, geophysical methods is necessary.

As with any other in situ treatment, it is important to construct a test section prior to beginning "production" jet grouting. Preferably, this would occur prior to final design to verify feasibility of the method in the actual foundation soils, and to establish in a general way the details of equipment and procedures that produce the best results (e.g., whether to jet with compressed air in addition to water and

cement grout, and what pressures and nozzle velocities work best). After the
contract has been let, the contractor should construct a test section to demonstrate
that the specific equipment and methods intended for use will produce effective
treatment, and then adjust them as required, before beginning production. In two
known cases, jet grouting was considered for improving dam foundations
(USACE's Tuttle Creek Dam and Reclamation's MIAD) but then rejected on the
basis of poor results in test sections.

G.3.5.2   Deep Soil Mixing and Related Techniques

Like jet grouting, DSM can be used to construct columns, shear walls (individual
walls, or walls arranged in a lattice pattern), or massive blocks of soil-cement in
materials ranging from gravel to clay [4, 12, 21]. (This is also called the deep
mixing method [DMM].)

DSM uses hollow-stem augers and mixing paddles, which are advanced into the
soil while Portland cement grout (slurry) is pumped through the tip of the auger.
The auger flights and mixing paddles mix the grout with the surrounding soil
during penetration to the design depth and during withdrawal. To create walls or
blocks, the columns formed by individual augers are overlapped. Figure G12
shows DSM equipment working at Reclamation's Jackson Lake Dam in
Wyoming. There are rigs capable of producing as many as six 3-foot-diameter
columns at one time. One significant advantage over jet grouting is better control
of the dimensions with DSM and less opportunity for undersized columns or
untreated layers. Cutter soil mixing (CSM) is a related technique that uses soil
cutting equipment to break up the soil and mix it with cement, instead of augers
and paddles. The cost of DSM is moderate to high relative to other foundation
improvement methods.

To date, Reclamation has used DSM to modify one dam. The original
embankment of Jackson Lake Dam consisted primarily of hydraulic fill, and the
foundation contained large amounts of very loose silt. The embankment was
removed completely, and most of the foundation was treated with dynamic
compaction. Portions of the foundation that were too deep for dynamic
compaction were reinforced with a hexagonal honeycomb pattern of DSM
walls [4]. There, the primary intent of the walls was to reduce the cyclic shear
strain in the loose foundation soil, reducing the potential for liquefaction. DSM
was also used to create a deep, positive seepage cutoff. The City of
San Francisco's Sunset Dam was modified in 2006, using overlapped DSM
columns to create shear walls oriented upstream-downstream, with an earthfill
berm placed over them [22]. The USACE built a similar modification at its
Clemson Upper and Lower Diversion Dams in South Carolina [23].

In the right circumstances, DSM walls could reduce the cyclic shear strain in the
foundation soil, so that it does not become liquefied. A grid of DSM walls was
used to good effect to create nonliquefiable zones around bearing piles in the
foundation of the Oriental Hotel in Kobe, Japan [24]. During the 1995

Hyogoken-Nanbu earthquake, the walls prevented major liquefaction effects in the near-surface soil, apparently by reducing the cyclic shear strain. Nearby untreated areas showed major lateral spreading and other damage, but the area of the hotel showed only minor damage. Critical to that function is the ability of the walls to withstand the shaking without extensive breakage. The alternative concept is to provide foundation reinforcement that would prevent instability, even if the walls were cracked by the shaking and the foundation soil was liquefied; this would require massive DSM blocks, rather than thin walls or columns.

Figure G4. DSM wall construction, Jackson Lake Dam, Wyoming.

There are some important distinctions between the use of DSM for isolating liquefiable soils to reduce the cyclic strain of soil near the ground surface (as at the Oriental Hotel) and its use for reinforcement to maintain the stability of an embankment. When it is used to provide stiffening for approximately level ground, some cracking during the course of the earthquake may be tolerable, and the forces that the walls must resist in order to keep the strains small are relatively modest because there is no overlying mass. In contrast, DSM in a dam foundation would act as a stiff structural connection between firm soil below the weak material and the mass of the embankment above it. Upward-propagating, horizontal shaking would be transmitted to the embankment, mostly by the DSM

walls because they are stiff compared to liquefiable soil. For this reason, the
stresses could be much higher than in DSM used to isolate near-surface soil.
Furthermore, at the end of an earthquake, the DSM walls may still be needed in
order to maintain static stability of the embankment; if they are cracked
extensively, they may not be able to perform that function.

Nguyen et al. [25] describe dynamic structural analysis of square grids of DSM
walls in level ground. There were two important results:

(1) The shear strains within the soil inside the grid cannot be modeled as if
they are strain-compatible with the walls; the strain in portions of the soil
can actually be much higher and liquefaction may still be possible even
without any damage to the walls.

(2) Second, the confined soil applies normal force to walls oriented transverse
to the direction of shaking, whether upstream-downstream or cross-valley.
This creates bending moments and tensile stresses. Although not modeled
by Nguyen et al., the thickness of the wall varies because it is constructed
as overlapping cylinders; this can adversely affect the walls' ability to
resist bending about a vertical axis.

With thin elements (walls or columns) in the foundation, it is not adequate to
assign strength or stiffness to the treated zone by an area-weighted average of the
soil and the soil-cement. Unless the cemented material is massive, tens of feet in
any dimension, dynamic structural-analysis methods are required. Generally, the
analysis needs to be 3D. Structural failure could result from:

- Crushing of soil-cement at compressive stress concentrations

- Tensile stress in the soil-cement (which has nearly zero tensile strength)

- Complementary shear along column interfaces (where the walls are
thinnest and overlap of adjacent columns may not be complete)

- Buckling of walls due to in-plane compression

- Bending of walls due to unbalanced normal force (perhaps from
cross-valley shaking)

Figure G13 shows some of the failure modes. The analysis must somehow
address the brittleness of soil-cement and the transfer of forces among soft soils,
stiffer soils, and the soil-cement walls.

The strength of the soil-cement created by DSM is generally expected to be lower
than soil-cement mixed conventionally, using a pug mill before placement, or on
the fill using rotary equipment. Uniformity cannot be expected in soil-cement

mixed in place without inspection, and the strength of the walls would be governed by the weakest zones and any thinner zones, such as at poorly overlapping columns. These may not be detected by strength testing of drill cores recovered from the soil-cement. Once cracked, the walls may not be any stronger than the surrounding liquefied soil, particularly if they are slender with respect to the weak layer's thickness.

a. Cross section of dam with downstream DSM reinforcement and stability berm

Inertial forces applied to DSM structure
DSM reinforcement
Liquefiable or other weak foundation soil
Top of bedrock or stronger soil
A Acceleration in bedrock

b. Structural failure modes of DSM reinforcement

Bending of transverse walls
Shaking in both directions
Separation of transverse and longitudinal walls
Tensile separation and overturning
Complementary shear on column interface
Bending or toppling
Sliding at contact with hard foundation

Figure G13. Failure modes of DSM walls under lateral loading.

A possibly superior alternative to mixing soil-cement in place with augers and paddles is to excavate a slurry-supported trench using a long-reach backhoe, clamshell, or a tool that resembles a chainsaw, and then construct a high-strength, cement-bentonite (CB) wall in the trench, similar to what is commonly done for cutoff walls, but with more cementitious material for greater strength. After rejecting jet grouting, to prevent instability in case of foundation liquefaction at Tuttle Creek Dam, the USACE selected CB walls constructed this way to create a large number of upstream-downstream shear walls along the downstream toe [26]. This method appears to have some significant advantages over DSM, notably, better uniformity of the materials and wall thickness. With DSM or jet grouting, the soil-cement in the overlaps of the columns may not be as strong as within the columns themselves, and the interface is narrower than the column diameter. This could make the interface between individual DSM or jet-grout columns the weakest surface for failure of the walls by vertical shear stresses (the complementary stress from application of a horizontal shear force by the earthquake and the embankment slope). Incomplete overlap would exacerbate the problem. The CB shear walls at Tuttle Creek would not have this issue, although slurry-supported walls have their own issues, including disposal of waste slurry and the potential for trench collapse.

DSM walls are practically impervious, so if they are used under the downstream portion of a dam embankment, it may be necessary to leave gaps in the walls or to provide filtered drain pipes or other measures to allow seepage to pass.

Given the difficulties mentioned above, thin DSM walls are not likely to be accepted for a seismic modification of a Reclamation dam. DSM is more likely to be selected if it is used to create massive blocks that would either be less prone to cracking in strong shaking and/or be better able to provide reinforcement (as a frictional material) after being cracked and broken.

G.3.5.3   Permeation Grouting

Soil can also be improved by permeation grouting, in which very thin grouts are pumped into the void spaces. This is generally limited to clean, coarse sands and gravels. Permeation grouting can be useful where an improvement in the *average* value of some soil property, such as strength, compressibility, or permeability, would improve the overall performance. However, for providing lateral resistance, as in a shear key for stabilizing a dam, permeation grouting would not be reliable; a single silty layer that would not accept grout could form a plane of weakness through the whole foundation. There may be sites where this method could be used, but in general, it would not be considered for a dam.

G.3.5.4   Commentary on Cementing Methods

When evaluating cementation methods to remediate seismic deficiencies of dam embankments, the following issues must be considered:

- With the exception of DSM in the foundation of Jackson Lake Dam and jet grouting at Wickiup Dam, Reclamation has not used cementing methods to remediate dams for seismic deficiencies. Other agencies and dam owners have used them more, but details of analysis have not been widely published.

  Soil-cement and cement-bentonite are strong in compression and fairly strong in shear, but they are brittle and lack tensile strength. The treatment must be designed so that either: (1) it does not crack under the strongest earthquake loadings possible at the site, or (2) once it is cracked, it still has sufficient strength for post-earthquake stability. The modification of Wickiup Dam was designed on the basis of frictional strength of granular material, assuming that the massive soil-cement blocks created by jet grouting would be cracked.

- The analysis of foundations treated with relatively thin walls of cemented material (DSM, CB, or single rows of jet-grout columns) is complex, and methods are not yet well established in practice (2015). Thin vertical elements must be evaluated using structural analysis methods. Among the required analyses are bending of upstream-downstream walls due to cross-valley shaking, bending of cross-valley walls due to pressure from static and dynamic loads from the embankment, and complementary shear on vertical surfaces. Because soil-cement mixed in situ cannot be inspected directly (only by examining and testing drill cores), the analysis must allow for potential flaws at column overlaps, undersized jet-grout columns, and locally poor mixing. Thin elements cannot be assumed to remain in alignment after cracking and maintain good contact for frictional resistance, especially if they are surrounded by liquefied soils that offer little lateral support and may intrude into cracks.

- Regardless of which in situ cementing method is selected, extensive post-treatment verification (quality control) is required; the costs need to be considered in the selection of the preferred method. (The risk of delays and cost overruns from inadequate results also needs to be considered.) The verification program would have to include coring of the treated material to determine material properties and continuity; geophysical testing may be useful to help verify continuity. The verification program would also need to verify that there is a good contact with the underlying stronger material. If the stronger material is soil, the treatment can be designed to penetrate several feet into it, but if it is bedrock, that may not be feasible without drilling into it.

- Cementing methods create impermeable zones in the foundation. (In situ densification may also reduce the permeability, but not to the same degree.) On the downstream side of an embankment, this could impair drainage, increasing the pore-water pressure in the embankment and foundation, and

adversely affecting stability of the embankment for static or dynamic loading conditions. It may be necessary to provide for drainage using relief wells, gaps in the treatment, etc., or, possibly, to select a different method of improving the foundation. Three-dimensional stability analysis may be needed for determining how wide the gaps between treated areas can be, and 3D seepage analysis may be needed for determining what drainage measures are required. Stone columns would have less effect on drainage.

- The dynamic site response would be altered by stiffening portions of the foundation, possibly resulting in slightly stronger shaking of the dam embankment. More importantly, the cemented elements would "attract" the load because they are stiffer than the surrounding soil. Under horizontal dynamic loading, untreated loose soil would contribute little stiffness compared to intact soil-cement or cement bentonite. It may be reasonable to assume that practically all of the horizontal force is carried by the soil-cement, as long as it remains intact.

- For either limit-equilibrium or FEM/FDM analysis, one cannot model the strength and elastic properties of a zone treated with thin walls or columns by a simple weighted average of the properties of the uncemented and cemented materials, whether the latter is assumed to be cracked or uncracked. However, with massive blocks of soil-cement (as at Wickiup Dam), cracked or uncracked material can be analyzed as zones of material.

G.3.6 Drainage to Improve Embankment Performance

Drainage methods can be divided into pre-earthquake drainage, and rapid drainage of excess pore-water pressure in "real time," during and immediately following shaking. The former is intended to reduce pore-water pressure during normal operation, improve slope stability, or to desaturate loose granular soil, rendering it nonliquefiable. It can be subdivided into passive drainage, using only gravity to provide the drainage, and active drainage provided by pumped wells, wellpoints, or sumps.

For most embankment dams, drainage, regardless of category, would not be used as the primary defense against liquefaction and deformation. It would be a secondary defense used in combination with methods described in previous paragraphs for densifying or reinforcing foundation soils. Because of the difficulty in making precise predictions of seepage, especially the transient flow associated with liquefaction, generous margins of safety should be built into any drain design.

Drainage features generally need filters to protect the embankment and foundation against internal erosion. For design of filters, refer to Reclamation's *Design Standards No. 13 – Embankment Dams* [27], Chapter 5, "Protective Filters."

Particularly for drains that would flow under normal conditions (or flood surcharge), filters must follow the standard requirements of Chapter 5. If a filtered blanket drain, chimney drain, or similar feature is to be constructed, it may be necessary to extend it into areas that have not previously experienced seepage, but could have new seepage as a result of an earthquake. These would require engineered filters as well.

In filters for the unknown quantities of seepage from cracks resulting from an earthquake, or in filters for drains to reduce water levels prior to an earthquake, adequate permeability is very important. It would typically be necessary to use a two-stage filter-drain, with sandy material for the filter and the coarsest, most pervious drainage material that can provide adequate particle retention for the filter. (Possibly, a third material would be needed as an intermediate filter.)

Flow through cracks is a 3D problem, although only two-dimensional (2D) seepage analysis is common in dam practice. A simple method to estimate required drain capacity for seepage from deep transverse cracks using 2D methods would be to assume that the cracks make the core act similar to jointed rock, with the depth, width, and spacing of the cracks judged from the expected deformation and differential settlement. Snow [28] suggests a procedure for estimating an equivalent permeability to allow the seepage to be modeled as Darcy flow, considering the spacing and opening of the fractures (recognizing the substantial imprecision in both predicting crack properties and estimating equivalent permeability from the crack properties). Instead, one could assume that the cracks would act as deep, narrow, open channels that would conduct reservoir water to the filter and drain with little head loss, compared to the head loss that would occur in the filter and drain, where there would be Darcy flow. Under that assumption, a 2D analysis would overestimate the flow volume or flux by orders of magnitude because the total width of the cracks would be a very small fraction of the length of the dam. The flow volume or flux so calculated would need to be adjusted to account for the finite crack width. This approach was used for checking the capacity of the drains in the overlay for the seismic modification of MIAD in California. (See figure G14.) Wide, deep cracks were assumed to transmit full reservoir head to the upstream side of the drain. The seepage calculations were then done in two stages. First, the flow volume was calculated in a 2D FEM analysis, assuming full reservoir head as the boundary condition at the drain's upstream side. Then, it was assumed that the actual flow volume could be approximated by reducing the calculated flow volume in proportion to the thickness of the cracks, estimated to be about 2.5 percent of the length of the dam. A second 2D analysis was then performed, this time with a flux boundary condition at the upstream side of the drain, instead of the head boundary condition, with the flux at each node being 2.5 percent of the flux from the first analysis. This approximation indicated that the proposed drain had adequate capacity as designed. While this was thought to be very conservative,

the conservatism did not increase the cost of modifying MIAD. With clean, coarse drain material available, the minimum dimensions of a constructible, robust drain were more than enough to provide the necessary capacity. The flow quantity could be more critical to the design for projects other than MIAD, if material like that is not available.

Figure G14. Two-stage filter being installed within overlay at MIAD in California. The filter is the light gray band crossing the picture from the lower left corner.

Regardless of the type of foundation treatment, the design process should include seepage analysis to verify that the design would not back up pore-water pressure under the embankment in such a way that static or dynamic stability could be adversely affected. Additional drainage may be necessary. Design of drainage features is described in *Design Standards No.13 – Embankment Dams* [27], Chapter 2, "Embankment Design," and Chapter 8, "Seepage Analysis and Control."

G.3.6.1 Pre-Earthquake Drainage
G.3.6.1.1 Passive Drainage. Permanent features for pre-earthquake drainage would be essentially the same as those used in typical embankment dam designs, such as relief wells, deeply incised toe drains, and improved surface drainage, which are primarily passive measures that do not require pumping. Modification by in situ densification can result in decreased permeability, which may need to be offset by additional relief wells, blanket drains, or other features. Soil-cement

and cement-bentonite are practically impervious, but shear keys created by excavation and replacement can generally include filters and drains within the backfill to avoid any increase in piezometric levels.

Sasaki et al. [29] report that a levee that had been modified with a gravel toe drain to lower the phreatic level within the embankment performed well during the 2003 North Miyagi earthquake; nearby levees without toe drains suffered severe damage.

At Reclamation's Casitas and Bradbury Dams, the bottom portions of the compacted earthfill keys were filled with cobbles, thereby both putting the strongest available material in the narrowest part of the key and providing a continuous, highly pervious drainage layer. In both cases, there is a two-stage filter to prevent internal erosion from the foundation alluvium into the cobbles. At Reclamation's Deer Creek Dam in Utah, the drainage layer was constructed as a gravel blanket drain (with filters) approximately at the level of the original ground surface, rather than at the bottom of the key. This location was selected to make it easier to monitor foundation seepage than if the drainage was at the base of the shear key.

For Jackson Lake Dam, the upstream cutoff and the DSM honeycomb under the upstream slope embankment provide nearly positive seepage cutoff, but the reconstructed embankment included a filtered toe drain

G.3.6.1.2 Active Dewatering. Though uncommon, active dewatering systems have been used to lower groundwater levels in an effort to prevent liquefaction of materials during strong seismic shaking. Materials that are made unsaturated by dewatering would be nonliquefiable, and simply lowering the piezometric level would reduce the cyclic stress ratio resulting from a given earthquake loading. Experiments by Eseller-Bayat et al. [30] suggest that reducing the saturation to 80 percent would be adequate in medium-density soils, but 60 percent saturation may be needed in very loose ones. Active pumping from wells or sumps is likely to be used only as a temporary measure because of the ongoing maintenance and power costs, and because layers containing fines may not be fully desaturated by gravity flow to the wells.

At Bradbury Dam, a dewatering system was needed for excavation for the earthfill key to stabilize the downstream slope in case of liquefaction. The wells were installed and operated well ahead of the beginning of construction, both to allow time to debug the dewatering system prior to the contractor beginning excavation, and to reduce the risk in the interim by desaturating the clean sand and gravel in the foundation to make them less prone to liquefaction [5]. The excavation was located adjacent to a large spillway stilling basin that could not be unwatered for the duration of excavation and backfilling. With pervious alluvium

between the excavation and stilling basin, it was necessary to construct a soil-bentonite cutoff wall to make dewatering quantities manageable. When the key was being backfilled, and the cutoff was no longer needed to prevent water flowing upstream into the excavation, large gaps were cut into it so that it would not inhibit seepage from the reservoir moving downstream.

Materials with large amounts of fines may remain saturated due to capillarity, and, therefore, still be susceptible to liquefaction, even if the piezometric level has been lowered. If so, dewatering would not provide positive protection against liquefaction, so the suitability of dewatering to prevent liquefaction needs to be judged with consideration of the stratigraphy at a very small scale. The reliability of a dewatering system is also an issue. Particularly at sites where the groundwater would recover rapidly in case of system outage, frequent inspection and maintenance are necessary. If an earthquake were to cause failure of the dewatering system, followed by rapid recovery of the groundwater, the foundation could be vulnerable to liquefaction in aftershocks. The cost of powering the pumps and providing backup power can be significant, and wells and pumps generally lose efficiency with time, so they require regular maintenance. Therefore, use of dewatering systems for preventing liquefaction is generally limited to short-term use at sites with high annual probability of earthquake loading. It is most likely to be selected for interim reduction in risk prior to and during construction of some other type of foundation treatment. (Most other methods would not have the recurring expenses, with the possible exception of drain maintenance.)

G.3.6.2 Drainage for Rapid Pressure Relief During and After an Earthquake

It is possible to drain excess pore pressure from loose, saturated soil as it develops, not necessarily fully precluding liquefaction, but minimizing its effects. It has been proposed that in very pervious soils, drainage of excess pore-water pressure could be accomplished with vertical drains within the soil, much like drains used to hasten the progress of consolidation of clay by radial flow [31]. That has been implemented at a number of sites other than dams [32]. The original idea was large-diameter auger holes backfilled with clean gravel; more recently, the focus has been on slotted pipe drains with fabric "socks."

After an earthquake, a dam embankment still provides a large static driving force for slope movement. In a number of the case histories of earthquake-induced flow slides, the slide occurred minutes or hours after the end of shaking, likely due to void redistribution and formation of loosened zones with high excess pore pressure. Void redistribution could cause instability, even if the dam initially survived the earthquake with only modest deformations (See appendix F). If, instead of migrating upward to where it can create loosened zones, water expelled from liquefied soil as it settles is collected in drains, it would not cause the drastic loss of effective stress that causes flow slides.

No case histories of dams stabilized with earthquake drains were located during preparation of this appendix. However, Sasaki et al. [29] report relatively good performance of a levee embankment with drains in the 2011 Tohoku earthquake in Japan; an adjacent levee without drains behaved poorly. It should be noted, however, that typical drain construction practice includes vibration, which tends to densify the surrounding sand. It is, therefore, not clear how much benefit came from densification and how much came from drainage. In contrast, gravel drains installed at the Jensen Filtration Plant failed to prevent liquefaction and lateral spreading during the 1994 Northridge earthquake; there, the permeability of the treated soils and/or of drains themselves apparently was too low [33]. Some centrifuge and larger-scale experiments have shown benefit from vertical slotted pipe drains [32, 34, 35]. Again, it should be noted that in the experiments, the drains were installed either with vibration that apparently caused some densification around them, or they were installed under ideal conditions, including very pervious soil, and installation procedures that would not produce "smear" along the walls of drill holes to affect permeability.

The viability of drainage for dissipating enough excess pore-water pressure to maintain stability would be governed by the permeability of the soil to be treated; the volume of water that would need to be drained rapidly (up to 2 percent of the soil volume); head losses through the sock, slots, and any "smear" of the walls of the hole; and the spacing of the drains. There must be a free surface to which the expelled water can drain, or else unsaturated highly pervious material (clean coarse gravel or cobbles) with enough void space to act as a reservoir for the expelled water.

At this time (2015), Reclamation does not rely on drainage as the primary means of protecting a high-hazard dam. However, in highly pervious soils, earthquake drains may be used to provide redundancy for an additional margin of safety.

Reclamation has made use of a different drainage concept to prevent excess pore-water pressure migrating from liquefied foundation material into a treated area. On the downstream side of MIAD, lines of closely spaced, small stone columns or "mini-columns" were installed between untreated foundation material and foundation material that had been densified using stone columns, with very little vibration in order to minimize intrusion of the native material into the voids of the gravel in the mini-columns. Voids in the unsaturated portion of the stone columns above the static water table would act as a reservoir for water expelled from the liquefied material.

G.3.7 Verification of Foundation Improvement

Verification of adequate foundation treatment requires two things:
(1) demonstrating that the design is adequate and (2) quality control during
construction. Procedures and the level of difficulty vary considerably among
methods. Documentation needs to be timely and thorough.

G.3.7.1   Excavation and Replacement

With foundation treatment by excavation and replacement, verification is simple
and inexpensive. Ordinarily, placement of the fill can be observed as it occurs,
and conventional embankment construction control is all that is needed. This
would require sand cone, ring, and/or nuclear density tests, and laboratory
maximum-density tests to verify that the shear-key fill has been compacted to the
specified minimum density. Typically, the minimum is 95 to 98 percent of the
laboratory maximum density as determined by American Society for Testing and
Materials (ASTM) D 698 (Proctor-type impact test) for material containing
substantial amounts of fines, and either ASTM D 4253-00 (vibrating table) or
ASTM D 7382-08 (vibratory hammer) for free-draining coarser soils. It was
formerly common for compaction of sands and gravels with only small amounts
of fines to be controlled by the relative density test. However, compaction is now
generally controlled by the percentage of the maximum density for all materials,
which eliminates the uncertainty and additional work of performing the
minimum-density test. As needed, gradations and permeability of the materials
are measured by conventional laboratory tests or infiltrometer tests on the fill, and
quantities are measured by surveying and counting truckloads.

It is very important to map, evaluate, and document the condition and
acceptability of the foundation at the bottom of the excavation upon which the
backfill materials are to be placed. This is necessary to verify the designers'
assumptions about the foundation materials at the contact (integrity,
strength, roughness, liquefaction resistance, etc,). For a soil foundation,
(e.g., Reclamation's Pineview and Deer Creek Dams), this would include
laboratory testing and in situ density tests for calculating relative density or
relative compaction. For a rock foundation, geologic mapping and surface
characteristics are needed. Photogrammetry was used to obtain a permanent
3D record of the geology and surface roughness at the bottom of the key block
excavation at Mormon Island. Figure G15 shows the prepared surface, with lines
painted on the bedrock to simplify mapping and highlight important features of
the surface.

Figure G15. Bedrock painted for geologic mapping and photogrammetry at the bottom of the MIAD key block (2011).

G.3.7.2 In Situ Densification

Verification of in situ methods of foundation improvement generally requires much more effort and entails much greater uncertainty because the work is not exposed in plain sight. Densification is usually verified by penetration testing, using the SPT, the CPT, and/or the Becker hammer penetration test (BPT); shear-wave velocity, V_S, can also be used. Typically, acceptance criteria are established based on a liquefaction triggering correlation with SPT or CPT, described in appendices B and C, respectively. In material that is too coarse for SPT or CPT, the BPT may be used to estimate an equivalent SPT blow count. SPTs or CPT soundings are typically done at the centers of the areas among columns or DC impact locations, on the assumption that they would be the least likely locations for adequate treatment to have occurred. The acceptance criteria would be based on the adjusted SPT blow count or CPT tip resistance needed to provide a suitably low probability of liquefaction under the maximum cyclic shear stress ratios that the foundation could experience. Drilling and sampling are needed also because liquefaction potential depends on fines content and Atterberg limits, in addition to the penetration resistance, and the CPT and BPT do not provide samples the way the SPT does. Historically, Reclamation has used all three tests, but SPT is the most prominent one because a sample is retrieved with each test, and it is possible to test below dense material that would cause refusal of the CPT. BPT, and especially CPT, have the advantage of producing more

continuous readings of penetration resistance, and they are generally faster, which are important considerations when construction schedules are involved.

Complications arise when material is added to the foundation, as with stone columns. The gravel does not form neat cylindrical columns; instead, it may deviate and spread unpredictably. Soundings or drill holes between columns often end up penetrating the column material, instead of the treated native soil, so the meaning of the data is less clear.

Caution is required with densification methods that increase the horizontal effective stress and the value of K_0. The increase could have a modest effect on penetration resistance (SPT N or CPT q_c) or on shear-wave velocity (V_S). More importantly, however, CPT friction ratio is sensitive to K_0. The interpretation of soil properties from the friction ratio is empirical, and it depends on having typical K_0 values. Higher K_0 may cause the CPT to predict higher fines content and, therefore, greater resistance to liquefaction *for a given CPT tip resistance*; the result is unconservative. If the post-treatment K_0 exceeds typical values like 0.4 to 0.5, an adjustment may be needed [36]. The Harder-Seed method of BPT analysis contains implicit assumptions about the rod friction, which is a function of the horizontal effective normal stress, so it too could be unconservative if K_0 is atypically high. (Refer to appendix D.) The Sy-Campanella method should not be affected as much because the effects of rod friction are explicitly measured and accounted for, but it requires post-processing that could slow the acceptance or rejection of areas that have been treated. Verification testing usually occurs within a few days after densification so that the contractor can proceed with treating other areas or perform other work, and so that inadequately densified areas can be retreated while it is still practical to do so. It should not occur too soon, however. Any in situ test results are likely to be influenced by pore pressures generated by the various densification processes; hence, they should not occur immediately after treatment, even in very pervious granular soils. Once the excess pore-water pressures have dissipated (probably by the next day in granular soils), the tests may initially indicate poor densification but improve for days and even years. It has been shown at a number of sites, however, that penetration resistance and V_S continue to increase for some time after all excess pore-water pressure generated by compaction has had time to dissipate. The best known case is Jebba Dam in Nigeria, where blast densification was used to improve the foundation prior to construction. Initially, the SPT blow counts were less than they were prior to treatment, but they increased dramatically in subsequent weeks [37]. Similar behavior has been observed after dynamic compaction [5, 38]. Prior to deep dynamic compaction on the upstream side of MIAD, cross-hole V_S in the untreated foundation material was very low: as low as 460 feet per second (ft/s). Dynamic compaction was completed in late 1990, but a new cased, cross-hole triplet was not drilled and tested until January of 1992 (so there was no measurement immediately after compaction). With the exception of a layer near the bottom of the profile (which was too deep or too impermeable to be improved much by DDC), the 1992 values

were all much higher (950 ft/s or more), indicating successful treatment.
Subsequent measurements in the same triplet in 1994 and 2000 found
successively higher measurements, increasing tens of feet per second between
each pair of readings. (No measurements have been taken since 2000.)

The observed increases in penetration resistance and V_S with time suggest that
applying construction acceptance criteria to in situ measurements soon after
treatment could introduce a moderate amount of conservatism, with respect to an
earthquake that would occur tens to hundreds of years later after treatment. It is
not, however, recommended to assume that much additional improvement in
liquefaction resistance would occur with aging before an earthquake would occur
at the site. An earthquake is just as likely to occur in the first year after
construction as it is in the 19th or 53rd year, and any predicted increase in
liquefaction resistance would be speculative.

G.3.7.3   Cementing Methods

For cementation methods that create soil-cement or similar material in place,
verification of treatment is more complicated. Not only must the soil-cement or
cement-bentonite have adequate compressive and shear strength, but there must
be continuity of intact material without gaps between columns, or weak or poorly
treated zones within the good material. Continuous coring of the cemented
material can identify untreated zones or weak material, but an extensive coring
program is needed to verify good treatment at column overlaps, changes in strata,
and contact with bedrock below the treated zone. Laboratory strength
measurements on recovered cores (usually unconfined compression tests or
triaxial tests) can determine the strength properties of the intact cemented
material, but they only test a few cubic inches at a time, not the behavior of the
soil-cement structure as a whole, analogous to the difference between properties
of rock cores and of rock masses. Soil-cement is much stiffer and stronger than
soil; therefore, it needs to be tested as if it were weak rock, rather than soil, with
the strain/deformation measurements made directly on the specimen, rather than
outside a triaxial cell, as is usually done with soil specimens. Geophysical testing
may be helpful in verifying continuity, but methods have not been well
established.

G.4   Preventing Internal Erosion

Instability and deformation are not the only potential failure modes that can result
from an earthquake. Internal erosion resulting from transverse cracking of the
embankment is thought to have caused failure of at least two dams in the United
States (Rogers Dam and Coleman Dam, both diversion dams affected by the
1952 Fallon, Nevada Earthquake) [39]. Another dam apparently showed the
initial stages of internal erosion simply from being shaken (Chatsworth Dam,
California). Fortunately, deep transverse cracks are uncommon, but an

embankment that undergoes large displacement could be cracked by differential
settlement. The loss of freeboard compounds the potential for failure by
shortening the seepage path and reducing the amount of embankment material
that would have to be eroded to cause a breach.

The two main countermeasures are: (1) filters to stop movement of eroded
particles, and (2) upstream crackstoppers that would be washed into a transverse
crack and help to plug it, halting, or at least delaying, the progress of internal
erosion.

Most of the earthfill keys that Reclamation has constructed included filters and
drains, at least up to the original ground surface. (See Figure G1 and G16.)
When Reclamation modified Casitas Dam in California, continuous filters were
included from the bottom of the key to the top of the embankment. The crest of
the dam had to be widened with an overlay (as discussed below). Within the
overlay, there is a chimney drain that consists of processed clean sand. It was not
equipped with a separate drain zone, because it was thought that the sand had
adequate permeability to handle the seepage until the reservoir could be lowered
following an earthquake strong enough to damage the embankment. Cracks
through the core, should they occur, would be at discrete locations along the axis,
and 3D flow would allow the seepage to spread out in the cross-valley direction in
a way that a 2D seepage analysis would not predict. This would make the
separate drainage zone less critical. (Drainage was provided within the key,
below the original ground surface, so as not to interfere with seepage under
normal operating conditions.) The modification of Deer Creek Dam, Utah,
completed in 2008, included a chimney filter extending from the invert of the key
trench to 12 feet above the top of active storage, so that the core would be
protected in the unlikely event of very large settlement. (It is considered unlikely
because of the large berm, overlay, and earthfill key to maintain stability of the
downstream slope.)

Conceptually, design of filters for this purpose is the same as described in *Design
Standard No. 13 – Embankment Dams* [27], Chapter 5, "Protective Features,"
although there are some additional considerations. First, filters in the upper part
of an embankment could remain dry for many years until they are suddenly called
upon to undergo large deformations during an earthquake, without leaving any
cracks that do not heal immediately upon the arrival of water. This requires that
the filter material be very clean, lacking fines and fine sands that could create
apparent cohesion by capillarity, and especially, free of any sort of cementing
agent, such as salts [40]. Any tendency toward cementing contributes to potential
for cracks to remain open. Cementing agents are most likely to exist in borrow
areas located above the water table in dry climates, where infiltrating salts would
tend to be deposited. Petrographic examination of potential filter materials is
generally required, regardless of origin. Washed sand is preferred, and washing
may actually be necessary for some sources. It is also important that filters are
not compacted too much.
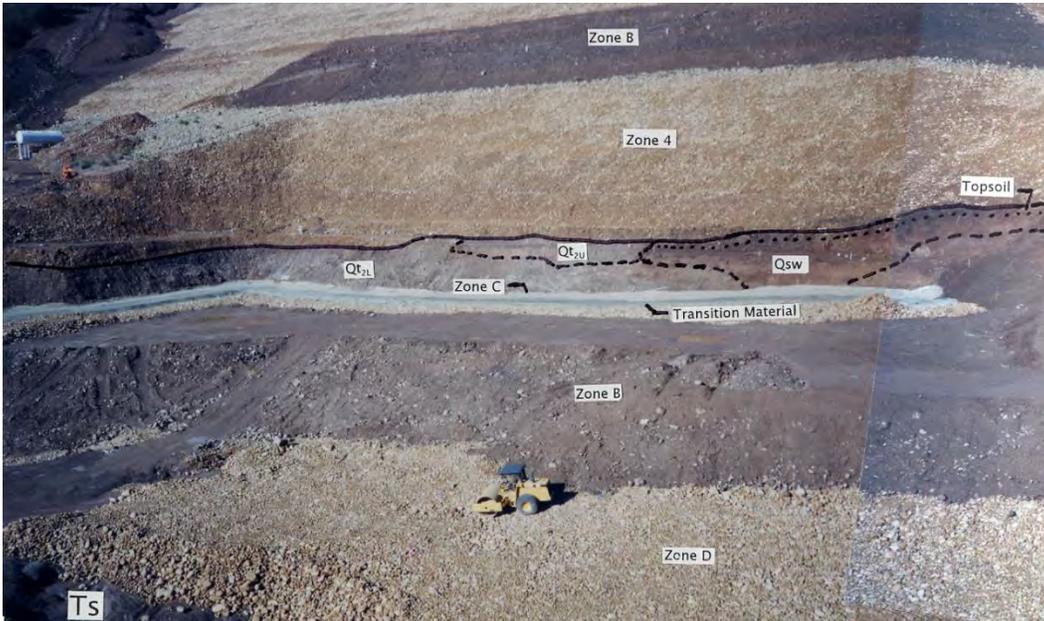
Figure G16. Filter (Zone C) transition and drain (Zone D) in shear key, Casitas Dam, California. Zone B (darkest material at the top and middle of the photo) is compacted miscellaneous fill for berm and remainder of key.

Milligan [41] wrote, "Compaction of filters should be minimal. Excessive compaction, particularly of crushed rock, can lead to the creation of sufficient fines in the filter to make them susceptible to cracking." Excessive compaction can also create a thin layer with low permeability at the top of each lift, due to particle breakage and higher density. This affects the vertical permeability of the filter zone much more than the horizontal permeability. Compaction is usually specified as relative compaction ("D" value) between 90 and 94 percent of the laboratory maximum, or as relative density of 70 to 75 percent. Reclamation currently uses the former, but many earlier Reclamation projects were controlled by relative density (RD). It is important that filters be able to deform without leaving open cracks, and higher densities decrease the ability of a filter to collapse and "self-heal." The greater tendency for denser filters to sustain cracks was among the findings of experiments by Redlinger et al. [42] and Reclamation [43].

If they are wide enough, cracks in the core and upstream zones could allow water at nearly full reservoir head to reach the filter. The filter must be capable of remaining in place, through some combination of drainage to relieve high pore pressure and sufficient weight or confinement to resist uplift or blowout. This would generally require a berm of sufficient height to counteract the uplift pressures and/or a separate drain zone that is more pervious than the filter, unless analysis shows otherwise.

Depending on the dam core's gradation, no-erosion filters required by Reclamation's *Design Standards No. 13 – Embankment Dams* [27], Chapter 5,

"Protective Filters," commonly require the maximum D_{15} to be as low as 0.7 millimeters (corresponding roughly to the U.S. Standard No. 30 sieve), or occasionally even less. This limits their permeability, possibly making it too low for the amount of water they would have to pass if the embankment core is cracked, making the drains less effective. Filter and drain gradations for seismic remediation may need to be compromises between particle retention, (which favors a finer filter) and adequate permeability and reduced capillarity (which favor coarser filters). It may be acceptable (case by case) to relax the filter criteria normally used for dams and allow slightly coarser material. This would be acceptable only in situations where limited particle movement after an earthquake could be tolerated. As a minimum requirement, a filter would have to be finer than the "excessive erosion" boundary, as defined in Foster and Fell [44], instead of the typical "no-erosion" filter generally required by chapter 5 of Design Standards No. 13. Filters that experience significant seepage in normal operation should still be designed by chapter 5. Refer to Foster and Fell [44] for the behavior of filters that do not strictly meet a no-erosion criterion. **The rationale for any deviation from the normal filter design criteria in chapter 5 of Design Standards No. 13 requires formal review, approval, and documentation in a technical memorandum.**

It is common to use ASTM C33 fine concrete aggregate as a filter in dams because of its easy availability and well-defined properties, which include meeting particle-retention criteria for nearly any base soil. However, it can include a small amount of fines and up to 10 percent sand passing the U.S. Standard No. 100 sieve, 0.15 millimeter, which limits its permeability. Therefore, filter material conforming strictly to the standard C33 fine aggregate is often not appropriate; instead, one should use the coarsest readily available sand that meets the particle retention criteria in chapter 5. This, along with avoiding excessive compaction, would also help minimize the potential for cracks in the filter. Chapter 5 of Design Standards No. 13 [27] describes a modified C-33 fine aggregate gradation that limits the fines content to a maximum of 2 percent in the stockpile and 5 percent in place. This gradation would provide the same particle retention as the standard C33 sand, while somewhat decreasing the potential for it to sustain a crack. Modified C-33 is commercially available in many places; however, the permeability is still limited to that of fine sand.

As a general rule, earthfill shear keys should include filtered drains, so that the compacted fill does not inhibit seepage under normal conditions or after an earthquake. It is also good practice to extend the filter well above the normal reservoir level, so that it remains above the reservoir following possible settlement of the embankment. Filters should be thick enough to remain continuous after embankment deformation.

Upstream crackstoppers have been used as backup protection against erosion through transverse cracks caused by an earthquake. They consist of a clean sand-and-gravel mixture that could drop into an open crack, or be washed into it

by flowing water, and help to plug it, thereby halting (or at least delaying) erosion of a breach. Even if it does not actually get washed into cracks and plug them, an upstream zone containing sand and fine gravel will still cause some head loss in water flowing through it, which could also reduce erosion of the core. (The permeability of the crackstopper is governed by the finer material in it.) If the crackstopper material does get washed into the crack, there would need to be a downstream zone that would remain in place and prevent it from being carried all the way through the crack, where it would provide no benefit. Crackstoppers have been constructed at a number of dams since the 1930s [45], but to date (2015), none of them have actually been tested by an earthquake. Most embankment dams contain a transition zone or pervious upstream shell to provide drainage and filtration for reverse flow during reservoir drawdown; this may also provide some crackstopper capability. Crackstoppers, whether they are designed as such or are existing materials that could act as a crackstoppers, should be regarded as providing redundancy, rather than being the primary defense against erosion through cracks.

G.5 Other Protective Measures

G.5.1 Crest Raises

Embankment crests can be raised for two purposes: (1) providing additional freeboard to reduce the risk that embankment deformation would allow overtopping, and (2) preventing overtopping by seiche waves. Reclamation raised the crests of Pineview and Deer Creek Dams, both in Utah, because even with modifications to stabilize the downstream slopes, there was still thought to be potential for large settlements to encroach on the freeboard because the upstream slopes could not be stabilized without draining the reservoirs. The Deer Creek raise is conventional earthfill and was placed on the existing embankment crest. The unconventional raise of Pineview Dam was constructed entirely downstream of the embankment crest because, otherwise, it would have been difficult to restore full use of the existing highway that crosses the dam. The upstream side of the raise is supported by a retaining wall along the downstream side of the crest. The downstream side of the raise is an extension of the 2H:1V (horizontal:vertical) slope of an overlay placed on the downstream slope. Within the raise are earthfill core material, a filter, a transition, and flowthrough rockfill. Should large movements of the upstream slope cause severe cracking and enough settlement that the raise would be exposed to the reservoir, the rockfill in the raise and overlay would protect the embankment from erosion by acting as a drain for water passing through the damaged crest raise.

When the embankment for Jackson Lake Dam was reconstructed after removal, it was given very generous freeboard, in part because the reservoir basin was on the hanging wall of a large normal fault. Rupture of the fault could cause the basin to

tilt away from the dam, so that water would initially rush away from the dam (fortunately), but there could be a large seiche wave returning to the dam. The additional freeboard was designed to prevent overtopping by the possible seiche, something that actually happened at Hebgen Lake Dam in1959 [46]. As an alternative to a crest raise, the very small embankments at Lake Tahoe Dam were protected from seiche wave overtopping by concrete overlays, with blocks of polystyrene foam below them to prevent freezing of the soil below, which could have caused heaving of the concrete.

G.5.2 Overlays and Embankment Widening

There have been cases where both slopes of the embankment could have become unstable, or at least displaced enough to contribute to large crest settlements, but because of water operations or other reasons, it was not possible or practical to stabilize both slopes using foundation treatments and berms. This situation can sometimes be addressed by stabilizing the downstream slope and building an overlay that widens the crest on its downstream side, so that failure of the upstream slope would not cause release of the reservoir. This approach was used at Salmon Lake and Casitas Dams. In both cases, the post-earthquake factor of safety against instability of the downstream slope was very low prior to the modification, due to the presence of liquefiable alluvium. At Casitas Dam, the downstream side was stabilized with a compacted earthfill shear key and a large berm. The cutoff trench of the dam was offset upstream of the centerline, so it, in effect, created a small shear key under the upstream slope, and post-earthquake stability of the upstream slope was marginal (unlike the downstream slope, which had factors of safety well below 1.0). Whether the calculated post-liquefaction factor of safety for the upstream slope was above or below 1.0 was sensitive to the assumed strength of the liquefied alluvium, with only very conservative strength estimates indicating instability. Sliding was, therefore, considered unlikely, but it was not completely ruled out. Draining the reservoir to work at the upstream toe would have almost completely eliminated project benefits for at least one water year, so instead of stabilizing the slope, the crest was widened on its downstream side to as much as 110 feet (tapering narrower toward the abutments, where the foundation was bedrock, rather than alluvium, and the width was not needed). (Refer to figures G17a and G17b.) In effect, the overlay made the upstream slope sacrificial by providing a new dam embankment that would contain the reservoir if the upstream slope slid away. The overlay covered much of the downstream face of the embankment down to the top of the stability berm or abutments. It included a chimney filter and bidirectional geogrids to help maintain the integrity of the remnant crest against both instability and transverse cracking. A similar design (without the geogrids) was constructed at Salmon Lake Dam; see figure G9a.

Figure G17a. Casitas Dam stability berm and widened crest.
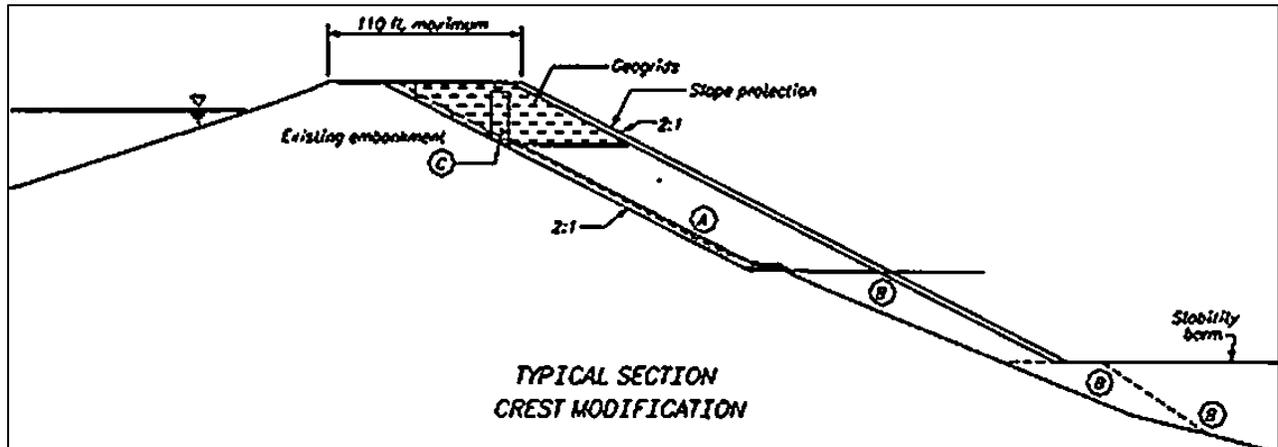
17b. Casitas Dam overlay with filter (zone C) and geogrid reinforcement.

As mentioned above, the modification of Pineview Dam included an overlay that is integral with the crest raise. In addition to providing a base for the raise, the overlay includes flow-through rockfill to safely convey seepage that might come through a badly cracked remnant of the crest raise and the upper part of the existing dam and erode the embankment. Figure G18 shows the Pineview overlay under construction.

**Figure G18. Placement of flowthrough rockfill, transition, and filter zones,
downstream to upstream (left to right), Pineview Dam modification, Utah.**

G.5.3 Embankment Reinforcement

In addition to reinforcement in the overlay on Casitas Dam (figure G17b),
geogrids have also been used as tensile reinforcement at the base of embankments
to prevent spreading of the embankment upstream and downstream. Two
examples are Jackson Lake Dam (figure G19) and a dam belonging to another
agency, for which Reclamation designed modifications. In both cases, the
embankment was removed completely, then it was reconstructed after foundation
improvement. The geogrids were oriented with their strong direction upstream-
downstream.
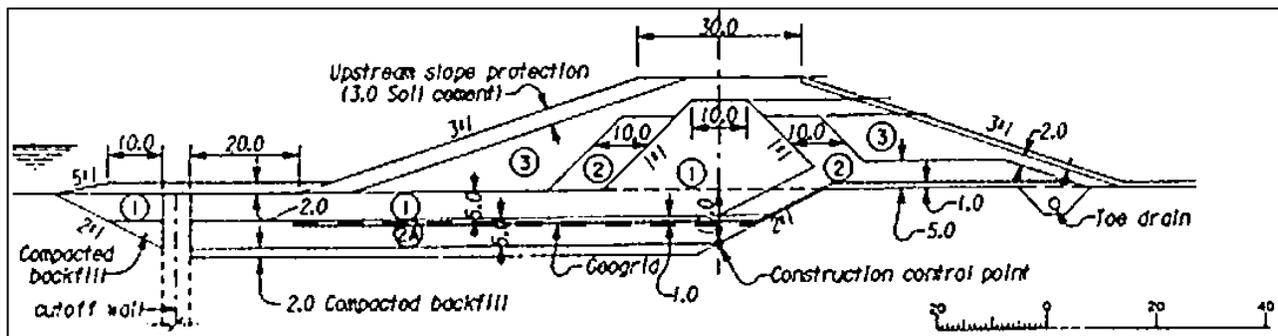
 **Figure G19. Geogrids for tensile reinforcement of embankment foundation, Jackson Lake Dam,
Wyoming. Heavy dashed line shows location of geogrids.**

With continuous geogrids across the embankment from the upstream side to the downstream side, it was necessary to provide sand filters around the downstream geogrids because they could form a vulnerability for initiation of internal erosion.

The longevity of geogrids buried deep in a foundation, away from oxygen, light, and temperature fluctuations, is unlikely to be a problem. Refer to Koerner [47] for details of testing geogrids and protecting them from the elements.

G.6   Analysis of Modification Designs

The level of analysis required for acceptance of a modification design depends on the type of modification, the severity of the potential loading, and the characteristics of the dam and foundation, including the amount of pre-earthquake freeboard, properties of foundation soils, and the type of foundation treatment.

Any or all of the following may be needed:

- Equivalent-linear dynamic response. The commonly used relationships for triggering of liquefaction all are referenced to cyclic stresses from equivalent-linear analysis. Equivalent-linear response analysis is also used to find the acceleration time history for Newmark's sliding-block procedure for estimating settlement.

- Liquefaction triggering, using correlations with "indices" of density, such as SPT or V_s.

- Post-earthquake static stability of the embankment with liquefied material in the foundation or embankment, if applicable.

- Newmark's numerical sliding-block procedure for embankment deformation.

- The simplified deformation chart solutions by Newmark [48] and Makdisi and H. Seed [49]. (A newer chart solution developed by Bray and Travasarou [50] is available, but it has not yet been evaluated by Reclamation.)

- Nonlinear FEM or FDM analysis of dynamic deformation (primarily due to *shear* strain). The earthquake loading would occur very rapidly, so undrained shear strengths are often needed.

- Settlement due to post-earthquake *volumetric* strain as excess pore-water pressure dissipates.

- Cracking potential. Differential movements between two portions of the dam have the potential to create longitudinal and transverse cracks. Cracks could occur at abrupt changes in embankment height or foundation materials, for example, part of an embankment on loose alluvium adjacent to part on bedrock, particularly steep abutments, or appurtenant structures within the embankment.

- Two- or three-dimensional dynamic structural analysis of foundation reinforcement by soil-cement or other "stiff" material, particularly if the reinforcement is in the form of walls or columns, for which bending loads can be very important. There may also need to be detailed analysis of the transfer of forces from the embankment to the reinforcement to the firm foundation material below it. Brittle behavior and potential flaws, e.g., incompletely overlapped jet-grout columns, must be accounted for in the structural analysis,.

- Filter compatibility for areas of the dam with potential for cracks to form, or with existing high gradients and unfiltered seepage, where strong shaking could precipitate internal erosion.

- Seepage analysis for normal operation after construction.

- Seepage analysis and dewatering for construction.

- Hydraulic calculations for reservoir seiche waves or overtopping flow.

- Risk-reduction analysis to verify that the proposed modification provides the necessary level of safety.

- Construction risk analysis to verify that the construction process does not create undue risk for the downstream public or construction personnel.

References

[1] *Performance of Improved Ground During the Loma Prieta Earthquake*, Report No. UCB/EERC-91/12, J.K. Mitchell, and F.J. Wentz, University of California at Berkeley, Berkeley, California, 1991.

[2] "Soil Improvement for Earthquake Hazard Mitigation," Soil Improvement and Geosynthetics Committees of the Geotechnical Engineering Division of the American Society of Civil Engineers (ASCE), *Geotechnical Special Publication,* No. 49, October 22-26, 1995.

[3] "Aspects of Compaction Grouting of Liquefiable Soil," R.W. Boulanger, and R.F. Hayden, *Journal of Geotechnical Engineering,* American Society of Civil Engineers (ASCE), Vol. 121, No. 12, pp. 844-855, 1995.

[4] "Ground Improvement, Ground Reinforcement, Ground Treatment – Developments, 1987-1997," *Geotechnical Special Publication*, American Society of Civil Engineers (ASCE), No. 69, 1997.

[5] "Dewatering for Interim Mitigation of Liquefaction Hazard at Bradbury Dam – Ground Improvement, Ground Reinforcement, Ground Treatment – Developments, 1987-1997," D.R. Gillette, and R.M. Bliss, *Geotechnical Special Publication,* American Society of Civil Engineers (ASCE), No. 69, pp. 525-542, 1997.

[6] "Theoretical and Practical Aspects of Dynamic Consolidation," L. Ménard, and Y. Broise, *Géotechnique,* Vol. 25, No. 1, pp. 3-18, 1975.

[7] "Dynamic Compaction to Remediate Liquefiable Embankment Foundation Soils," M.G. Stevens, K. Dise, and J.L. Von Thun*, Proceedings, U.S./Japan Fourth International Workshop on Remediation of Liquefiable Soils,* Public Works Research Institute, Tsukuba City, Japan, 1994.

[8] "Dynamic Compaction to Remediate Liquefiable Embankment Foundation Soils," K.M. Dise, M.G. Stevens, and J.L. Von Thun, I*n Situ Deep Soil Improvement,* Geotechnical Publication, American Society of Civil Engineers (ASCE), No. 45, pp. 1-25, 1994.

[9] "Ground Response to Dynamic Compaction," P. Mayne, J. Jones, Jr., and J. Dumas, *Journal of Geotechnical Engineering,* Vol. 110, No. 6, pp. 757-774, 1984.

[10] "Ground Improvement Using Rapid Impact Compaction," H. Kristiansen, and M. Davies, *Proceedings, 13th World Conference on Earthquake Engineering,* Vancouver, BC, Canada, 2004.

[11] *Application of the Rapid Impact Compaction (RIC) Technique for Risk Mitigation in Problematic Soils*, C.J. Serridge, and O. Synac, International Association for Engineering Geology and the Environment (IAEG), Nottingham, United Kingdom, 2006.

[12] "State of Practice for Liquefaction Mitigation in North America," R.F. Hayden, and J.I. Baez, Public Works Research Institute, *Proceedings, U.S./Japan Fourth International Workshop on Remediation of Liquefiable Soils,* Tsukuba City, Japan, 1994.

[13] "Numerical Modeling of the Seismic Response of Columnar Reinforced Ground," C.G. Olgun, and J.R. Martin*, Proceedings, Geotechnical Earthquake Engineering and Soil Dynamics IV,* American Society of Civil Engineers (ASCE), Reston, Virginia, pp. 433-451, 2008.

[14] "Numerical Study of Shear Stress Distribution for Discrete Columns of Liquefiable Soils," D. Rayamajhi, T.V. Nguyen, S.A. Ashford, R.W. Boulanger, J. Lu, A. Elgamal, and L. Shao, *Journal of Geotechnical Geoenvironmental Engineering,* Vol. 140, No. 3, 2014.

[15] "Seismic Upgrade of the Seymour Falls Dam, Design Phase," D. Siu, F. Huber, L. Murray, and W. Lozinski, *Proceedings, 13th World Conference on Earthquake Engineering,* Vancouver, BC, Canada, 2004.

[16] "Earth Foundation Treatment at Jebba Dam Site," V.Z. Solymar, C.C. Iloabchie, R.C. Gupta, and L.R. Williams, *Journal of Geotechnical Engineering,* Vol.110, No. 10, pp. 1415-1429, 1984.

[17] "Investigation of Predictive Methodologies for Explosive Compaction," W.A. Narin van Court, and J.K. Mitchell, *Proceedings, Geo Institute Specialty Conference on Geotechnical Earthquake Engineering and Soil Dynamics,* American Society of Civil Engineers (ASCE), Seattle, Washington, pp. 39-653, 1998.

[18] "Reduction of Liquefaction Potential by Compaction Grouting at Pinopolis West Dam, SC," J.I. Baez, and J.F. Henry, *Proceedings, Specialty Conference on Geotechnical Practices in Dam Rehabilitation,* Special Geotechnical Publication, American Society of Civil Engineers (ASCE), Raleigh, North Carolina, No. 35, pp. 493-506, 1993.

[19] "Deep Chemical Mixing Method Using Cement as Hardening Agent, Recent Developments in Ground Improvement Techniques," Suzuki, Yoshio, *Proceedings, International Symposium,* Bangkok, Thailand, pp. 299-340, 1985.

[20] "Jet Grouting and Safety of Tuttle Creek Dam," T.D. Stark, P.J. Axtell,
F.C. Walberg, J.C. Dillon, G.M. Bellew, and D.L. Mathews, *DFI Journal,*
Deep Foundations Institute (DFI), Vol. 6, No. 1, pp. 3-20, 2012.

[21] *An Introduction to the Deep Soil Mixing Methods as Used in Geotechnical
Applications*, Publication No. FHWA-99-138, Federal Highway
Administration, 2000.

[22] "Cement Deep Soil Mixing Remediation of Sunset North Basin Dam,"
R.F. Barron, C. Kramer, W.A. Herlache, J. Wright, H. Fung, and C. Liu,
*Proceedings, 23rd Annual Conference of the Association of State Dam
Safety Officials,* pp. 181-199, 2006.

[23] "Deep Soil Mixing for the Seismic Remediation of the Clemson Upper and
Lower Diversion Dams," L. Wooten, and B. Foreman, *Proceedings,
25th USSD Annual Meeting and Conference,* United States Society on
Dams, Denver, Colorado, 2005.

[24] "Performance of Soil Improvement Techniques in Earthquakes,"
E.A. Hausler, and N. Sitar, *Proceedings, 4th International Conference on
Recent Advances in Geotechnical Earthquake Engineering and Soil
Dynamics,* San Diego, California, 2001.

[25] "Design of DSM Grids for Liquefaction Remediation," T. Nguyen,
D. Rayamajhi, R. Boulanger, S. Ashford, J. Lu, A. Elgamal, and L. Shao,
Journal of Geotechnical Geoenvironmental Engineering, Vol. 139,
No. 11, pp. 1923-1933, 2013.

[26] "Seismic Retrofit of Tuttle Creek Dam." F. Walberg, T. Stark, P. Nicholson,
G. Castro, P. Byrne, P. Axtell, J. Dillon, W. Empson, J. Topi, D. Mathews,
and G. Bellew, *Journal of Geotechnical Geoenvironmental Engineering,*
Vol. 139, No. 6, pp. 975-986, 2013.

[27] *Design Standards No. 13 - Embankment Dams*, Chapter 5, "Protective
Filters," Bureau of Reclamation, Dam Safety Office, Denver, Colorado,
2011.

[28] "Rock Fracture Spacings, Openings and Porosities," D.T. Snow, *Journal of
the Soil Mechanics and Foundations Division,* American Society of Civil
Engineers (ASCE), Vol. 94, pp. 73-91, 1968.

[29] "Reconnaissance Report on Damage in and round River Levees Caused by
the 2011 Off the Pacific Coast of Tohoku Earthquake," Y. Sasaki,
I. Towhata, K. Miyamoto, M. Shirato, A. Narita, T. Sasaki, and S. Sako,
Soils and Foundations, Vol. 52, No. 5, pp. 1016-1032, 2012.

[30] "Liquefaction Response of Partially Saturated Sands, I: Experimental Results," E. Eseller-Bayat, M.K. Yegian, A. Alshawabkeh, and S. Gokyer, *Journal of Geotechnical Geoenvironmental Engineering,* Vol. 139, No.6, pp. 863-871, 2013.

[31] "Stabilization of Potentially Liquefiable Sand Deposits Using Gravel Drains," H.B. Seed, and J.R. Booker, *Journal of Geotechnical Engineering Division,* American Society of Civil Engineers (ASCE), Vol. 103, pp. 757-768, 1977.

[32] "Liquefaction Hazard Mitigation by Prefabricated Vertical Drains," K.M. Rollins, R.R. Goughnour, J.K.S. Anderson, and S.F. Wade, *Proceedings, 5th International Conference on Case Histories in Geotechnical Engineering,* New York, New York, 2004.

[33] "Drainage Capacity of Stone Columns or Gravel Drains for Mitigating Liquefaction," R.W. Boulanger, I.M. Idriss, D.P. Stewart, Y. Hashash, and B. Schmidt, *Proceedings, Geotechnical Earthquake Engineering and Soil Dynamics III,* Geotechnical Special Publication, American Society of Civil Engineers (ASCE), Seattle, Washington, Vol. 1, No. 75, pp. 678-690, 1998.

[34] "Centrifuge Modeling of Prefabricated Vertical Drains for Liquefaction Remediation," R. Howell, E. Rathje, R. Kamai, and R. Boulanger, *Journal of Geotechnical and Geoenvironmental Engineering,* Vol. 138, No. 3, pp. 262–271, 2012.

[35] "Effect of Prefabricated Vertical Drains on Pore Pressure Generation in Liquefiable Sand," E.M. Rathje, W.J. Chang, B.R. Cox, and K.H. Stokoe, Jr., *Proceedings, 11th International Conference on Soil Dynamics and Earthquake Engineering and 3rd International Conference on Earthquake Geotechnical Engineering,* Berkeley, California, Vol. 2, pp. 529-536.

[36] "Lateral Stress Effects on CPT Liquefaction Resistance Correlations," R. Salgado, R.W. Boulanger, and J.K. Mitchell, *Journal of Geotechnical Engineering,* American Society of Civil Engineers (ASCE), Vol. 123, No. 8, pp. 726-735, 2004.

[37] "Time Dependent Strength Gain in Freshly Deposited or Densified Sand," J.K. Mitchell, and V.Z. Solymar, *Journal of Geotechnical Engineering,* American Society of Civil Engineers (ASCE), Vol. 110, No. 11, pp. 1559-1576, 1984.

[38] "Delayed Soil Improvement After Dynamic Compaction," R.G. Lukas, *Ground Improvement, Ground Reinforcement, Ground Treatment - Developments 1987-1997,* Geotechnical Special Publication, American Society of Civil Engineers (ASCE), No. 69, pp. 409-420, 1997.

[39] "On the Seismic Behavior of Earth Dams," N.N. Ambraseys, *Proceedings, Second World Conference on Earthquake Engineering,* Japan, 1960, Vol. I, pp. 331-354, 1960.

[40] "A New Test for Cementation Potential of Embankment Dam Granular Filter Material," R.V. Rinehart, and M.W. Pabst, *Geotechnical Testing Journal,* American Society for Testing and Materials (ASTM), Vol. 37, No. 3, 2014.

[41] "Some Uncertainties in Embankment Dam Engineering," V. Milligan, *Journal of Geotechnical and Geoenvironmental Engineering,* Vol. 129, No. 9, pp. 785-797, 2003.

[42] "Lessons Learned from Large-Scale Filter Testing," C. Redlinger, C. Rudkin, D. Hanneman, W. Engemoen, P. Irey, and T. Howard, *Proceedings, 6th International Conference on Scour and Erosion,* Paris, France, 2012.

[43] *Large-Scale Filter Performance Tests*, Report DSO-2014-05, Bureau of Reclamation, Dam Safety Office, Denver, Colorado, 2014.

[44] "Assessing Embankment Dam Filters Which Do Not Satisfy Design Criteria," M.A. Foster, and E. Fell, *Journal of Geotechnical and Geoenvironmental Engineering,* Vol. 127, No. 4, pp. 398-407, 2001.

[45] "Earthquake-Proof Earth Dams," F.H. Tibbetts, *Engineering News-Record,* pp. 10-15, July 2, 1936.

[46] "The Hebgen Lake, Montana, Earthquake of August 17, 1959," Professional Paper No. 435, U.S. Geological Survey, Washington, DC, 1964.

[47] *Designing with Geosynthetics*, R.M. Koerner, 5th edition, Prentice Hall, Upper Saddle River, New Jersey, 2005.

[48] "Effects of Earthquakes on Dams and Embankments," N.M. Newmark, *Géotechnique,* Vol. 15, No. 2, pp. 139 -160, 1965.

[49] "A Simplified Procedure for Estimating Earthquake-Induced Deformations in Dams and Embankments," Report No. UCB/EERC-77/19, F.I. Makdisi, and H.B. Seed, University of California Earthquake Engineering Research Center, Berkeley, California, 1977.

[50] "Simplified Procedure for Estimating Earthquake-Induced Deviatoric Slope Displacements," J.D. Bray, and T. Travasarou, *Journal of Geotechnical Geoenvironmental Engineering,* Vol. 133, No. 4, pp. 381-392, 2007.